THE OLIGOMERISATION OF PROPENE OVER NICKEL OXIDE SILICA ALUMINA

BY

STEFAN MATHIAS HARMS
B.Sc. (Eng) (Cape Town)

Submitted to the University of Cape Town in
fulfilment of the requirements for the degree
Master of Science in Engineering
(1987)

SYNOPSIS

A synthesis technique was developed for the preparation of a nickel oxide silica alumina catalyst. The propene oligomerisation activity and the selectivity of the catalysts prepared by homogeneous decomposition deposition (HDD) were investigated and compared with nickel oxide silica alumina catalysts prepared by the techniques of impregnation (IMP) and co-precipitation (SG). Amongst others, the effect of the nickel content, reaction temperature and pressure, and water content of the feed, on the activity and selectivity, were investigated. Also investigated were the lifetime of the various catalysts and, in the case of HDD type catalysts, the ability to oligomerise high molecular weight hydrocarbons (C_6).

Nickel oxide silica alumina prepared by the HDD method is more active for the propene oligomerisation than catalysts prepared by the IMP and SG methods. The product spectrum in the case of IMP and HDD type catalysts are similar, with a propene dimer (C_6) being the main product. In the case of SG type catalysts, however, a shift to heavier products was observed, i.e., propene dimer (C_6) and trimer (C_9) were formed in equal quantities. It is proposed that the increase in activity of HDD type catalysts was due to a large extent of metal dispersion and distribution and a stronger interaction between the metal and the support. It is also proposed that the metal is readily accessible to the reactant molecules.

The activity and selectivity of catalysts prepared by the HDD method were independent of the nickel content. This was not the case for IMP and SG type catalysts, both of which showed decreasing activity with increasing nickel content when the nickel content was increased beyond 5 wt%.

The lifetimes of the various catalysts were also examined. From the results obtained, over the first 10 h, the lifetime of HDD type catalysts was superior to that of the other catalysts studied. The activity and selectivity of the various catalysts were sensitive to the reaction conditions. Thus moving into the vapour phase, by either increasing the temperature at a fixed pressure or decreasing the pressure at a fixed temperature, was in each case accompanied by a shift to heavier products and a decrease in activity.

THE OLIGOMERISATION OF PROPENE OVER NICKEL OXIDE SILICA ALUMINA

BY

STEFAN MATHIAS HARMS
B.Sc. (Eng) (Cape Town)

Submitted to the University of Cape Town in
fulfilment of the requirements for the degree
Master of Science in Engineering
(1987)

SYNOPSIS

A synthesis technique was developed for the preparation of a nickel oxide silica alumina catalyst. The propene oligomerisation activity and the selectivity of the catalysts prepared by homogeneous decomposition deposition (HDD) were investigated and compared with nickel oxide silica alumina catalysts prepared by the techniques of impregnation (IMP) and co-precipitation (SG). Amongst others, the effect of the nickel content, reaction temperature and pressure, and water content of the feed, on the activity and selectivity, were investigated. Also investigated were the lifetime of the various catalysts and, in the case of HDD type catalysts, the ability to oligomerise high molecular weight hydrocarbons (C_6).

Nickel oxide silica alumina prepared by the HDD method is more active for the propene oligomerisation than catalysts prepared by the IMP and SG methods. The product spectrum in the case of IMP and HDD type catalysts are similar, with a propene dimer (C_6) being the main product. In the case of SG type catalysts, however, a shift to heavier products was observed, i.e., propene dimer (C_6) and trimer (C_9) were formed in equal quantities. It is proposed that the increase in activity of HDD type catalysts was due to a large extent of metal dispersion and distribution and a stronger interaction between the metal and the support. It is also proposed that the metal is readily accessible to the reactant molecules.

The activity and selectivity of catalysts prepared by the HDD method were independent of the nickel content. This was not the case for IMP and SG type catalysts, both of which showed decreasing activity with increasing nickel content when the nickel content was increased beyond 5 wt%.

The lifetimes of the various ctalysts were also examined. From the results obtained, over the first 10 h, the lifetime of HDD type catalysts was superior to that of the other catalysts studied. The activity and selectivity of the various catalysts were sensitive to the reaction conditions. Thus moving into the vapour phase, by either increasing the temperature at a fixed pressure or decreasing the pressure at a fixed temperature, was in each case accompanied by a shift to heavier products and a decrease in activity.

The catalysts studied were very sensitive to the feed moisture content. The introduction of an undried feed resulted in a high initial activity followed by rapid deactivation. IMP and HDD type catalysts, after being exposed to a wet feed, were shown to be able to regain their normal activity and selectivity after calcination.

ACKNOWLEDGEMENTS

I would like to express my sincere appreciation to Dr. M. Kojima and Prof. C.T. O'Connor for their assistance and guidance throughout the duration of my study.

Many thanks to Messrs D. McClean, L. Jacobs, P.M. Dickens, K. Moller and S.Schwarz, for their friendship and helpful advice over the years.

The following people and institutions are also gratefully acknowledged :

SASOL and the Council for Sientific and Industrial Research for financial assistance.

All on the Chemical Engineering Department staff.

Dr. K Herzog for his assistance with the TG-DTA analysis.

Miss B. Williams for the mass spectroscopic analysis.

Dr. M. Rautenbach for the use of his computer programm.

A special thanks to Alexandra for her help and patience.

I would also like to thank my mother, Ingeborg, for her continuous support and patience.

TABLE OF CONTENT

PAGE

LIST OF FIGURES

PAGE

CHAPTER 3

CHAPTER 4

PAGE

PAGE

PAGE

LIST OF TABLES

PAGE

PAGE

CHAPTER 7

7.A APPENDIX A

1. INTRODUCTION

In South Africa the oil from coal industry has developed the first commercial process whereby synthetic fuels are produced from coal via gasification using Fisher Tropsch catalysts. It started in 1943 when the American rights to the Fischer Tropsch process were purchased by South Africa. In 1950 the South African Oil, Coal and Gas Corporation (SASOL) was formed. The first plant Sasol I with a capacity of 4130 barrels/day went into operation in 1954 (Dutkuwicz, 1980). It used two type of reactors, namely the Arge fixed bed and synthol fluidised bed reactors. Two further plants, Sasol II and Sasol III which are improved and enlarged versions of Sasol I, were later built each having a capacity of 35900 barrels/day (Dutkuwicz, 1980). In both of these plants only the synthol reactors are used. Due to the nature of the process Sasol produces large quantities of light hydrocarbon gases amounting to approximately $1.5 \cdot 10^6$ m^2/day. These are partly reticulated to local industry and partly converted via a catalytic oligomerisation process to light fuels thereby increasing the overall production in terms of barrels of liquid fuel produced per ton of coal processed. Currently Sasol I can more than satisfy the local demand and therefore the light hydrocarbons from Sasol II and Sasol III represent excess supply.

The catalytic oligomerisation process referred to above uses the conventional phosphoric acid catalyst to oligomerise the light hydrocarbons to liquid fuels. This process however produces poor quality petrol and diesel and the catalyst is corrosive.

The present study investigated an alternative catalyst for the catalytic oligomerisation of light hydrocarbons to liquid fuels using a nickel oxide silica alumina catalyst synthesised via a method adopted by the author from work done by van Dillen et al (1976). Although nickel oxide silica alumina catalysts have been widely studied (Tahahashi et al., 1969: Hogan et al., 1955, Holm 1957, etc.) the synthesis method developed in this work will produced, it is hoped, a more active catalyst with greater resistance to deactivation and greater selectivity to linear C_6 than those recorded for nickel oxide silica alumina catalysts produced via the standard impregnation technique. In this way it is hoped to produce a better quality diesel than possible over the standard impregnated nickel oxide silica alumina.

1.1 Heterogeneous catalysis

As the silica alumina support in a nickel oxide silica alumina catalyst is a catalytically active solid oxide insulator its catalytic properties as well as those of nickel oxide on silica alumina have to be examined. In what follows, a brief review of the catalytic properties of both is given.

The oxides and halides of the lower elements of groups III, IV and V of the periodic table tend to catalyse positive ion or 'acid' type reactions such as polymerisation, alkylation, cracking and isomerisation. One of the most active solid oxide insulators is silica alumina. In Figure 1.1 (Clark, 1953), the rate of reaction is plotted against the weight percent silica in a silica alumina catalysts for various reactions, viz., hydrogen transfer, propene polymerisation, ethene hydrogenation and hydrogen deuterium exchange. It can be seen from this figure that the reaction velocity constants of the acid type reactions such as hydrogen transfer and propene polymerisation roughly parallel the changes in catalyst acidity.

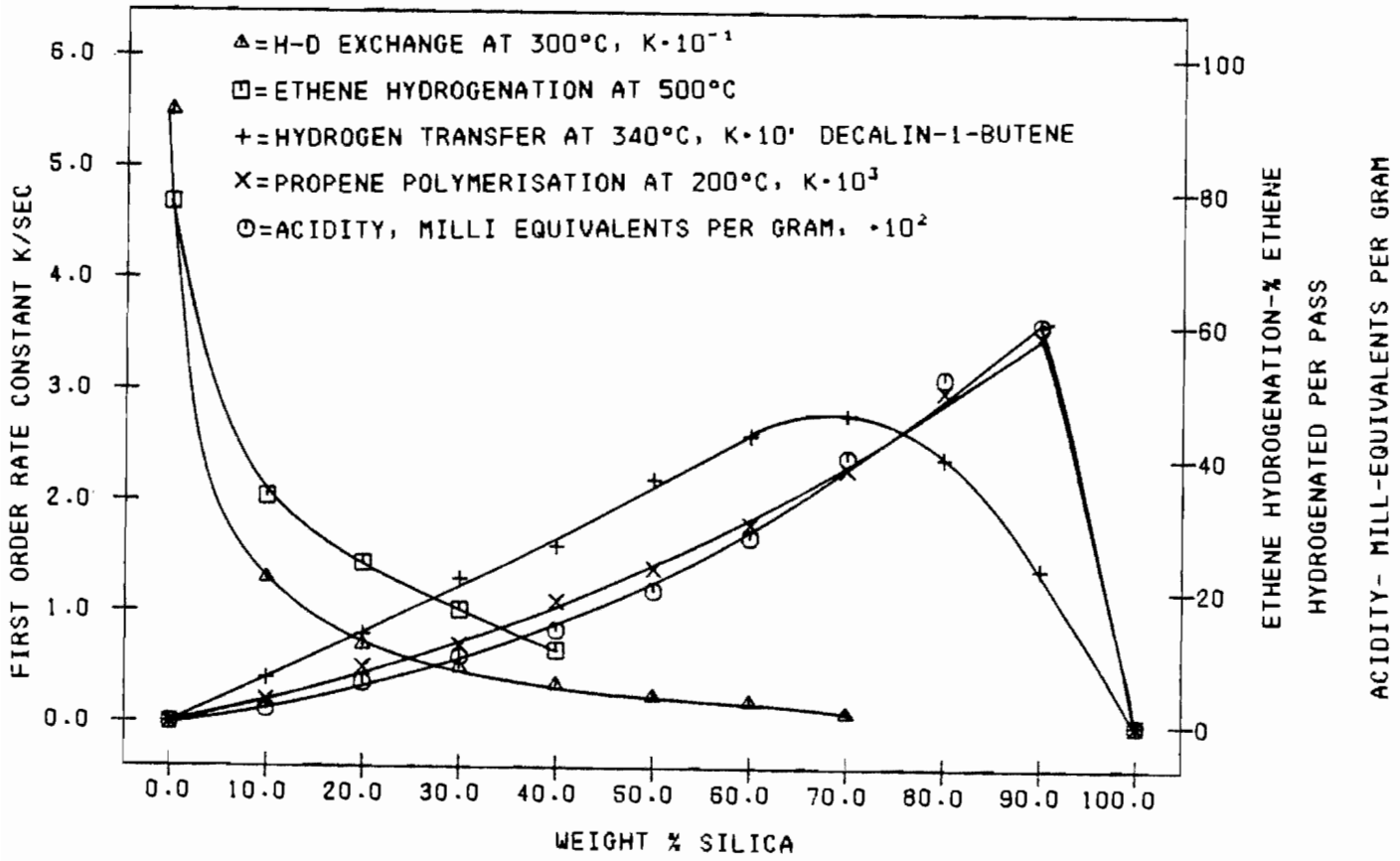

FIGURE 1.1 ACTIVITY OF SILICA ALUMINA CATALYSTS FOR VARIOUS REACTIONS AS A FUNCTION OF SILICA TO ALUMINA RATIO

The reactions which occur readily on the transition metal oxides, such as hydrogen-deuterium exchange which gives a reasonably good indication of hydrogenation-dehydrogenation activity, and ethene hydrogenation, proceed slowly even on pure alumina and the rate decrease to insignificant values with increasing silica content. Conversely, transition metals are poor catalysts for acid-type reactions.

Transition metal oxides alone, or supported on weakly acid oxides such as alumina, show only a small activity for acid type reactions such as the polymerisation of the low boiling point olefins. When, however, these oxides are supported on strong acid oxides such as silica alumina, they are capable of giving an increased activity as indicated in Figure 1.2 (Clark, 1953), which shows data on the polymerisation of propene. The details of the mechanism by which these metal oxides supported on silica alumina give an activity greater than that over silica alumina alone are not clear. Using Tamele's method of butylamine titration, there are some indications of an increase in acid content of the active metal oxide promoted catalyst over that of silica alumina alone (Clark, 1953). A detailed discussion of the mechanisms proposed and nature of the active sites is given elsewhere.

The following conclusions may therefore be drawn from Figure 1.2 with respect to propene polymerisation:

- the oxides of metals in group V and higher of the periodic table loaded on silica alumina alone give increased activity over silica alumina
- the oxides of metals in group IV and lower of the periodic table give activity below that of silica alumina.
- reducing the metal oxides causes the activity of the catalyst to drop below that of silica alumina.

1.2 Polymerisation using heterogeneous catalysts

1.2.1 Kinetics of the overall process

The overall kinetics of the process can be summarised by five steps. It must however be noted that at times some of these steps are not present. The steps are:

Step 1: Diffusion of reactants through the Nernst diffusion layer, a liquid film surrounding the catalyst particle, to the outer surface of the catalyst.

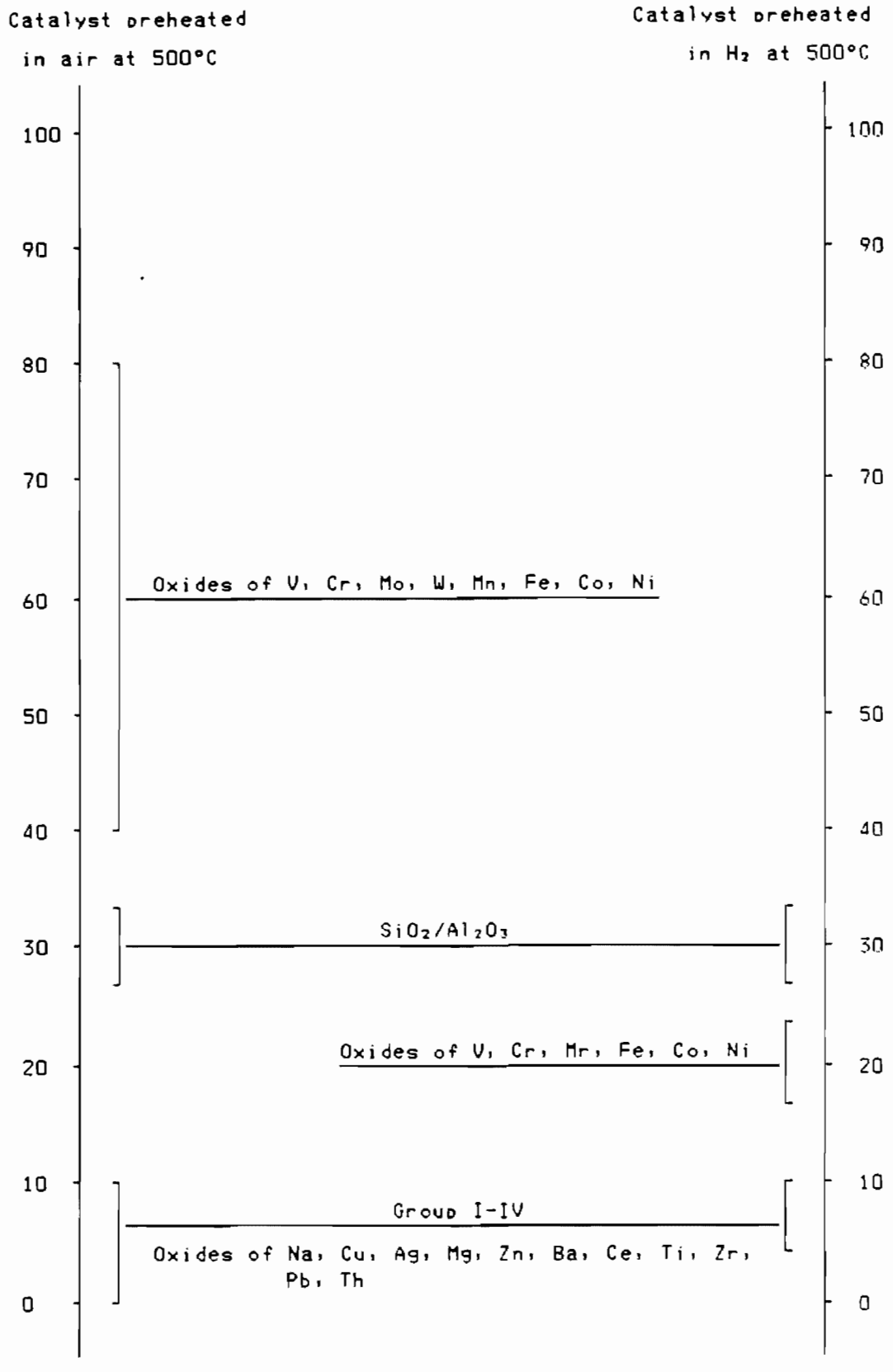

Fig 1.2 Ranges of conversion for polymerisation of propene on metal oxide silica alumina catalysts: 4 wt% metal oxide impregnated on support.

Step 2: Penetration and diffusion of the reactants through the blanket of graphitic carbon and/or hydrocarbon deposits to the internal surface and into the unreacted core.

Step 3: Reaction of the reactants at an active site.

Step 4: Diffusion of the products through the unreacted core and the blanket of graphitic carbon and/or hydrocarbon deposits back to the outer surface of the solid.

Step 5: Diffusion of the products through the fluid film back into the main body of the fluid.

The resistances of the different steps usually vary greatly from one another. The step with the highest resistance is considered to be the rate controlling step. This rate controlling step can often be identified via simple tests (see Levenspiel, 1972).

For optimum catalyst utilisation, a high matrix diffusivity is desirable. At any given condition, if the rate of chemical reaction is higher than the rate of diffusion, reactants cannot be supplied fast enough to the active site to establish an equilibrium concentration. The reaction therefore occurs only in the outer shell of the catalyst particles and a significant number of active sites inside the particle are unused. Large matrix diffusion resistance therefore results in molecules reacting before they penetrate into the interior of the catalyst particle. The rate is then controlled by either film diffusion or the rate of chemical reaction on the active surface, whichever is the slower step.

The overall reaction rate is also influenced by the reaction temperature. The rate of diffusion, however, increases at a slower rate than that of the chemical reaction and so at high temperatures pore diffusion or film diffusion becomes the rate controlling step. Insufficient agitation and a high viscosity of the solution can result in large film thickness and hence favour a film diffusion controlling mechanism.

1.2.2 Polymerisation

To date, the most widely accepted mechanism for the polymerisation of olefins is that proposed by Whitmore (1934) and involves the carbonium ion. One of the most pronounced characteristics of acid catalysed reactions involving the carbonium ion is the lack of specificity (Langlois, 1953). Almost never is only a single product formed and even under the mildest conditions a large number of compounds are formed. Schmerling and Ipatieff (1950) have distinguished two classes of polymerisation: "true polymerisation" in which the reaction products are mono-olefins with molecular weights intergral multiples of the monomer molecular weight, and "conjunct polymerisation" in which the reaction products are a complex mixture of olefins, diolefins, paraffins, naphthenes, cyclo-olefins and aromatics. Both will now be discussed in detail.

1.2.2.1 True polymerisation

The carbonium ion is formed in the presence of a hydrogen acid by the addition of a proton to the electron pair of the double bond, i.e.,

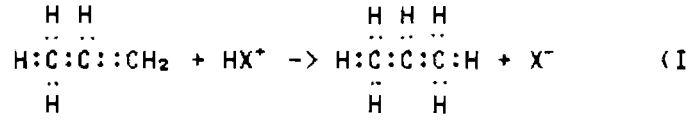

(I)

It is not proposed that a free alkyl carbonium ion exists in the hydrocarbon solution, but that it remains within a short distance from the anion of the catalysts and that the two exist in the form of an ion pair (Langlois, 1953). As the degree of separation of the carbonium ion from the Bronsted site is of no importance in the explanation of the reaction mechanism, it is sufficient to postulate the existence of an alkene with a positive charge on a particular carbon atom. The term carbonium ions will be used in subsequent discussions and represented as shown in equation (I) above without showing the anion, although its presence somewhere near the positive charge is to be understood (Langlois, 1953).

The halide catalysts are acidic only in so far as they are electron acceptors. Hunter and Yohe (1933) postulated that the active complex, in the absence of hydrogen halide promoters, is formed by the addition of the catalysts to the olefin. In this way the metal halide functions in a manner similar to that of a proton and may be considered to be an acidic catalyst (Schmeling and Ipatieff, 1950).

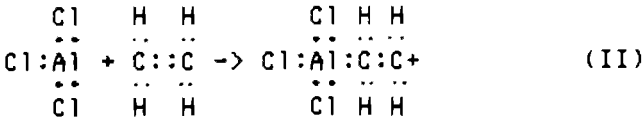

(II)

It has, however, been found that the halide catalyst requires a co-catalyst such as water, tert-butyl alcohol or acetic acid, all of which contain an active proton, to be active for polymerisation. Fontana and Kidder (1948) found that the polymerisation of propene on a halide catalyst was approximately proportional to the concentration of the promotor used which was confirmed by Norrish and Russel (1952) who found that in the polymerisation of isobutene with stannic chloride, a co-catalyst such as water was necessary, that the rate of reaction was proportional to the concentration of the co-catalyst and that the maximum rate was achieved when water and stannic chloride were present in equimolar proportions.

It is thus probable that the reactions proceed through an intermediate from the reaction of the olefin, metal hydride and promotor, with the latter serving as the source of the proton necessary for the production of the carbonium ion, viz.,

$$R\text{-}CH{=}CH_2 + BF_3 + H_2O \langle\text{-}\rangle R\text{-}\overset{+}{C}H\text{-}CH_3 + BF_3OH^- \qquad \text{(III)}$$

It appears that reaction (II) does not occur to any appreciable extent, or if it did, that the resulting complex would not have any appreciable activity for the initiation of polymerisation. It is probable, therefore, that in all cases the effective catalyst for the acid catalysed polymerisation of olefins are acids in the more restricted sense that they must be able to supply a proton to initiate the reaction (Langlois, 1953).

Of the olefins of low molecular weight, isobutene is polymerised the most readily with acid catalysts. N-butene and propene are polymerised less readily, while ethene is polymerised only with difficulty. From this, and information drawn from the composition of the reaction products, Whitmore (1934) reached the conclusion that a tertiary carbonium ion is the most stable, a secondary ion less stable, and a primary ion least stable. Evans and Polanyi (1947) calculated proton affinities of the doubly bonded carbons in isobutene, propene and ethene. Their calculations showed the proton affinity of the primary carbon of the double bond to be in the order isobutene > propene > ethene and furthermore that the proton affinity of the primary carbon of the double bond is greater than that of a secondary or tertiary carbon

of the double bond for the cases of propene and isobutene. These calculations confirm the early empirical observations. In accordance with this concept we should expect the following carbonium ions from isobutene and propene.

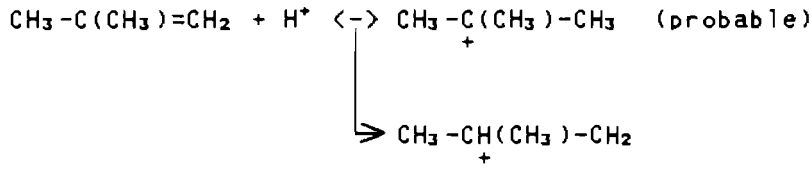

and

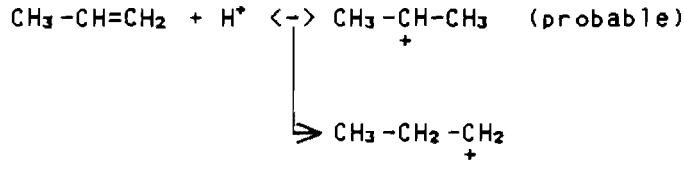

The possibility of the formation of minor quantities of the two less favoured isomers cannot be excluded, particularly at high temperatures, but the species indicated should be the predominant ones. Whitmore (1934) postulated that a carbonium ion, once formed, may undergo a variety of reactions:

Addition of a negative ion X, with the net result being the addition of HX to the double bond,

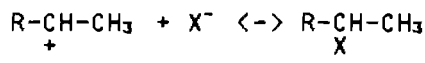

Addition to the double bond of an olefin to form a new carbonium ion: this is the polymerisation step.

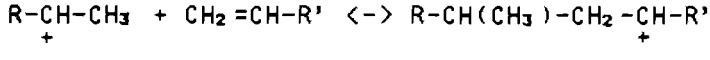

Elimination of a proton to form the original olefin or a different one.

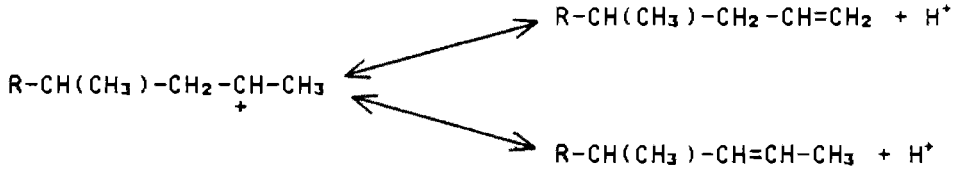

Migration of a proton with its bonding electrons from another carbon to the atom deficient in electrons leaving a new carbonium ion.

$$CH_3-CH(CH_3)-\overset{+}{C}H-CH_3 \;<\!\!-\!\!>\; CH_3-\overset{+}{C}(CH_3)-CH_2-CH_3$$

Migration of a methyl group with its two electrons to the positive carbon atom, generating a new carbonium ion with a new skeletal arrangement.

$$CH_3-C(CH_3)_2-CH(CH_3)-\overset{+}{C}H-CH_3 \;<\!\!-\!\!>\; CH_3-\overset{+}{C}(CH_3)-CH(CH_3)-CH(CH_3)-CH_3$$

Extraction of hydrogen from another molecule to form a saturated molecule and a new carbonium ion.

$$RH + \overset{+}{R'} \;<\!\!-\!\!>\; \overset{+}{R} + R'H$$

All the above reactions are indicated to be reversible, but the reactions may not occur at similar rates. Usually one will be favoured over the other.

1.2.2.2 Conjunct polymerisation

Conjunct polymerisation, that is, polymerisation accompanied by the formation of saturated hydrocarbons, occurs only under specific conditions such as at high temperatures and over highly acidic catalysts. Evidence in support of a carbonium ion mechanism to explain the formation of conjunct polymers was obtained by Bartlett et al (1944). The mechanism involves the removal from the oligomer of a hydrogen atom with its bonding electrons by the carbonium ion. The mechanism may be illustrated as follows:

$$R-CH_2-CH_2-CH=CH-R' + H^+ \;<\!\!-\!\!>\; R-CH_2-CH_2-\overset{+}{C}H-CH_2-R'$$

$$R-CH_2-CH_2-\overset{+}{C}H-CH_2-R' + R-CH_2-CH_2-CH=CH-R' \;<\!\!-\!\!>$$

$$R-CH_2-CH_2-CH_2-CH_2-R' + R-CH_2-\overset{+}{C}H-CH=CH-R'$$

$$R-CH_2-\overset{+}{C}H-CH=CH-R' \;<\!\!-\!\!>\; R-CH=CH-CH=CH-R'$$

For conjunct polymerisation the significant reaction steps are:

- initiation by proton addition;
- propagation by olefin addition;

- chain termination by proton expulsion,
- chain termination by proton transfer,
- chain termination by addition of hydride ion,
- depolymerisation to same or chain length other than that of the original olefin,
- isomerisation,
- hydrogen exchange,
- cyclysation, equivalent to self-alkylation or self-polymerisation, and
- loss of hydride ion.

1.2.3 Polymerisation on silica alumina

1.2.3.1 Nature of active sites on silica alumina

Silica aluminas differ widely in properties and have been the subject of much research (Mizuno et al., 1976; Finch and Clark, 1969; Peri, 1976). The nature of the active sites in the polymeric olefin formation is controversial because of the lack of conclusive evidence.

Ozaki and Kimura (1964) speculated that the olefin chemisorbed on Lewis acid sites as a monomer. Hirschler (1970) concluded that Bronsted acid sites were the active sites over silica alumina on the basis of the similarity in composition of polymeric species formed over silica alumina and those formed over deammoniated Y-zeolite. On the contrary, Weeks et al (1974) concluded that the active sites were Lewis sites formed upon dehydroxylation of Y-zeolite because no significant difference was found between products over deammoniated and dehydroxylated zeolites. Peri (1976) regarded an alpha site, a pair consisting of a Lewis site and an oxide ion, to be active. Holm et al (1959) and Sato et al (1965) reported that propene polymerisation at an elevated temperature varied in proportion to the Bronsted acid content. However, objections have been raised to their determination of the Bronsted acid content (Forni, 1974). Mizuno et al (1976), on the other hand, showed that the catalytic activity for the polymeric olefin formation declined sharply as the extent of selective poisoning of the Lewis acid sites increased.

1.2.3.2 Structure of the products and proposed mechanism on silica alumina

Silica-alumina has a low activity for the oligomerisation of propene at low reaction temperatures, the main product being propene trimers.

The mixture of propene dimers formed on silica-alumina was characterised by Fel'dblyum and Baranova (1971) and found to contain a relatively high content of 4-methyl-2 and 4-methyl-1-pentene. According to the carbonium ion mechanism as postulated by Whitmore (1934), these are the primary dimerisation products which isomerise into the thermodynamically more stable methylpentenes.

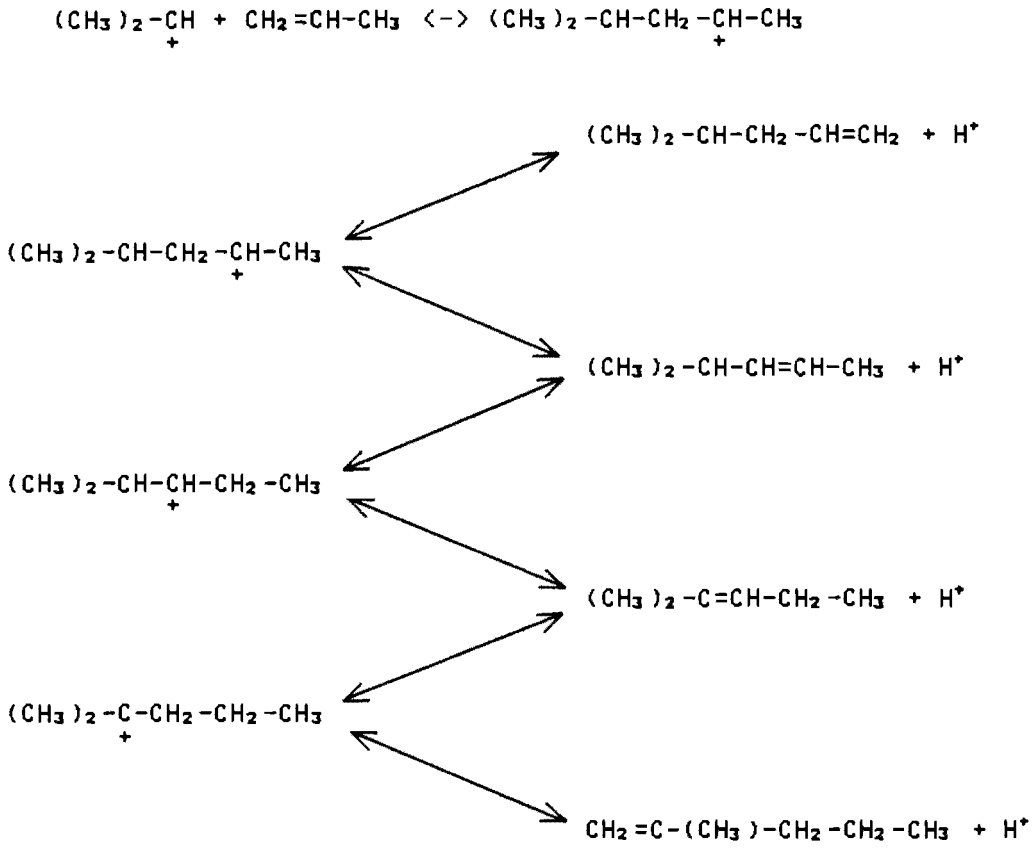

The 2,3-dimethylbutenes may form on silica alumina either as a result of the skeletal isomerisation of the 2-methyl-3-pentyl cation as suggested by Shephard et al (1962), or by the irregular (anti-Mrkovnikov) addition of the isopropyl cation to propene as suggested by Fel'dblyum and Baranova (1971). The second route is more likely since skeletal isomerisation of the isohexene cation should lead with even greater ease to the production of 3-methyl pentenes, which are, however, practically absent from the mixture of propene dimers.

Fel'dblyum and Baranova (1971) further suggested that hexenes are formed over silica alumina catalyst via the anomalous addition of a proton to propene. That the main reaction product on silica alumina is a propene trimer was explained by Fel'dblyum and Baranova (1971) by suggesting that the initially formed 4-methyl-2-pentyl cation rapidly isomerises to the more stable tert-2-methyl-2-pentyl cation and the rate of the reaction of the latter with propene is higher than the rate of

desorption of the dimer from the active center of the catalyst. At the same time the reaction of the 2-methyl-2 pentyl cation with propene should lead to the formation of the propene trimer with a 4,4 dimethyl heptane carbon skeleton. This was found to be the case by Fel'dblyum and Baranova (1971).

It can thus be seen that the silica alumina carrier leads to the oligomerisation of propene by a carbonium ion mechanism, as proposed by Whitmore (1948), with the product being a propene trimer.

1.2.4 Polymerisation on nickel oxide silica alumina

1.2.4.1 Nature of active sites on nickel oxide silica alumina

Hogen et al (1955) established that hexenes and methyl pentenes were the main products formed during the oligomerisation of propene under the influence of nickel oxide on silica alumina. While explaining this observation from the standpoint of the carbonium ion mechanism, Hogan et al (1955) at the same time admitted that the reaction mechanisms differed substantially from that found in the usual acid catalysts. It was proposed by Ushida and Imai (1962) that two types of protonic acid centers existed and they ascribed the observed product selectivity to the isomerisation of the olefin over the protonic acid site attached to the aluminium. Imai et al (1968), however, proposed that 3-methyl-1- and 3-methyl-2-pentenes were formed via a cyclo butene intermediate. At the conditions used by Imai et al (1968), i.e., a temperature of 200°C, skeletal isomerisation of the primary oligomers was entirely possible. At lower reaction temperatures, e.g., 64°C as used by Fel'dblyum and Baranova (1971), 3-methyl-pentenes were hardly formed. The dimerisation reactivity of ethene, propene and 1-butene under the influence of nickel oxide on silica alumina was established by Ozaki et al (1968) to vary in the ratio of 100:10:1, i.e., in an order opposite to that which occurs on typical acidic catalysts. This was explained by them via the existence of hydrogen atoms on the catalyst surface. The hydrogen atoms were capable of adding to the olefin to form free radicals which are then involved in the dimerisation. According to Ozaki et al (1968), the role of the acidic carrier is unimportant. Schultz et al (1966) examined the dimerisation of propene in the presence of cobalt oxide on a non-acidic carrier, activated charcoal. A positive result was obtained with cobalt oxide, while nickel oxide on the same support was inactive.

In view of the foregoing the nature of the products from the oligomerisation of propene under the influence of nickel oxide on silica

alumina is discussed in greater detail below to deepen our understanding of the reaction mechanism and the active sites.

1.2.4.2 Structure of the products on nickel oxide silica alumina

The deposition of nickel oxide on silica alumina changes the selectivity of the catalyst, the preferential product now being a propene dimer. The high content of hexenes in the resultant dimer is not due to the occurrence of isomerisation or to the greater tendency of the methyl pentenes as opposed to that of the hexenes to react further, but was ascribed by Fel'dblyum and Baranova (1971) to be a characteristic feature of nickel oxide on silica alumina catalysts, when used for the dimerisation of propene.

There exists a close analogy in the mechanism, as shown in Table 1.1 (Fel'dblyum et al., 1974) between homogeneous catalysis based on nickel salts and organoaluminium compounds, and heterogeneous catalysts based on nickel oxide on an acid carrier. The similarity in the mechanisms is based on the proposal that during the dimerisation of the olefins on the oxides of group VIII metals, a complex hydride is formed. In the case of nickel oxide, the source of the active site is assumed to be an unusually low degree of oxidation at a defect site in the nickel oxide crystal lattice. The dimerisation of propene catalysed by the complex hydrides of the transition metal (HM) should lead to the formation of 4 methyl-1- and 4-methyl-2-pentenes as the primary products, with subsequent isomerisation as shown below.

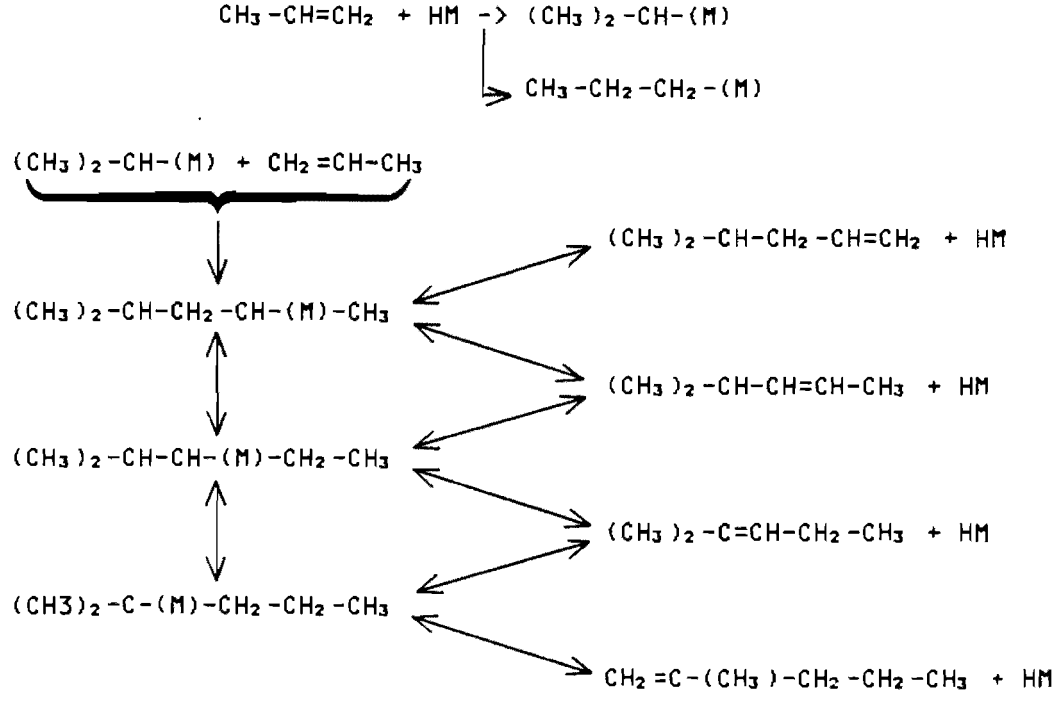

Table 1.1 : Analogy in the mechanism of the catalytic action of homogeneous and heterogeneous system for the dimerisation of olefins

Catalyst mechanism	Homogeneous ($NiCl_2$-R_nAlCl_{3-n})	Heterogeneous (NiO-SiO_2-Al_2O_3)
Structure of active site	$HNiCl \cdot R_nAlCl_{3-n}$	$HNi(O)_{n-1}$ on silica Alumina
Path of the formation of active site	Reaction of NiCl with R_nAlCl_{3-n}	Reduction of $Ni(O)_n$ and reaction of $Ni(O)_{n-1}$ with the olefin
Initiation stage of the reaction	1,2-Cis-addition of HNiCl to the olefin	1,2-Cis-addition of $HNi(O)_{n-1}$ to the olefin
Propagation stage of the reaction	Entry of a co-oordinated olefin at the nickel-carbon σ bond	Entry of a co-ordinated olefin at the nickel-carbon σ bond
Catalyst regeneration step	Cis-elimination of an olefin from HNiCl	Cis-elimination of olefin to form $HNi(O)_{n-1}$
Reasons for termination of reaction	Thermal decomposition and reduction of HNiCl	Reduction of $HNi(O)_{n-1}$ to metal

The formation of hexenes is explained by an alternative route in the cis 1,2 addition of HM to propene:

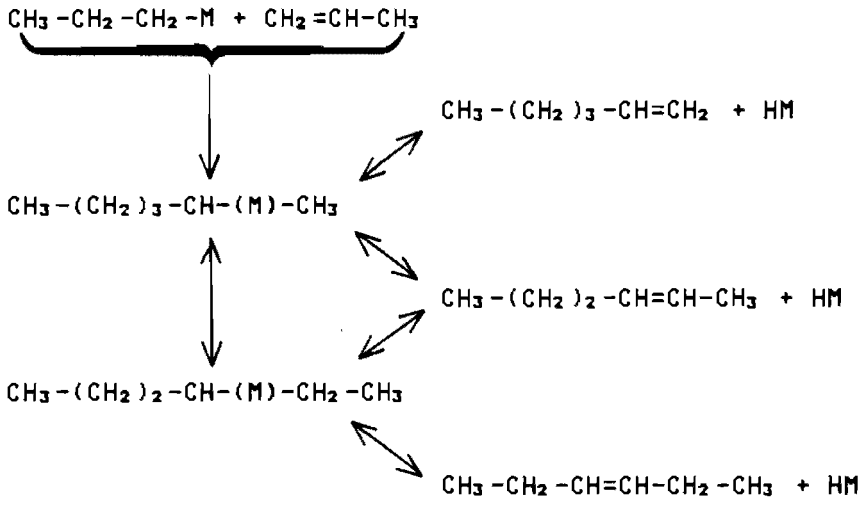

With the addition of a third propene molecule at the nickel carbon sigma bond, trimers (C_9) with a carbon skeleton of 2,4 dimethyl heptane and 4-methyl-octane were expected to form. This was confirmed by Fel'dblyum and Baranova (1971).

The absence of olefins with a 4,4-dimethyl-heptane carbon skeleton in the propene trimer, formed under the influence of nickel oxide on silica alumina, rules out the possibility of the reaction of tert-hexyl derivatives of the transition metal with propene and this results from their instability. This accounts for the dimerising action of the catalyst.

From the structure of the products formed and the analogy between homogeneous catalyst based on nickel salts and organoaluminium compounds, and heterogeneous catalysts based on nickel oxide on silica alumina, it must be supposed that complex hydrides of the transition metal are responsible for the catalytic actions of nickel oxide silica alumina in the oligomerisation of propene.

1.2.5 Thermodynamics

Figure 1.3 shows the free energy changes which occur during the dimerisation of C_2 to C_6 mono-olefins as a function of temperature. The free energy change for the dimerisation of ethene to 1-butene is much lower than the dimerisation of the other light olefins (Ublad et al., 1958).

The dimerisation of terminal bonded olefins, e.g., propene, to isomers of corresponding higher olefins at a given temperature is much more favourable than that for the dimerisation to the higher terminal olefin

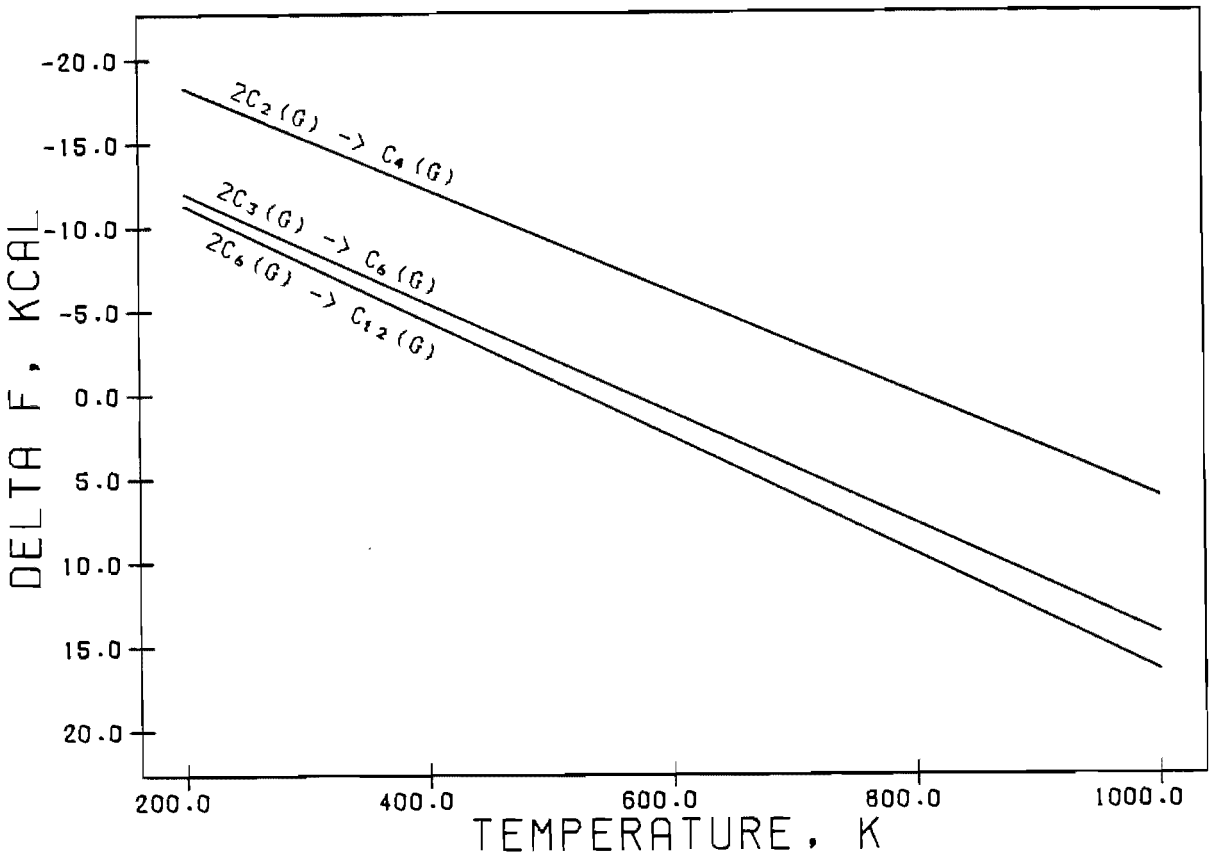

FIG 1.3 FREE ENERGY CHANGE DURING DIMERISATION

as shown in Figure 1.4. Hence the equilibrium conversion of an alpha olefin to a higher alpha-olefin will always be less than the corresponding conversion of an alpha-olefin to an iso-olefin. Dimerisation of beta-olefins or iso-olefins to corresponding higher olefins will be similar to the alpha-olefin-alpha-dimer relationship. Dimerisation of beta olefins or iso-olefins to higher alpha olefins will however always be the least favourable reaction (Ublad et al., 1958).

Figure 1.5 shows the effect of pressure on the dimerisation equilibrium. The relationship shown is that of the product of the equilibrium constant and reaction pressure in atmospheres to the percentage conversion for any dimerisation reaction

Figure 1.6 shows the free energy change for the formation of higher olefins as a function of temperature for the monomers propene and 1-butene, respectively. These figures show that above 550°C for both propene and 1-butene the reverse reaction, i.e., cracking, occurs. Clearly at higher temperatures the lower oligomers will predominate whereas at low temperatures the higher polymers will predominate at equilibrium (Oblad et al., 1958).

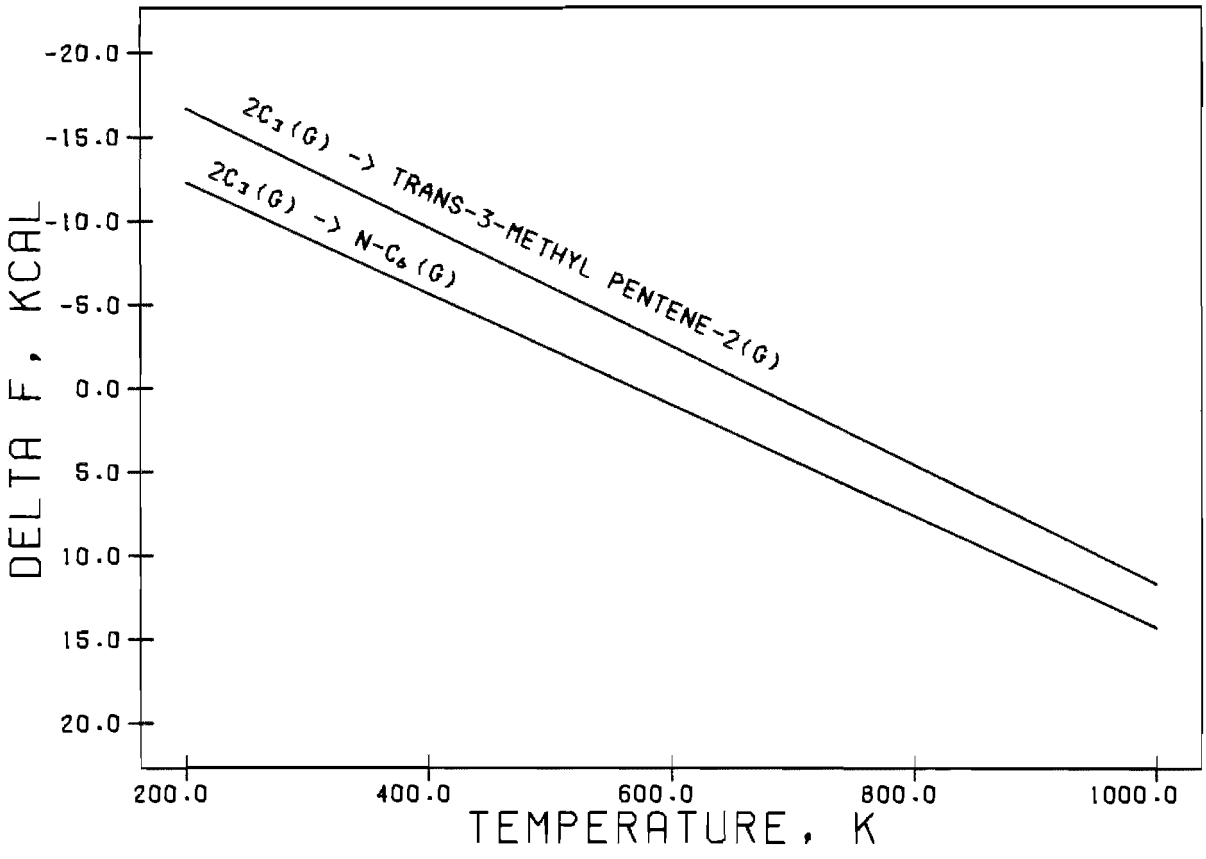

FIG 1.4 FREE ENERGY CHANGE DURING DIMERISATION

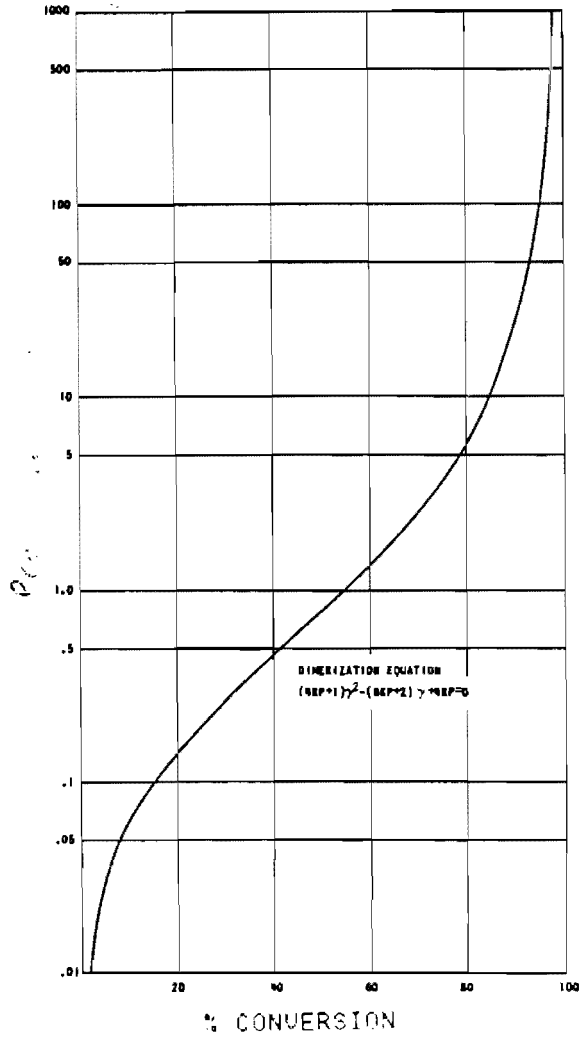

FIG 1.5 CONVERSION OBTAINABLE IN DIMERISATION REACTIONS

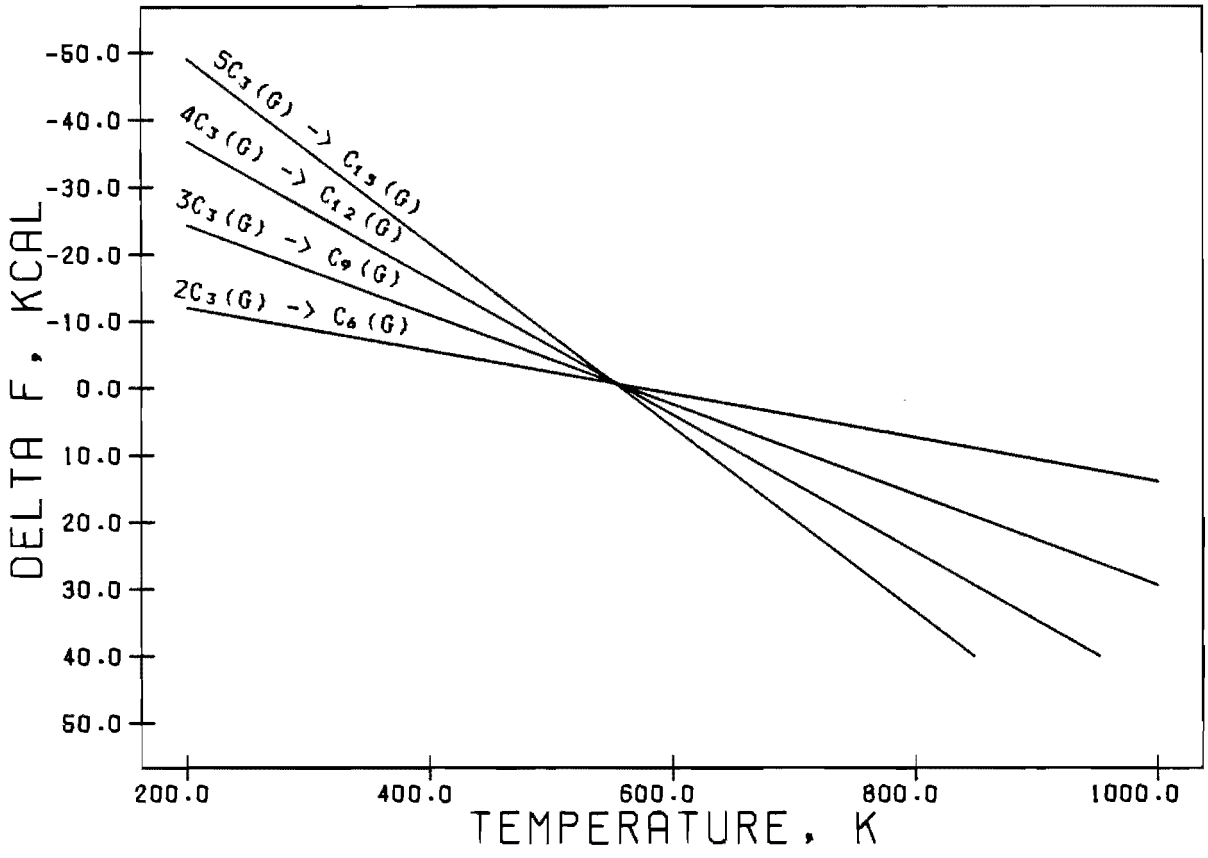

FIG 1.6 POLYMERISATION OF PROPENE

1.3 Catalyst characterisation

1.3.1 Introduction

There are a number of advantages in depositing catalytically active metals on a support such as alumina, charcoal, silica and silica alumina. The metal can be highly dispersed as small crystallites throughout the pore system of the support and as a result a large active metal surface is produced relative to the weight of the metal used. In a pelleted, granular or other physical form, a supported metal catalyst provides for flow of gases through the reactor and rapid diffusion of reactants and reaction products through the porous catalyst to and from the active site (Boreskov, 1976; Cervello et al., 1976). The support can also improve dissipation of reaction heat, retard the sintering of metal crystallites with resultant loss of active surface and increase poison resistance. For these reasons supported metal catalysts are widely used in chemical processing. It must be recognised however that the support may also have a catalytic role to perform and the resultant bifunctional catalyst may have properties different from those of the support or the metal alone.

To achieve greater understanding of the way in which good catalysts can be prepared more information is needed about the effect of the synthesis method and the structure of the catalysts. Both will now be discussed in detail.

1.3.2 Catalyst synthesis methods

When a porous solid comes into contact with a liquid, capillary forces of several hundred atmospheres draw the liquid into the pores. The active component may then be adsorbed on the walls of the pore in which case the method of preparation is described as adsorption from solution or ion exchange. Here the volume of solution used will be larger than the pore volume of the support. In other preparation methods where adsorption is small, the catalyst is produced by drying out of the support wetted with a solution of the active component and the term impregnation is used (Maatman and Prater, 1957). At a high degree of loading, greater than 5 %, the above methods do not lead to uniform distribution, viz., uniform location of the metal crystallites within the support, or uniform dispersion, viz., uniform size of the metal crystallites throughout the support. This can, however, be overcome by starting from a mixture in which the constituents of the active component and the support are mixed on an atomic scale. Under certain conditions a precipitate will be formed with the active phase, atomically spread throughout the support. This method of production is termed co-precipitation and discussed in detail by Holm et al (1957).

The factors affecting dispersion and distribution in the various synthesis routes will now be discussed.

1.3.2.1 Preparation with adsorption

Catalysts are often made by immersing a porous support in a solution of an active material. Catalytic properties can be influenced by the amount and distribution of this material on the internal surface of the support which in turn depends on whether the active material (solute) or the solvent adsorbs on the support and the fraction of pore volume accessible to the solute. In Figure 1.7, the quantity of active material found in different parts of a system, consisting of an external solution and a single pore which adsorbs activating material, is shown for four conditions. Figure 1.7a shows the distribution of the active material in the system, when the solution reaches the end of the pore. The assumption is made that the rate of penetration and rate of diffusion of the solute into the pore are slow compared to the rate of adsorption. All active material in the penetrating liquid thus adsorbs on the wall

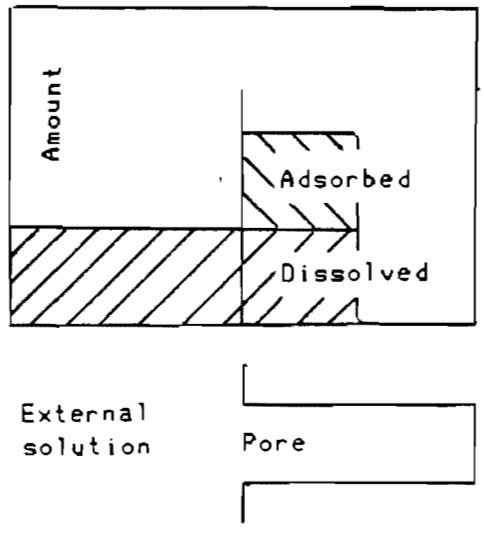

A: Immediately after filling

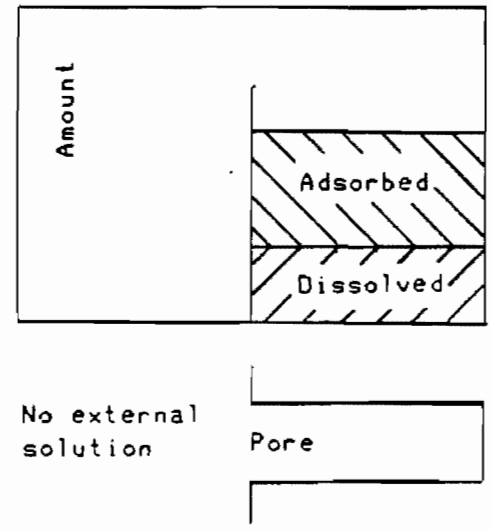

B: After it was filled and allowed to equilibrate

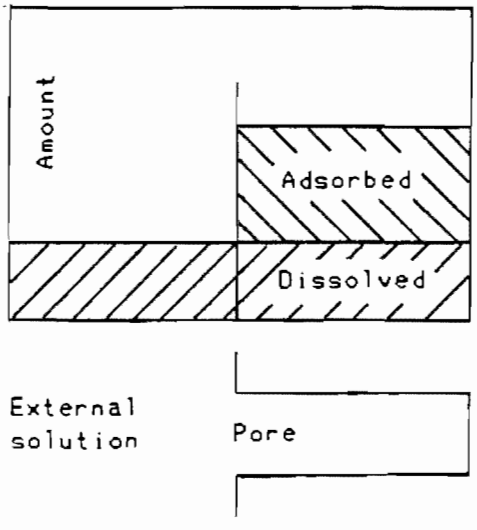

C: After equilibration in the presence of an excess of external solution

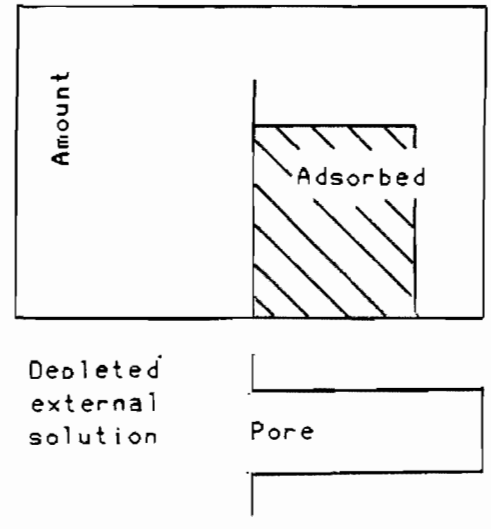

D: After external solution depleted of solute but before equilibration

Fig 1.7 Conditions of a pore adsorbing activating material in solution

of the first part of the pore. The liquid which passes further into the pore contains no active material. If at this time the solvent is removed from the pore by drying, the active material is found only in the part of the pore nearest to the external solution. If instead of drying the catalyst at this time the pore is simply removed from the external solution but left filled with liquid another phenomenon may be observed. If the active material can desorb at a reasonable rate redistribution occurs by desorption and migration by diffusion. This ultimately results in a uniform distribution of active material within the pore as shown in Figure 1.7b. This process can be used in catalyst preparation if the rate of desorption is rapid enough. If the pore is however left in contact with the external solution additional active material is supplied by the external solution by diffusion to the adsorption sites until either equilibrium with the external solution is reached bringing about a uniform distribution as shown in Figure 1.7c, or the external solution is depleted of active material before the distribution is uniform as shown in Figure 1.7d (Maatman and Prater, 1957).

It can thus be seen that the amount of active material found in a porous support can be much larger than that contained in the original pore volume of liquid penetrating the support. If on the other hand the pores are accessible to the solvent but are too small for the solute to enter or if the solvent is adsorbed in preference to the solute, the quantity of active material may be extremely low.

1.3.2.2 Drying of adsorbent solids

In the case of an adsorbent solid, the drying process is not expected to alter the distribution of the active material since it is adsorbed to the solid. However, if the adsorptive properties of the material were to alter during heating and prior to evaporation of the solvent, as by thermal decomposition to a soluble species which does not adsorb on the support, the distribution of the solute would be markedly altered. This condition is discussed below.

1.3.2.3 Preparation without adsorption

In this case, a porous support is submerged in a solution containing the active material and the metal salt is drawn into the pores by capillary forces. The solvent is then evaporated and the salt decomposed by calcination or reduction. The metal content can be calculated from the concentration of the solution.

For impregnated type catalysts, Dorling et al (1971) predicted that up to a certain metal content, the number of crystallites would increase, the mean crystallite size would vary slowly and the metal area would be approximately proportional to the metal content. Beyond this metal content, the number of crystallites would remain constant if only one crystal formed in each pore during drying. Hence the metal crystallites would increase in size and the metal area would be proportional to (metal content)$^{2/3}$. Dorling et al (1971) predicted that the crystallite size distribution would reflect the pore size distribution of the support.

1.3.2.4 Drying of non-adsorbed solids

As a result of evaporation of the solvent, deposition of the solute begins when the solution becomes saturated. If all the liquid could be evaporated instantaneously the active material would deposit locally and uniformly throughout the support. Evaporation, however, does not occur instantaneously but starts at the outer periphery of the particles and proceeds from regions of larger pore diameters to smaller pores. This uneven evaporation is the result of the higher vapour pressure of the liquid in the larger pores, while liquid which evaporates from small pores is replaced by liquid drawn, by capillary action, from the larger pores as illustrated in Figure 1.8.

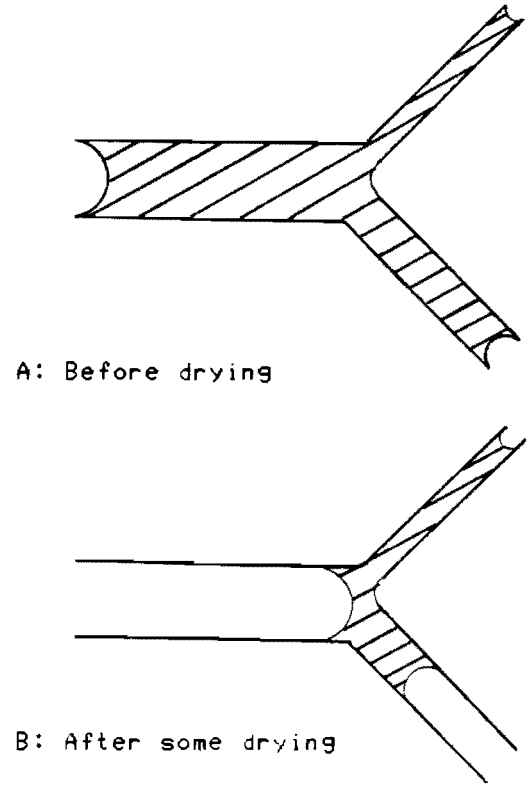

Figure 1.8 Intersecting pores of diferent sizes before drying (A) and after evaporation of some of the pore volume liquid (B)

Thus, when drying proceeds slowly enough, there is a tendency for the active material, which is increasing in concentration as the liquid volume decreases, to redistribute by diffusion into the remaining fluid. This results in an enrichment of the active material in the smaller pores and towards the center of the particle (Maatman and Prater, 1957).

1.3.3 Homogeneous decomposition deposition

It can be seen from the above discussion that, producing a catalyst by impregnation or ion exchange with high metal contents leads to the formation of crystallites with non-uniform distribution and low dispersion. As an active supported catalyst system calls for a highly dispersed particle with uniform distribution on a highly porous thermally stable support such as silica alumina, it would be desirable to combine the high degree of penetration of the solute into the support observed during impregnation with a controlled ion exchange-type precipitation. The procedure studied by van Dillen (1976) for the manufacture of highly dispersed nickel silica catalysts with uniform distribution, and a similar system used by Higley (1984) to produce nickel oxide on silica alumina catalysts, was investigated.

In the case of this work a suspension of nickel nitrate hexahydrate and silica alumina was prepared. To precipitate the nickel salt onto the support the pH had to be lowered. This was achieved by Higley (1984) via the injection of ammonium hydroxide and in the case of this work by the slow and homogeneous decomposition of urea. The reason for using urea as the source of hydroxyl ions as opposed to ammonium hydroxide is discussed below. A detailed discussion of the synthesis procedure is given in Section 3.6.3.

1.3.3.1 Theory of homogeneous decomposition deposition

When the concentration of a homogeneous solution is raised at a constant temperature, as shown by path A in Figure 1.9, the solubility curve is reached. Crossing the solubility curve does not generally lead to the formation of a precipitate but to a metastable state. When, however, the concentration on the solubility curve is exceeded by a critical amount, nuclei of the precipitate are spontaneously generated, bringing about the transition to the equilibrium state. The concentration where nuclei start to develop spontaneously in homogeneous solutions is indicated by the supersolubility curve which is also shown in Figure 1.9 (Walton, 1969). The fact that no precipitate grows when the solubility curve is crossed is due to the considerable surface energy of very small

particles of the precipitate. Thus, raising the concentration of a solution to the value on the supersolubility curve leads to the formation of a limited number of nuclei. If the homogeneity of the solution is maintained the concentration of the solution will remain between that of the solubility and supersolubility curves where no new nuclei can develop. Therefore, as a result of precipitation from a homogeneous solution, a small number of large particles of the precipitate are formed. Pouring a precipitant into the suspension on the other hand gives rise to an inhomogeneous solution as the concentration will locally be increased far beyond that of the supersolubility curve, as shown by path B in Figure 1.9. This gives rise to the formation of a large number of nuclei. Before the concentration has decreased by homogenizing the solution, the nuclei have grown sufficiently to be stable at the lower concentration. Working with an inhomogeneous solution therefore results in a relatively large number of small particles (Cartwright et al., 1967).

It was concluded by Hermans and Geus (1979) that pouring a precipitant into a suspension of a porous carrier leads to precipitation of the active material where the precipitant enters the suspension and the precipitate will not develop uniformly over the surface of the support. Precipitation from a homogeneous solution, on the other hand, proceeds equally in the pores of the support and in the bulk of the solution and so eliminates the inhomogeneous addition of the precipitate to the support.

In order to produce a catalyst with high dispersion and uniform distribution, a sufficiently strong interaction of the precipitating compound with the support is necessary. This interaction must decrease the nucleation barrier so that nucleation at the surface of the support can proceed at a concentration between the solubility and supersolubility curves. The precipitate can then nucleate at the surface of the support, whereas nucleation in the bulk of the solution is prevented. In addition, nucleation at the surface must be rapid to avoid the growth of a small number of nuclei to large particles of the precipitate (Hermans and Geus, 1979).

1.3.3.2 Nickel oxide silica alumina preparation using homogeneous decomposition deposition

Higley (1984) showed that incorporating nickel onto silica alumina by the injection of a hydroxide-containing solution (ammonium hydroxide)

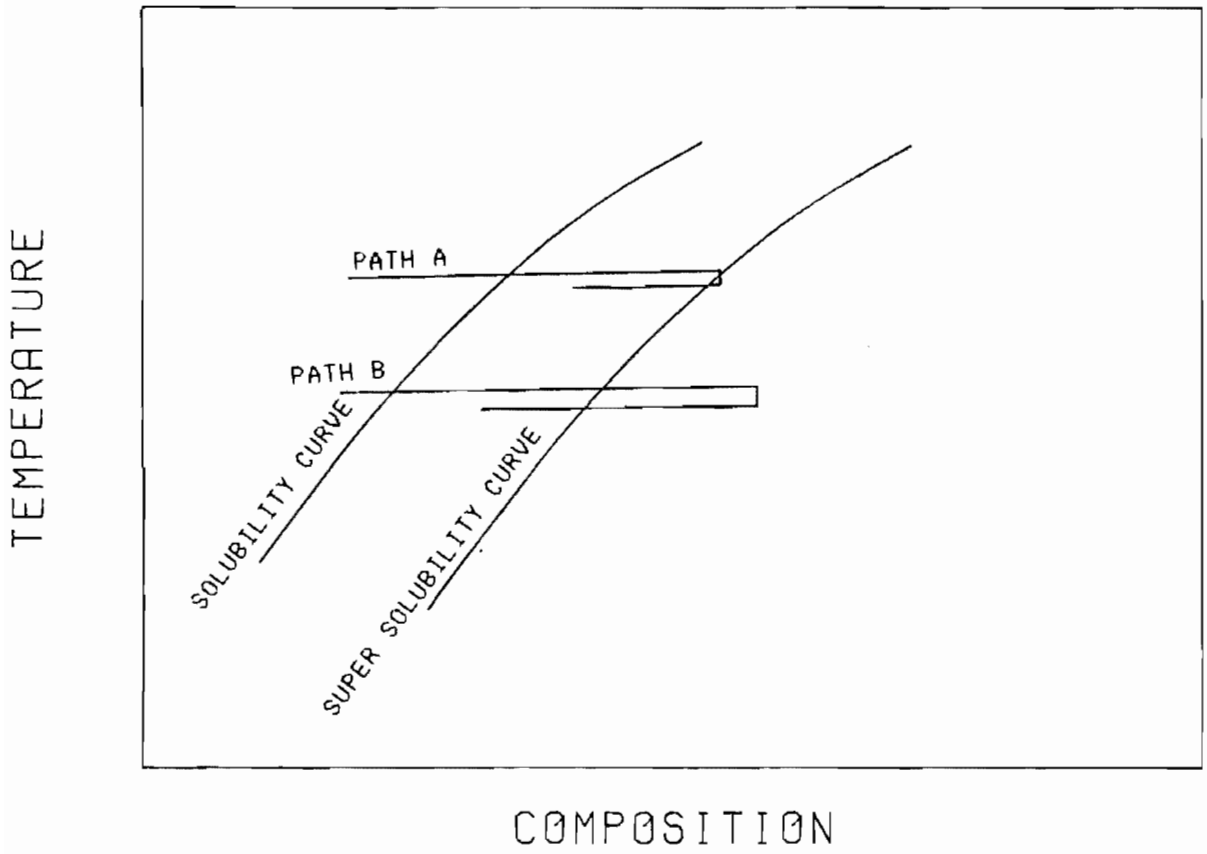

FIG 1.9 PHASE DIAGRAM

resulted in a catalyst active for the oligomerisation of olefins. In view of the above discussion, however, it seems likely that the synthesis procedure developed by Higley (1984) resulted in a catalyst with high dispersion but nonuniform distribution. Using a homogeneous system, with the slow hydrolysis of urea as a source of hydroxyl ions as developed by van Dillen et al (1976) for the preparation of nickel silica catalysts, the catalyst produced would have a high dispersion and a uniform distribution of the metal crystallites throughout the support.

1.3.4 Co-precipitation

This method for preparing supported metal catalysts is usually associated with nickel silica catalysts. The technique involves mixing of the constituents on an atomic level under condition favouring precipitation. The resulting catalyst is one where small crystals are uniformly distributed throughout the catalyst matrix. Subsequently this type of catalysts can be made with nickel contents up to 20 wt% without affecting crystal size or distribution.

1.4 Physical characteristics of the catalyst

The properties which characterise a catalyst are shown in Table 1.2 and discussed below.

Table 1.2 : Characterisation of supported metal catalysts

Support properties	Metal dispersion and location	Nature of active component
Total area	Total surface area	Metal support interaction, e.g., oxidation state
Pore structure	Metal surface area	
Surface chemical properties, e.g., surface acidity	Crystal size distribution	
	Crystal size and location	

1.4.1 Properties of silica alumina

1.4.1.1 Surface area

The surface area of silica alumina is not only a function of the alumina content but also of the synthesis procedure used. In the case of co-precipitation used by Holm et al (1959), the surface areas for the entire range from pure alumina to pure silica were consistently higher than that established by Ward and Hansford (1969) for an impregnated catalyst. The results obtained by both Ward and Hansford (1969) and Holm et al (1959) are shown in Figure 1.10, as are the results for the commercial catalyst used by Ward and Hansford (1969).

1.4.1.2 Pore structure

Ramser and Hill (1958) studied the pore diameter distribution of a commercial silica alumina catalyst using nitrogen isotherms. The results obtained by them are shown in Table 1.3. No data was, however, available as to the silica to alumina ratio of the catalyst used by them.

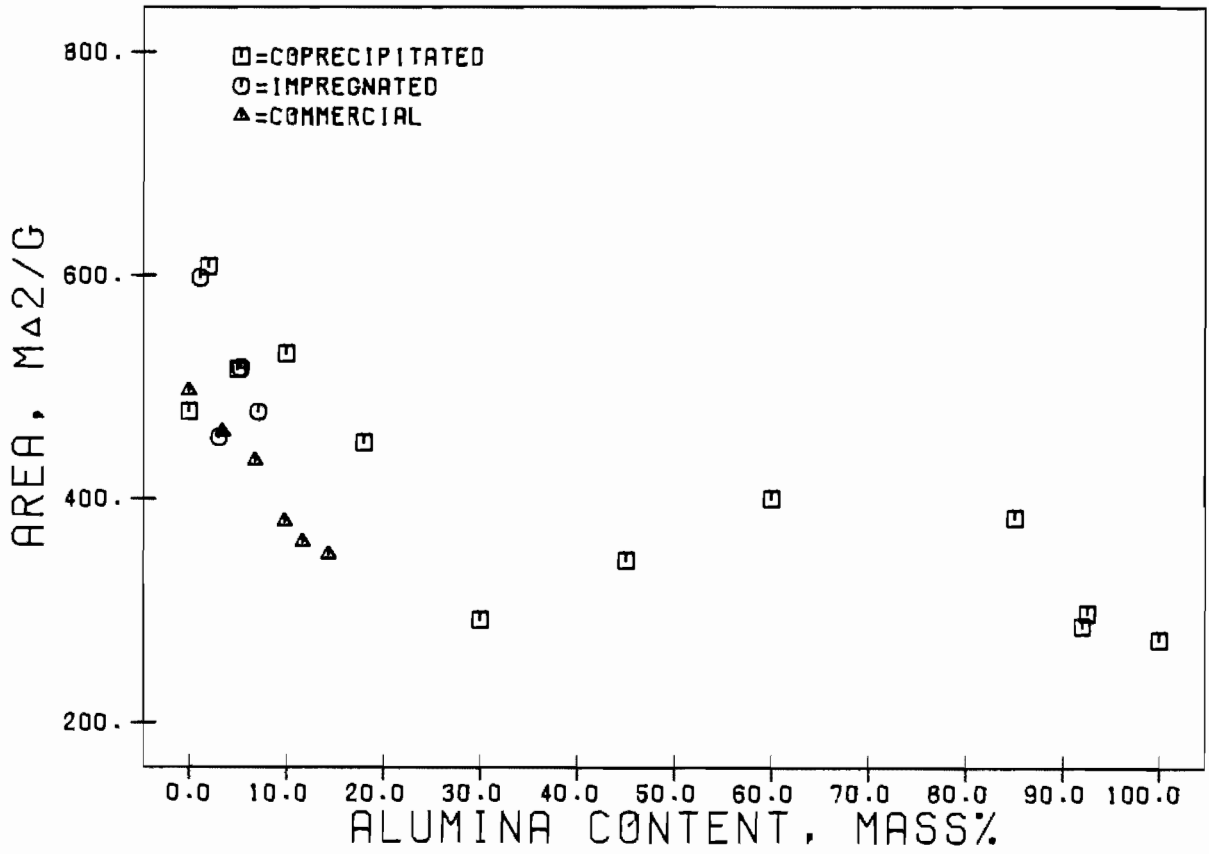

FIG 1.10 SILICA ALUMINA SURFACE AREA (MΔ2/G) VS ALUMINA CONTENT (MASS%)

Table 1.3 : Pore volume and size distribution of fresh catalyst and adsorbents (Ramser and Hill, 1958)

Catalyst code	Surface area (m^2/g)	Pore volume (cm^3/g)	Average pore radius (A)
Commercial	542.1	0.585	15.7 ± 9.6
Silica	500.2	0.608	17.7 ± 10.8
Alumina	462.0	0.619	17.9 ± 12.6
Alumina	166.6	1.142	30.1 ± 56.8
Silica	771.2	0.426	10.5 ± 4.3

1.4.1.3 Surface acidity

Holm et al (1959), using a butylamine titration technique as proposed by Tamele (1947), determined the total acid content of a co-precipitated silica alumina catalyst. They also determined the Bronsted acid content of the catalyst using a base exchange reaction via ammonium acetate. In this way the Lewis acid content of the support could be established. The results obtained, for the entire range from pure silica to pure alumina, are shown in Table 1.4.

Table 1.4 : Acid content (total and Bronsed) for silica alumina heat treated at 550°C

Alumina content (wt%)	Protonic acid content (meq/g)	Total acid content (meq/g)		Acid strength index (K)
100	0.00	0.14		-
92.5	0.06	0.43		-
92	0.04	0.41		-
85	0.07	0.39		$2.3*10^{-7}$
60	0.19	0.42		$4.7*10^{-6}$
45	0.34	0.46		$1.1*10^{-5}$
30	0.45	0.40		$3.9*10^{-5}$
18	0.80	0.40		$6.1*10^{-5}$
10	0.77	0.40		$1.4*10^{-4}$
5	0.61	0.31		$2.4*10^{-4}$
2	0.38	-		$2.5*10^{-4}$
0	0.13	0.03	approx.	$1.1*10^{-3}$

1.4.2 Properties of nickel oxide on silica alumina

1.4.2.1 Total surface area

The total surface area of nickel oxide on silica alumina was examined by Holm et al (1957) for an impregnated and a co-precipitated catalyst. The silica to alumina weight ratio was held constant at 9 to 1 throughout. The results obtained, as a function of nickel loading, are given in Table 1.5. Ushida and Imai (1962), using a co-precipitated nickel oxide silica alumina catalyst, with the nickel content fixed at 4 wt% but varying the alumina content from 0 to 46 wt%, also measured the surface

area of the catalyst. Their results of surface area as a function of alumina content are shown in Table 1.6. In an independent study, Imai and Ushida (1965) measured the surface area of a nickel oxide on silica alumina catalyst with a fixed alumina content of 4.3 wt% varying nickel content. These results are shown in Table 1.7.

Table 1.5 : Surface area of nickel oxide silica alumina prepared by impregnation and coprecipitation, as a function of nickel content; the silica to alumina weight ratio of 9:1

Synthesis technique	Nickel content (wt%)	Surface area (m^2/g)
Impregnated	0.85	300
	1.71	300
	3.15	300
	10.80	253
Coprecipitated	0.73	373
	2.54	374
	4.48	388
	8.30	248
	17.26	259
	37.82	302
	60.26	219

1.4.2.2 Metal surface area and crystal size

The metal surface area of an impregnated nickel oxide on synthetic zeolite was examined by Brooks and Christopher (1968) using hydrogen chemisoption and the average nickel crystallite size using X-ray diffraction line-broadening. They found that the nickel areas estimated from H_2 chemisorption and from average nickel crystallite size determined by X-ray diffraction line-broadening were in good agreement. The results obtained by them for a series of supports and nickel loading are shown in Table 1.8.

Table 1.6 : Surface area of nickel oxide silica alumina as a function of the alumina content. Nickel content held constant at 6.1 wt%.

Alumina content (wt%)	Surface area (m^2/g)
0.0	275
2.8	338
5.1	360
9.6	281
29.2	138
49.0	181

Table 1.7 : Surface area of nickel oxide silica alumina as a function of nickel content. Alumina content was held at 4.3 wt%.

Nickel content (wt%)	Surface area (m^2/g)
0.0	283
2.51	344
4.98	355
7.44	368
9.87	344

1.4.2.3 Pore volume and size distribution

The pore volume and average pore radius was examined by Uchida and Imai (1962) for a catalyst with a fixed nickel content but varying alumina content, and by Imai and Uchida (1965) for a catalyst with a fixed alumina content of 4.3 wt% but varying nickel content. The results obtained by them are shown in Tables 1.9 and 1.10, respectively.

Table 1.8 : Nickel metal area from H_2 chemisorption at 250°C and 100 mmHg H_2 vapour pressure, and from X-Ray diffraction line-broadening

Catalyst code	Nickel content (g·Ni/g·cat)	Total nickel area, H_2 chemisorption (m^2·Ni/g·cat.)	X-ray line broad Diameter (A)	Area (m^2·Ni/g·cat)
G56-1	0.145	4.8	155	6.0
G56-2	0.131	4.2	175	4.8
G56-3	0.071	1.9	715	0.6
NiDavZ14	0.059	2.7	185	2.0
NiZeolon	0.032	0.7	680	0.3

Table 1.9 : Pore volume and radius of a nickel alumina catalyst with varying alumina content. Nickel content held at 4 wt%.

Alumina content (wt%)	Pore volume (cm^3/g)	Average pore radius (A)
0.00	0.518	38.4
8.63	0.349	25.3
17.52	0.349	35.7
26.70	0.349	48.4
36.17	0.387	47.7
45.95	0.416	46.8

1.4.2.4 Metal support interaction

The valence of nickel oxide on silica alumina was measured by Holm et al (1957) using hydrogen reduction, as proposed by Hill and Selwood (1949). They found that no abnormalities existed with regard to the chemical valence of nickel in either the co-precipitated or impregnated catalysts. These results were confirmed by Ushida and Imai (1962) who,

however, reported that for catalysts with an alumina content higher than 8.6 wt% or lower than 2.6 wt%, the valence of nickel was slightly higher than two. The slight valence increase in the case of higher aluminum content could be explained since the larger the aluminum content the larger the amount of nickel oxide which could be combined with alumina.

Table 1.10 : Pore volume and radius of a nickel oxide silica alumina catalyst with varying nickel content. Alumina content held at 4.3 wt% throughout.

Nickel content (wt%)	Pore volume (cm^3/g)
0.00	0.37
2.51	0.40
4.98	0.38
7.44	0.40
9.87	0.36

1.5 Catalyst polymerisation properties

1.5.1 Silica alumina properties

1.5.1.1 Effect of silica to alumina ratio

The propene polymerisation activity was examined by Holm et al (1959) for a coprecipitated silica alumina catalyst with varying silica content. The catalyst was activated by drying in air at a temperature of 550°C for 16 h and the polymerisation activity determined by passing propene over the catalyst while raising the temperature from 30 to 300°C. The maximum conversion obtained for each activation temperature was considered to be indicative of the polymerisation activity. The results obtained by Holm et al (1959) showed that a catalyst with a silica to alumina weight ratio of 7 to 1 was the most active for the polymerisation of propene. Johnson (1955) examined the polymerisation activity of propene at 200°C for an impregnated silica alumina catalyst with varying silica content, and found that for a catalyst dried at 200°C the optimum silica to alumina weight ratio was 9 to 1. Tamele (1950), also working at 200°C and using a catalyst dried at 500°C, reached the same conclusion as Johnson (1955).

1.5.1.2 Effect of reaction temperatures

Silica alumina required temperatures higher than 200°C to be active for the polymerisation of propene (Takahashi et al., 1972). This was also shown by Fel'dblyum and Baranova (1971), who, working at 64°C, recorded a conversion of only 6%. The dependence of temperature for propene polymerisation over silica alumina was investigated by Takahashi et al (1972) in a flow through system at a pressure of 50 atm. The results obtained by them are shown in Table 1.11.

Table 1.11 : Propene oligomerisation on silica alumina at a constant pressure of 50 atm and varying temperature. Silica to alumina ratio used was 94 to 3 throughout.

Reaction temperature (°C)	Propene conversion (wt%)
200	12.6
250	40.7
300	64.1
350	67.9

1.5.1.3 Effect of space velocity

The relationship between the space velocity and polymerisation activity, expressed in terms of propene conversion, was examined by Takahashi et al (1972) for a catalyst with a silica to alumina weight ratio of 9 to 1 at a temperature of 200°C and a pressure of 50 atm. The results obtained show that an inverse relationship exists between space velocity and propene conversion.

1.5.1.4 Product spectrum

At the temperatures needed in the presence of silica alumina for propene polymerisation, dimerisation is a minor reaction with the main product being the propene trimer. The effect of temperature on the product spectrum at a pressure of 50 atm with a catalyst having a silica to alumina ratio of 94 to 3, as established by Takahashi et al (1972), is shown in Table 1.12 as are the results of Fel'dblyum and Baranova (1971).

Table 1.12 : Product distribution of propene oligomerised over silica alumina as a function of temperature. Reaction pressure is 50 atm.

Researcher	Fel'dblyum and Baranova (1971)	Takahashi et al (1972)			
Silica to alumina ratio	9:1	94:3			
Reaction temperature (°C)	64	200	250	300	350
Propene conversion (wt%)	6	12.6	40.7	64.1	67.9
Product spectrum					
Dimer (C_6)	15	8.8	15.9	23.3	28.5
Trimer (C_9)	75.6	43.8	36.2	30.7	23.1
Tetramer$^+$ (C_{12+})	9.4	44.8	44.8	43.6	45.5

1.5.1.5 Effect of activation

Holm et al (1959) examined the propene polymerisation activity of a catalyst with a silica to alumina weight ratio of 9 to 1 as a function of the activation temperature. Activation was achieved by holding the catalyst at each temperature for 16 h under dry air. They found that the optimum activation temperature with regards to propene oligomerisation was 550°C.

1.5.2 Nickel oxide silica alumina properties

1.5.2.1 Effect of synthesis procedure

The two methods available for incorporating nickel onto silica alumina are impregnation and coprecipitation. The exact synthesis procedure and nature of the catalyst has been discussed previously. Holm et al (1957) examined the polymerisation activity of catalysts prepared by these

methods and concluded that for coprecipitated catalysts the maximum propene polymerisation activity was approximately 50% greater than that for catalysts prepared by impregnation.

1.5.2.2 Effect of metal content

Hogan et al (1955), using a commercial catalyst with a silica to alumina weight ratio of 9 to 1, concluded that when the metal was loaded onto the support by impregnation, the most active catalyst for the polymerisation of propene contained between 3 and 5 wt% nickel. Holm et al (1957), using a co-precipitated and impregnated nickel oxide on silica alumina catalyst, established that for both methods of loading the maximum polymerisation activity per unit volume was also obtained for a catalyst holding between 3 and 5 wt% nickel. Takahashi et al (1969), using a commercial silica alumina with an alumina content of 13 wt%, showed that for an impregnated catalyst a nickel content of 13 wt% was optimum for the conversion of propene. To maximize the yield of propene dimer, however, the optimal nickel content was found to be 9.7 wt%. When a co-precipitated, as opposed to impregnated, catalyst was used, Takahasi et al (1969) found that a nickel content between 3 and 5 wt% gave the optimum results for propene dimerisation.

1.5.2.3 Effect of reaction temperature and pressure

Hogan et al (1955) showed that when the reaction temperature was varied from 35 to 130°C, the rate of reaction was highest in the range of 70°C to 93°C, with a sharp decline in conversion when the pseudo-critical temperature of 96°C of the feed was exceeded and the system was essentially in the vapour phase. They concluded that the optimum reaction conditions for the dimerisation of propene were a temperature of 70°C and a pressure of 40 atm. Takahashi et al (1969) also examined the effect of temperature and pressure with respect to propene conversion and dimer yield, and concluded that as long as the system remained in the liquid phase, the formation of dimers dominated with a shift to heavier products as soon as the system moved into the vapour phase. The optimum conditions for the dimerisation of propene according to Takahasi et al (1969) were a temperature of 70 to 80°C with the pressure ranging from 30 to 35 atm. The above conclusions can easily be represented graphically as shown in Figure 1.11.

1.5.2.4 Effect of feed composition and space velocity

Takahasi et al (1972) found that when pure propene was fed the surface temperature of the catalysts rose far above the set reaction temperature. Consequently, although the system was essentially in the

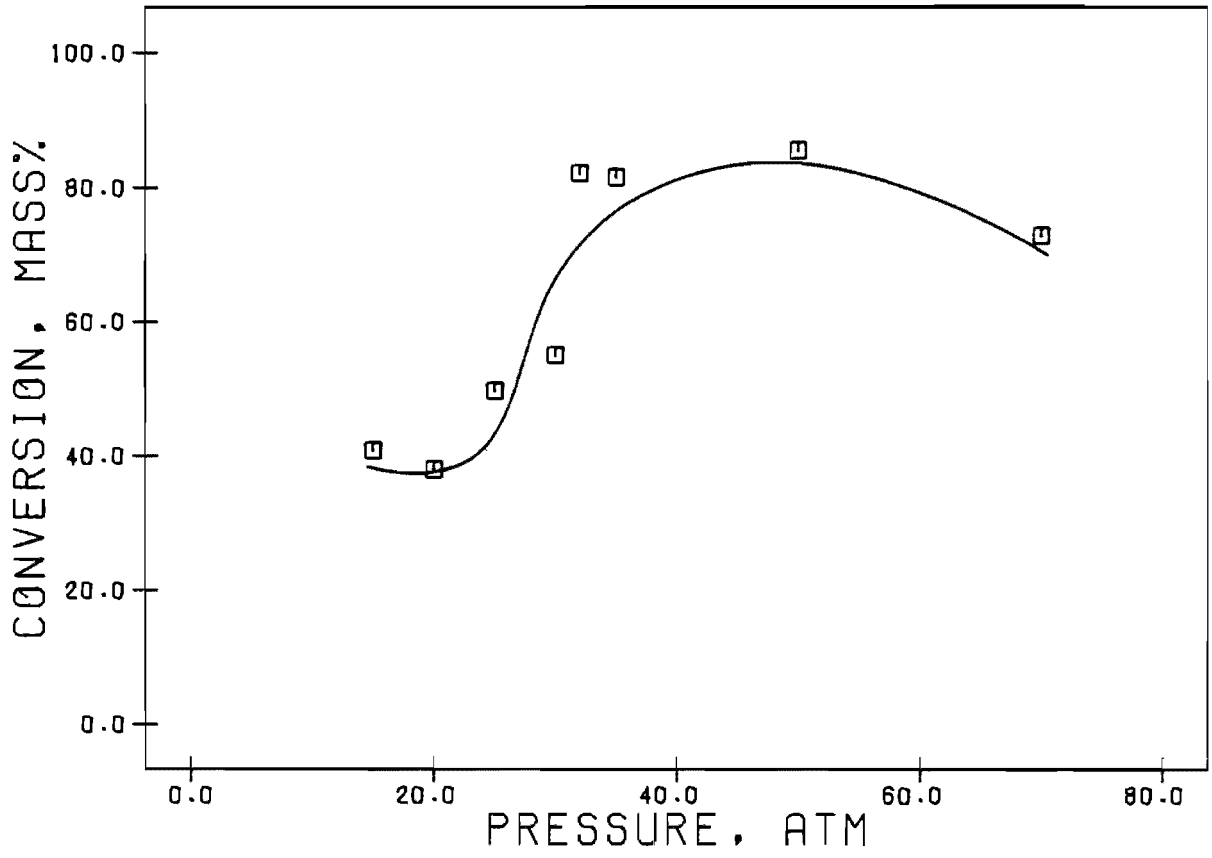

FIG 1.11 PROPENE CONVERSION (MASS%) VS PRESSURE (ATM)

liquid phase, a vapour phase reaction was taking place at the surface of the catalyst, with a corresponding shift to heavier products, and rapid deactivation of the catalyst. It was therefore necessary to use a mixture of propene and an inert diluent such as propane which served as a heat sink and so controlled the catalyst surface temperature. Hogan et al(1955) varied the propene concentration in the feed from 7 to 37 vol% at space velocities of 2, 4 and 8 and concluded that the rate of polymer production increased linearly with propene concentration. A first order relationship between propene concentration and rate of polymer formation was obtained. Hogan et al (1955) did not indicate how dimer selectivity was affected as a function of feed composition. Takahashi et al (1969), using a 2.17 to 1 mixture of propene to propane, with trace impurities of ethane, ethene and butenes, concluded that the optimum space velocity for the production of a propene dimer, at the conditions of temperature and pressure discussed earlier, was 750 g of propene per liter of catalyst per hour.

1.5.2.5 Effect of feed impurities

Hogan et al (1955) stated that the catalyst became deactivated if allowed to absorb as little as 0.5 wt% moisture. This type of contamination was, however, totally reversible. Other impurities, such

as acetelyne and carbon monoxide, acted as severe poisons to nickel oxide silica alumina while oxygen sulphur compounds and butadienes had only a moderate poisoning effect. The poisoning effect of these materials was apparently not reversible as the catalyst did not regenerate to any extent after removal of the contaminant from the feed. Takahashi (1969), on the other hand, stated that the Scientific Design Company had shown that by introducing water or alcohol with the feed, the conversion of propene could be doubled without affecting dimerisation activity.

1.5.2.6 Effect of activation procedure

The activation time, temperature and gas flow rates were examined by Takahashi et al (1969) with respect to acidity, structure and propene dimerisation activity of the catalyst. They found, when using 200 ml of catalyst, that a space velocity of 100 h^{-1} of dry air at a temperature between 500 and 600°C was optimal, and that the activity of the catalysts increased with increasing activation time up to 5 h above which the activity did not change. Three distinct temperature regions were identified by Takahashi et al (1969): between 300 and 500°C physisorbed water was removed, between 500 and 600°C the concentration of protonic sites was highest and above 600°C Lewis sites were formed which could not be hydrated back to Bronsted sites.

1.5.2.7 Effect of regeneration

The polymerisation activity of the nickel oxide silica alumina catalysts declined at a rate determined largely by the amount and type of impurities in the feed, and eventually regeneration was required (Hogan et al., 1955). The regeneration procedure was to strip the catalyst free of hydrocarbon vapours and preheat it to a combustion temperature (about 400°C) with dry inert gas. The small amount of residual deposits were then burnt off in dry air at 500°C and the catalyst cooled under dry air (Hogan et al., 1955). After repeated regeneration the nickel oxide promotor underwent changes which caused the activity to decline. The catalyst could, however, be restored to its initial activity by wetting with a nitric acid solution followed by a normal activation.

1.5.2.8 Product spectrum

Takahasi et al (1969) together with Hogan et al (1955) found that the reaction conditions had a large influence on dimer composition. The results obtained by Takahashi et al (1969) at various reaction conditions are shown in Table 1.13. The products obtained by Hogan et al (1955) for once through propene conversion using a catalyst with 4 wt%

nickel at 75°C and 40 atm and the results of Fel'dblyum and Baranova (1971), using a temperature of 64°C and a pressure of 50 atm and a catalyst containing 4.5 wt% nickel, are also shown in Table 1.13. Hogan et al (1955) working with fixed feed composition and reaction conditions studied the effect of varying the space velocity on the product spectrum. The results obtained by Hogan et al (1955) are shown in Table 1.14.

1.5.2.9 Lifetime

Hogan et al (1955) examined the lifetime of an impregnated nickel oxide silica alumina catalyst using a cracked gas, containing 25 mol% ethene, 10 mol% propene and 12 mol% butenes with butane as liquid diluent. A 100 h run was done by Hogan et al (1955) and data was obtained on conversion and on the properties of the products in butene-butane recycle operation. The reaction conditions used were a temperature of 65 to 75°C and a pressure of 34 atm with feed rates of 600 standard volumes of cracked gas and 4 liquid volumes of butane-butenes per hour per volume of catalyst. The catalyst used contained 4 wt% nickel with a silica to alumina weight ratio of 9 to 1. Hogan et al (1955) showed that the activity of the catalyst with respect to total olefin conversion after 100 h on stream dropped from 99 to 96%. The average rate of polymer production was 350 g/h/l·cat. The polymer composition by volume was 13% pentenes, 26% hexenes, 20% heptenes and 41% octenes through decenes.

In an indepndent study Allum (1974) prepared a nickel oxide silica alumina catalyst by first impregnating silica gel with aluminium and then with nickel. The final catalyst contained 1.45 wt% aluminium, 0.36 wt% sodium and 0.7 wt% nickel. The catalyst, which was activated for 4 h at 550°C under dry nitrogen, was used to oligomerise 1-butene in daily batches at 80°C and 54 atm in a 3 l rocking autoclave for 24 consecutive days. The activity of the catalyst decreased from 0.20 grams of product per gram of catalyst per hour (1st day) to 0.14 grams of product per gram of catalyst per hour (24th day). Of the liquid oligomers 65 wt% were octenes on the first day which rose to 85 wt% octenes on the 24th day.

1.6 Conclusion

As can be seen from the above discussion, nickel oxide on silica alumina catalysts prepared by impregnation and coprecipitation have been studied in great detail. The technique of homogeneous decomposition deposition for incorporating nickel into silica alumina is a much simpler technique than coprecipitation, and it is hoped that the catalytic properties with

respect to lifetime, selectivity and activity are comparable to, if not better than, the properties of coprecipitated or impregnated nickel oxide silica alumina catalysts.

Table 1.13 : Relationship between product distribution and reaction conditions.

a) Takahashi et al (1969); silica to alumina weight ratio of 87 to 13; nickel content 13 wt%.
b) Hogan et al (1955); silica to alumina weight ratio of 9 to 1; nickel content 4 wt%.
c) Fel'dblyum and Baranova (1971); silica to alumina weight ratio of 9 to 1; nickel content 4.5 wt%.
d) Distillation cut off temperature

Temperature (°C)	Pressure (atm)	C_6 ≈100°C[d]	C_9 ≈155°C[d]	C_{12} ≈185°C[d]	C_{12+} ≈185°C+[d]
[a] 65	35	47.8	33.5	9.7	2.2
80	35	46.5	38.0	9.5	1.8
90-95	35	38.0	34.0	19.0	2.4
120	35	23.0	38.0	26.0	9.8
75	15	18.5	21.0	39.5	13.7
75	20	24.6	25.0	35.0	9.0
75	25	30.5	28.0	30.0	3.6
75	30	40.1	31.0	15.0	6.6
75	32	52.0	27.0	14.0	2.8
80	35	46.5	35.0	9.5	1.8
75-80	50	43.0	34.0	13.5	3.0
75	70	43.5	25.0	22.0	2.5
[b] 75	40	72.0	19.0	6.0	3.0
[c] 64	40	77.2	20.2	2.6	-

Table 1.14 : Propene conversion and product spectrum as a function of space velocity; silica to alumina ratio is 9 to 1 throughout

Conversion (wt%)	Space velocity	C_6	C_9	C_{12}	C_{15}^+
53	2	77.7	16.0	6.1	2.4
68	4	73.7	20.0	7.0	3.2
83	8	65.6	21.0	8.8	6.4

1.7 OBJECTIVE OF RESEARCH

The aim of this study was to investigate the propene oligomerisation properties of $NiO/SiO_2-Al_2O_3$ catalysts, synthesised using three different techniques, impregnation, co-precipitation and homogeneous decomposition deposition. The effect of the following factors on the activity, selectivity and lifetime of these catalysts for propene oligomerisation were investigated:

(i) Nickel content of catalysts;
(ii) Reaction pressure and temperature;
(iii) Weight hourly space velocity;
(iv) Reactor temperature stability; and
(v) Propene feed moisture content.

2. DESIGN OF ISOTHERMAL REACTOR

2.1 Introduction

In order to facilitate interpretation of reactor data, it was important that the reactor used in this study was as isothermal as possible. Various attempts have been made to achieve this. Hogan et al (1955) surrounded the reactor with an electrically heated jacket containing a liquid which was boiled at a temperature fixed by the pressure of an inert gas applied to the top of the reflux condenser. Imai (1968), on the other hand, inserted the reactor into a heated bed of iron powder. In the case of the present work a similar system was used to achieve isothermal conditions. A detailed description of the design of this reactor will now be given.

2.2 Fluidisation theory

If a fluid passes upward through a bed of solids at a low velocity, the pressure drop across the bed is the same as that for a downward flow. As the fluid velocity increases the particles become rearranged so that they offer less resistance to the flow and the bed starts to expand. This process continues as the velocity is increased, with the total frictional force remaining equal to the weight of the particles, until the bed has assumed the lowest stable form of packing. If the velocity is then increased further, the individual particles separate from one another and become freely supported in the fluid. At this stage the bed is said to be fluidised. Further increases in fluid velocity cause the particles to separate still further from one another and pressure differences remain approximately equal to the weight per unit area of the bed. The above phenomenon can be represented graphically if the pressure drop across the bed is plotted against fluid velocity through the bed using logarithmic co-ordinates.

Thus in Figure 2.1, (Coulson and Richardson, 1980) a linear relation is obtained on a log log scale up to the point where bed expansion takes place (A). The slope of the curve then gradually diminishes as the bed expands. As the velocity is increased, the pressure drop passes through a maximum value (B) and finally falls slightly before attaining an approximate constant value independent of fluid velocity (CD). The section (CD) of the curve is an indication of the quality of fluidisation, for if the pressure drop is constant as the fluid velocity

increases, channeling is absent. Point (B), which lies above (CD), identifies the point where the frictional forces between the particles is being overcome prior to rearrangement. The point of minimum fluidisation velocity, i.e., the fluidising point, is shown on this curve at (E) (Coulson and Richardson, 1980).

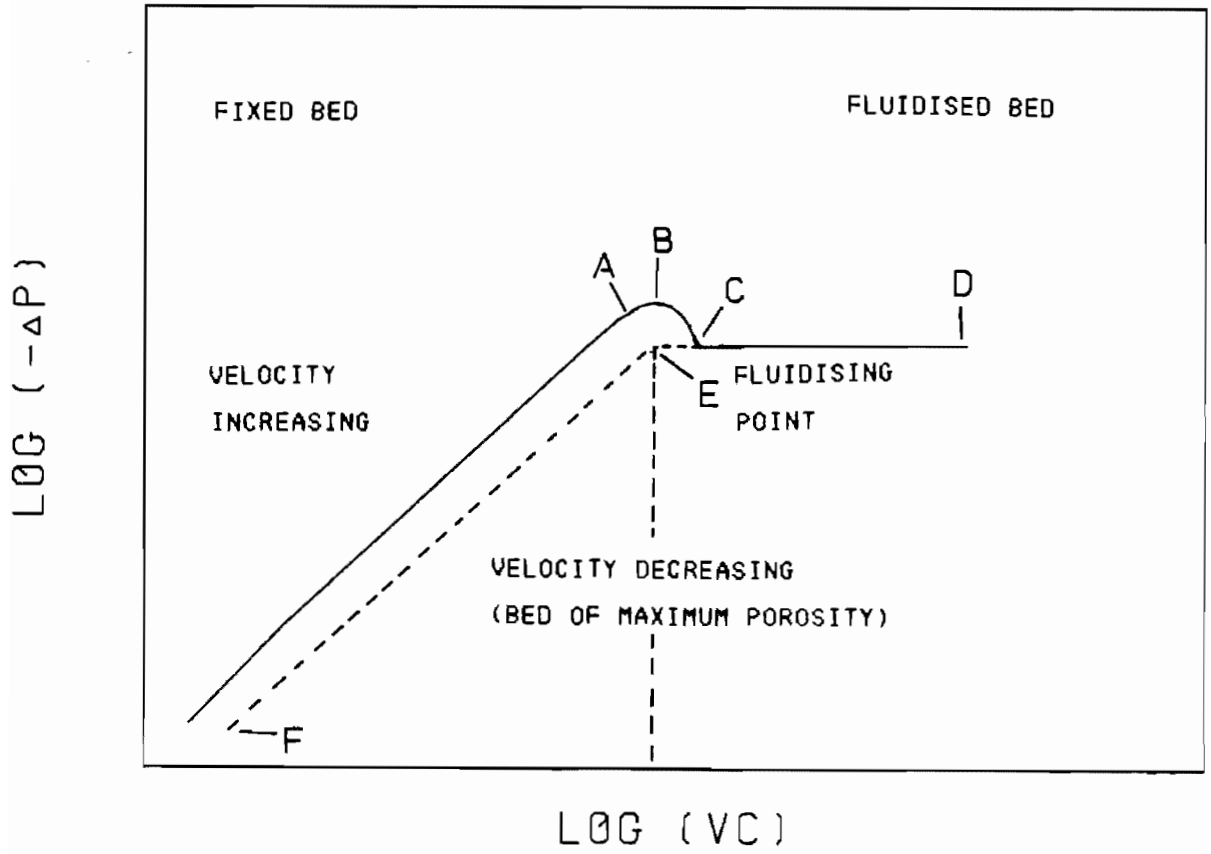

FIG 2.1 PRESSURE DROP OVER FIXED AND FLUIDISED BEDS

2.3 Heat transfer

Fluidised beds have good heat transfer properties and are ideal in a system where close control of temperature is required. The intimate mixing which takes place in the bed ensures that heat transfer throughout the system is very rapid and that uniform temperatures are quickly attained.

Three mechanisms have been suggested to explain this improvement in heat transfer coefficient. An increase of up to one-hundred fold as compared with the value obtained with a gas alone at the same velocity can be attained by the presence of the solid. Coulson and Richardson (1980) stated that the particles, whose heat capacity per unit volume is many times greater than that of the gas, act as heat transferring agents. As a result of their rapid movement within the bed they pass from the bulk of the bed to the layers of gas in close contact with the heat transfer

surface, exchanging heat at this point and returning to the body of the bed. This, together with the extremely short physical contact time of the particle with the surface, ensures that the thermal conductivity of the particle is not an important factor. The second mechanism proposed by Coulson and Richardson (1980) is the erosion of the lamminar sublayer by the particles and the subsequent reduction in its effective thickness. A third mechanism suggested by Mickley and Fairbanks (1955) is that "packets" of particles move to the heat transfer surface and an unsteady heat transfer process takes place.

Many equations are available in the literature to calculate the convection heat transfer coefficient of the gas solid system. One equation which seems to be the most reliable is that of Dow and Jakob (1951). The Nusselt number with respect to the tube diameter is expressed as a function of four dimensionless groups: the ratio of tube diameter to length, ratio of tube to particle diameter, ratio of heat capacity per unit volume of the solid to that of the fluid, and finally the tube Reynolds number. These relations are combined as shown below,

$$\frac{h \cdot d_t}{k} = 0.55\left(\frac{d_t}{l}\right)^{0.65}\left(\frac{d_t}{d}\right)^{0.17}\left(\frac{(1-\epsilon)\cdot p_s \cdot c_s}{\epsilon \cdot p \cdot c_p}\right)^{0.25}\left(\frac{u_c \cdot d_t \cdot p}{\mu}\right)^{0.8}$$

where h is the heat transfer coefficient,
k is the thermal conductivity of the gas,
d is the particle diameter,
d_t is the tube diameter,
l is the length of the bed,
ϵ is the bed voidage,
p_s is the density of the solid,
p is the density of the gas,
c_s is the specific heat of the solid,
c_p is the specific heat of the gas,
μ is the viscosity of the gas, and
u_c is the superficial velocity based on the empty tube,

At the present stage of our knowledge the above equation seems the most reliable and will thus be used to estimate heat transfer coefficients and optimum particle diameter.

2.4 Fluidising medium

Various materials were investigated. It was assumed that each material had a discreet size fraction. As a high heat transfer coefficient was important if the fluidised bed was to perform its function effectively,

the equation developed by Dow and Jakob (1951) as discussed above was used to compare the various solids. Furthermore two bed temperatures were used to identify any changes in heat transfer coefficients as a function of bed temperature. The results are shown in Figures 2.2 and 2.3. It can be seen from these figures that a maximum exists at a particle size of approximately 150 μm, and that the convective heat transfer coefficient drops slightly as the bed temperature is increased.

Copper powder gave the best results, a heat transfer coefficient in excess of 1000 W/m^2 K for a particle of 150 μm. The explosive and toxic nature of metallic dust at the temperatures reached during calcination made this an undesirable solution. Sand, however, was less dependant on both the particle size and bed temperature, is totally inert and readily available. It was thus decided that sand would be used as fluidising medium.

2.4.1 Sand data

Two sands were readily available. These were coded by the manufacturer as No. 1 and No. 12. Their size distributions are shown in Table 2.1. As the actual material had a size range rather than a discreet particle size, an effective particle diameter had to be established. Using the relation suggested by Leva (1959),

$$d = 1/\Sigma(x_i/d_i)$$

where d is the effective particle size and x_i is the size fraction of particles of size d_i, the effective particle size was calculated.

The efficiency of fluidisation (Leva, 1959) of sands with wide (No. 12) as opposed to narrow (No. 2) size distributions effectively eliminated sand No 12 from further consideration.

2.5 Optimisation of the fluidised bed

As discussed in Section 2.1 a bed of solids becomes fluidised only when the superficial velocity exceeds the minimum fluidisation velocity. As it is important for the bed to be totally fluidised the minimum fluidising velocity has to be found. For this reason the system was modified as shown in Figure 2.4. An attempt was made to measure the pressure drop across the bed itself but was found not to be possible as the fluidising medium would block the tapping point at the bottom of the bed.

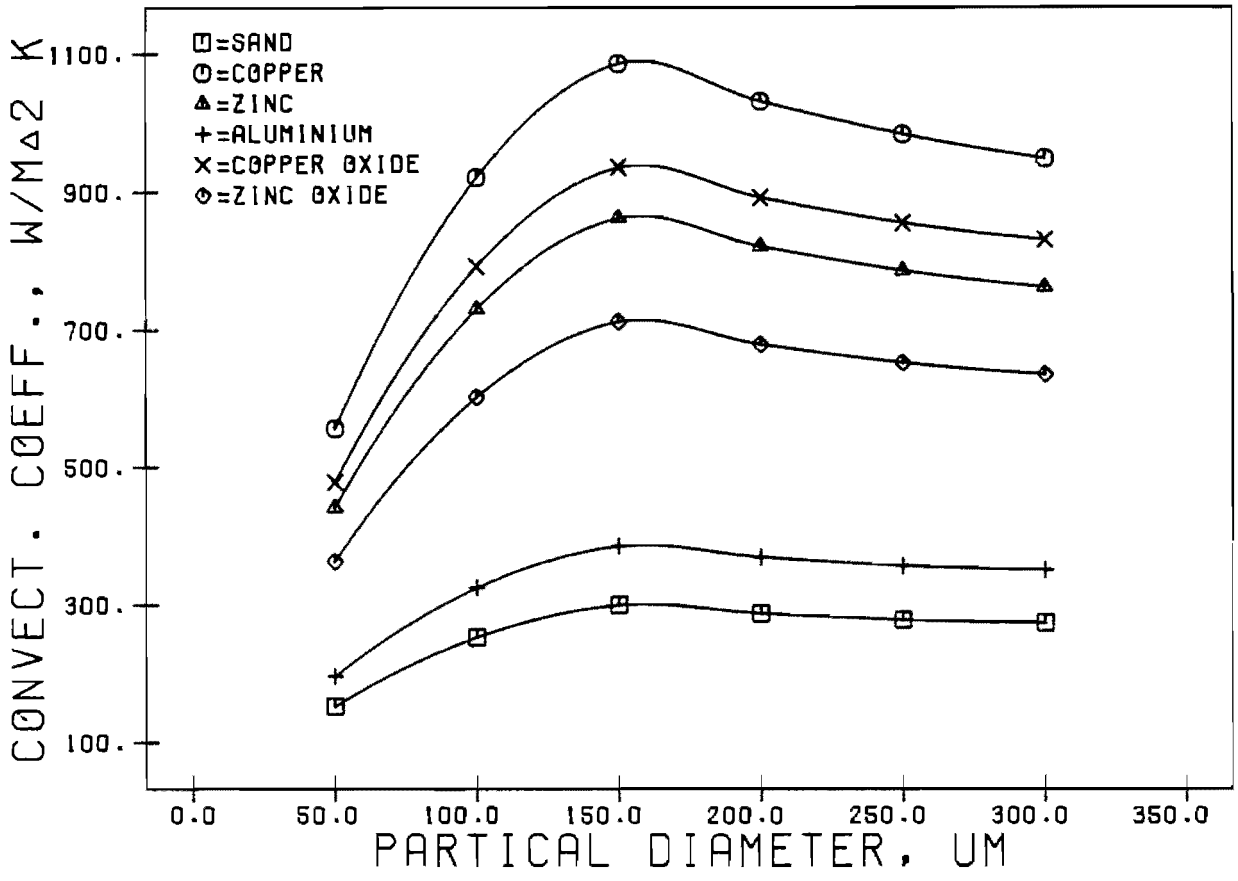

FIG 2.2 CONVECTION COEFFICIENT (W/M△2 K) VS PARTICAL SIZE (UM); 25'C

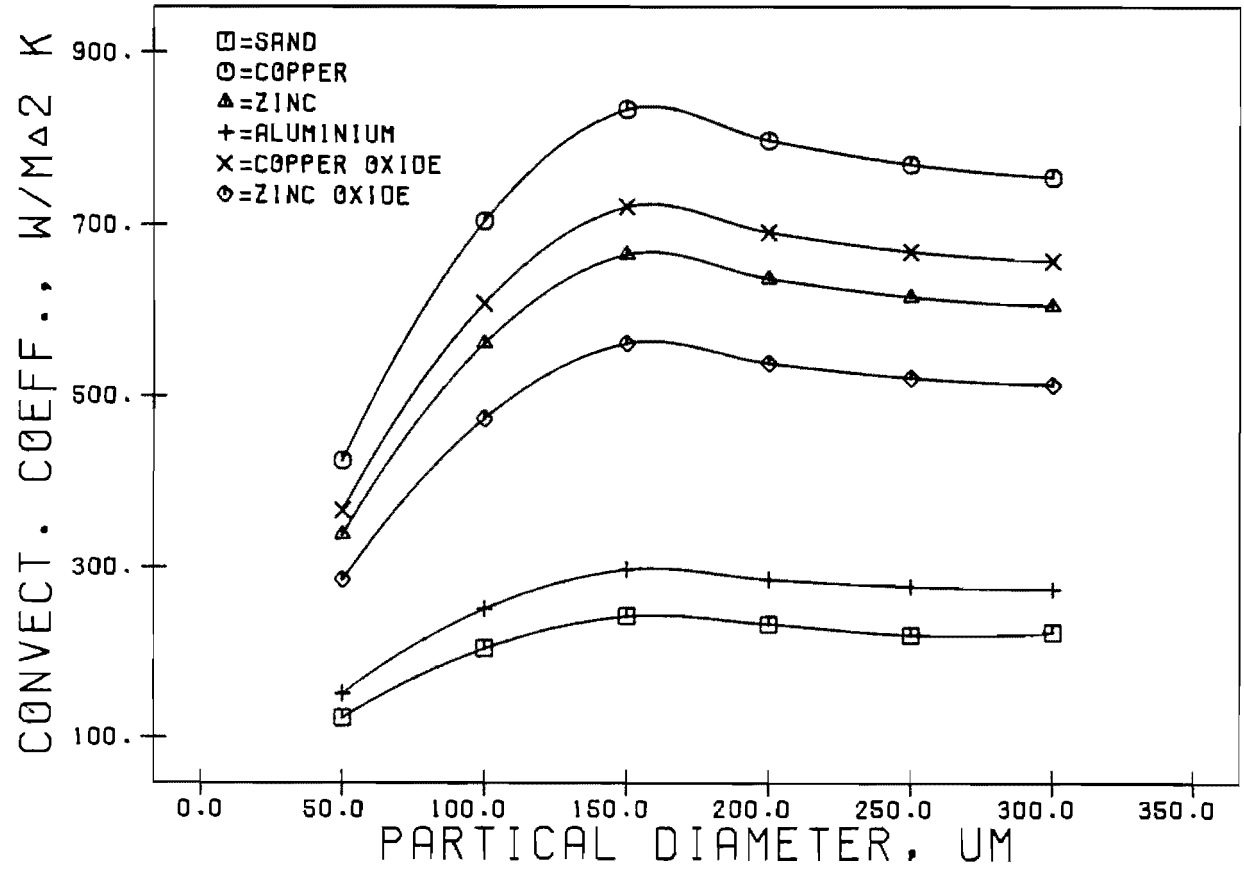

FIG 2.3 CONVECTION COEFFICIENT (W/M△2 K) VS PARTICAL SIZE (UM); 190'C

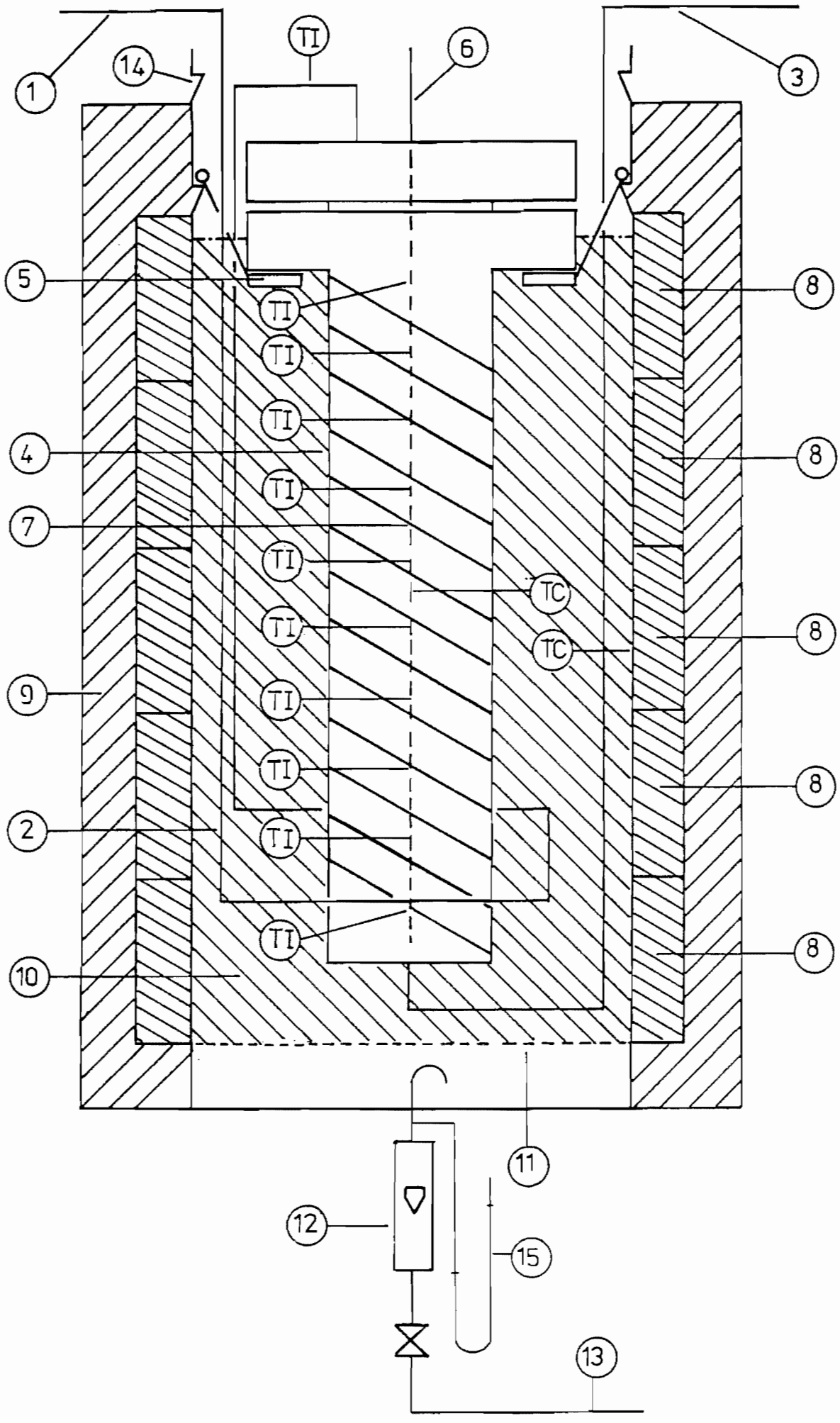

FIG 2.4 REACTOR MODIFICATIONS TO MEASURE PRESSURE DROP

Key to Figure 2.4

1 Feed inlet
2 Feed preheater
3 Product outlet
4 Integral reactor
5 Reactor support
6 Thermowell
7 Tubular embedded element (1.0 kW)
8 Mica band elements (0.5 kW)
9 Insulation
10 Fluidised sand bed
11 Gas distributor
12 Rotameter
13 Air supply
14 Disengagement zone support
15 U-tube manometer

The procedure used to determine the data to prepare a plot of pressure drop across the bed vs. the superficial velocity through the bed is discussed below.

Table 2.1 Sand size fractions

Size (μm)	No. 12 (wt%)	No. 2 (wt%)
-420	0.6	-
420-350	-	0.1
350-297	19.0	0.4
297-250	-	2.1
250-210	33.6	8.6
210-177	-	20.2
177-149	28.9	15.3
149-125	-	24.2
125-105	15.5	12.5
105-74	2.2	11.7
74 -	0.2	4.9
Mean size (μm)	166.8	124.3

2.5.1 Airflow optimisation

The calibration chart of the rotameter could be approximated using

$$V_c = 1.983 + 0.585 \cdot TR + 0.005 \cdot TR^2$$

where V_c is the volumetric flowrate in l/min at 15°C (T_c) and 760 mmHg (P_c), and TR is the rotameter tube reading. Using ideal gas behavior, this can be corrected to the actual temperature (T_r) and pressure (P_r) in the rotameter using:

$$V_r = (V_c \cdot P_c \cdot T_r)/(T_c \cdot P_r)$$

where V_r is the volumetric flowrate at rotameter temperature and pressure.

The pressure in the rotameter was that measured at the inlet to the bed and was use to calculate the actual flowrate at each tube reading. If the log of the pressure drop across the bed and ~~disk~~ was plotted against the log of the superficial velocity a straight line was obtained. The graph is shown in Figure 2.5. The shape of this curve does not correspond to that of the curve as discussed in Section 2.1. This is due to the fact that the pressure drop across the ~~disk~~ was included in the calculation.

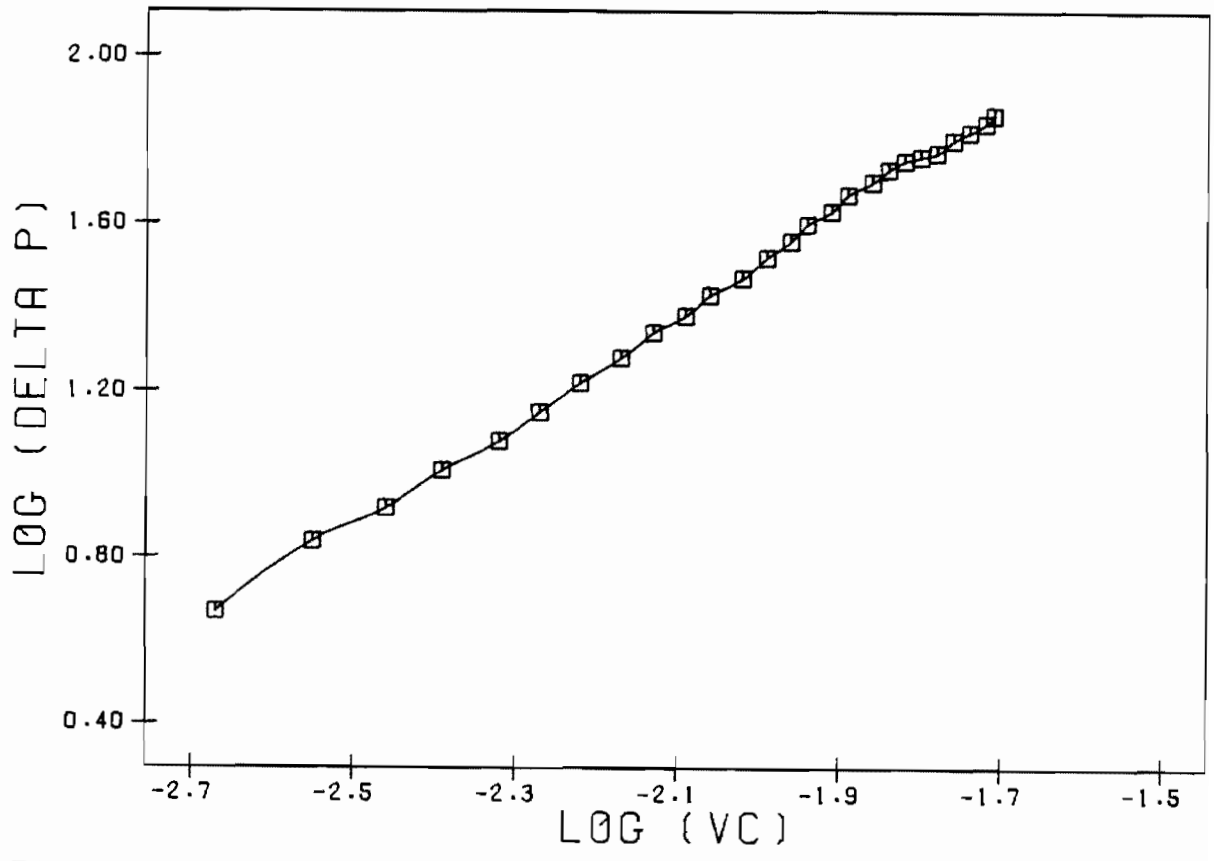

FIG 2.5 PRESSURE DROP VS SUPPERFICIAL VELOCITY ACROSS DISK AND BED

Having previously determined the pressure drop across the disk, the actual pressure in the bottom of the bed could be calculated at each rotameter tube reading using:

$$P_b = P_r - P_d$$

where P_b is the pressure in mmHg at the bottom of the bed above the disk, and P_d is the pressure in mmHg in the rotameter when no sand was in the bed.

This corrected pressure was then used to calculate the actual flowrate through the bed. The temperatures of the rotameter and bed were assumed to be identical and so

$$V_b = (P_r \cdot V_r)/P_b$$

where V_b is the air flowrate at the bottom of the bed in l/min. Using the above procedure and plotting the log of the pressure drop across the bed (P_b) against the log of the superficial velocity (V_b) a curve of the classic shape is obtained as shown in Figure 2.6 without the integral reactor and in Figure 2.7 with the integral reactor in the bed. In both cases the minimum fluidisation velocity was found to be 12.1 l/min (Point E on Figures 2.6 and 2.7) and channeling was absent (Part CD in Figures 2.6 and 2.7 is flat.)

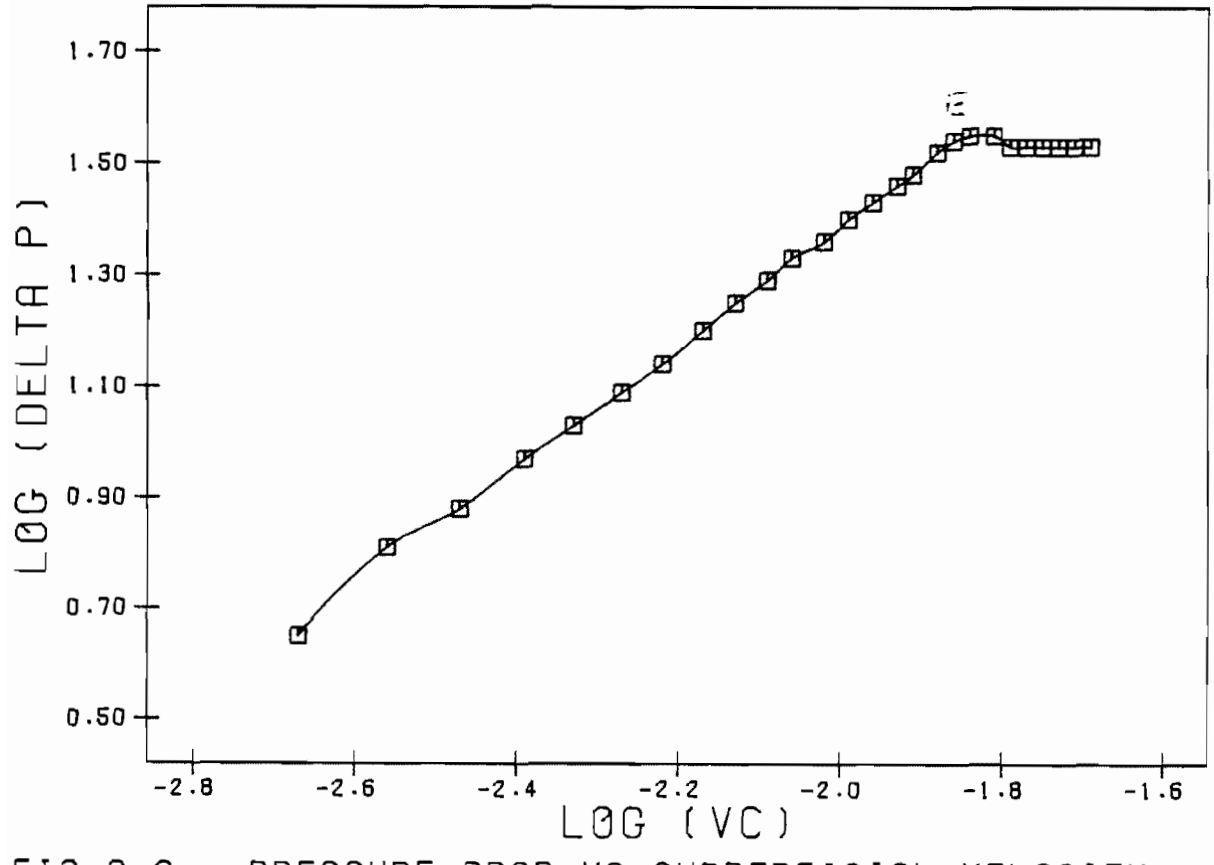

FIG 2.6 PRESSURE DROP VS SUPPERFICIAL VELOCITY INTEGRAL REACTOR ABSENT

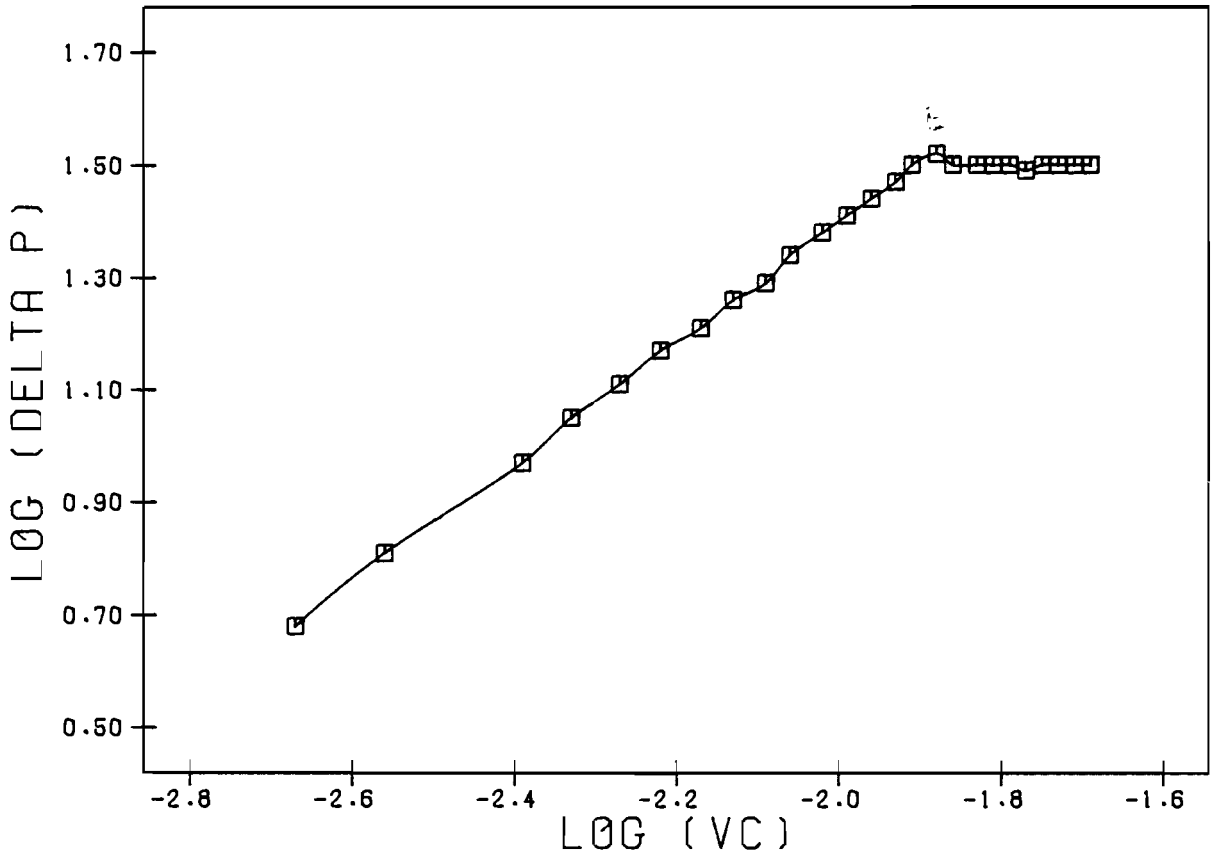

FIG 2.7 PRESSURE DROP VS SUPPERFICIAL VELOCITY; INTEGRAL REACTOR PRESENT

2.5.2 Temperature correction

As the temperature in the bed increased to reaction conditions the superficial velocity increased at a fixed rotameter setting This resulted in a change in the quality of fluidisation. It was thus desirable to develop a relationship between the bed temperature and the rotameter tube reading at the minimum fluidisation velocity. As the temperature of the gas was raised to 330°C within 2.5 mm above the distributor, as shown by Heertjie and McKibbins (1956), the only assumptions that had to be made was that the pressure drop across the bed and disk was independent of temperature and that the ideal gas law applied. Thus:

$$V_r = (P_b \cdot V_b \cdot T_r)/(T_b \cdot P_r)$$

To find the tube reading which corresponds to the air flowrate calculated above, the value had to be corrected to the rotameter calibration conditions using:

$$V_c = (V_r \cdot T_c \cdot P_r)/(P_c \cdot T_r)$$

Combining the above equation with that used to approximate the rotameter calibration chart and solving for TR we get

$$TR = -58.5 + ((3023.4 + 200 \cdot V_r)^{.5})$$

The resulting graph is shown in Figure 2.8. Using this graph it was ensured that the superficial velocity in the bed was close to the minimum fluidisation velocity at any bed temperature.

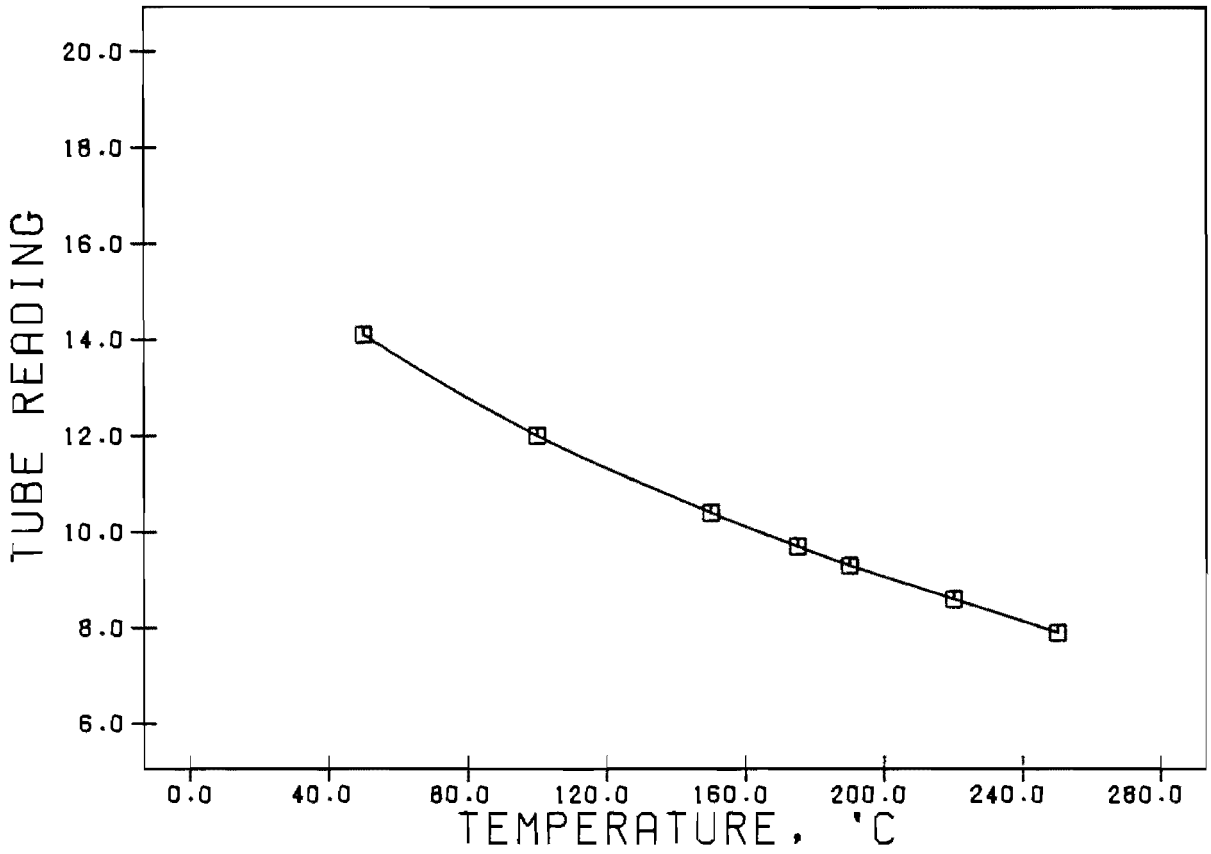

FIG 2.8 BED TEMPERATURE ('C) VS ROTAMETER SETTING; VB=12.1 L/MIN

3. EXPERIMENTAL METHODS

3.1 The reactor system

3.1.1 Layout

All experimental work was done in an integral high pressure reactor system. A diagram of this system is shown in Figure 3.1. The feed, a 4:1 mixture of propene/propane obtained from SASOL, was contained in a number seven Cadac cylinder mounted bottom up to ensure that only liquid emanated from it. Water and entrained impurities were removed from the feed by passing it through a bed of Union Carbide 3 A molecular sieves and through a 1 μm sintered metal filter.

The vapour pressure of the feed had to be lowered before it could be pumped by the Lewa high pressure diaphragm pump. To achieve this the feed was piped through a heat exchanger held at -15°C. The pump head was also cooled to this temperature. In this way cavitation was prevented and efficient working of the pump was ensured. From the delivery side of the pump the feed was piped through a preheater, where it was heated to within 20°C of the operating temperature, to the top of the integral reactor.

The products from the reactor were piped through a heat exchanger, held at 6°C, and a 20 μm sintered metal filter to the Grove Mity Mite back pressure regulator. Here the materials were released to atmospheric pressure. The back pressure regulator had to be heated to 60°C to prevent freezing of the products due to a Joule Thomson expansion and subsequent failure of the unit. To achieve this a water bath was used, the liquid being pumped through a pipe wrapped around the outside of the unit.

The products were then piped via a heat exchanger to a double walled catchpot where gas-liquid separation occurred. To ensure total separation the liberated gas was passed through a Davies double surface condenser held at -15°C, with the condensate fed back to the catchpot.

The catchpot was periodically drained and the liquid stored for later analysis. The flue gas was then piped through a 10 l surge tank to the wet gas flow meter. Finally the flue gas was passed through a sampling loop, which could be removed from the system, and vented to the atmosphere.

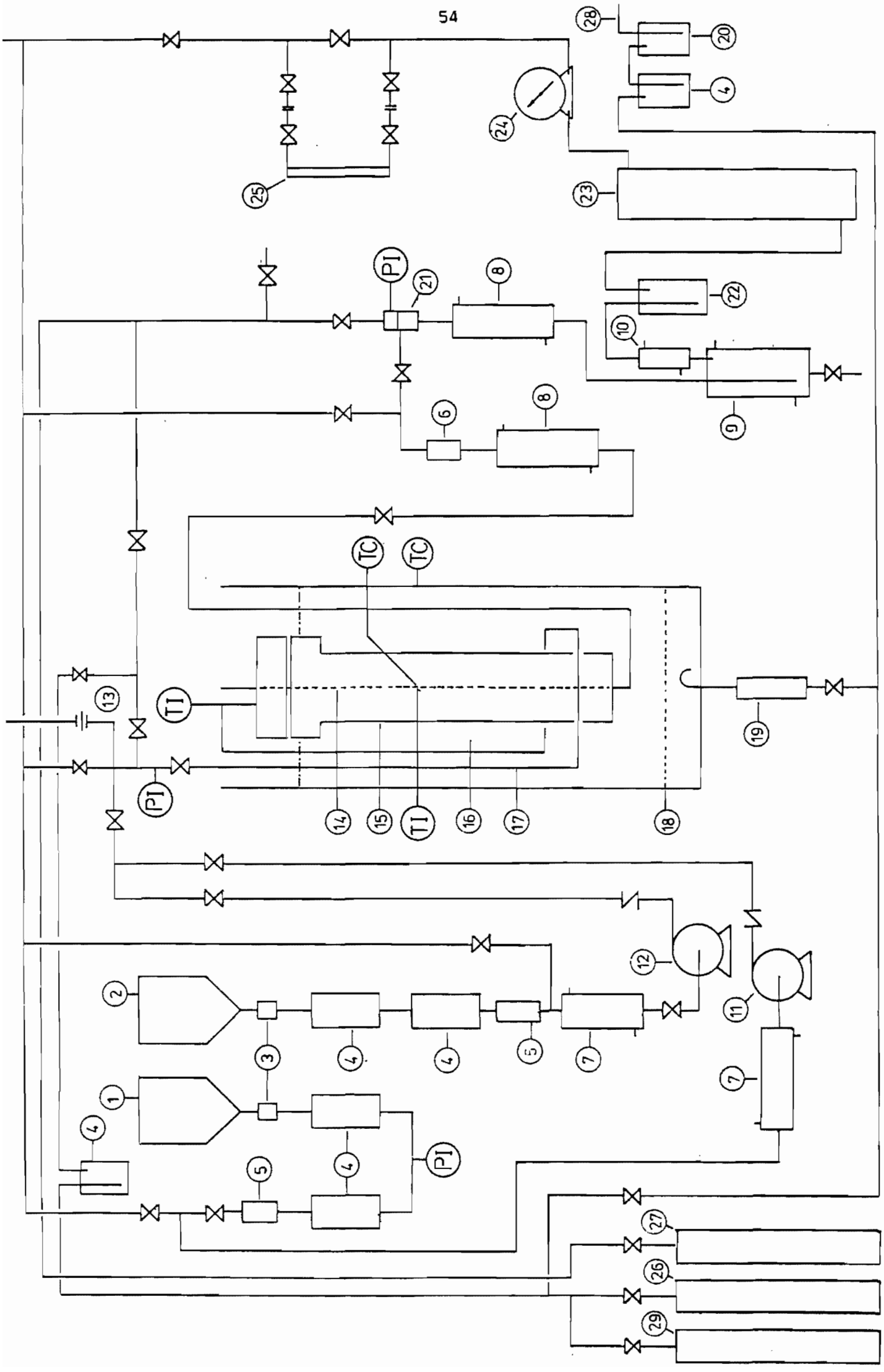

FIG 3.1 REACTOR SYSTEM

Key to Figure 3.1

1 Monomer feed cylinder
2 Dimer feed cylinder
3 Gas tight quick connector
4 3A molecular sieve holder
5 1μm sintered metal filter
6 20μm sintered metal filter
7 Glycol/ethanol cooler
8 Glycol/water cooler
9 Glycol/water cooled catchpot
10 Glycol/ethanol cooled condenser
11 Monomer pump
12 Dimer pump
13 Bursting disk (70 atm)
14 Thermowell
15 Reactor
16 Fluidised sand bed
17 Feed preheater
18 150μm sintered brass disk
19 10 mm rotameter
20 Oil condenser
21 Back pressure regulator
22 Condensation unit
23 Surge tank
24 Wet gas flow meter
25 Gas sampling loop
26 Nitrogen bottle (high purity)
27 Nitrogen bottle
28 Air supply
29 Hydrogen bottle (high purity)

A separate line was used to purge the reactor with wet or dry hydrogen, nitrogen or air depending on the pretreatment required by the catalyst. Vent lines were installed to prevent air locks in the system during start up.

The safety of the line was ensured by a bursting disk set at 70 atm and a pressure relief valve in the pump which permitted internal circulation if the delivery side pressure exceeded the set point.

Two cooling circuits were employed. An ethylene glycol/water mixture at 6°C was used to cool the catchpot and all product heat exchangers, while

an ethanol/water mixture at -10°C was used to cool the feed heat exchanger, pump head and the flue gas condenser.

3.2 Reactor

Before any statement could be made about the effects of temperature on a reaction in an integral reactor, the latter had to be as nearly isothermal as possible. Various attempts have been made to achieve isothermality, e.g. Hogan et al (1955) surrounded the reactor with an electrically heated jacket containing a liquid which was boiled at a temperature fixed by the pressure of inert gas applied to the top of the reflux condenser. Imai (1968), on the other hand, inserted the reactor into a heated fluidised bed of iron powder. In the present work the system used by Imai (1968) was adopted. Sand was however substituted for iron powder as the explosive and toxic nature of metallic dust at the temperatures reached during calcination made the latter undesirable. The final result was a reactor where the temperature in the catalyst bed could be held within 5°C of the set point. Each aspect of this design was discussed in Chapter 2, while a description of the reactor is given below. The reactor consisted of two distinct parts, the fluidised bed and the integral reactor. Both are shown in Figure 3.2

3.2.1 Fluidised Bed

The fluidised bed consisted of a rolled sheet metal chimney with a removable disengagement zone. An inverted tripod was suspended from the top of the chimney into which the reactor was hung. Air was injected into a sealed chamber at the bottom of the bed in such a way as to prevent impingement of the gas on the distributor (see Figure 3.2). The distributor used was a 150 μm sintered brass disk. Great care had to be taken to mount the gas distributor absolutely horizontally as severe channeling and corresponding loss in heat transfer efficiency would result otherwise. The air flow through the bed was controlled using a 10 mm gas rotameter with a stainless steel float.

Heat was supplied to the fluidised bed by five mica band elements strapped around the outside of the chimney. Each element was rated at 0.5 kW. The controlling thermocouple (chromel-alumel) was situated on the inside wall of the chimney half way up the bed. To prevent heat loss to the surroundings the entire unit was insulated using asbestos cloth.

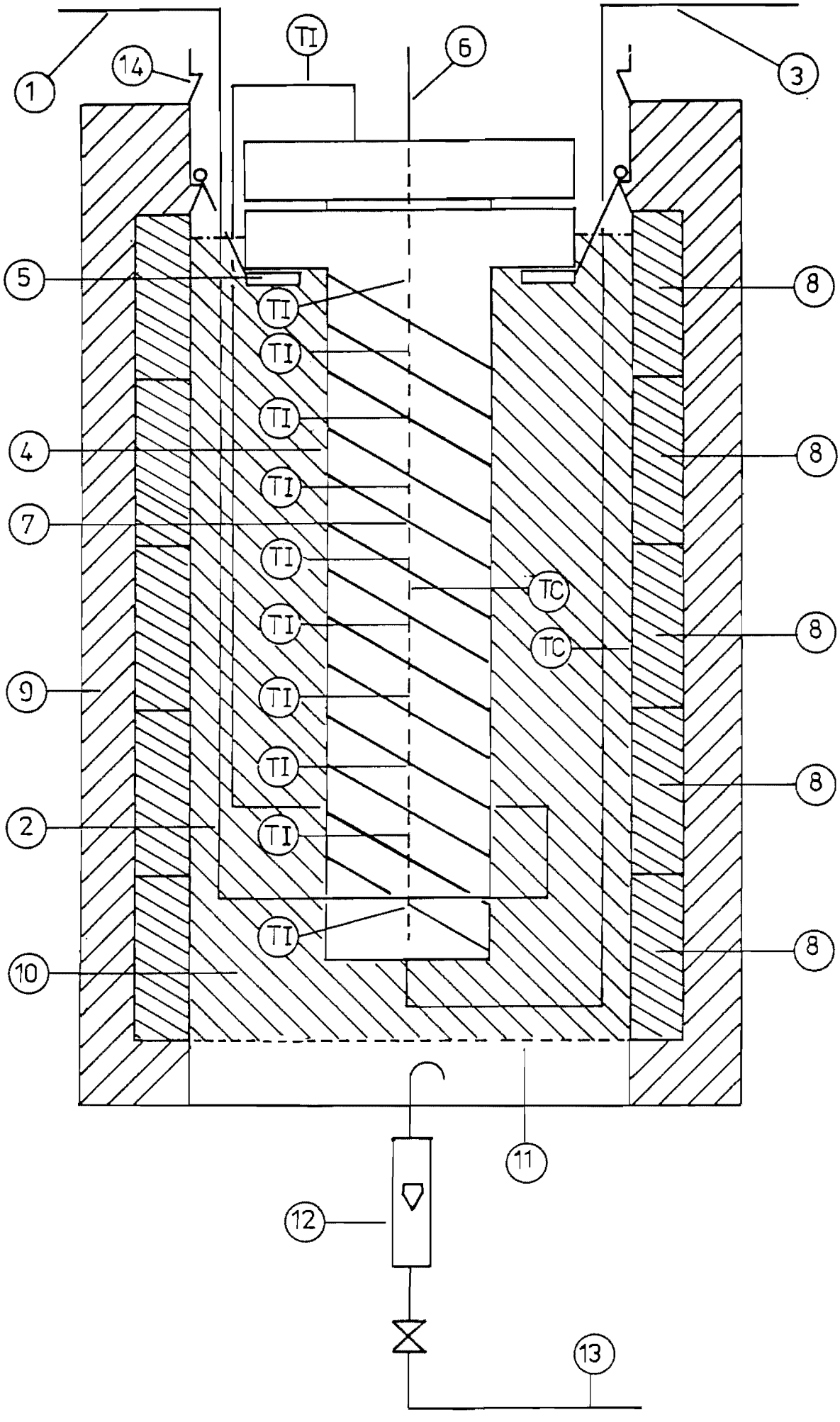

FIG 3.2 INTEGRAL REACTOR AND FLUIDISED SAND BED

Key to Figure 3.2

1 Feed inlet
2 Feed preheater
3 Product outlet
4 Integral reactor
5 Reactor support
6 Thermowell
7 Tubular embedded element (1.0 kW)
8 Mica band element
9 Insulation
10 Fluidised sand bed
11 Gas distributor
12 Rotameter
13 Air supply
14 Disengagement zone support

3.2.2 Integral Reactor

The reactor was a multi-component single seal unit with a bed diameter of 2.5 cm. Two distinct sections could be identified, cross-sections of which are shown in an exploded form in Figure 3.3.

The insert consisted of the top flange through which the thermowell and feed were passed and the catalyst bed jacket which was screwed into the bottom of this flange. The catalyst bed jacket was stoppered at its lower end by a perforated plug which prevented bed entrainment and centered the bottom end of the thermowell. Holes were drilled through the top flange to allow passage of the securing bolts. The sleeve consisted of the bottom flange to which the reactor jacket was welded, which in turn was sealed at its lower end by a concave plug through which the products were taped off. Securing bolts were anchored in the top surface of the bottom flange. Sealing was achieved by a groove in the bottom flange and a ridge in the top flange. These served as a seat for a laminated graphite nickel seal.

Separation of the units, upon completion of a run, was achieved with the aid of two 6 mm bolts. These bolts were screwed through holes in the top flange onto the top surface of the bottom flange. In this way the units could be forced apart.

Heat was supplied to the unit by a 1 kW tubular imbedded element wrapped around the outside of the reactor jacket. This element was used only

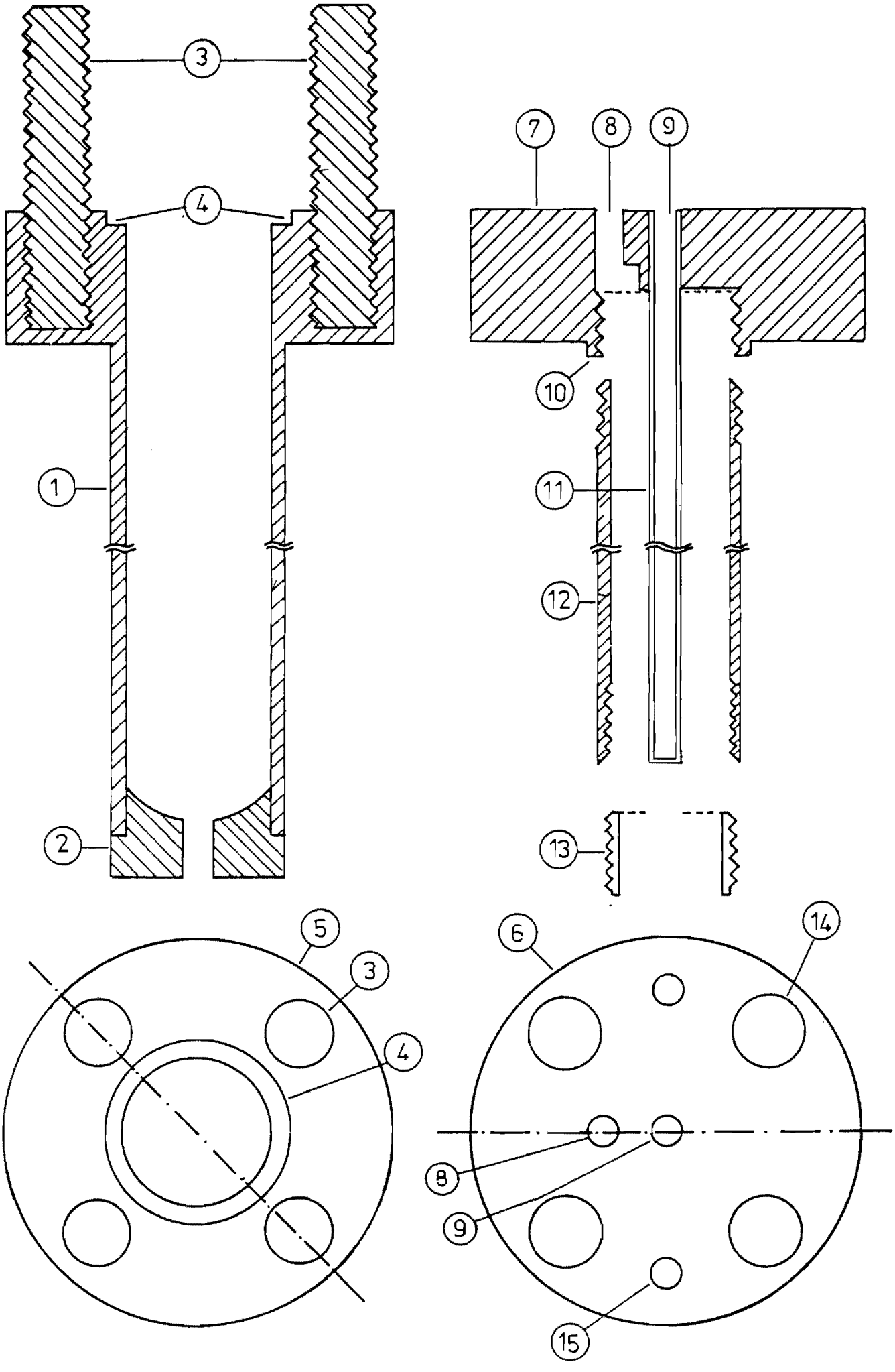

FIG 3.3 INTEGRAL REACTOR

Key to Figure 3.3

1 Reactor sleve
2 Plug
3 Sealing bolts
4 Sealing groove
5 Bottom flange
6 Top flange
7 Reactor insert
8 Feed inlet
9 Thermowell inlet
10 Sealing ridge
11 Thermowell
12 Bed seath
13 Purforated plug
14 Sealing bolt channel
15 Seperation bolt channel

during calcination. The controlling thermocouple (chromel-alumel) was placed halfway up the thermowell running down the center of the catalyst bed.

Temperatures of the reactor, fluidised bed and feed were monitored using a Digitron temperature display connected to 11 iron-constantan thermocouples. Ten of these were situated at regular intervals in the central thermowell to record the catalyst bed temperature profile and feed temperature. The fluidised bed thermocouple was mobile and could be moved throughout the bed.

3.3 Operation

3.3.1 Loading

For every run the reactor was packed in a similar way as shown in Figure 3.4. Four distinct regions were identified. These were, from the bottom up:

1 A region of void, capped with a wire mesh which prevented the catalyst and beads from blocking the reactor exit.
2 A layer of glass beads, which served as a disengagement zone and prevented catalyst entrainment.
3 The catalyst bed, which consisted of $^{1}/_{16}$ inch extrudates mixed with 2 mm glass beads in a ratio of 1:1 by volume. The beads served as a heat sink and catalyst diluent.

4 A plug of glass beads capped by a wire mesh. This ensured preheating and prevented movement of the bed during sudden pressure drops.

The depth of each layer was accurately measured to fix the number and position of the thermocouples in each region.

3.3.2 Calcination procedure

Prior to each run the catalyst was calcined. The purpose of calcination was to burn off organic intermediates incorporated in the catalyst during synthesis and to convert all the nickel nitrate to nickel oxide. At the same time the catalyst was freed of all but a trace of moisture (Hogan et al., 1955).

Calcination for all experimental work was carried out in-situ. Dry air was passed through the bed at a rate of 500 ml·gas/ml·cat·h while the temperature was stepped up in 50°C increments at intervals of 10 min. The activation was continued for an additional 4 h at 500°C.

Upon completion of this step, the activated catalyst was purged with dry nitrogen until the temperature of the bed dropped to 250°C. When this temperature was reached, the reactor was sealed at a pressure of 10 atm under dry nitrogen before being allowed to cool to room temperature.

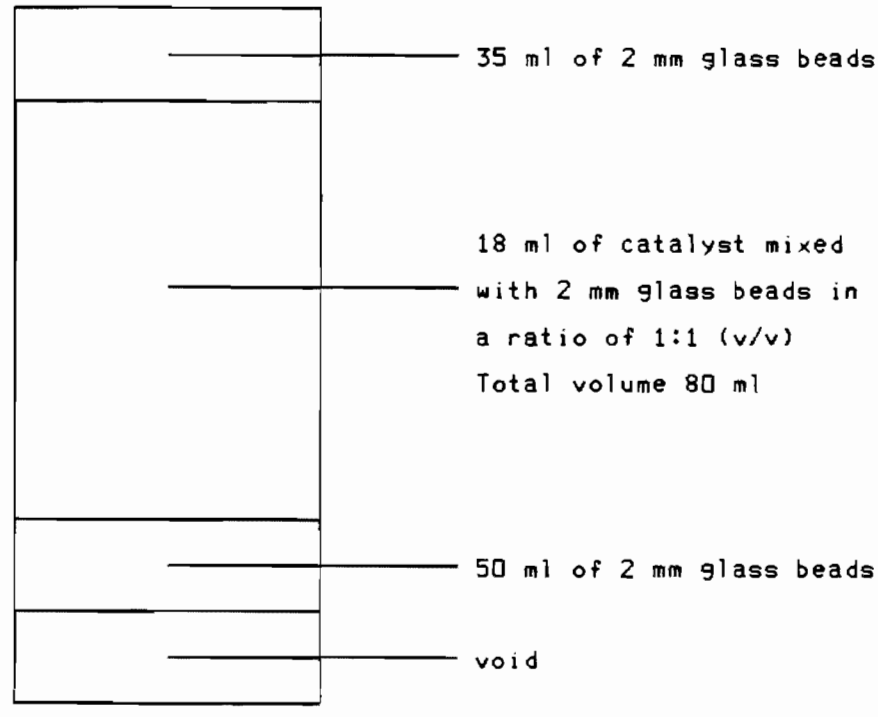

FIG 3.4 REACTOR BED

3.3.3 Start-up

Prior to introducing the reactants into the system, the cooling circuits and water bath were allowed to operate for a sufficiently long time to ensure that the temperatures reached steady state. The back pressure regulator was set to the desired value and the fluidising air set to the value determined previously.

The feed cylinder was then opened and the reactants allowed to flow to the inlet of the sealed reactor. All air was removed from the low pressure side via a vent line and the pump started. At this time the reactants were allowed to flow through the reactor and into the rest of the line. When the pressure in the system reached its set point, the pump setting was altered to give the correct feed rate. Once this had been achieved, the temperature of the bed was set to the desired value.

When the first drops of liquid were collected the feed cylinder was changed and the catchpot emptied. This was taken as time zero. Although a certain amount of data was lost during start-up, this persisted over a relatively small time fraction of the entire run. Little significant information was therefore lost. Furthermore, in this way the liquid left in the line and reactor at the end of a run did not affect the mass balance.

3.3.4 Steady state operation

To monitor the performance of the isothermal reactor and the catalyst, the following readings were taken at selected time intervals.

- bed temperature profile
- fluidised bed temperature
- fluidising air flow
- liquid mass and volume
- tail gas meter reading
- tail gas temperature
- G.C. analysis of tail gas
- G.C. analysis of liquid

The feed cylinder was changed when necessary. The mass of the used and fresh cylinder was noted.

3.3.5 Shut-down

When shutting down the system, the feed pump was switched off and the procedure as outlined above followed. The feed cylinder was however not replaced. Once the relevant data had been collected,

- the temperature controllers were switched off;
- the coolant and heating flows were stopped;
- the system pressure was released to atmosphere.

Temperature runaways did not occur during start up. However, it was found that the degree of control that could be exercised was sensitive to sand height and the position of the controlling thermocouple in the fluidised bed, which were consequently monitored by visual inspection throughout the run.

3.4 Data analysis

The data and collected during the run was analysed using a variety of procedures. These are discussed below.

3.4.1 Computation of results

A computer program was utilised to analyse the data obtained during the runs. The following was computed.

Mass balance. The percentage mass loss was calculated using

$$\% \text{ mass loss} = 1 - \left[\frac{(\text{total liquid out} + \text{total gas out})}{(\text{total weight of feed in})}\right] \cdot 100$$

where the (total liquid out) is measured directly by adding the weight of all liquid sampled. The (total gas out) was calculated using

$$\text{total gas out} = \frac{(P \cdot V \cdot M)}{(Z \cdot R \cdot T)}$$

where P = pressure in atm,
V = total volume of flue gas in liters,
M = molecular weight based on mean over entire run,
Z = compressibility factor (0.986),
R = universal gas constant (8.21×10^{-2} atm·l/gmole·K), and
T = gas meter temperature in K.

Two limiting cases of where mass loss could occur would be: 1) all mass was lost before the reactor in which case the mass out would be equal to the effective mass in, and 2) all mass was lost after the reactor in which case the mass in would be equal to the mass out plus the mass lost. To account for the mass lost it was assumed that the rate of mass loss was constant throughout the run and that the mass was lost in the form of gas. The calculated WHSV and conversion would depend upon where the mass loss occured. The equations used to calculate these are shown below.

Weight Hourly Space Velocity. This was the rate of feed in per hour per gram of catalyst and was calculated using

$$WHSV_n = \frac{\text{(mass of propene and propane passing over the catalyst)}}{\text{(total time)}\cdot\text{(catalyst mass)}}$$

where n = 1 if it was assumed that all mass was lost before the reactor,
n = 2 if it was assumed that all mass was lost after the reactor

Liquid production rate. This is an indication of the activity of the catalyst and is expressed in terms of grams of liquid product obtained per gram of catalyst per hour. As it was assumed that all mass lost was gas, the mass of liquid out was that measured and the LPR was calculated using,

$$LPR = \frac{\text{(mass of liquid out - mass of dissolved gas)}}{\text{(total time)}\cdot\text{(mass of catalyst)}}$$

Liquid mass % conversion. This is calculated using the formula,

$$\text{mass \% conversion} = \left[\frac{(LPR)}{WHSV_n \cdot (w)}\right] \cdot 100$$

where n = 1 if it was assumed that all mass was lost before the reactor
n = 2 if it was assumed that all mass was lost after the reactor
w is the mass fraction of propene in the feed

Liquid sample composition. The liquid product was grouped into oligomers of propene as dimer, trimer, tetramer, etc. The liquid composition was based on the mass percent output, the response factors having been set equal to one. It can be used to compare oligomer production rate between different runs and variations with time in a particular run.

Gas sample composition. This data is expressed in terms of mass % since all G.C. response factors have been determined.
Apart from the mass balance data all other results could be presented in graphical form as functions of time on stream. When the data was plotted in this way an average time between two sampling points was used. Data was recorded only from the time that the first drop of product was collected, this time being defined as time zero.

3.5 Analytical procedure

3.5.1 Gas analysis

Both the feed gas and flue gas were analysed on a Gow-Mac 750p gas chromatograph whose responses from the detector were monitored by a Varian 4270 intergrator. The packing used for this work was n-Octane/ Poracil C in a 5.5 m glass column with an inner diameter of 4 mm. Table 3.1 shows the typical composition of the feed used. The G.C. settings used together with a typical chromatogram of the feed with its retention times and response factors are shown in Appendix A, as is a discussion of the calibration procedure.

Table 3.1 : Feed Composition

Hydrocarbon	Mass%
Methane	0.0
Ethane	0.9
Propane	20
Propene	78
Iso-Butane	0.2
N-Butane	0.2
1-Butene	0.4
Iso-Butene	0.1
T2-Butene	0.1
C2-Butene	0.1
$C5^+$	0.2

3.5.2 Liquid analysis

Liquid samples were analysed by a Varian 3400 together with a Varian 8000 auto sampler. The packing used for this work was 3% Silicon/OV-101

on Chromosorb W-HP 100/120 mesh in a 3 m long glass column with an inner diameter of 4 mm. The responses from the G.C. were monitored by the Varian Vista 401 data system. This system could be programmed to give an integral analysis of the results. The G.C. settings as well as a discussion of the optimisation and calibration procedure used are given in Appendix A.

Due to the complex nature of the liquid products the analysis of the liquid spectra was difficult. To facilitate product analysis it was decided that the liquid product analysis be based on carbon number groupings rather than on individual components. The groupings chosen are shown in Table 3.2.

Table 3.2 : Carbon number groupings used for liquid analysis

Group	Range
Monomer (C_3)	C_3-C_4
Dimer (C_6)	C_5-C_7
Trimer (C_9)	C_8-C_{10}
Tetramer (C_{12})	C_{11}-C_{13}
Pentamer (C_{15})	C_{14}-C_{16}
Heptamer (C_{18})	C_{17}-C_{19}
Hexamer+ (C_{21})	C_{20}+

3.5.3 Nuclear magnetic resonance

The hydrocarbon functional group distribution of C_6 to C_{18} propene oligomerisation products was determined using ^1H NMR. Conventional methods of spectral analysis for propene oligomers were inadequate because of the great variety of head to tail and tail to tail fragments generated and because of the greater influence from end groups.

As ^{13}C NMR was not available at the time of this work, only a partial analysis of the liquid products was possible. The information thus obtained was that of the type of proton present: primary, secondary or tertiary. The characteristic proton chemical shift for the relevant protons are shown in Table 3.3 (Galya et al., 1985).

Table 3.3 : Structure definitions of terms and NMR spectral positions and area code (Galya et al., 1985).

Species	Structure	^{1}H Shift (ppm)	Area Code
Protonated aromatic and olefinic region.			
Olefinic CH_2	R-CH=CH_2	4.50-4.75	L
Olefinic CH	R-CH=CH-R	4.75-5.75	M
Aromatic CH	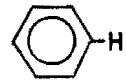	6.50-7.30	N
Aliphatic region			
α to aromatic CH_2	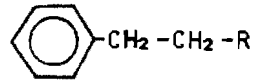	2.30-3.00	A
α to aromatic CH_3	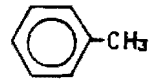	2.10-2.30	B
α to olefinic CH, CH_2	R_2-CH-CH=CH-CH_2-R	1.80-2.10	C
α to olefinic CH_3	R-CH=CH-CH_3	1.40-1.80	D
ß to olefinic CH, CH_2	R_2-CH-CH_2-CH=CH-CH_2-CH_2-R	1.00-1.40	E
CH_2 between isopropyl end groups and CH's	$(CH_3)_2$-CH-CH_2-CH(CH_3)-R	0.92-1.00	F
Terminal CH_3	CH_3-$(CH_2)_2$-CH=CH-R	0.84-0.92	G
Internal CH_3	R-CH(CH_3)-$(CH_2)_2$-CH=CH-R	0.70-0.84	H

Using the equations developed by Galya et al (1985) for the C_6 to C_{18} oligomerisation products of propene, each ^1H area was first converted to a carbon area before the percentage of each was calculated.

The carbon area of CH_3 was calculated using

$$CH_3 \text{ carbon area} = \frac{(\text{Area G} + \text{Area D} + \text{Area B} + \text{Area H})}{3}$$

and the carbon areas of CH_2 and CH were calculated using

$$CH_2 \text{ carbon area} = \frac{(\text{Area E} + \text{Area A} + \text{Area C})}{2} - \frac{(\text{Area H})}{6} + \text{Area F}$$

$$CH \text{ carbon area} = \frac{\text{Area H}}{3} + \text{Area F}$$

The degree of branching i.e. the CH_3 to CH_2, CH_3 to CH and CH to CH_2 ratios could be approximated (Galya et al., 1985) using:

$$\frac{CH_3}{CH_2} = \frac{2 \cdot (\text{AREA G} + \text{AREA D} + \text{AREA B} + \text{AREA H})}{3 \cdot (\text{AREA E} + \text{AREA A} + \text{AREA C}) - \text{AREA H} + 6 \cdot \text{AREA F}}$$

$$\frac{CH_3}{CH} = \frac{(\text{AREA G} + \text{AREA D} + \text{AREA B} + \text{AREA H})}{(\text{AREA H} + 3 \cdot \text{AREA F})}$$

$$\frac{CH}{CH_2} = \frac{2 \cdot (\text{Area H} + 3 \cdot \text{Area F})}{3 \cdot (\text{Area E} + \text{Area A} + \text{Area C}) - \text{Area H} + 6 \cdot \text{Area F}}$$

The above equations will be used to analyse the NMR spectra in this work.

3.5.4 TG/DTA

Thermogravimetry (TG) involves measuring the changes in sample mass with temperature using a thermobalance. This is a combination of a suitable electronic microbalance with a furnace and associated temperature programmer. The balance is in an enclosed system so that the atmosphere can be controlled. Differential Thermal Analysis (DTA) involves measuring the difference in the temperature between the sample and a reference material while both are being subjected to the same temperature program. Both TG (mass loss in wt%) and DTA (temperature difference between sample and reference material) are recorded as a function of furnace temperature. The furnace used in this work was a STA-780 Series with a Stanton Redcroft Thermal Analyser. The balance was

controlled by a Stanton Redcroft Balance Controller while the temperature in the furnace was controlled by a Stanton Redcroft Temperature Controller. The signals were amplified by a Stanton Redcroft DC amplifier and recorded by a Bondwell Personal Computer.

In this work 20 mg of sample was placed in the furnace and the temperature raised from 40°C to 850°C at a rate of 10°C/min in flowing air or nitrogen.

3.5.5 Water content determination

The water content of the feed was determined by measuring the dew point temperature of the water in the feed using a Panametrics Hygrometer (Model 700D) with an aluminium oxide sensor. Approximately 48 h was needed for the system to stabilise. Once this temperature had been measured the vapour pressure of the water in the feed was determined (at 1 atm) and the mole fraction of water in the feed determined. Using the above procedure it was found that the feed contained approximately 112 ppm (v/v) water.

3.5.6 Distillation

The liquid products obtained from the high pressure reactor runs were distilled in a glass distillation column, shown in Figure 3.5, to separate the C_6 from the heavier fractions. After the still was filled, up to 3 liters per batch, it was placed into a heating mantle and connected to the column with a Quick-fit connector. Upon heating the vapours from the still passed via a column packed with berl saddles to a condenser. Here the condensate was either directed back to the column as reflux liquid (plunger down), or to the catchpot (plunger up) as product. This separation was controlled by a solenoid operating a magnet fused to the plunger. The solenoid in turn was controlled by a timing device with which the total cycle time and reflux time could be set. The reflux ratio was then calculated by the ratio of the time the plunger was up to the time that the plunger was down. For all cases the reflux ratio used was 2:9. The cut off temperature was set by a thermostat at the top of the column. When the desired temperature was reached, power to the solenoid was discontinued and subsequently the plunger remained down (total reflux). The cut point temperature used was 62°C. The coolant used in the condensers was water. Dissolved gases did not condense and were vented to the atmosphere.

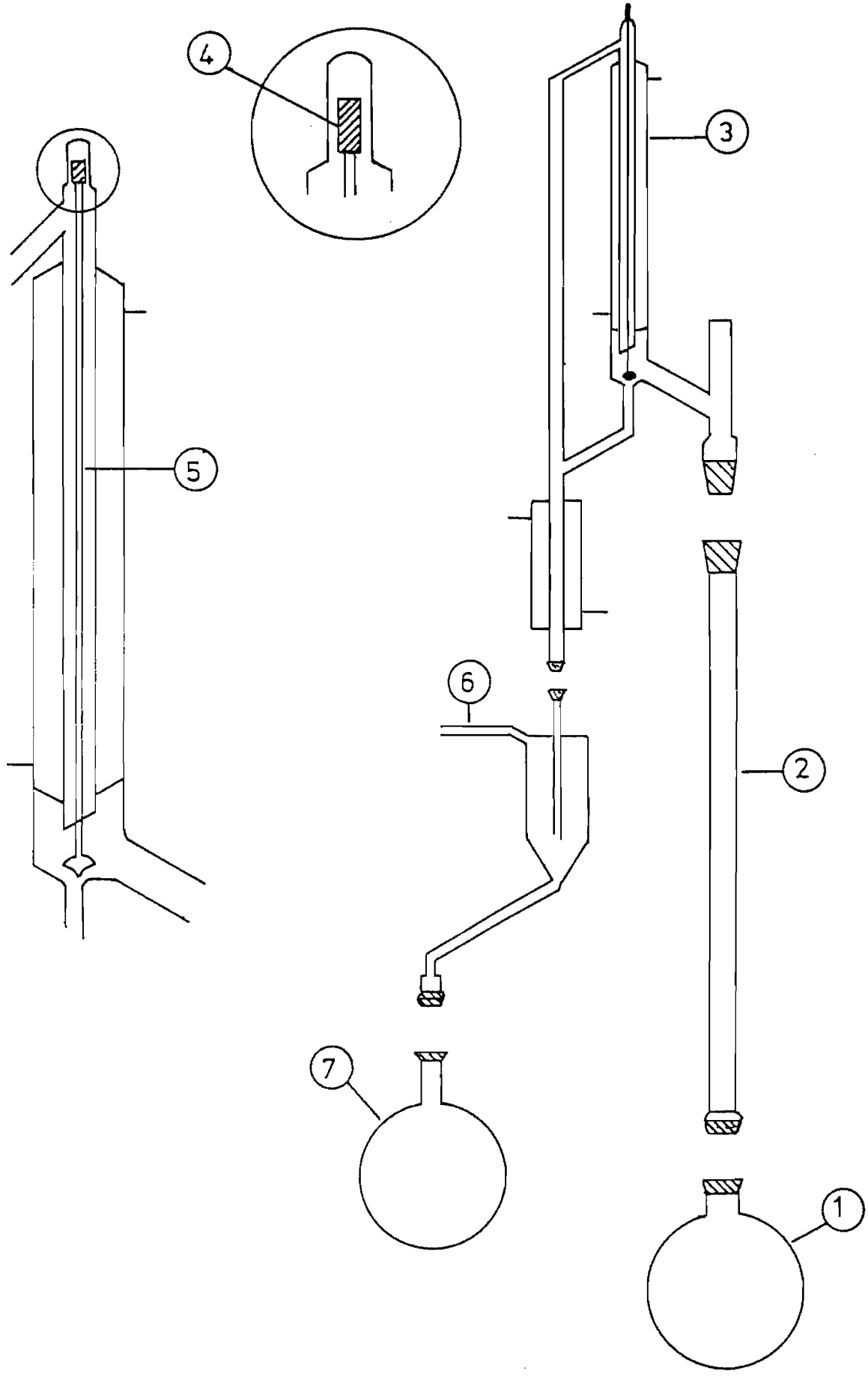

FIG 3.5 BATCH DISTILLATION UNIT

Key to Figure 3.5

1 Still
2 Berle saddle column
3 Reflux condenser
4 Magnet at top of plunger
5 Plunger assembly
6 Gas tapping point
7 Distillate receptacle

3.6 Catalyst synthesis

3.6.1 Support preparation

The silica-alumina support was received from Kali Chemie in the form of 4 mm spheres which were crushed in a ceramic ball mill to -500 μm. The silica to alumina ratio was 9:1 on a weight basis.

3.6.2 Impregnation

A previously determined mass of metal salt was dissolved in 500 ml of distilled water to which 50 g of silica alumina was added. The solution was boiled under reflux for 1 h with vigorous agitation throughout. The vessel was then opened to the atmosphere and while being agitated, most of the water boiled off. The concentrated solution was transferred to a ceramic pie dish and placed into an oven at 120°C where the remaining water was evaporated. Once the material was completely dry it was crushed, sieved and stored. The above was adopted from work by Hogan et al (1955) and Holm et al (1957).

3.6.2.1 Nickel concentration

The quantity of nickel needed to make a catalyst of known metal content was determined in a separate experiment. Using a constant mass of silica alumina, but varying the amount of nickel nitrate hexahydrate, a loading curve was constructed. The synthesis procedure used was that as discussed above. The nickel content of the material was determined using atomic absorption spectrophotometry. The loading curve is shown in Figure 3.6.

3.6.3 Homogeneous decomposition deposition

In this method 45 g of nickel salt was dissolved in 500 ml of distilled water to which 50 g of silica alumina was added. The solution was then heated under reflux to 100°C at which point 25 g of urea crystals were added. This was taken to be time zero. The solution was then refluxed,

while continuously being agitated, for a previously determined period of time, as discussed below. Excess water was removed by filtration in a Buchner funnel and the catalyst washed with 20 volumes of hot (90°C) distilled water per volume of catalyst. The catalyst was then dried at 110°C in a ceramic pie dish for 12 h before being crushed and stored. The above synthesis procedure was adopted from work done by Van Dillen et al (1977), Richardson and Dubus (1978) and Hermans and Geus (1979).

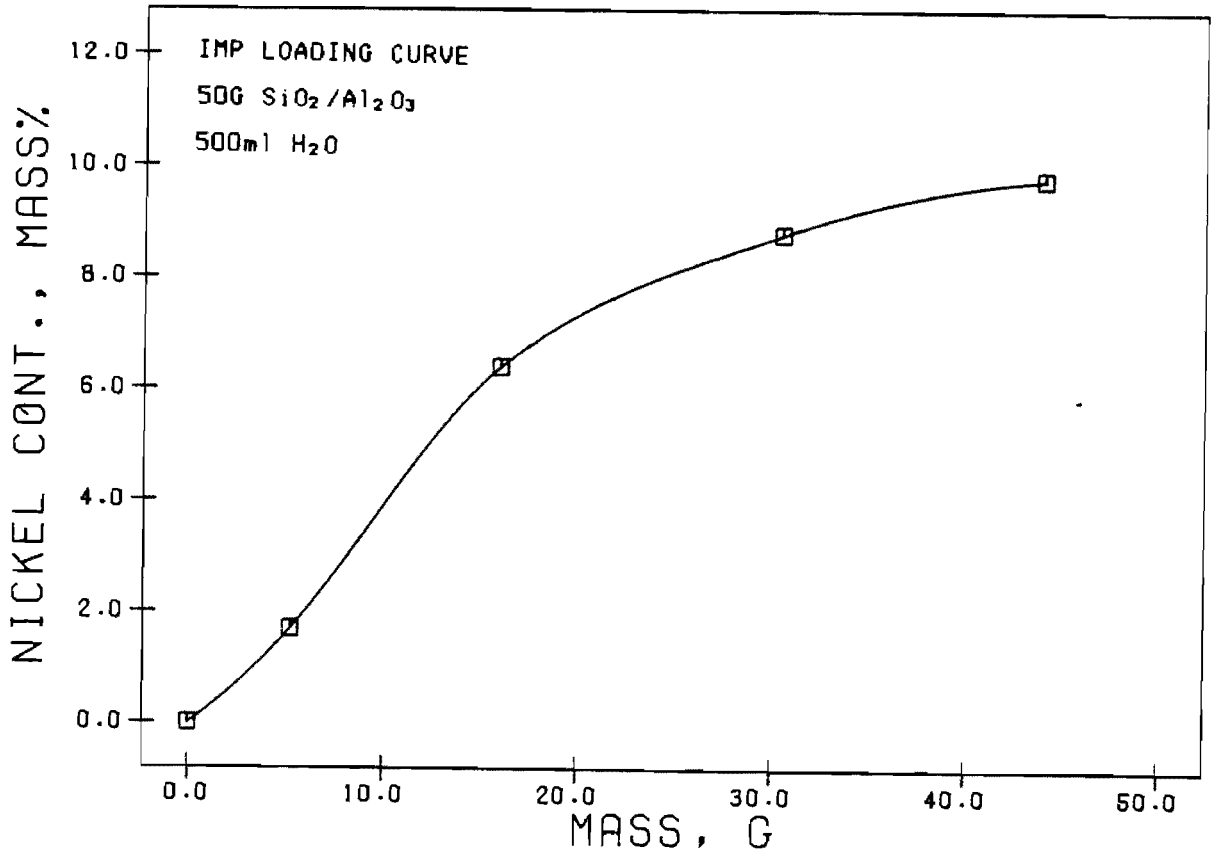

FIG 3.6 NICKEL CONTENT (MASS%) VS MASS OF NICKEL NITRATE HEXAHYDRATE (G)

3.6.3.1 Nickel concentration

The time required to load a desired quantity of nickel was determined in a separate experiment. All quantities of materials used were as discussed above, but while the mixture was boiling under reflux, samples of solution (5 ml) were taken, at discrete intervals. These samples were than washed and dried, in the usual manner, and their nickel content determined using atomic adsorption spectrophotometry. In this way the loading curve was constructed from which the time required to produce a catalyst of known metal content could be read. Two sets of starting conditions were used as shown in Figure 3.7.

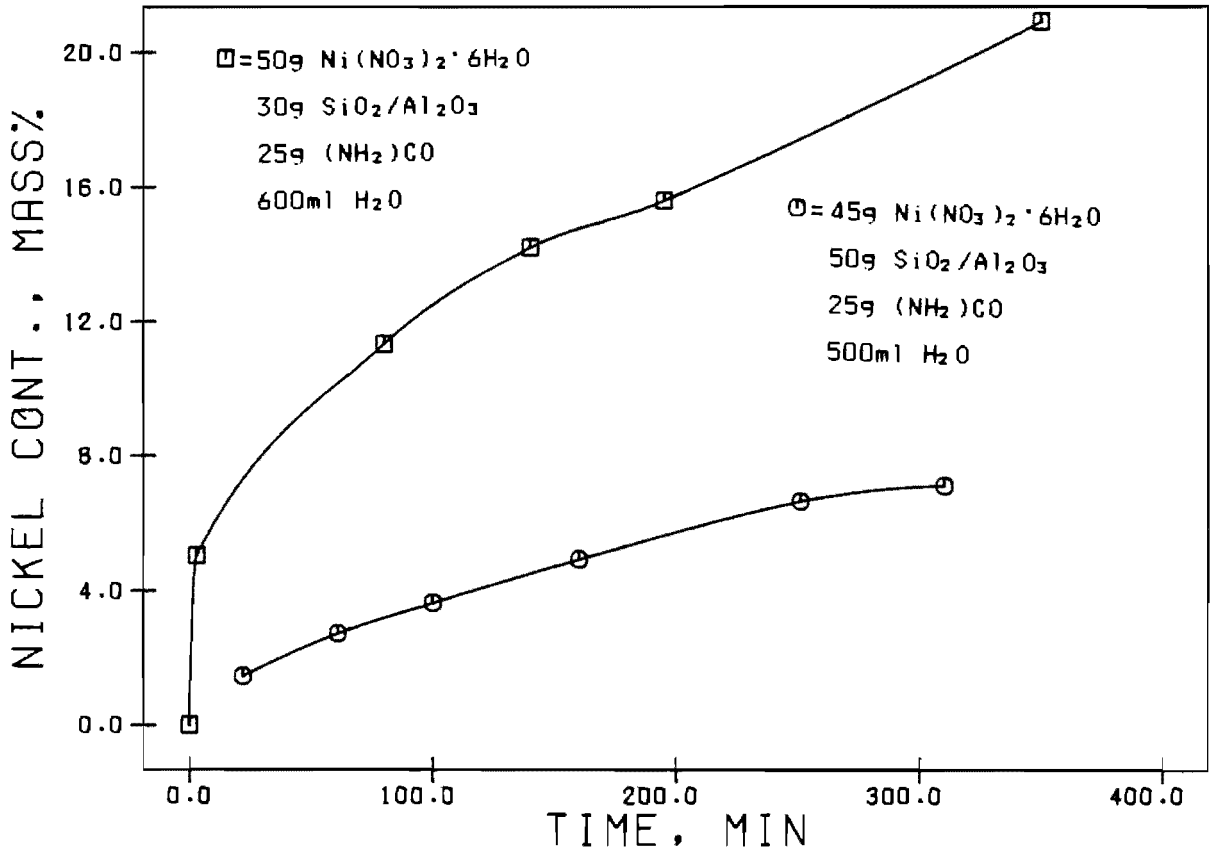

FIG 3.7 NICKEL CONTENT (MASS%) VS TIME (MIN)

3.6.4 Coprecipitation

Two solutions were prepared. One contained 180 g of sodium meta silicate in 1200 ml of distilled water and the other contained 42 g of aluminium nitrate nonahydrate and 11.7 g of nickel nitrate hexahydrate in 1000 ml of distilled water. It was important that the pH of the final solution was kept in the range of 8 $\pm$ 0.5. To achieve this caustic soda could be added to the sodium solution or nitric acid to the solution of the nitrates. In this work 82 ml of nitric acid (70 wt% HNO_3) was added to the solutions of the nitrates. The two solutions were mixed in a 4 l CSTR while being vigorously agitated and the pH adjusted using 5 g of sodium hydroxide in 100 ml of water. A gel formed after about 30 s and was allowed to stand for 1 h. This material was then filtered using a Buchner funnel, broken up and dried for 12 h at 110°C. The dried solid was washed twice by decantation with water and then washed with six or seven successive portions of 5% ammonium chloride. The ammonium wash involved soaking the catalyst for 1 h at 70°C in an excess of solution which was then drained using a Buchner funnel. In this way any sodium held in the solid was removed by base exchange. The catalyst was then washed with distilled water and dried at 110°C for 12 h before being

crushed, sieved and stored (Holm, 1957). The silica to alumina ratio of the final catalyst was 9:1 while the nickel content was 4 wt%.

3.6.5 Determination of nickel content

To determine the nickel content of the catalyst an accurately weighed sample, approximately 0.25 g, was added to 5 ml of hydrofluric acid in a teflon beaker. The solution was left for 12 h after which 5 ml of concentrated sulphuric acid and 5 ml of distilled water were added. This was again allowed to stand before being made up to 250 ml in a volumetric flask. In this way the catalyst was broken down into its individual elements and the nickel contents determined using the Varian SpectrAA-30 Atomic Adsorption spectrophotometer.

3.6.6 Extrudate manufacture

The powder form of nickel oxide silica alumina was found to be too fine for effective use in the high pressure intergral reactor as it caused an excessive pressure drop and downstream plugging problems. Breck (1980) suggested the use of an inorganic binder such as kaolinite in the formation of extrudates. This approach was found to be effective if the quantity of binder was greater than approximately 35 wt%. At lower binder mass fractions the material could not be extruded.

The binding process consisted of mixing the binder with the catalysts to form a homogeneous paste, the amount of water used carefully judged by visual inspection. When the paste had the desired consistency it was loaded into a previously wetted stainless steel piston and plunger assembly and extruded onto filter paper. The catalyst was then dried at 80°C for 12 h.

Breck (1980) further suggested that the extrudates be baked at 370°C for 12 h to convert the clay to an amorphous binder of considerable mechanical strength. It was however found that this was not necessary as the extrudates had sufficient strength after drying at 80°C.

4. RESULTS

Various types of catalyst synthesis procedures were examined. These were homogeneous decomposition deposition (HDD), impregnation (IMP) and, briefly, coprecipitation (SG), as well as the catalytic properties of the silica alumina support (SA). The silica to alumina weight ratio used throughout was 9 to 1. The criterion whereby the activity of the catalyst was measured was the liquid production rate (LPR). The selectivity of the catalyst, expressed in terms of mass% liquid composition, gave an indication of the relative amounts of the various oligomers formed.

The reaction conditions used were a temperature of 80°C and a pressure of 40 atm unless otherwise stated. The catalyst size fraction used was -500 μm, which was made into $^{1}/_{16}$ inch extrudates using 35 wt% kaolinite as binder.

As mentioned previously the feed used was a 4:1 mixture of propene/propane with trace impurities of C_4 and C_2 hydrocarbons unless otherwise stated. The exact composition of the feed is shown in Table 3.1.

The reaction conditions used in all experiments are summarised in Table 4.1. The $WHSV_1$ and $WHSV_2$ were calculated assuming the mass loss occurred before the reactor and after the reactor, respectively, in the form of gas. For the purpose of plotting the results it was assumed that all mass was lost before the reactor, i.e., $WHSV_1$ was used in all the figures.

4.1 Reproducibility of Data

Two runs were carried out under identical conditions of temperature, pressure and WHSV. The catalyst used in both runs was an HDD type catalyst with a nickel content of 1.5 wt%.

Figure 4.1 shows the LPR for each run as a function of time. It can clearly be seen that the largest discrepancies occurred during start-up.

Table: 4.1 Reaction data

Code	Nickel (wt%)	Temp (°C)	Press (atm)	$WHSV_1$ (g/g/h)	$WHSV_2$ (g/h/g)	Comment
HDD-1	1.5	80	40	4.2	4.5	
HDD-2	1.5	80	40	5.3	5.6	Reproducibility
HDD-3	1.5	80	40	5.2	5.6	Reproducibility
HDD-4	1.5	80	40	5.1	5.5	Wet feed
HDD-5	1.5	80	40	4.7	4.8	Regenerated HDD-4
HDD-6	1.5	200	40	4.9	5.5	Temp runaway
HDD-7	1.5	80	40	5.4	5.6	Regenerated HDD-6
HDD-8	1.5	150	40	4.3	4.7	
HDD-9	1.5	210	40	6.6	7.3	
HDD-10	2.2	80	40	5.0	5.5	
HDD-11	7.2	80	40	4.2	4.7	
HDD-12	11.7	80	40	4.9	5.2	
HDD-13	11.3	80	40	5.4	5.7	
HDD-14	11.3	80	40	10.8	11.7	
HDD-15	11.3	80	40	11.6	13.2	
HDD-16	11.7	80	20	6.7	7.4	
HDD-17	11.7	80	50	5.0	5.2	
HDD-18	1.5	80/200	40	5.5	-	Liquid feed (C_6)
HDD-19	1.5	80	40	8.8	-	Liquid + gas feed
HDD-20	1.5	200	40	7.7	-	Liquid + gas feed
IMP-1	0.8	80	40	4.7	4.8	
IMP-2	1.9	80	40	5.3	5.6	
IMP-3	2.2	80	40	4.8	4.9	
IMP-4	4.6	80	40	3.3	3.9	
IMP-5	6.3	80	40	4.9	5.4	
IMP-6	7.1	80	40	4.4	4.8	
IMP-7	9.8	80	40	5.2	5.5	
IMP-8	9.8	80	20	5.9	6.6	
IMP-9	9.8	80	50	5.0	5.3	
SG-1	1.5	80	40	5.2	5.5	
SG-2	1.5	80	20	5.9	6.1	
SG-3	3.0	80	40	3.7	4.1	
SA-1	-	80	40	4.0	4.1	
SA-2	-	150	40	6.2	6.3	
SA-3	-	200	40	3.5	4.2	

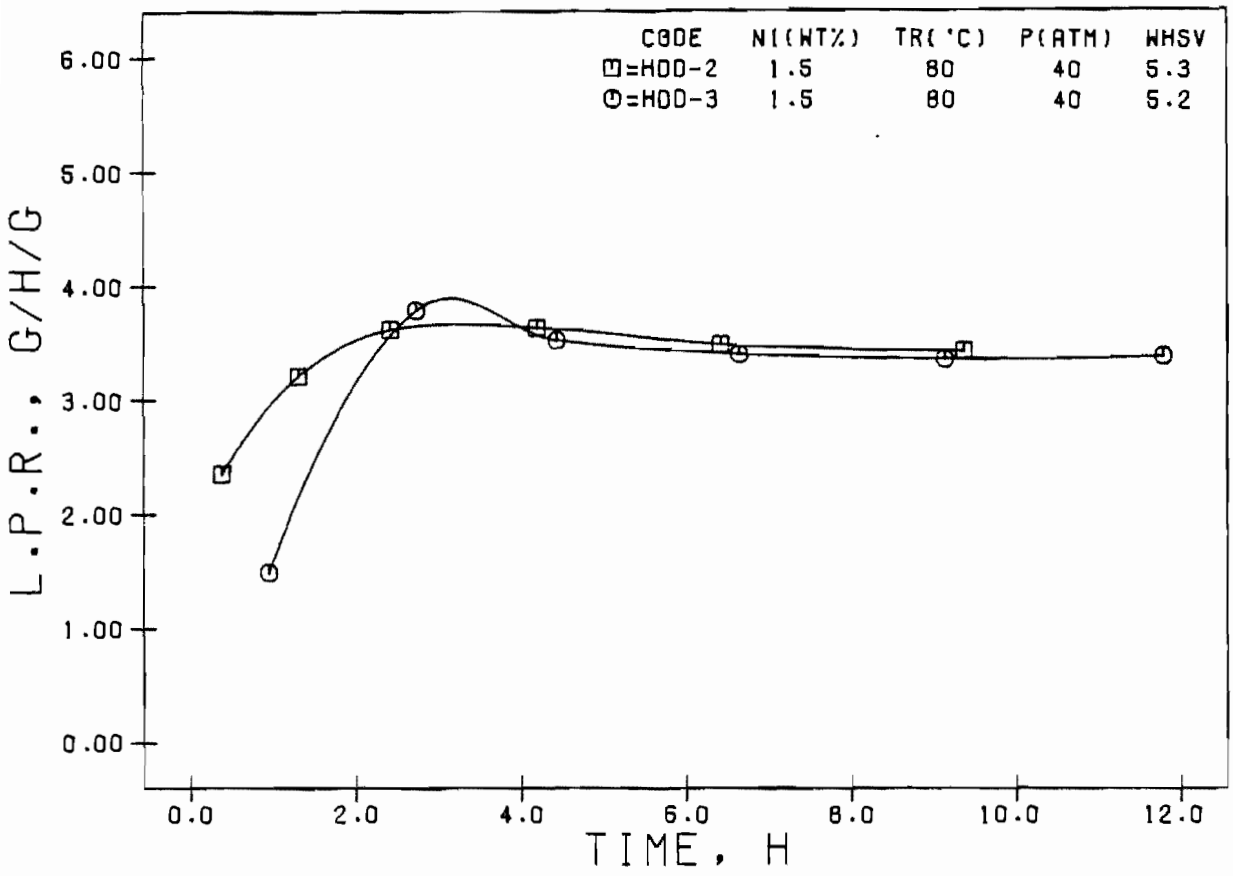

FIG 4.1 LIQUID PRODUCTION RATE (G/H/G) VS TIME (H)

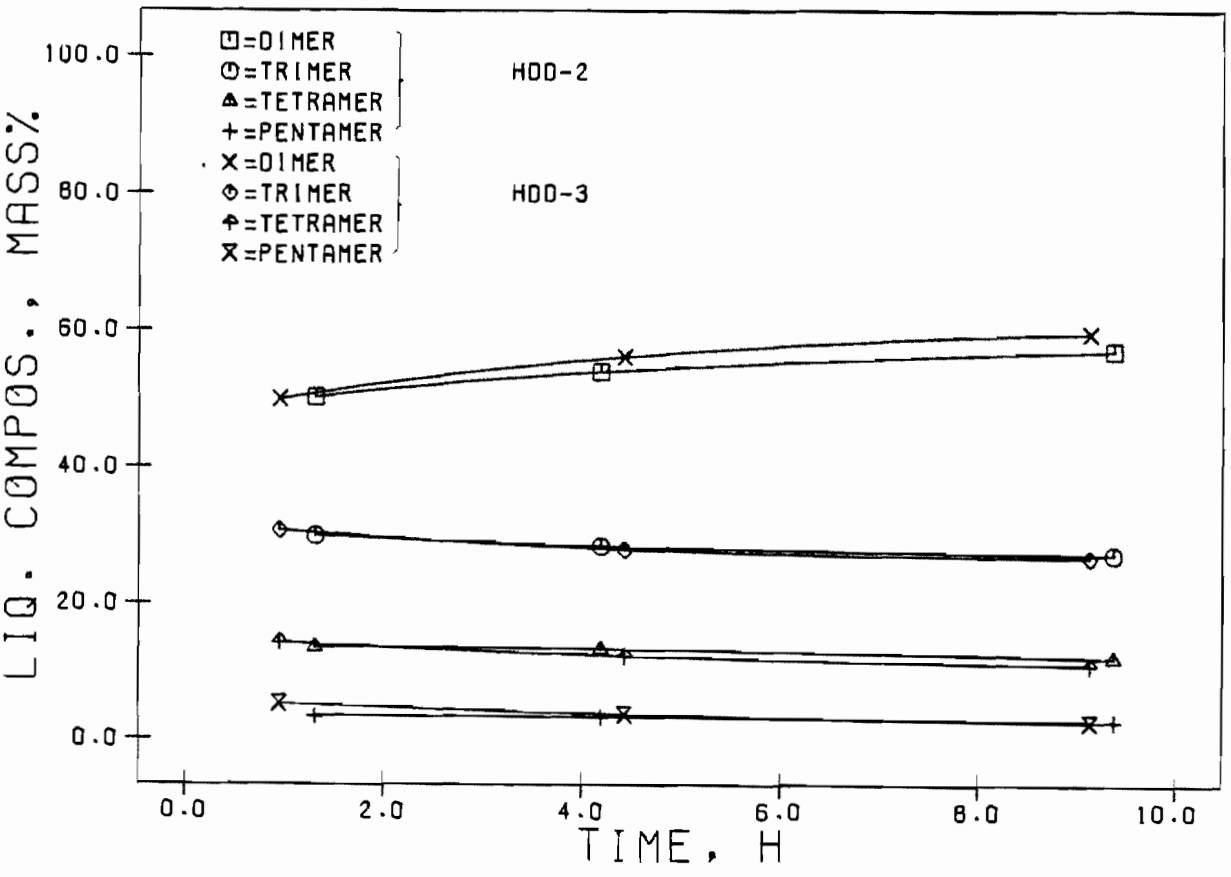

FIG 4.2 LIQUID COMPOSITION (MASS%) VS TIME (H)

Once steady state had been obtained, approximately after 4 h on stream, conversions were similar and the reproducibility acceptable.

Figure 4.2 shows selectivity as a function of time on stream. Here it can be seen that the dimer, trimer, tetrameter and pentamer were produced in similar quantities throughout the two runs.

It was thus concluded that at steady state adequate reproducibility was attained with respect to both selectivity and LPR.

4.2 Nickel content

In the case of HDD type catalysts, the nickel content was varied from 1.5 wt% to 11.7 wt%. It can be seen from Figure 4.3 that, while the LPR differed from run to run, this variation was due to WHSV differences, and no trend with increasing nickel content was observed. The LPR remained between 3 and 4 grams of product per gram of catalyst per hour over the range of nickel loadings examined. The selectivity of the catalyst, as shown in Figure 4.4, was also found to be essentially independent, both with respect to nickel content and time on stream although a slight decrease in dimer yield was observed with increasing nickel content.

In the case of IMP type catalysts, the nickel content was varied from 1.0 wt% to 9.8 wt%. An accurate statement about the effect of nickel content on the activity of IMP type catalysts could not be made due to differences in the WHSV. The selectivity, as a function of both time on stream and nickel content, is shown in Figure 4.6. The catalyst with 0.8 wt% nickel exibited the greatest selectivity towards trimers and the dimer yield increased slightly with increasing nickel content. No other marked changes in the selectivity were observed as a function of nickel content or time on stream.

4.3 Effect of pressure

In Figure 4.7 the LPR vs. time on stream is shown for an HDD type catalyst with a nickel content of 11.3 wt% at three different pressures. It can be seen from this figure that as the pressure was decreased from 50 atm to 20 atm the LPR remained constant although the WHSV was higher at lower pressures. This suggests that the activity of the catalysts dropped with decreasing pressure. The selectivity shown in Figure 4.8, as a function of time on stream and pressure was also dependent on the pressure used. It can be seen from Figure 4.8 that at 20 atm propene dimer accounted for approximately 70 wt% of the liquid product, while at

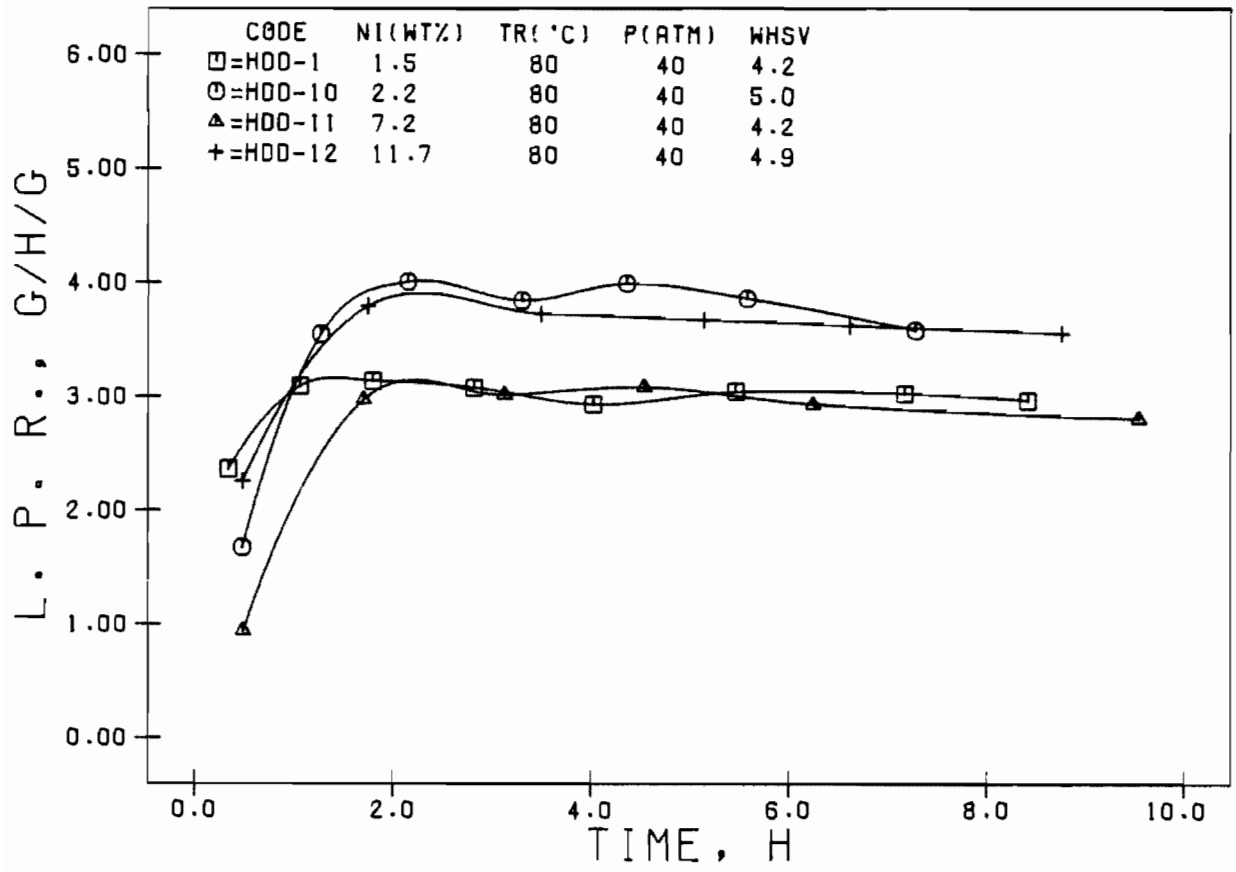

FIG 4.3 EFFECT OF NICKEL CONTENT (MASS%) ON LIQUID PRODUCTION RATE (G/H/G): HDD

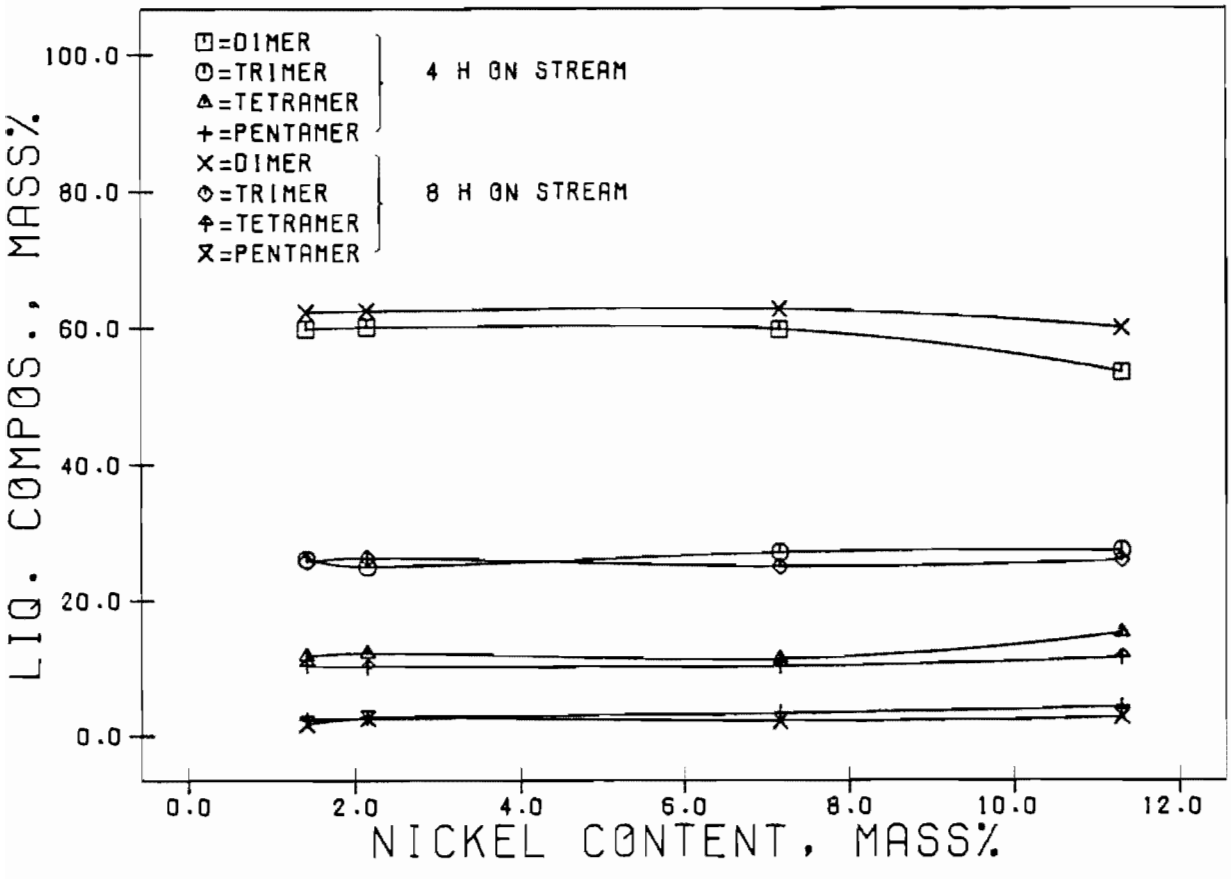

FIG 4.4 EFFECT OF NICKEL CONTENT (MASS%) ON LIQUID COMPOSITION (MASS%): HDD

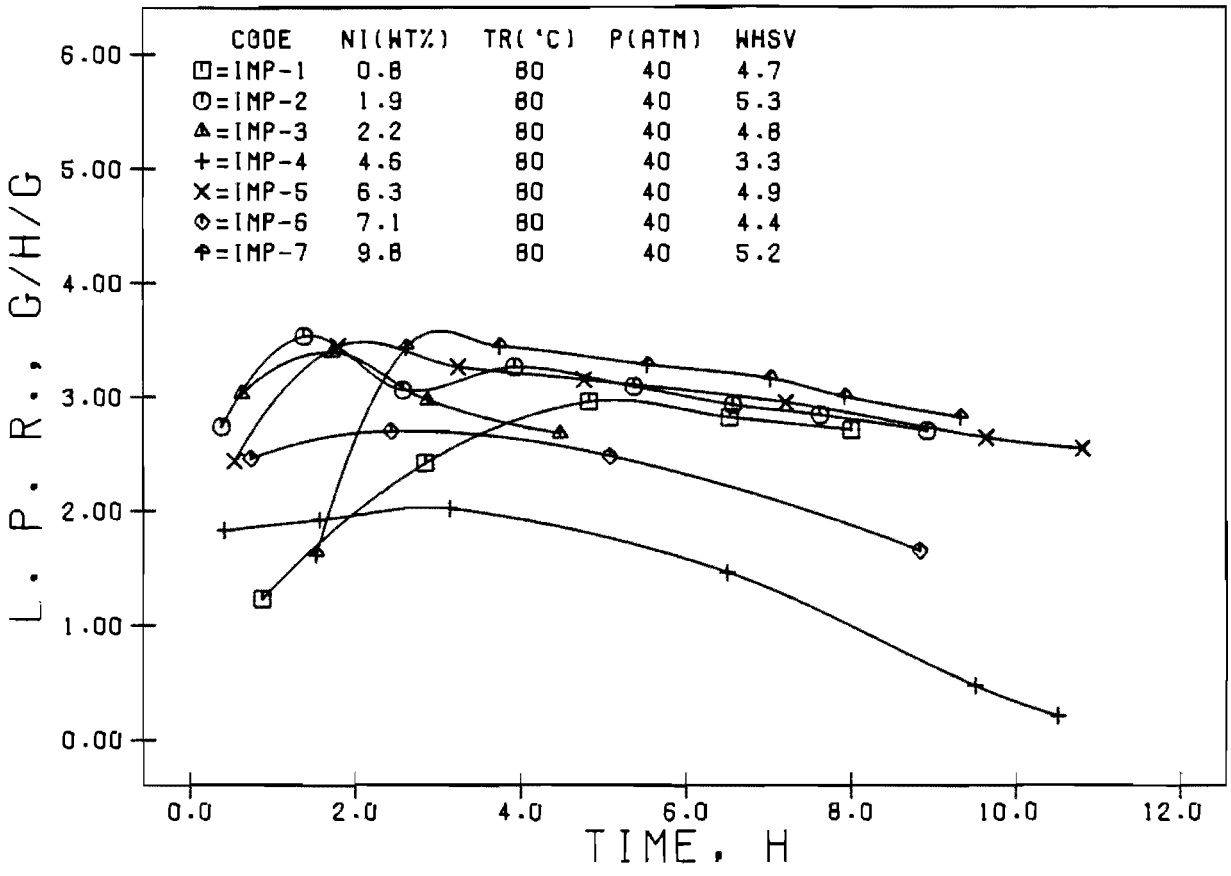

FIG 4.5 EFFECT OF NICKEL CONTENT (MASS%) ON LIQUID PRODUCTION RATE (G/H/G); IMP

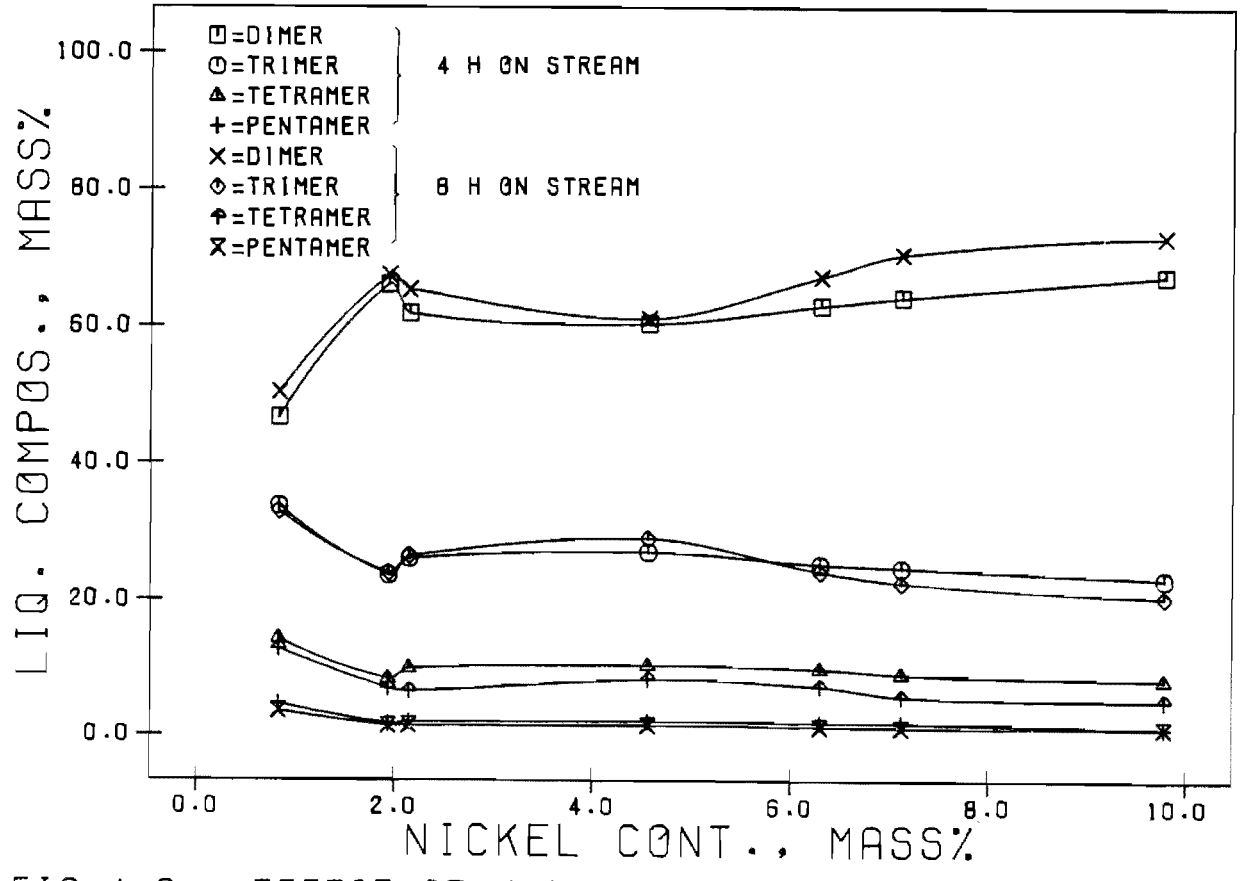

FIG 4.6 EFFECT OF NICKEL CONTENT (MASS%) ON LIQUID COMPOSITION (MASS%): IMP

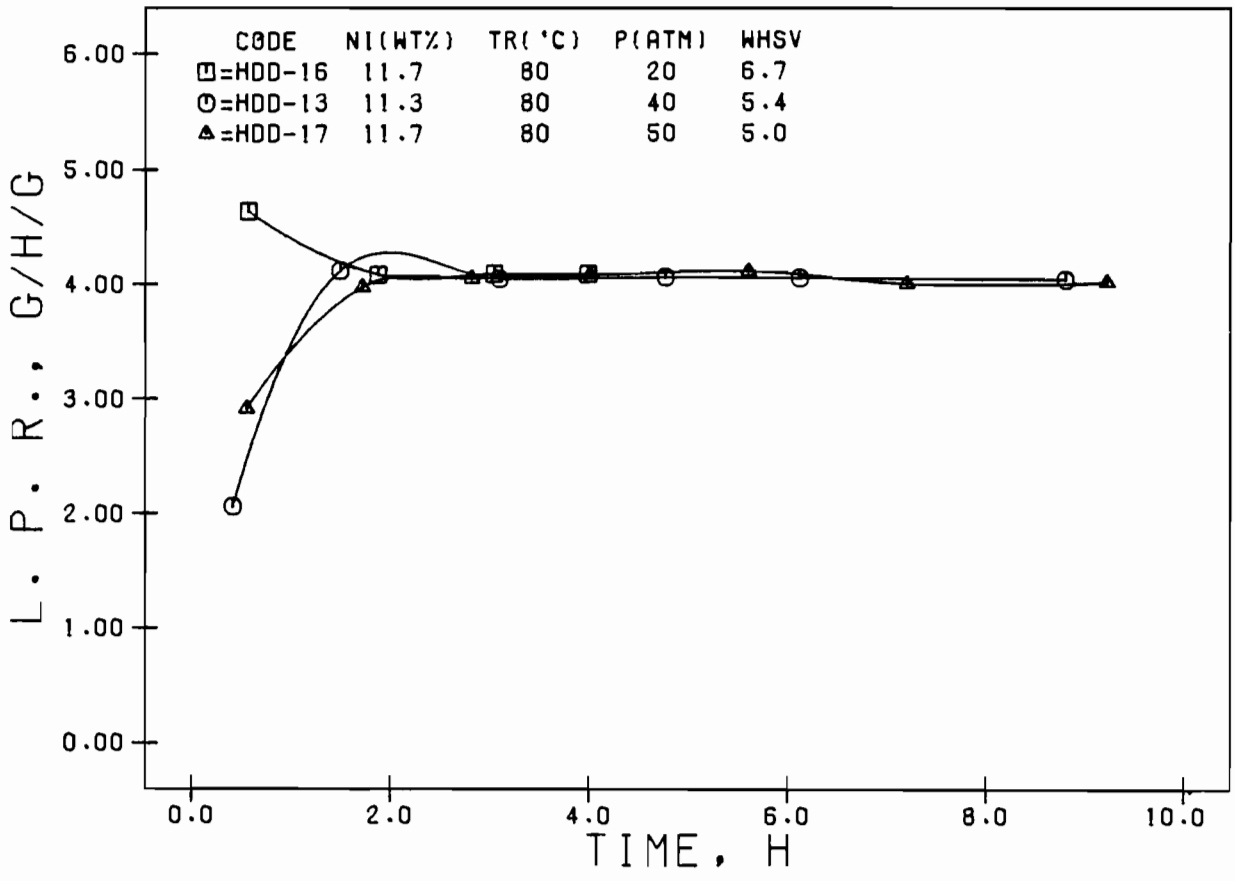

FIG 4.7 EFFECT OF PRESSURE (ATM) ON LIQUID PRODUCTION RATE (G/H/G); HDD

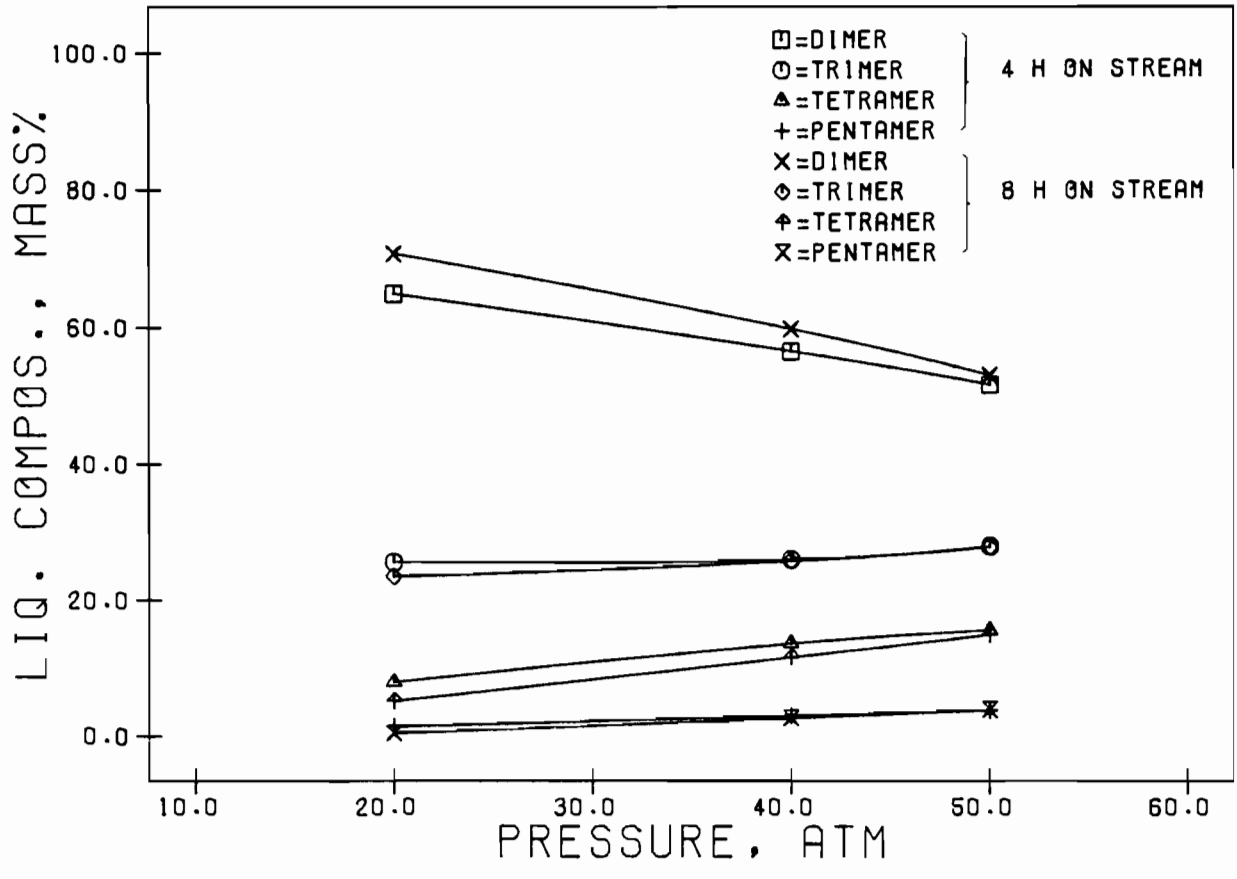

FIG 4.8 EFFECT OF PRESSURE (ATM) ON LIQUID COMPOSITION (MASS%); HDD

50 atm the liquid product contained only 50 wt% dimer. The observed shift to lighter products with decreasing pressure is consistent with thermodynamic predictions, although increasing the WHSV and hence decreasing the contact time, would result in the same shift in product spectrum.

In the case of an IMP type catalyst containing 9.8 wt% nickel, the LPR as well as the selectivity were very sensitive to the pressure used. The LPR at three distinct pressures is shown in Figure 4.9 as a function of time on stream. It can be seen that at 20 atm the catalyst rapidly deactivated and was practically inert after 7 h on stream. At the other pressures examined, i.e., 40 and 50 atm, no difference in the LPR was observed. The selectivity of the catalyst is shown in Figure 4.10 as a function of pressure. At 20 atm the liquid product contained approximately 30 wt% dimer which increased to 67 wt% at 40 atm dropping to 62 wt% at 50 atm. This trend, although opposite to that observed for HDD type catalysts, is in agreement with the data reported in the literature (Takahashi et al., 1969).

The LPR of a SG type catalyst with a nickel content of 1.5 wt% is shown in Figure 4.11 at two distinct pressures. At 40 atm the LPR was comparable to that of HDD and IMP type catalysts, while at 20 atm the catalyst was totally inert. The selectivity of the SG type catalyst at 40 atm differed markedly from that of an IMP and HDD type catalyst, in that the liquid not only contained a large percentage of dimers (40 wt%) but also an equally large percentage of trimers.

4.4 Bed temperature profile

Before any statement as to the effect of temperature could be made, the temperature throughout the bed had to be constant and not fluctuate excessively during a run.

In Figure 4.13 the temperature profile through the entire reactor is shown at 4 discrete times during a run. The catalyst bed started at position 4 and extended for 17.2 cm down the reactor to position 8. In this region of the reactor, viz., over the catalyst bed, a temperature deviation from the set point of not more than 4°C was observed at the times shown. In Figure 4.14 the temperature fluctuations with time were plotted at positions 4, 6 and 8. From this figure it can be seen that the amplitude of the temperature fluctuations with time were 4°C for position 4 and 6, and 3°C for position 8. It can thus be concluded that at 80°C the temperature throughout the bed and over the period of the

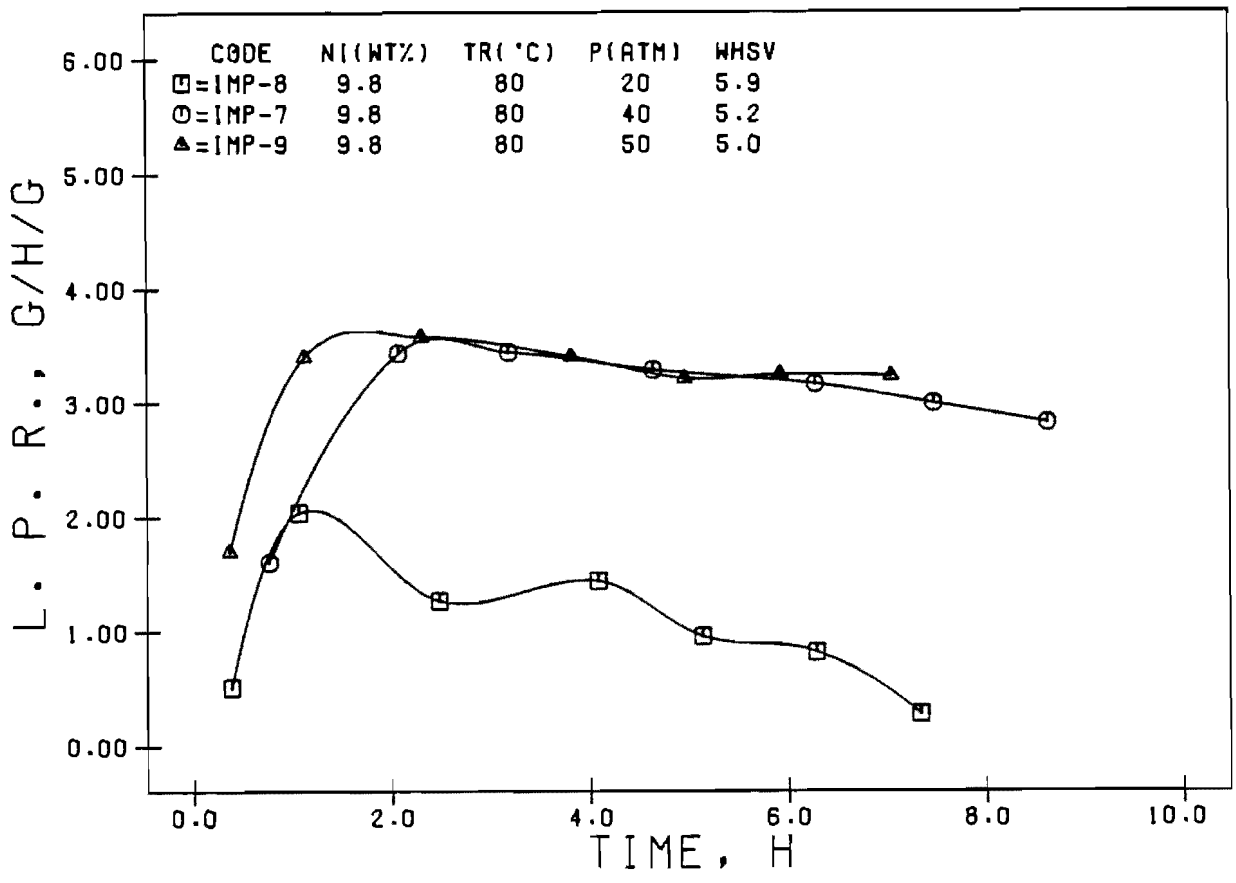

FIG 4.9 EFFECT OF PRESSURE (ATM) ON LIQUID PRODUCTION RATE (G/H/G); IMP

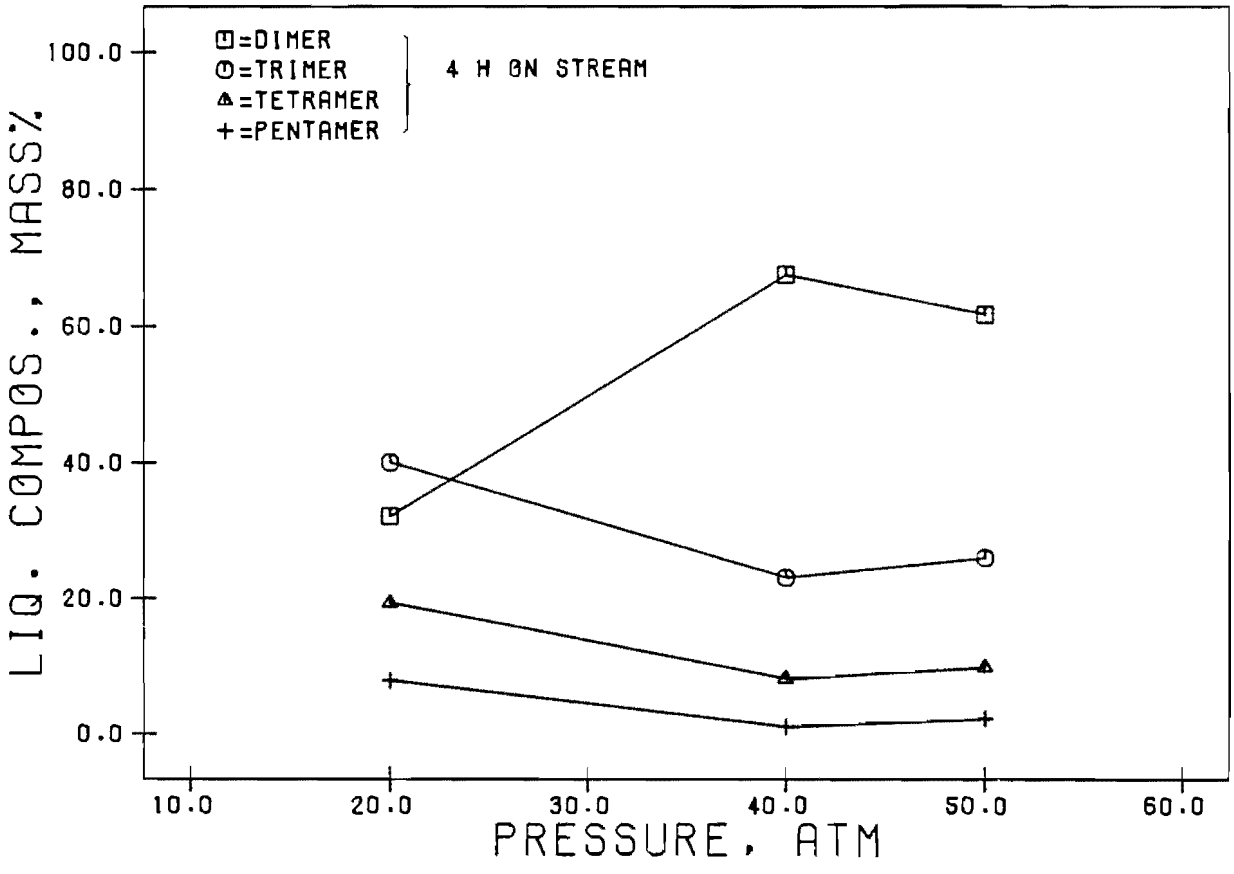

FIG 4.10 EFFECT OF PRESSURE (ATM) ON LIQUID COMPOSITION (MASS%); IMP

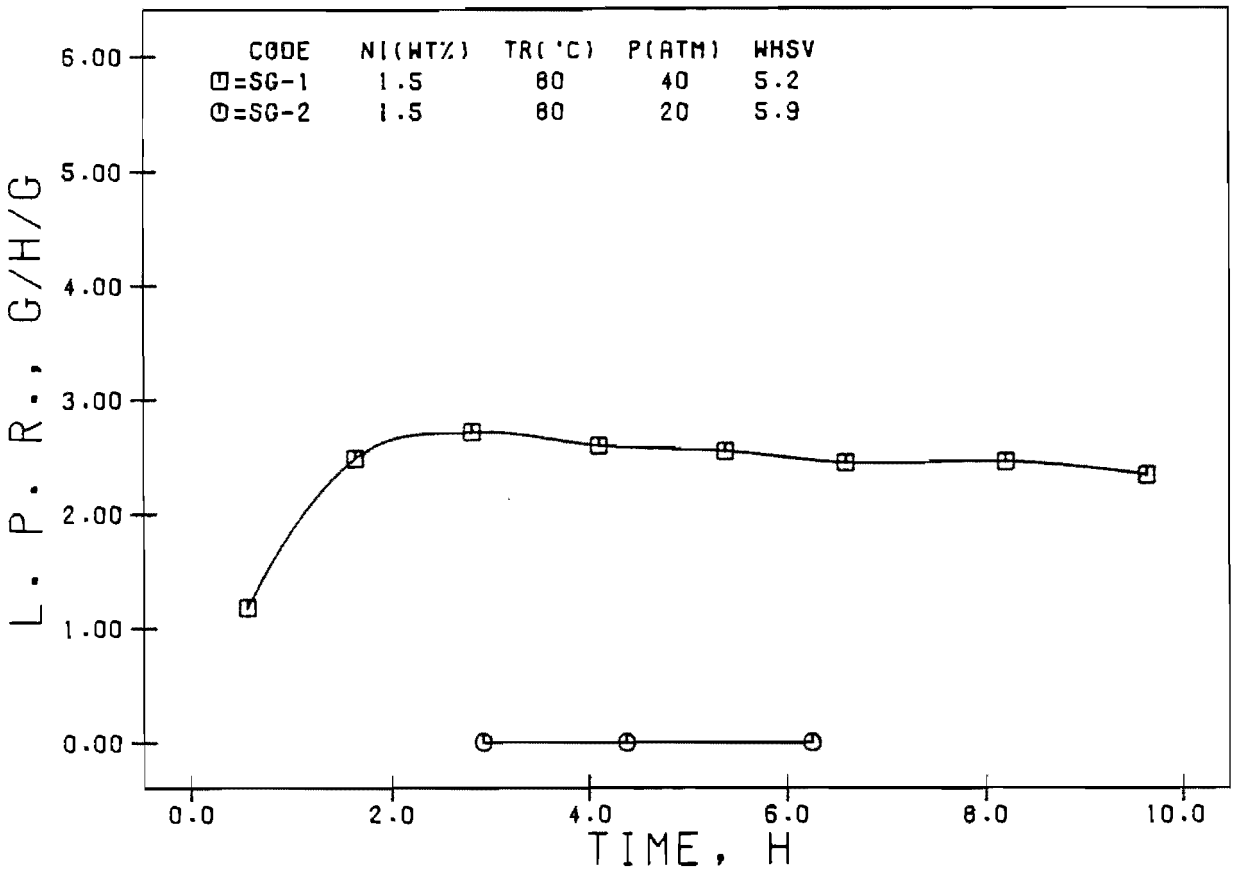

FIG 4.11 EFFECT OF PRESSURE (ATM) ON LIQUID PRODUCTION RATE (G/H/G); SG

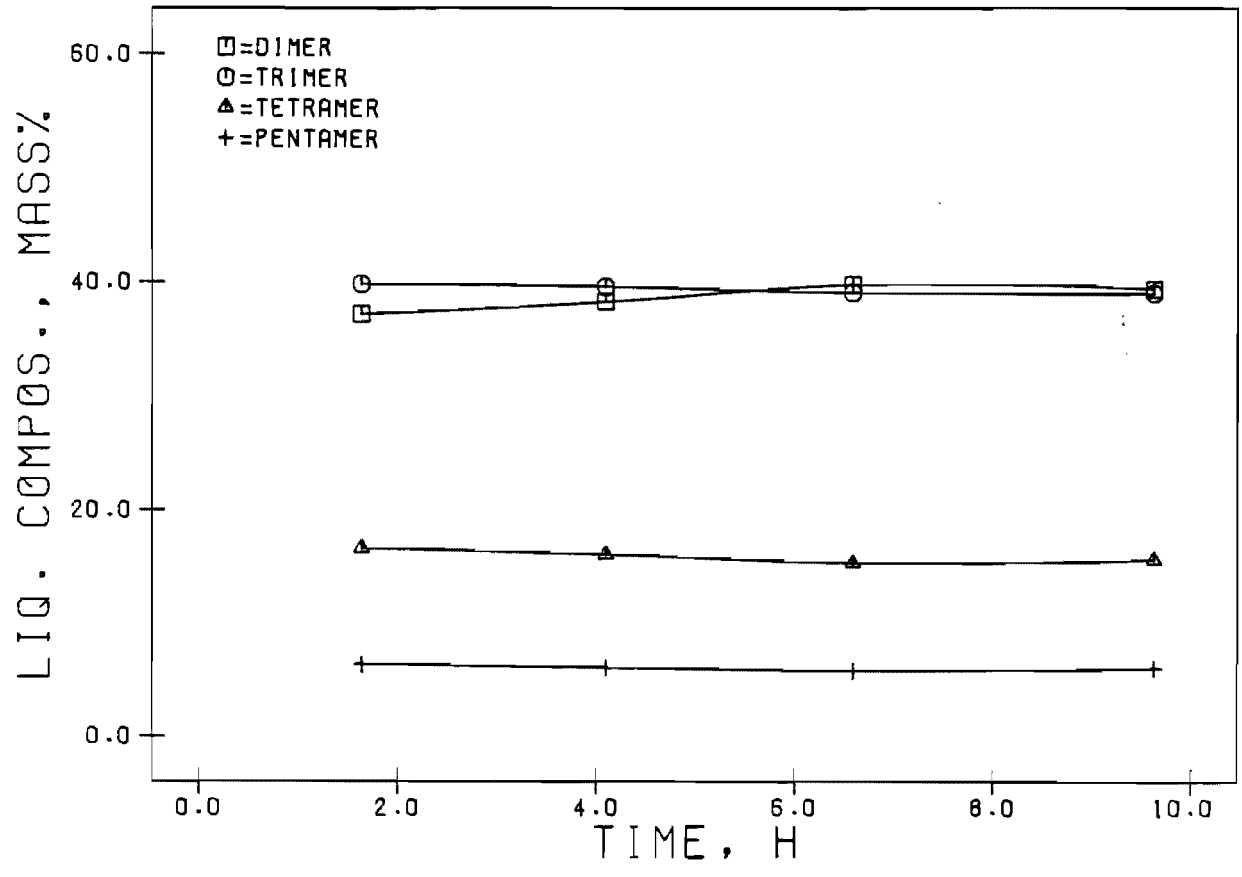

FIG 4.12 LIQUID COMPOSITION (MASS%) VS TIME (H) AT 40 ATM; SG

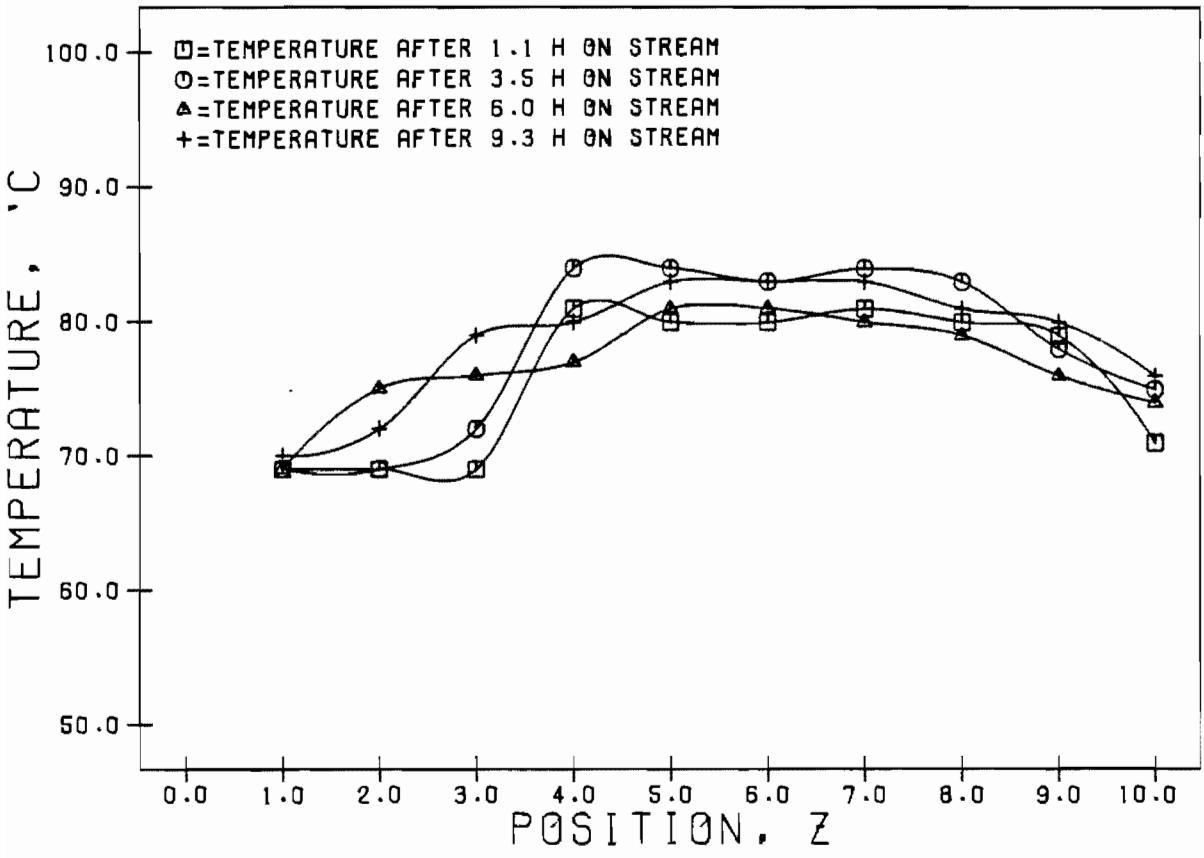

FIG 4.13 BED TEMPERATURE PROFILE ('C) VS POSITION (Z), SET POINT 80'C; SG-1

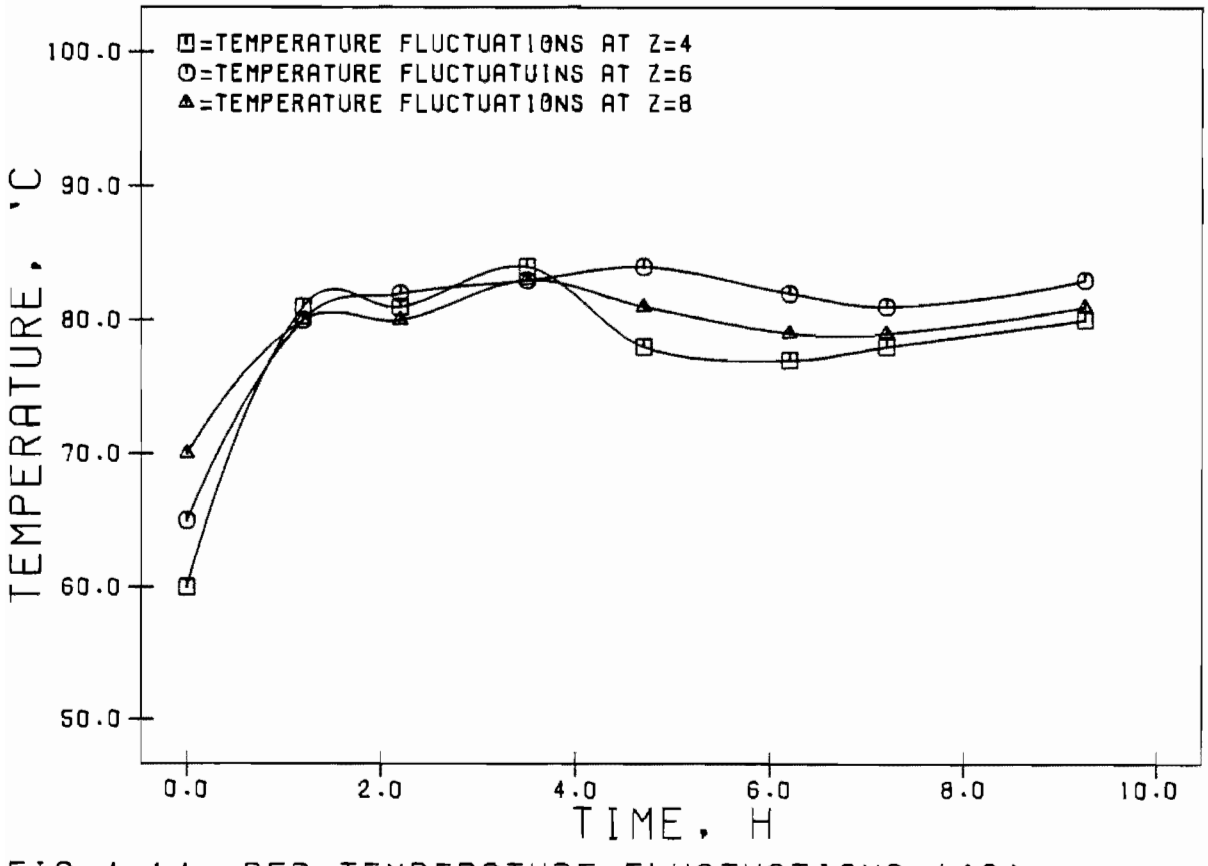

FIG 4.14 BED TEMPERATURE FLUCTUATIONS ('C) VS TIME (H), SET POINT 80'C; SG-1

run was controlled accurately enough to examine the effect of reaction temperature.

In Figure 4.15 the temperature profile through the bed is shown for 3 different times during a run at 210°C. During this run, from positions 4 to 7, i.e., over 75 % of the catalyst bed, the temperature deviation from the set point was less than 5°C at the times shown, while the temperature at position 8 was approximately 10°C below that of the rest of the bed. In Figure 4.16 the temperature variation with time at 3 different positions in the bed is shown. Excluding the start-up period, the amplitude of the temperature fluctuations with time at positions 4 and 6 was 3°C while the amplitude of the temperature fluctuations at position 8, although approximately 10°C below the set point, was 2°C. Thus, although a deviation from the set point existed at 210°C, the profile did not change markedly with time on stream.

4.4.1 Effect of temperature

The LPR for an HDD type catalyst, with a nickel content of 1.5 wt%, is shown in Figure 4.17 as a function of time on stream at 4 different temperatures. It can be seen from this figure that at 80°C and 40 atm, i.e., when the system was in the liquid phase, the LPR was higher than when the system moved into the vapour phase. As the temperature was raised from 80°C to 150°C a 50% decrease in LPR was observed while the WHSV was lower by 18%. Upon raising the temperature to 200°C a further drop in LPR of 10% was recorded although the WHSV was higher by 14%. At 210°C the high WHSV used makes a meaningful comparison impossible. However, from the recorded LPR it can be concluded that the activity of the catalysts decreased further.

Figure 4.18 shows liquid composition as both a function of time on stream and temperature. Increasing the temperature and moving into the vapour phase caused a dramatic drop in the dimer yield and an increase in trimer yield. Increasing the temperature still further resulted in the dimer recovering until at 210°C dimers and trimers were formed in equal quantities.

As at higher temperatures, i.e., above 150°C at 40 atm, silica alumina exhibits catalytic properties, the relationship between its activity and temperature was also examined. In Figure 4.19 the LPR as a function of time on stream is plotted for SA at 3 different temperatures. Reducing the temperature from 200°C to 150°C resulted in the maximum activity

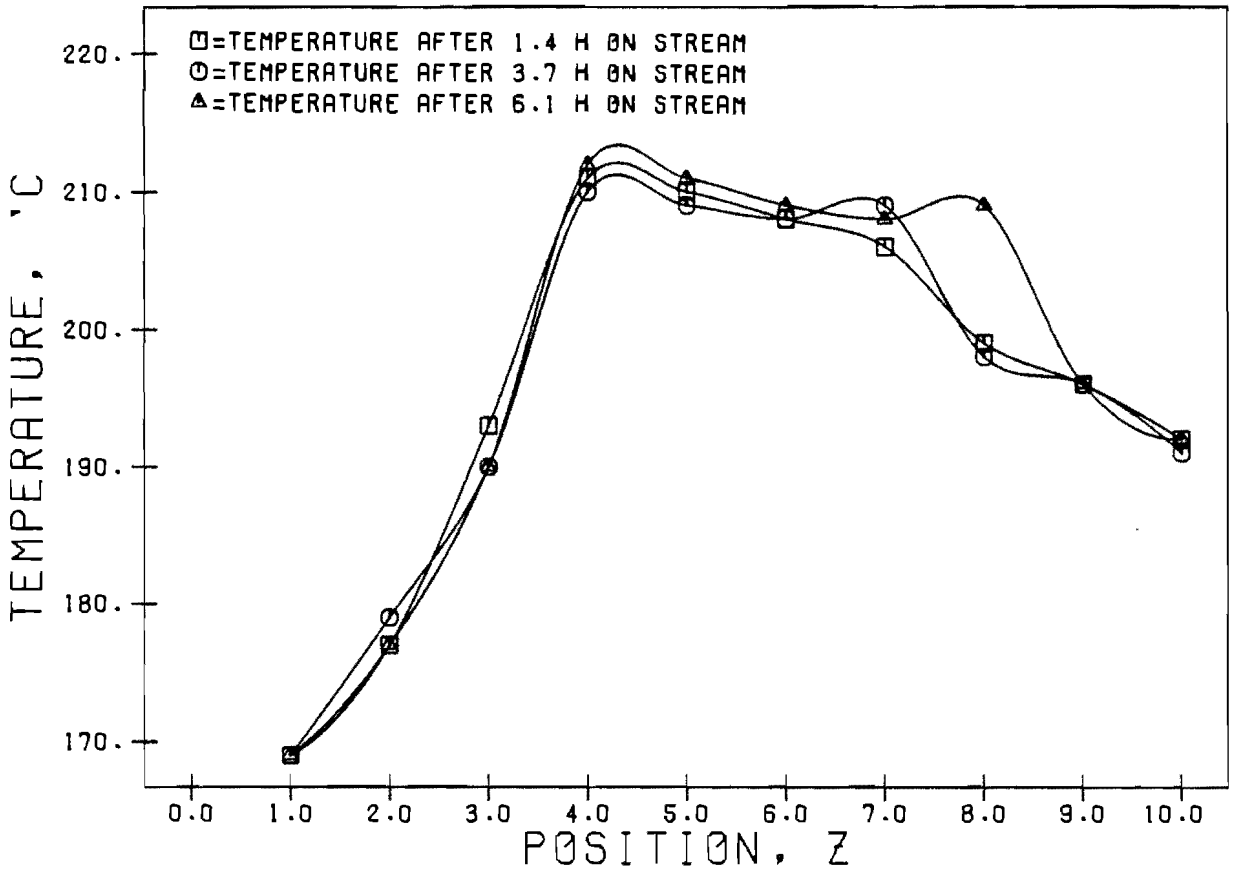

FIG 4.15 BED TEMPERATURE PROFILE ('C) VS POSITION (Z), SET POINT 210'C; HDD-9

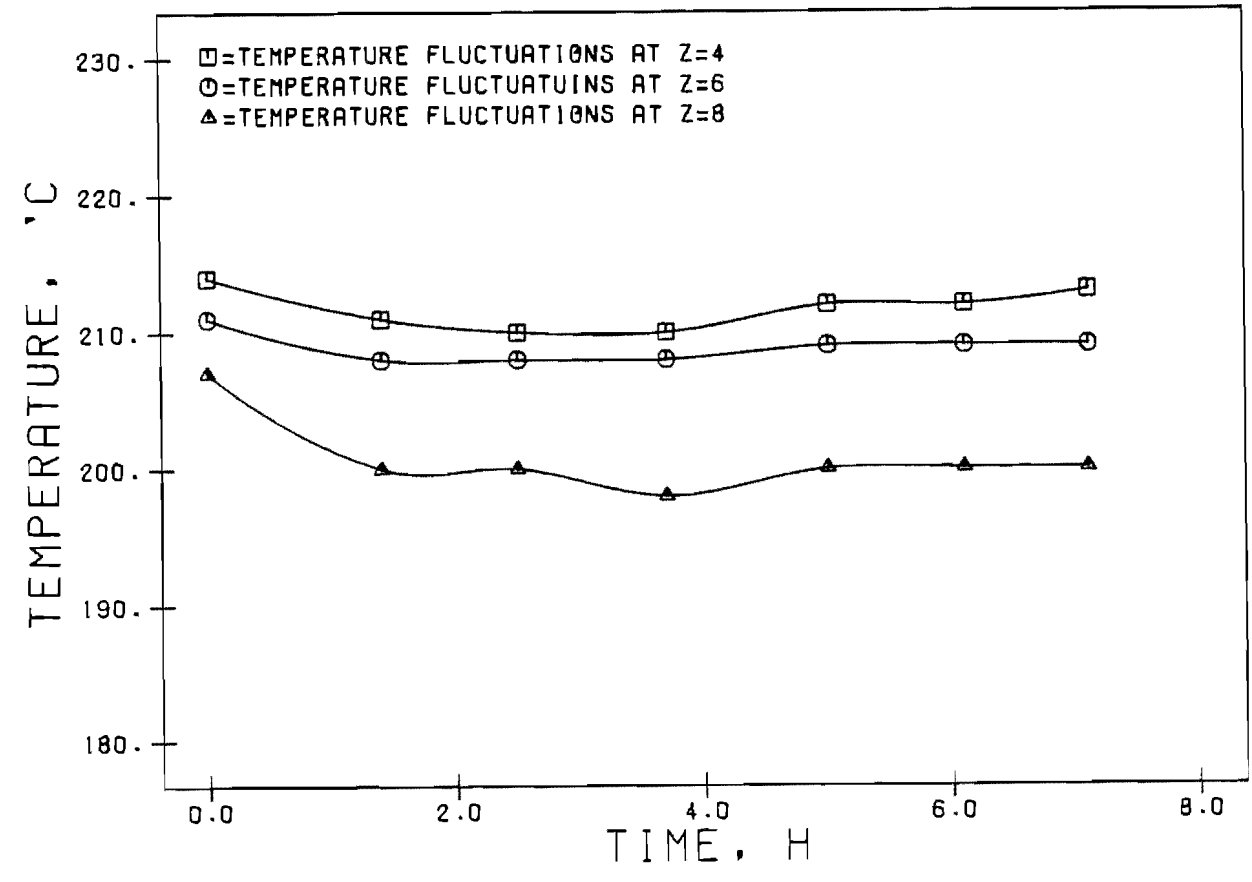

FIG 4.16 BED TEMPERATURE FLUCTUATIONS ('C) VS TIME (H), SET POINT 210'C; HDD-9

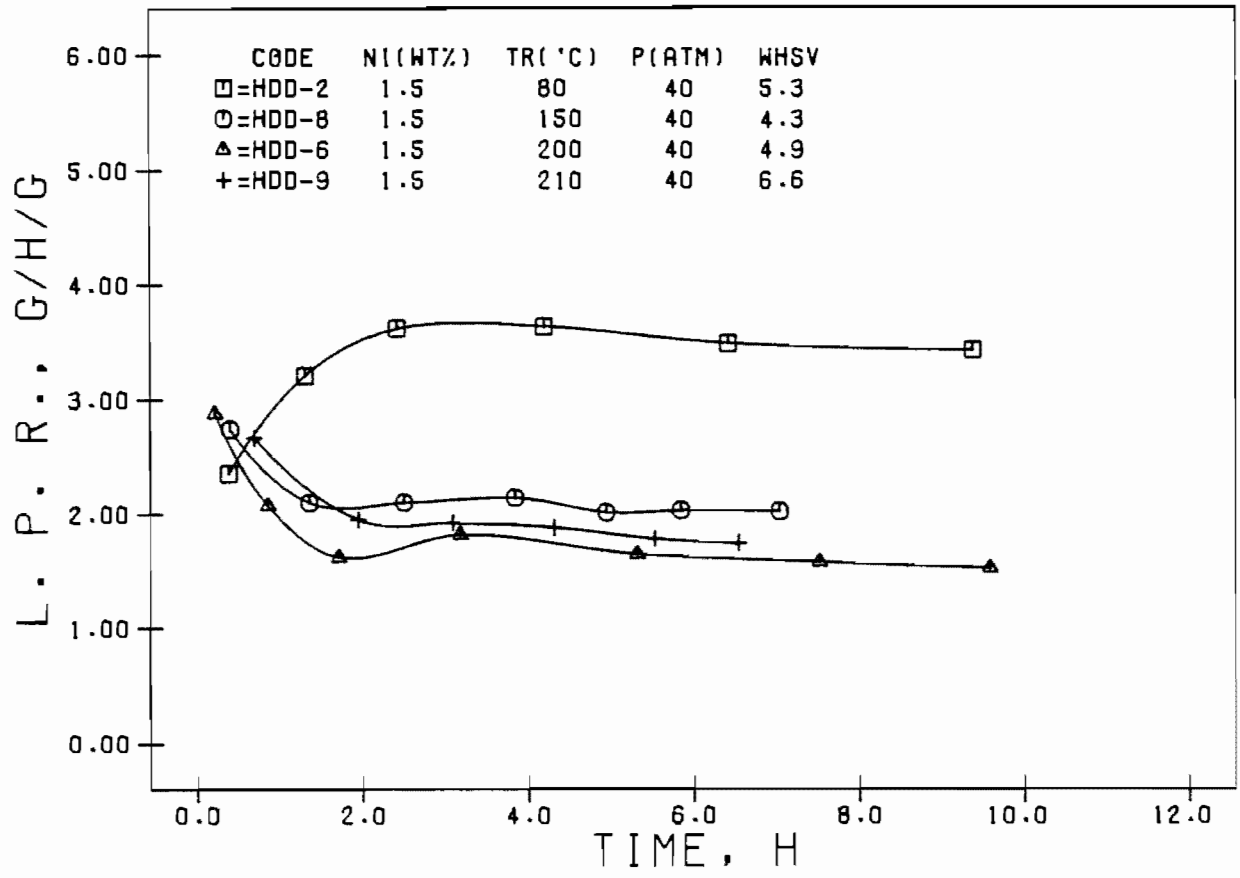

FIG 4.17 EFFECT OF TEMPERATURE ('C) ON LIQUID PRODUCTION RATE (G/H/G); HDD

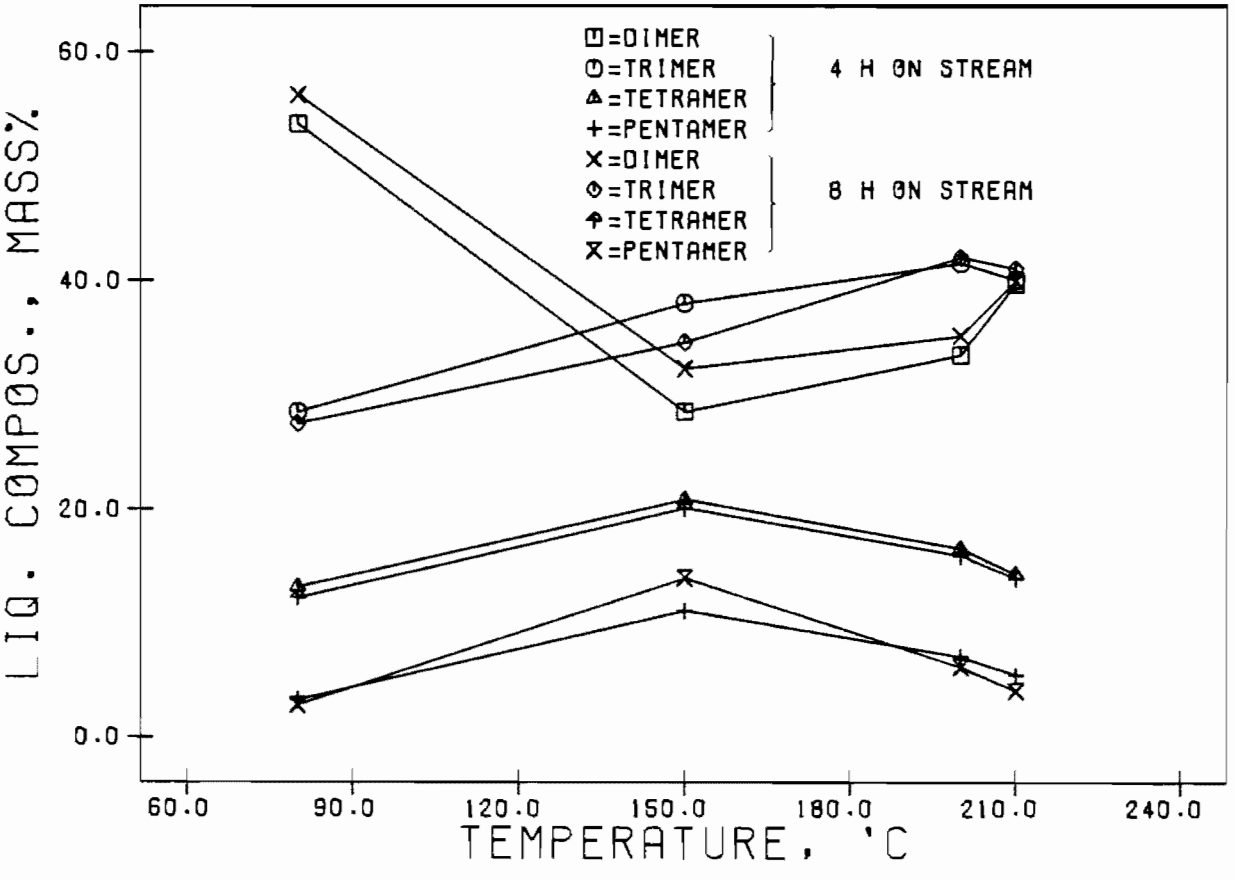

FIG 4.18 EFFECT OF TEMPERATURE ('C) ON LIQUID COMPOSITION (MASS%); HDD

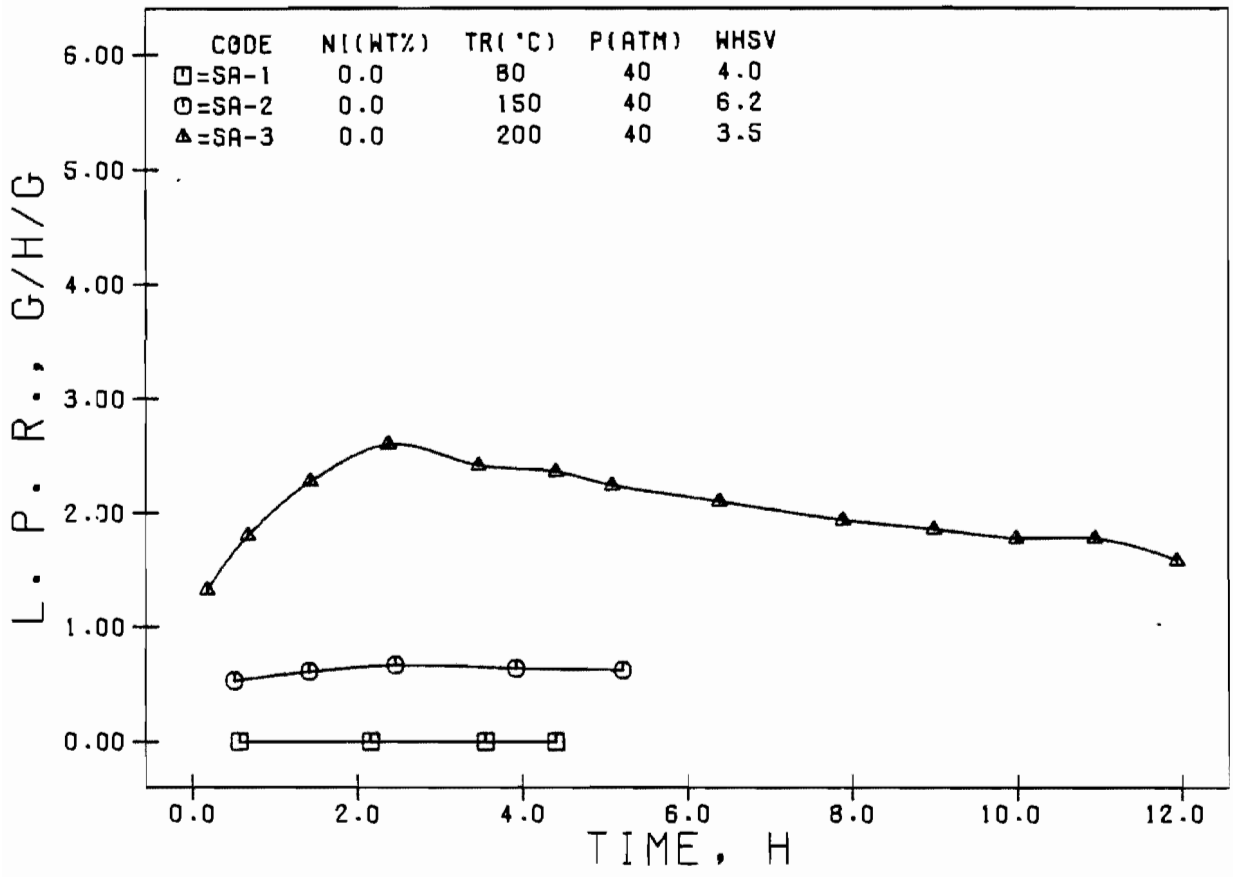

FIG 4.19 EFFECT OF TEMPERATURE ('C) ON LIQUID PRODUCTION RATE (G/H/G); SA

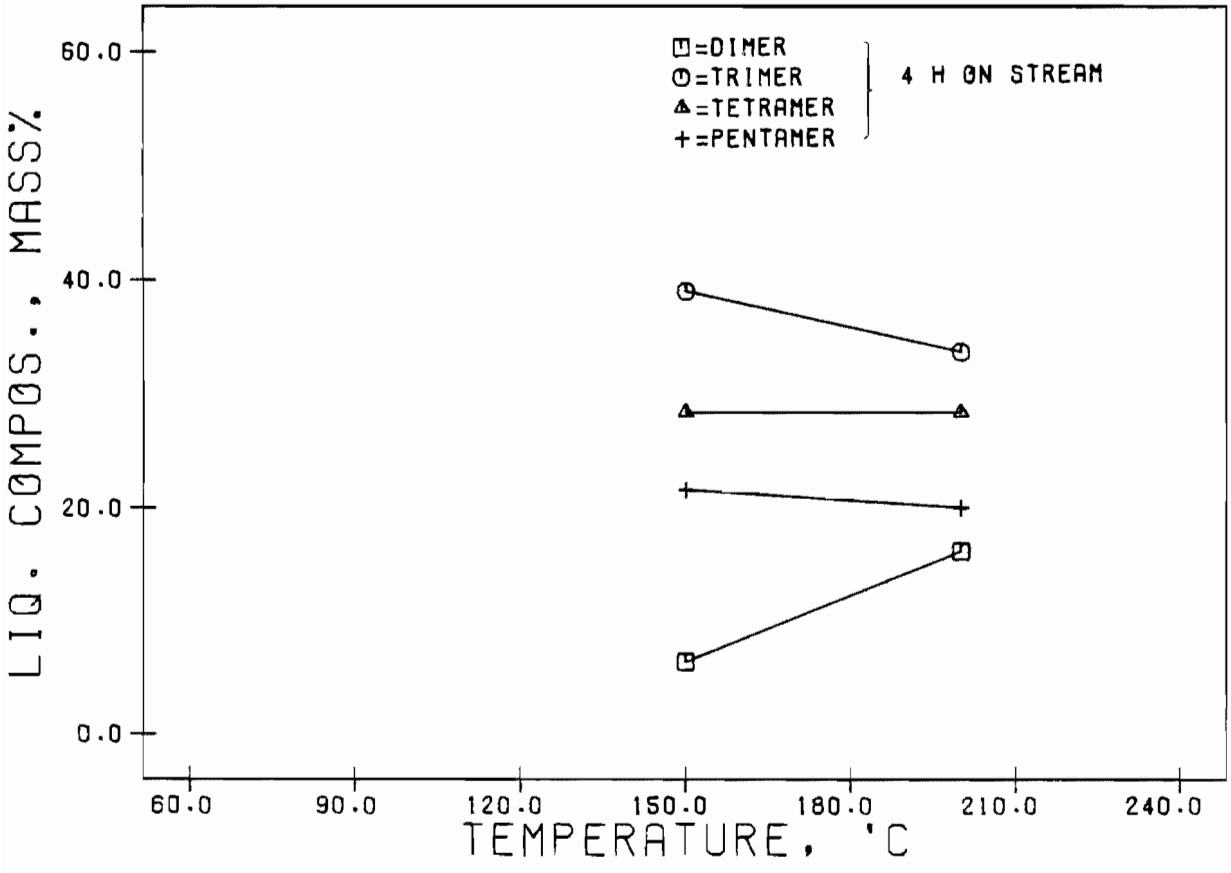

FIG 4.20 EFFECT OF TEMPERATURE ('C) ON LIQUID COMPOSITION (MASS%); SA

falling by approximately 72% while the WHSV increased by 55%. At 80°C the catalyst was inert. At 200°C the preferential product of silica alumina was propene trimer, which can be seen in Figure 4.20 where liquid composition is plotted against temperature. Decreasing the temperature to 150°C caused the trimer yield to increase at the expense of the dimer. Decreasing the temperature further resulted in the catalyst becoming inert, and so no liquid data was available.

4.5 Lifetime and selectivity

The lifetimes of HDD, IMP, SG and SA type catalyst were examined as well as their selectivity in long runs. In Figure 4.21 the LPR and WHSV as a function of time are plotted for an HDD type catalyst with a nickel content of 1.5 wt%. From this it can be seen that the LPR fluctuated with time due to WHSV fluctuations. Upon comparing points with equal WHSV it was found that the conversion had dropped by 12% after 100 h on stream. The selectivity with time on stream is shown in Figure 4.22. Selectivity changed slightly during the run, i.e., the quantity of dimer formed increased by 25% after 120 h at the expense of the tetramer and pentamer.

In Figure 4.23 the LPR as a function of time is plotted for an IMP type catalyst with a nickel content of 1.9 wt%. After 8 h on stream the activity of the catalyst dropped by 24% of its initial value. The selectivity, shown in Figure 4.24, remained approximately constant with the dimer yield increasing slightly at the expense of the tetramer and pentamer over the period of the run.

In Figure 4.25 the LPR as a function of time is plotted for an SG type catalyst with a nickel content of 1.5 wt%. After 10 h on stream the catalyst showed no signs of deactivation. The selectivity, shown as a function of time in Figure 4.26, also showed no changes over this period. Consequently, from the available data, no conclusive statement with respect to the lifetime of this catalyst could be made.

The lifetime of a SA type catalysts was examined at a temperature of 200°C and the LPR as a function of time is shown in Figure 4.27. Upon comparing points with equal WHSV it was found that the conversion had dropped by 24% over a period of 7.5 h. As shown in Figure 4.28 no significant change occurred in the selectivity over the period of this run.

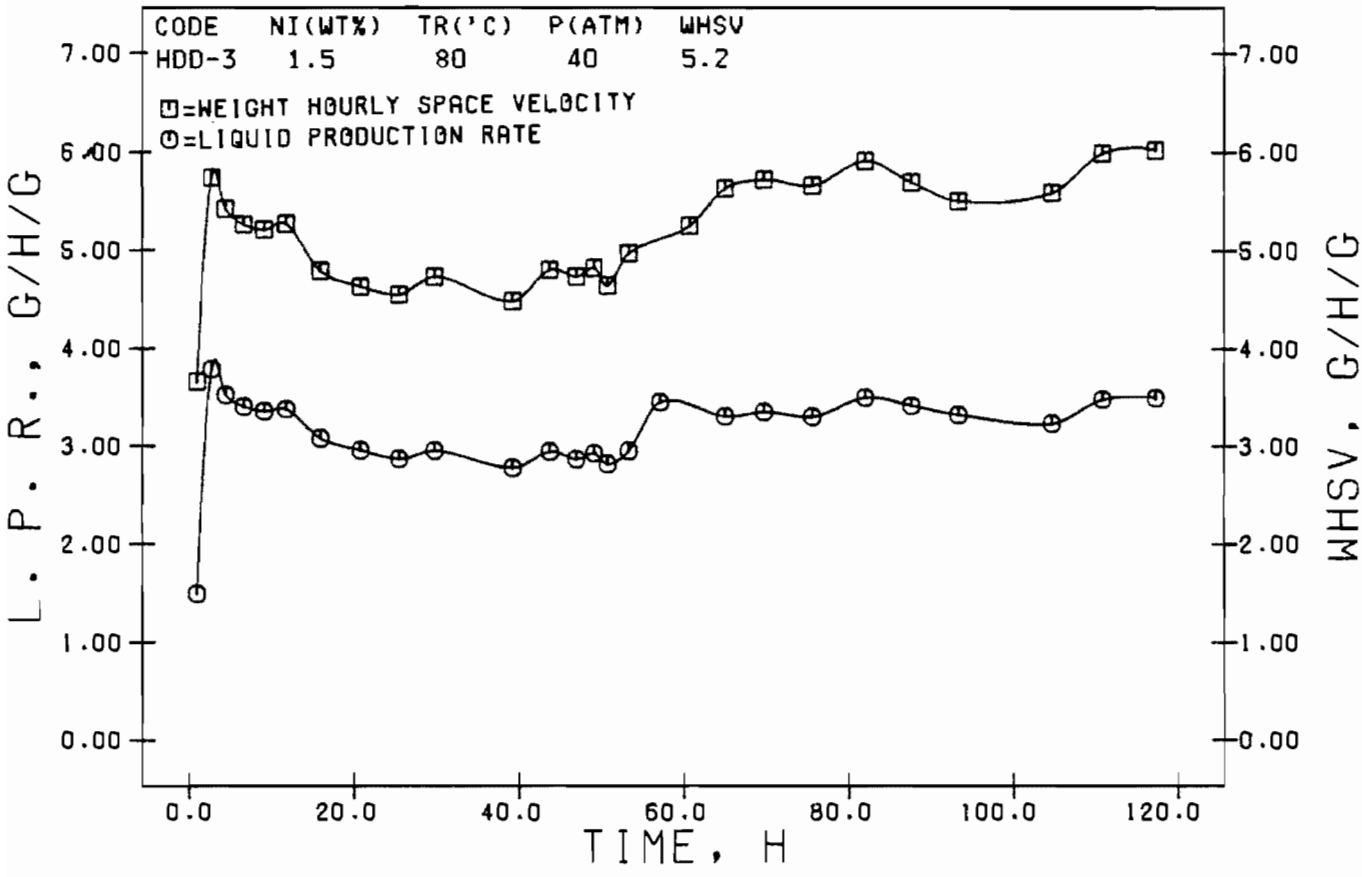

FIG 4.21 LIQUID PRODUCTION RATE (G/H/G) AND WEIGHT HOURLY SPACE VELOCITY (G/H/G) VS TIME (H) FOR HDD-3

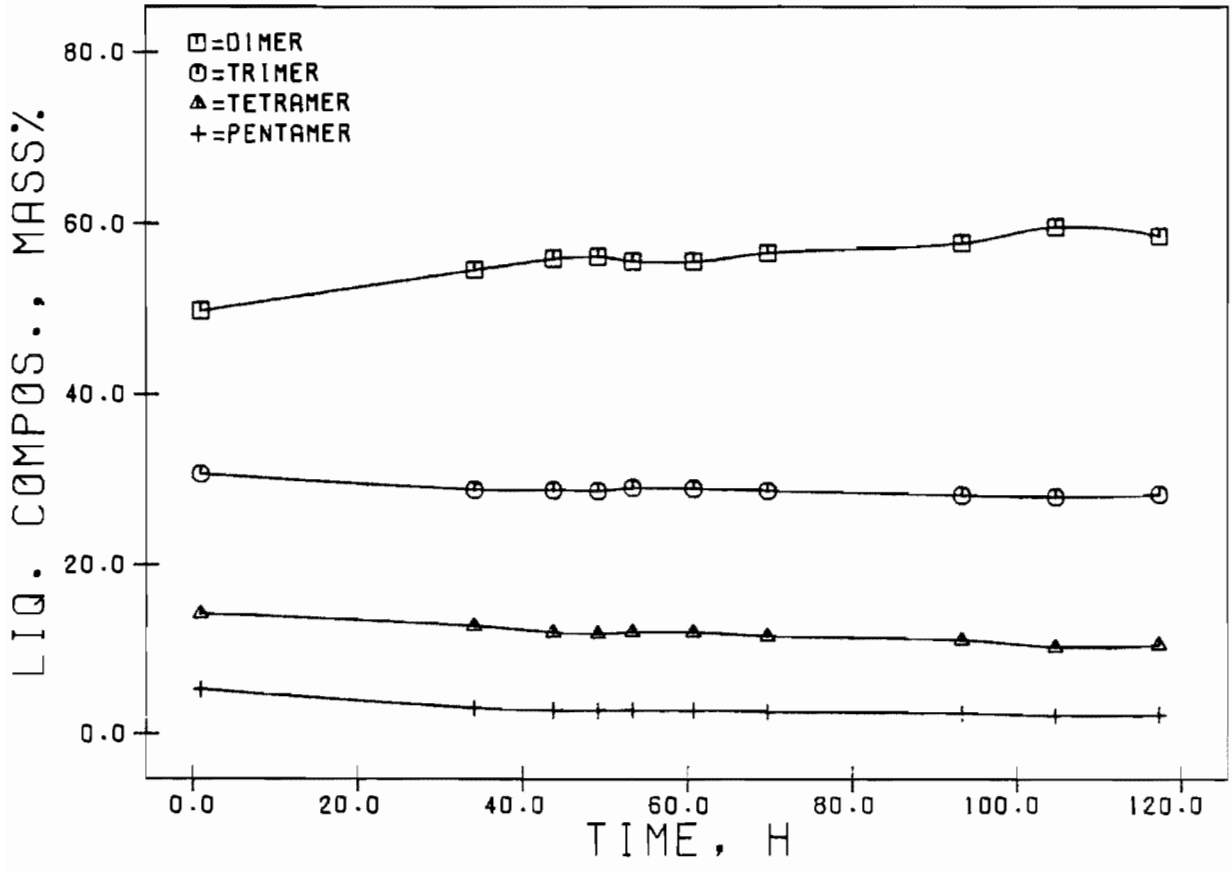

FIG 4.22 LIQUID COMPOSITION (MASS%) VS TIME (H) FOR HDD-3

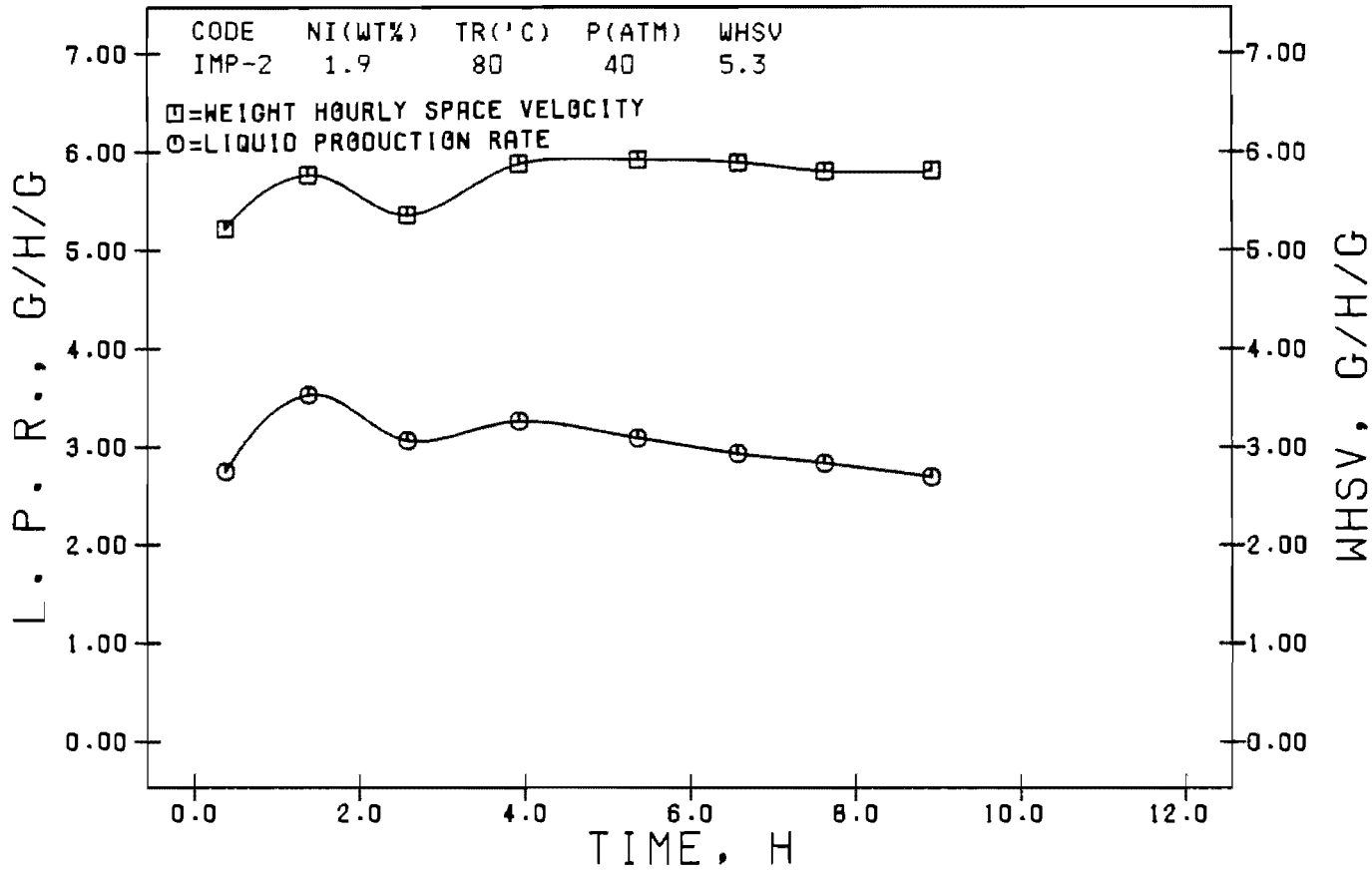

FIG 4.23 LIQUID PRODUCTION RATE (G/H/G) AND WEIGHT HOURLY SPACE VELOCITY (G/H/G) VS TIME (H) FOR IMP-2

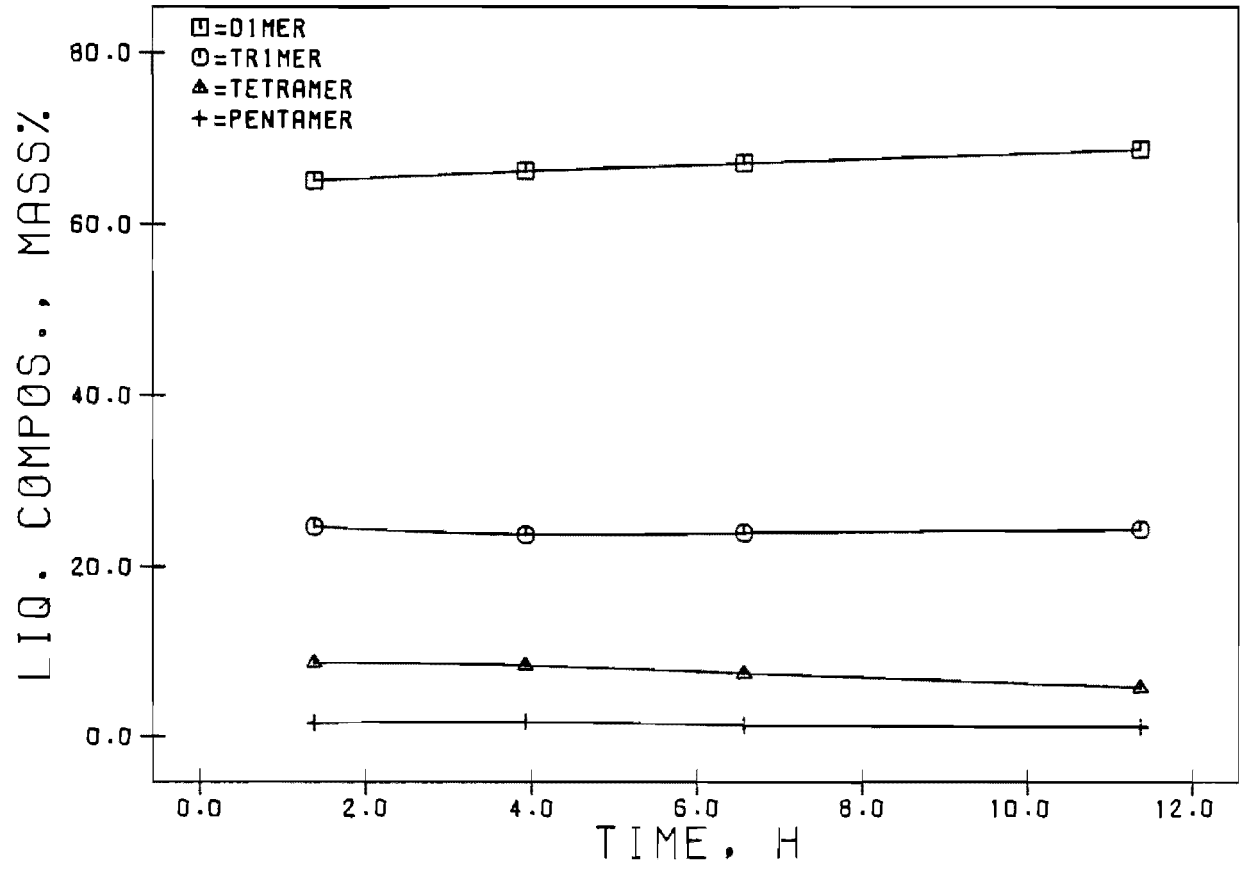

FIG 4.24 LIQUID COMPOSITION (MASS%) VS TIME (H) FOR IMP-2

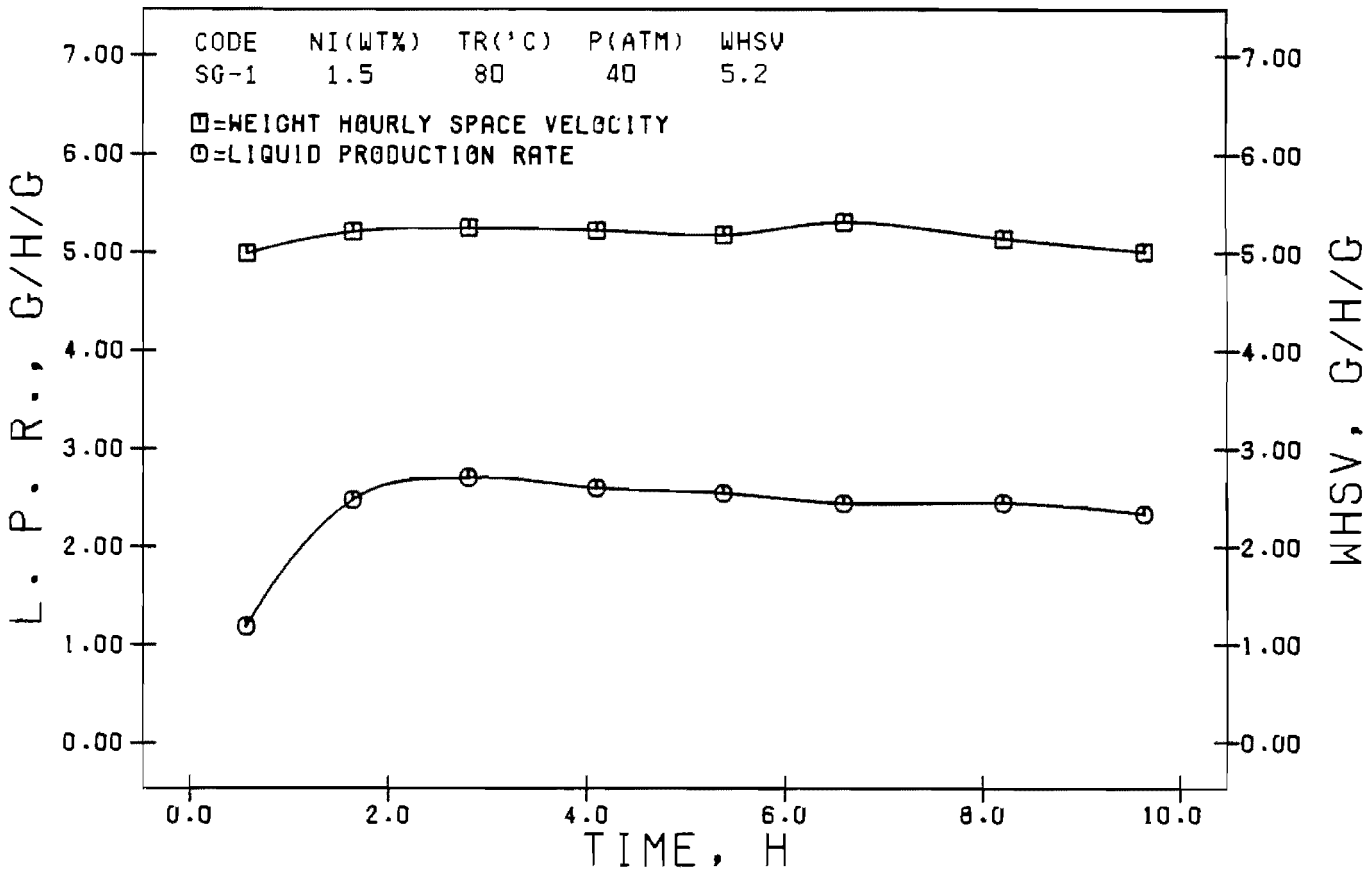

FIG 4.25 LIQUID PRODUCTION RATE (G/H/G) AND WEIGHT HOURLY SPACE VELOCITY (G/H/G) VS TIME (H) FOR SG-1

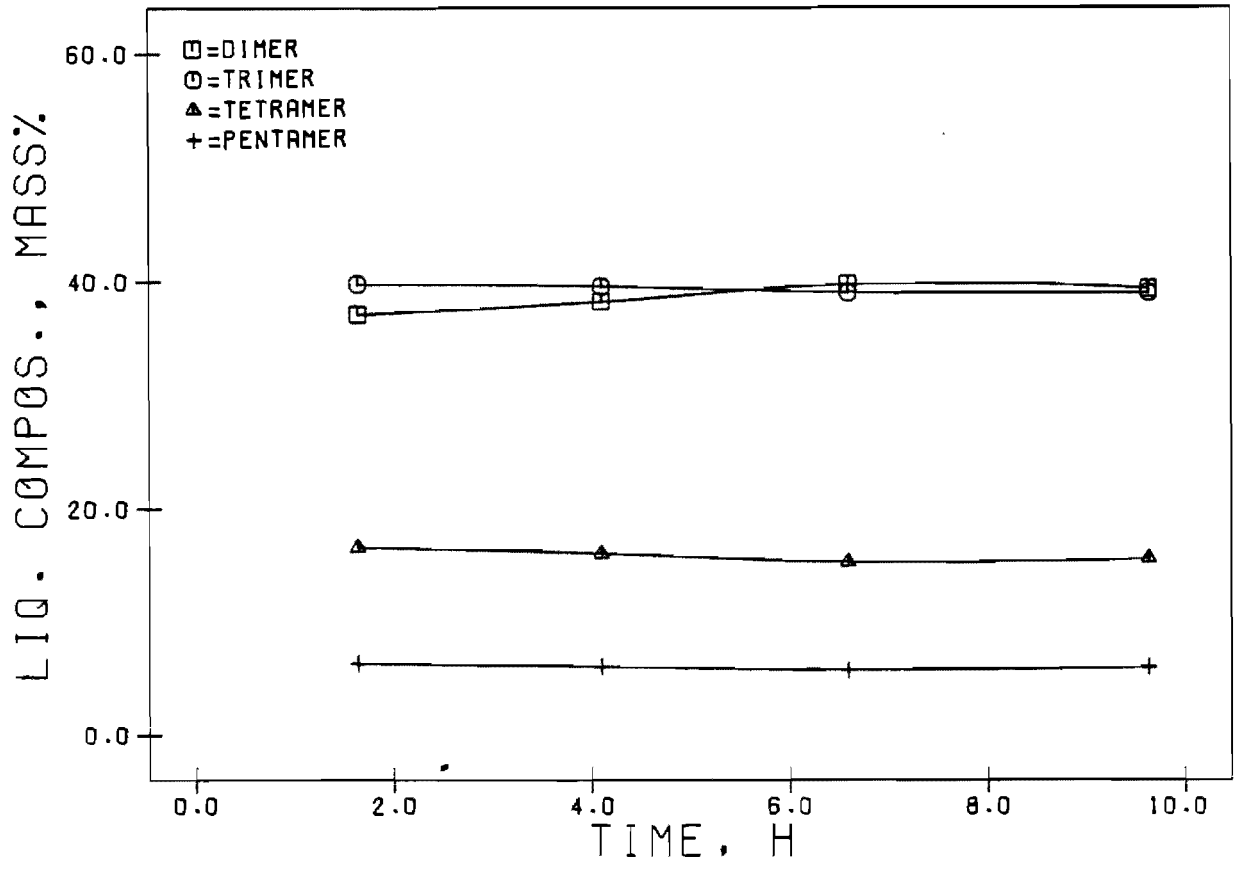

FIG 4.26 LIQUID COMPOSITION (MASS%) VS TIME (H) FOR SG-1

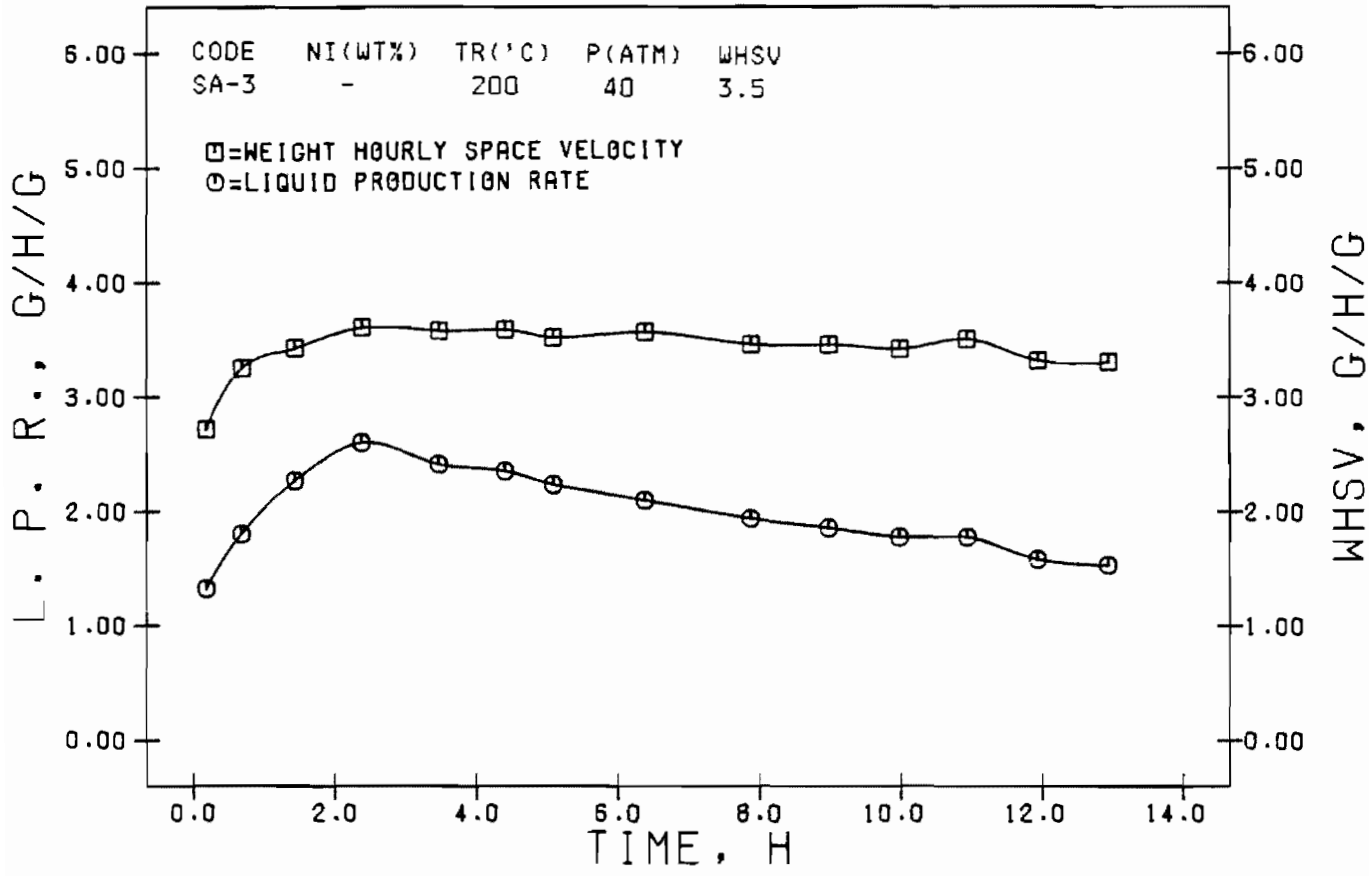

FIG 4.27 LIQUID PRODUCTION RATE (G/H/G) AND WEIGHT HOURLY SPACE VELOCITY (G/H/G) VS TIME (H) FOR SA-3

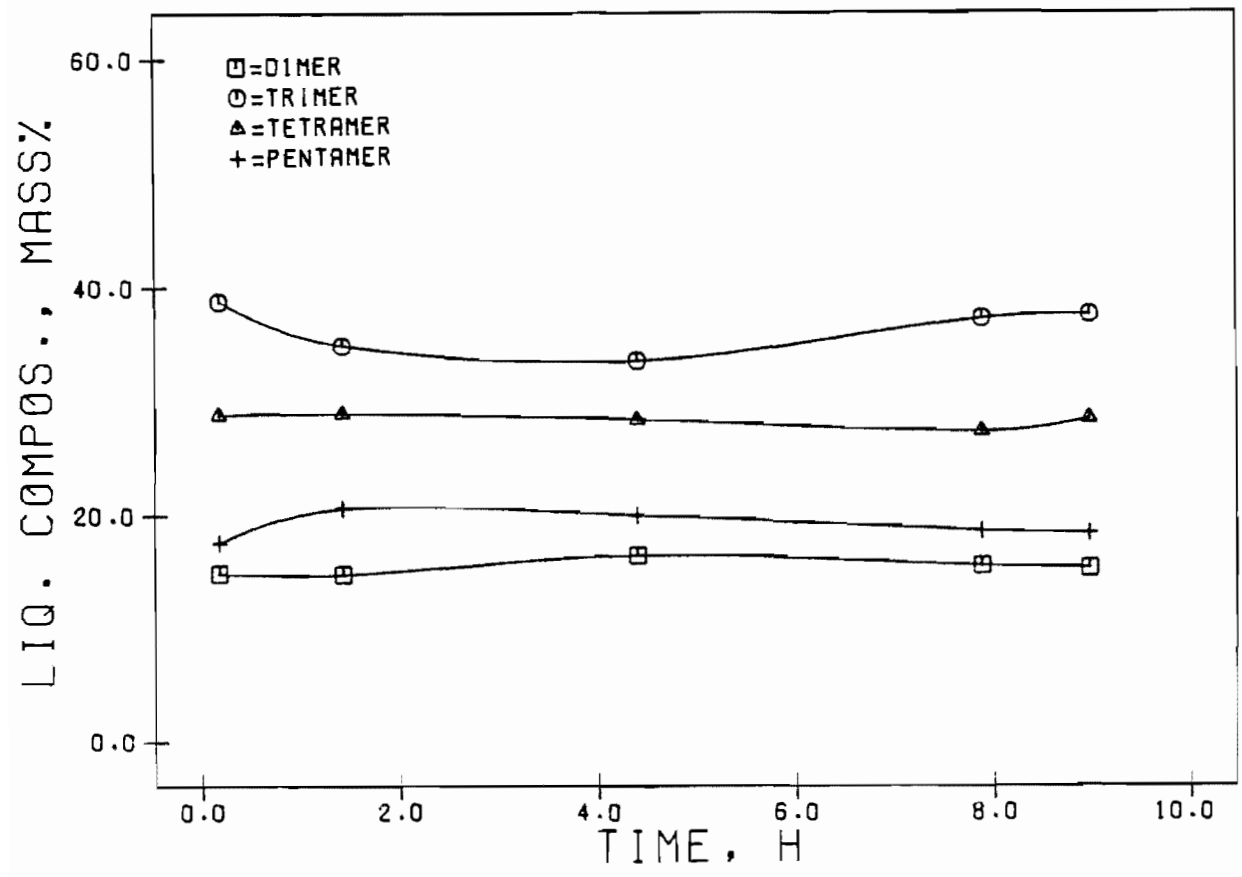

FIG 4.28 LIQUID COMPOSITION (MASS%) VS TIME (H) FOR SA-3

4.6 Effect of WHSV

The effect of the WHSV on the LPR and selectivity was examined. In Figure 4.29 the LPR of an HDD type catalyst with a nickel content ranging from 11.3 to 11.7 wt% is shown at four different WHSV. Figure 4.29 shows that increasing the WHSV increased the LPR and the rate of deactivation.

In Figure 4.30 the selectivity as a function of both time and WHSV is shown. This figure demonstrates how increasing the WHSV and consequently decreasing the conversion resulted in a higher dimer content of the liquid product at the expense of the tetramer and the pentamer. The quantity of trimer was not affected by changing WHSV in the range examined.

4.7 Effect of temperature runaway

The effect of operating the catalyst at 80°C was examined after operating it at 200°C. The aim of this experiment was to establish whether the activity or selectivity of the catalyst when rerun at 80°C was affected in any way by operating it first at a temperature higher than 80°C. Between the two runs the catalyst was calcined in the normal manner.

In Figure 4.31 the LPR of an HDD type catalyst with a nickel content of 1.5 wt% at 200°C is shown as a function of time on stream. After 11 h the run was stopped and the catalyst calcined in the normal manner and rerun at 80°C. The LPR as a function of time at 80°C is shown in Figure 4.31, together with the data obtained using a fresh catalyst at 80°C. It can be seen from this figure that using the catalyst first at 200°C did affect the activity and from Figure 4.32 the selectivity, causing a drop in LPR of 17% at steady state, and a shift to lighter products at the expence of the tetramer when the catalyst was re-used at 80°C.

4.8 Effect of water contamination

The aim of this experiment was to establish the effect of water on the activity and selectivity of an HDD type catalyst with a nickel content of 1.5 wt% (HDD-4) and to determine whether the catalyst could be regenerated to its normal activity and selectivity. For this purpose the feed, containing 112 ppm (v/v) water, was not dried before entering the bed and the activity with time was recorded under normal running

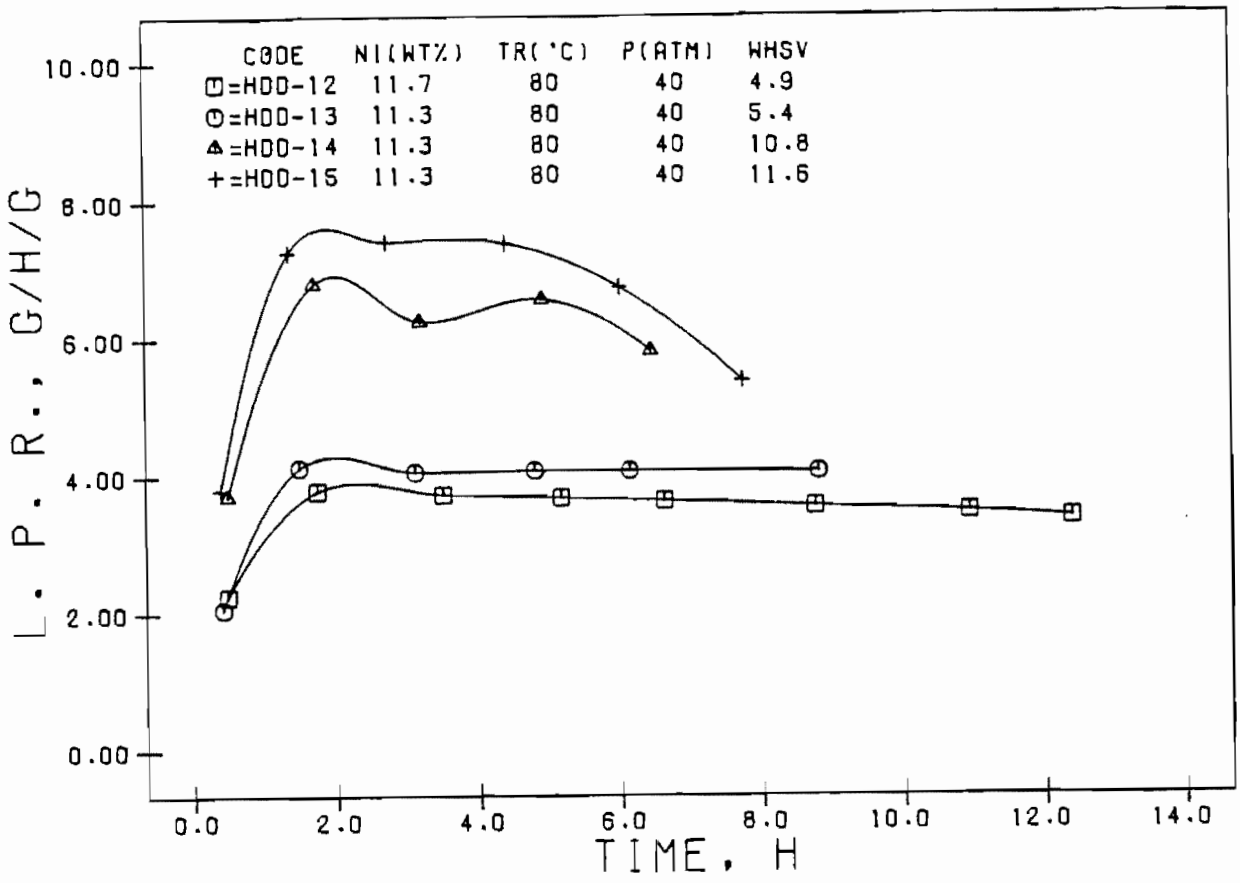

FIG 4.29 EFFECT OF WHSV (G/H/G) ON LIQUID PRODUCTION RATE (G/H/G); HDD

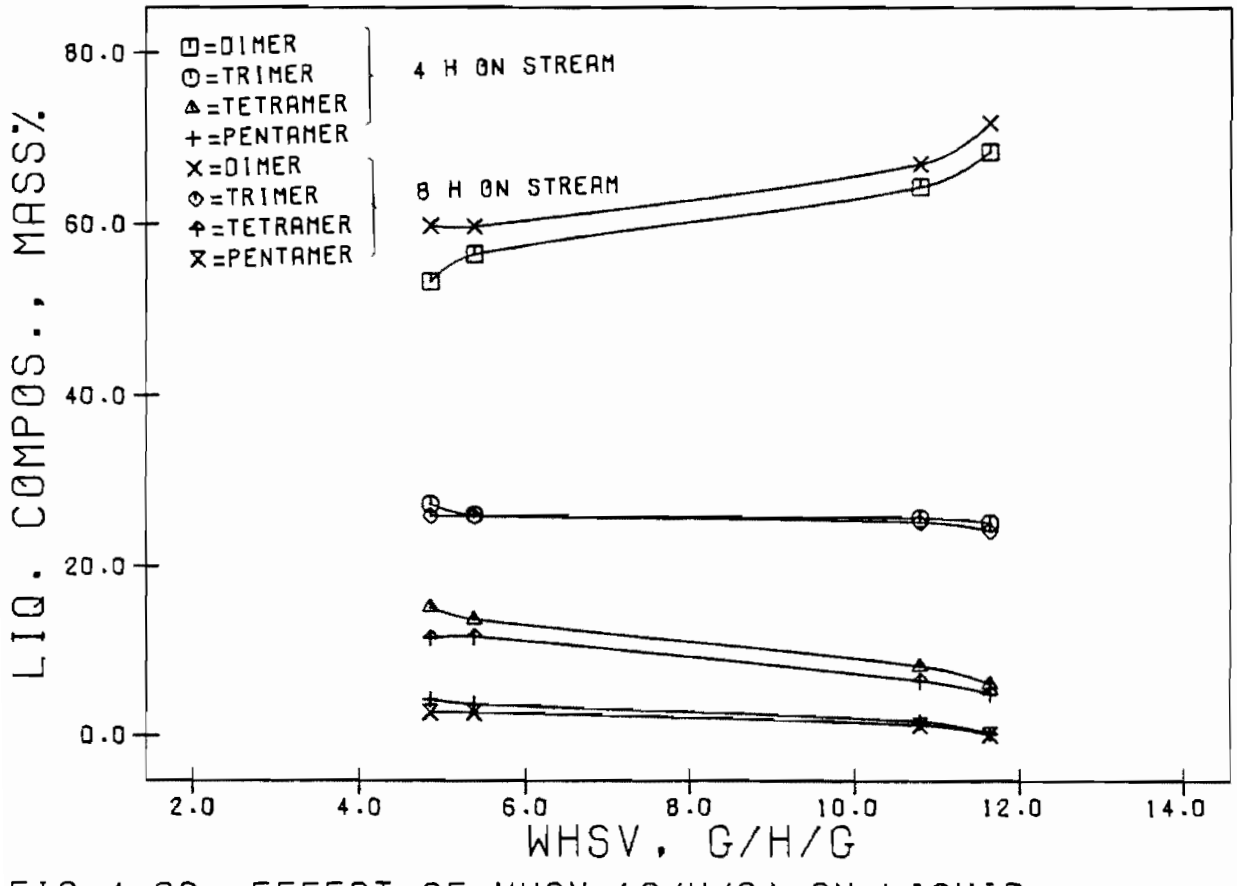

FIG 4.30 EFFECT OF WHSV (G/H/G) ON LIQUID COMPOSITION (MASS%); HDD

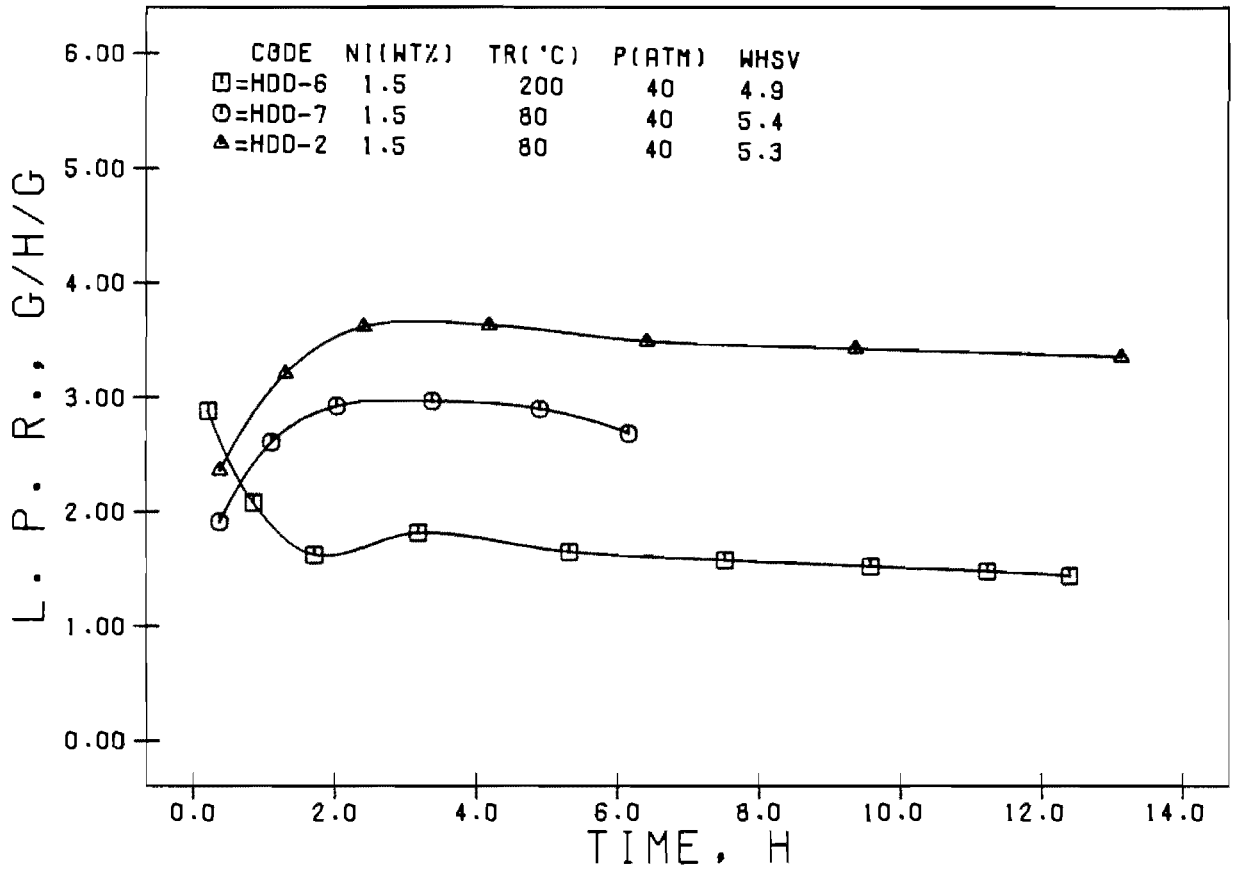

FIG 4.31 EFFECT OF TEMPERATURE RUNAWAY ON LIQUID PRODUCTION RATE (G/H/G); HDD-6 AND HDD-7 CONSECUTIVE RUNS USING SAME CATALYST

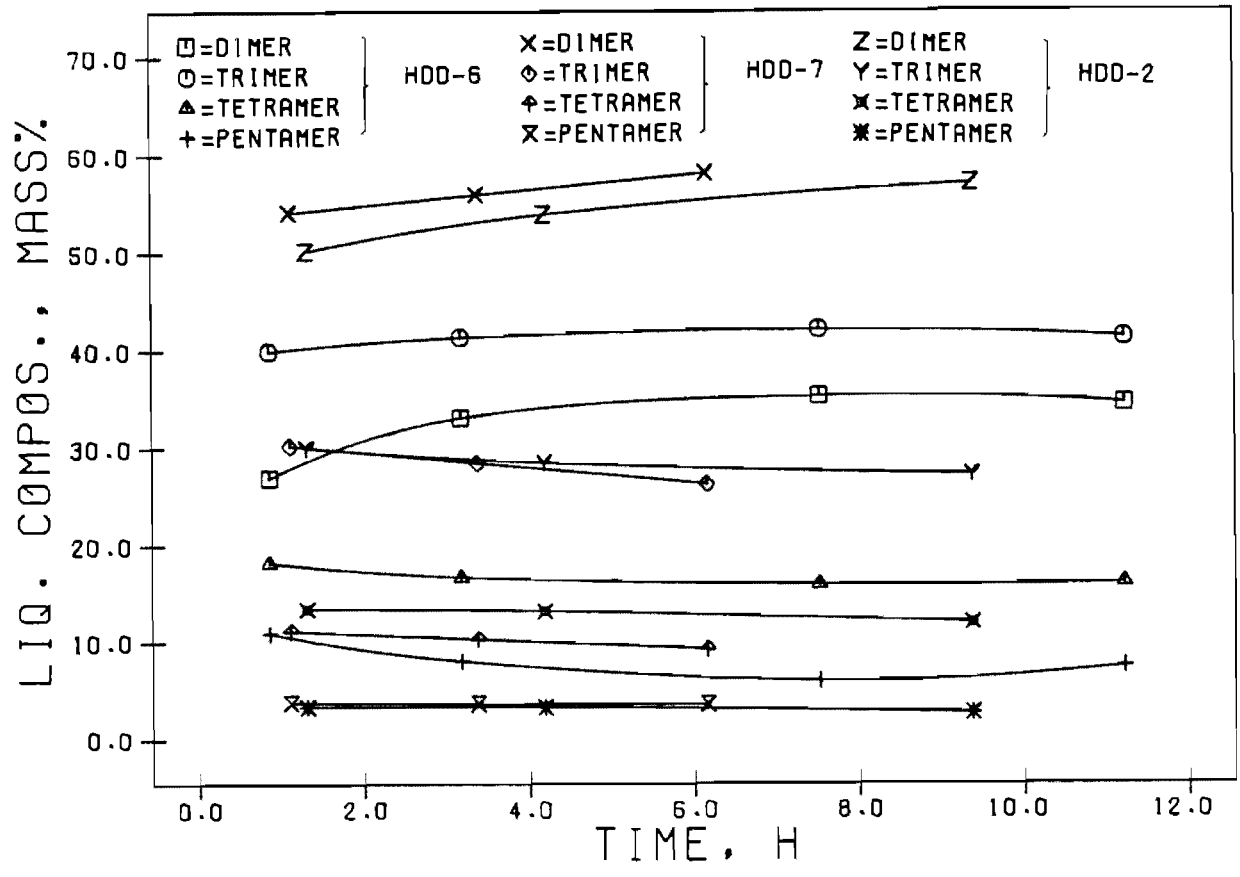

FIG 4.32 EFFECT OF TEMPERATURE RUNAWAY ON LIQUID COMPOSITION (MASS%)

conditions. It can be seen from Figure 4.33 how rapidly the catalyst deactivated, becoming totally inert in 4 h. The selectivity as shown in Figure 4.34 was also affected with the dimer rapidly becoming the main product.

Upon regenerating and operating the catalyst in the normal manner, (HDD-5) the catalyst showed an initial LPR higher than in HDD-1, due to a high WHSV which rapidly dropped to that of a catalyst in a dry run. For comparison the LPR vs time relation for a dry run using a fresh catalyst is also shown in Figure 4.33 (HDD-1). With regard to selectivity, no difference was observed for the regenerated or normal catalyst as shown in Figure 4.34.

4.9 Liquid feed (C_6)

In this experiment the -69°C fraction (dimer) from previous runs was fed through the reactor at 40 atm and 80°C. Once the catalyst had deactivated the temperature was raised to 200°C and the run continued. The catalyst used was a HDD type catalyst with a nickel content of 1.5 wt%. The feed composition was 99.4 wt% C_6 and 0.6 wt% C_3

To monitor the activity of the catalyst throughout the run, the LPR was calculated using

$$\text{LPR} = \frac{(\text{mass } C_{n=6} \text{ in} - \text{mass of } C_{n=6} \text{ out})}{(\text{time}) \cdot (\text{mass of catalyst})} \qquad \text{(I)}$$

while the conversion was calculated using

$$\text{Mass\% } C_{n=6} \text{ converted} = \left[\frac{(\text{mass } C_{n=6} \text{ in} - \text{mass } C_{n=6} \text{ out})}{\text{mass } C_{n=6} \text{ in}}\right] \cdot 100 \qquad \text{(II)}$$

It can be seen from Figure 4.35 that at 80°C the catalyst rapidly lost its activity. This also became apparent from the changes in the liquid composition with time on stream as shown in Figure 4.36. Upon raising the temperature to 200°C the catalyst regained activity, the conversion being 64% after 2.7 h on stream. The composition of the liquid product also changed markedly, the most abundant species in the product being a C_6 dimer (C_{12}) with trace quantities of C_{15} and trimer (C_{18}).

4.10 Liquid and gas feed (C_6 + C_3)

In this case, dimer (C_6) and monomer (C_3) were fed simultaneously to the reactor. The ratio of C_6 to C_3 was held at 1.1 g C_6/g C_3 throughout. Two runs using the same catalyst were carried out, one at 80°C and one at

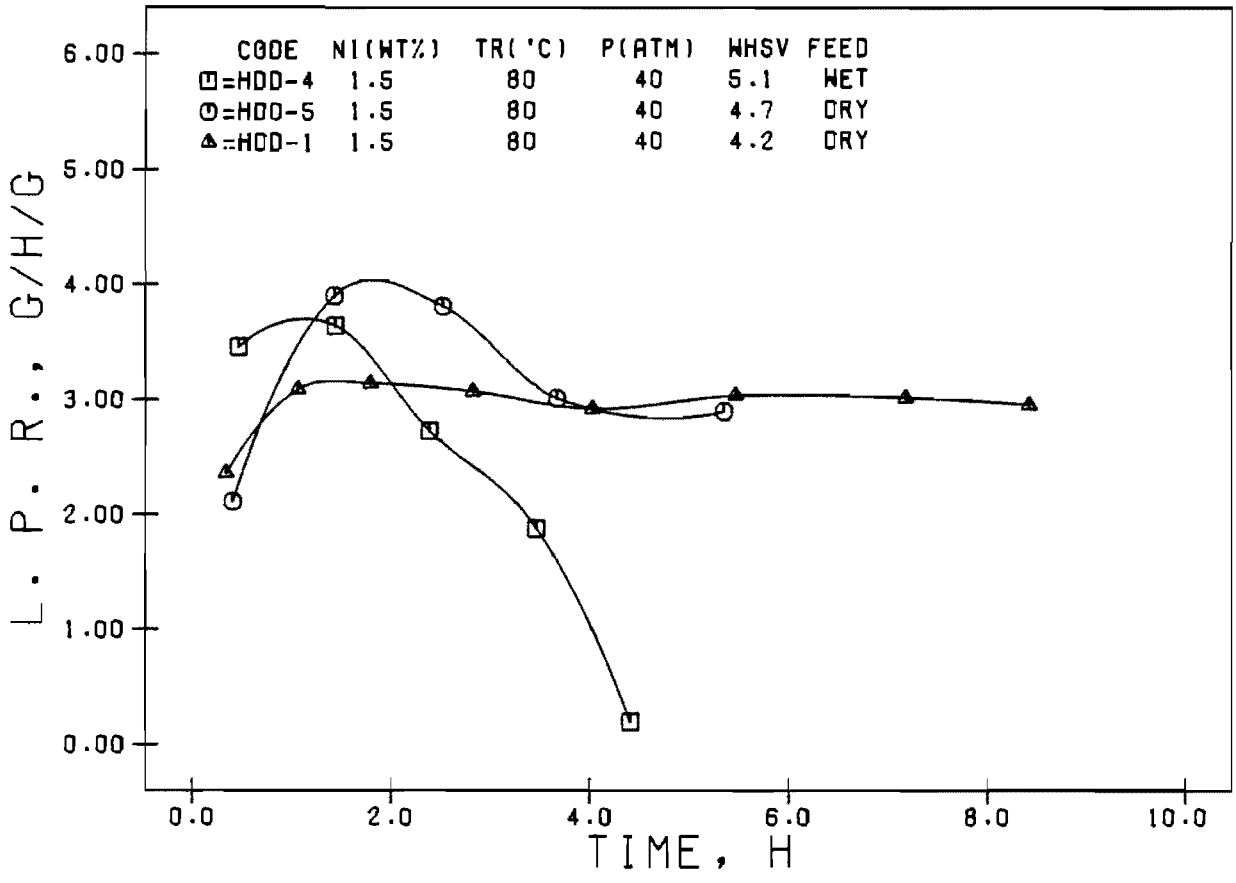

FIG 4.33 EFFECT OF WATER ON LIQUID PRODUCTION RATE (G/H/G); HDD-5 REGENERATION AFTER HDD-4

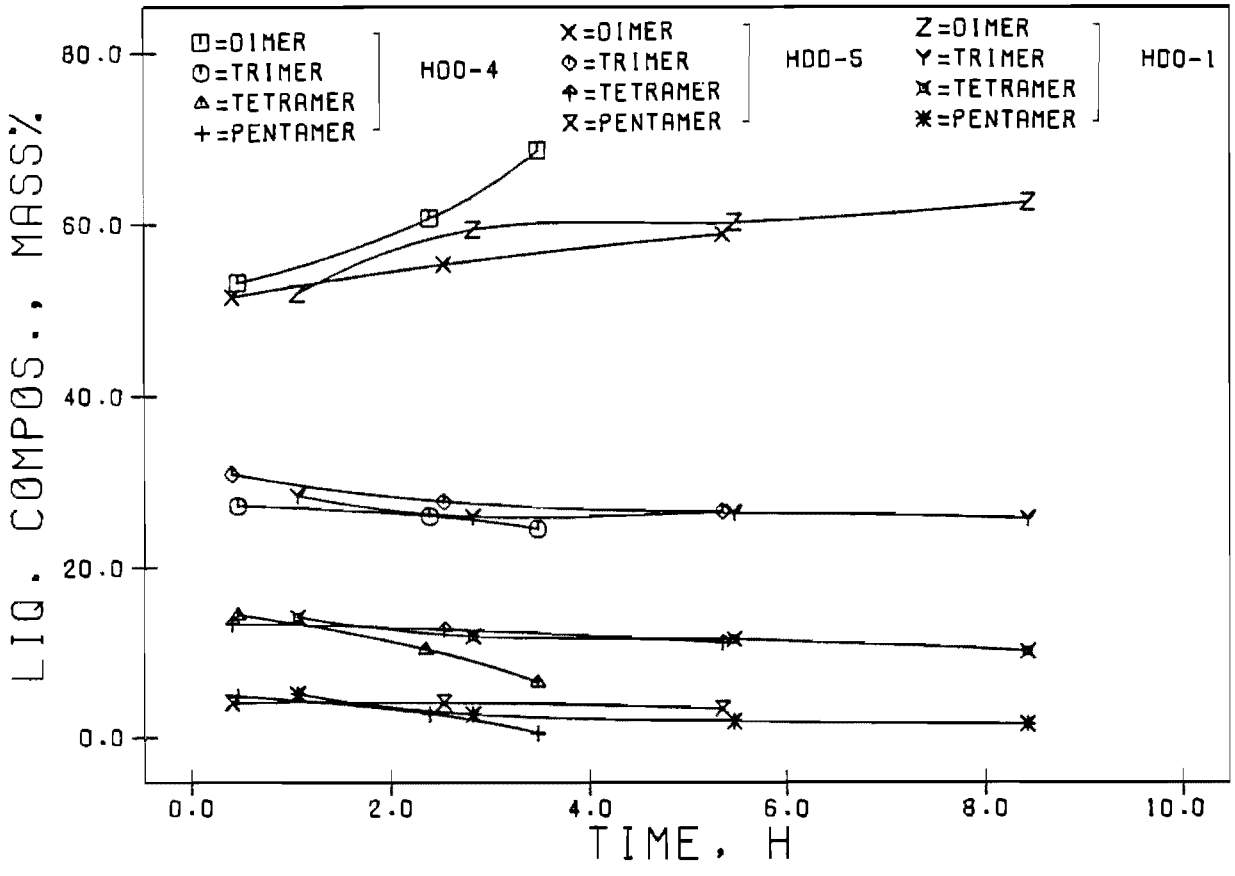

FIG 4.34 EFFECT OF WATER CONTAMINATION ON LIQUID COMPOSITION (GR/H/GR); HDD

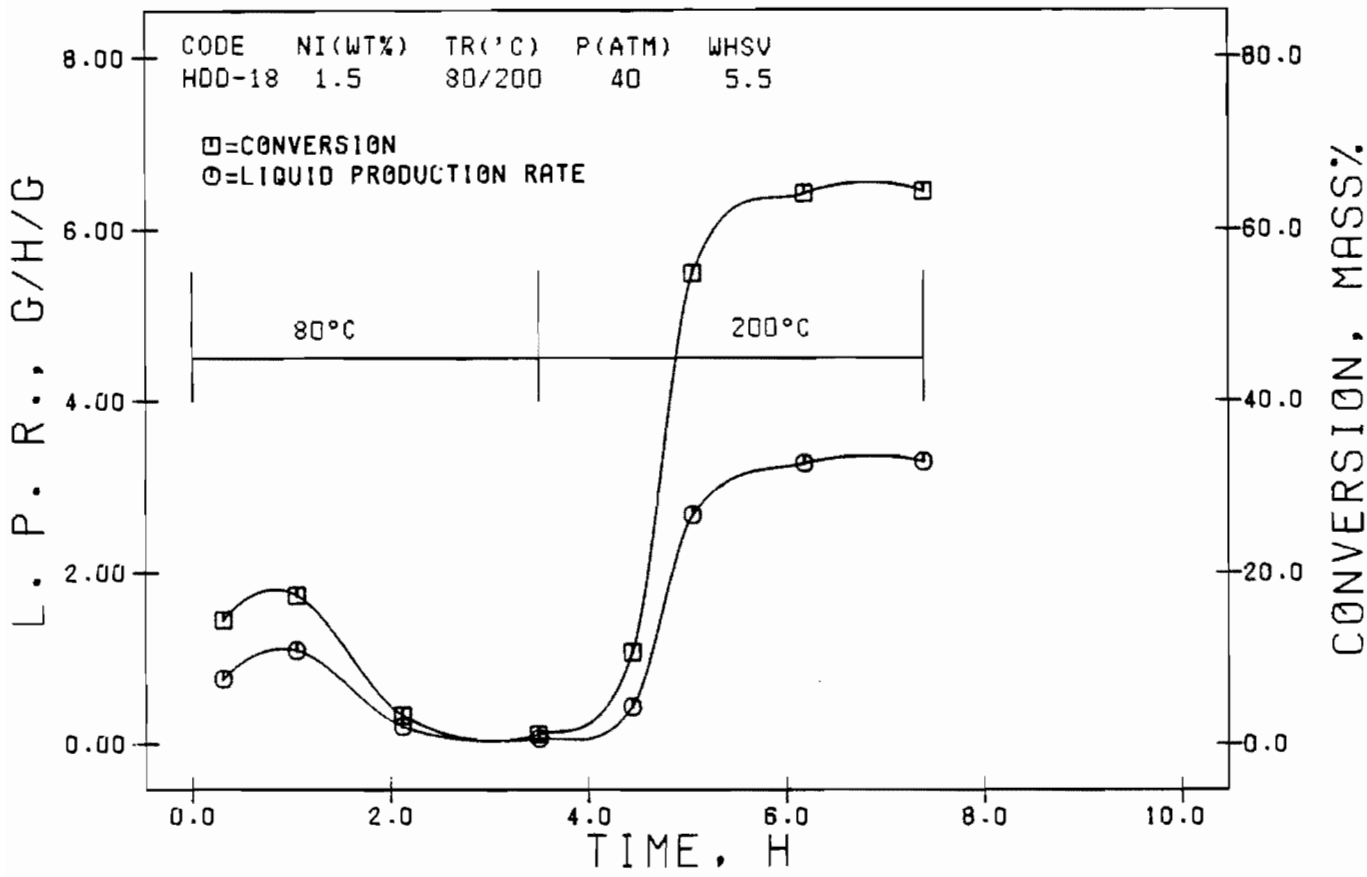

FIG 4.35 LIQUID PRODUCTION RATE (G/H/G) AND CONVERSION (MASS%) VS TIME (H); LIQUID (<69'C FRACTION) FEED; HDD-18

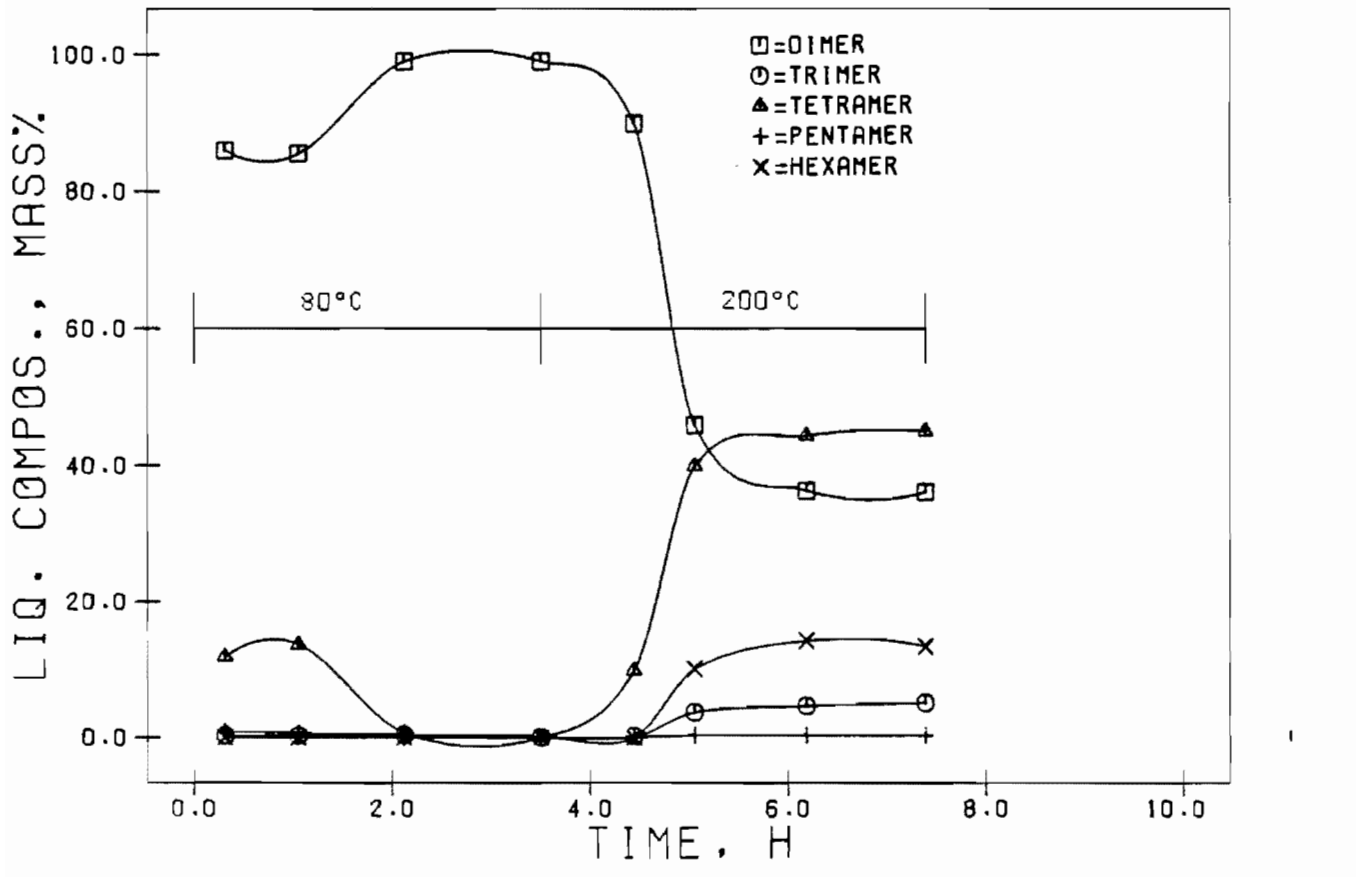

FIG 4.36 LIQUID COMPOSITION (MASS%) VS TIME (H); LIQUID (<69'C FRACTION) FEED; HDD-18

200°C. The catalyst, again an HDD type catalyst with a nickel content of 1.5 wt%, was activated in the normal manner between the runs.

To monitor the monomer utilization throughout the run the equations shown above for LPR and conversion with n=3 were used, i.e. a propene balance was done assuming no mass loss. The results are shown in Figure 4.37 for the run at 80°C and in Figure 4.39 for the run at 200°C.

Figure 4.38 shows that at 80°C the activity rapidly declined as the composition of the liquid product rapidly approached that of the C_6 feed. At 200°C, however, as shown in Figure 4.40, the liquid composition was steady and contained about 40 wt% dimer after 8 h on stream.

4.11 TG/DTA

In Figure 4.41 the TG and DTA curves for a fresh HDD type catalyst with a nickel content of 11.7 wt% are shown. The catalyst was held under flowing nitrogen throughout.

Up to 500°C, an exothermic peak, probably indicating the removal of chemisorbed water, was recorded. At approximately 530°C, the curve became endothermic probably due to the decomposition of the Ni-Urea complex to form NiO.

From the TG curve, it can be seen that the intermediate species formed were not stable until the final endothermic event at 530°C. Beyond this temperature the TG curve levelled out, indicating that a stable species was formed. The overall mass loss from the catalyst was 14 wt%.

To determine the quantity of water that the catalyst adsorbs, a previously calcined catalyst was exposed to air, and the TG and DTA curves were subsequently recorded. The results of this run using the same catalyst as before are shown in Figure 4.42. This figure shows a broad exothermic peak up to 600°C and an overall mass loss of 3.67 wt%

To establish the quantity of hydrocarbons adsorbed on the catalyst, the TG and DTA curves were recorded for a catalyst after it had been used for the oligomerisation of propene. The catalyst used was an HDD type catalyst with a nickel content of 11.7 wt%. The catalyst was exposed to flowing air while recording the TG and DTA curves. The results are shown in Figure 4.43.

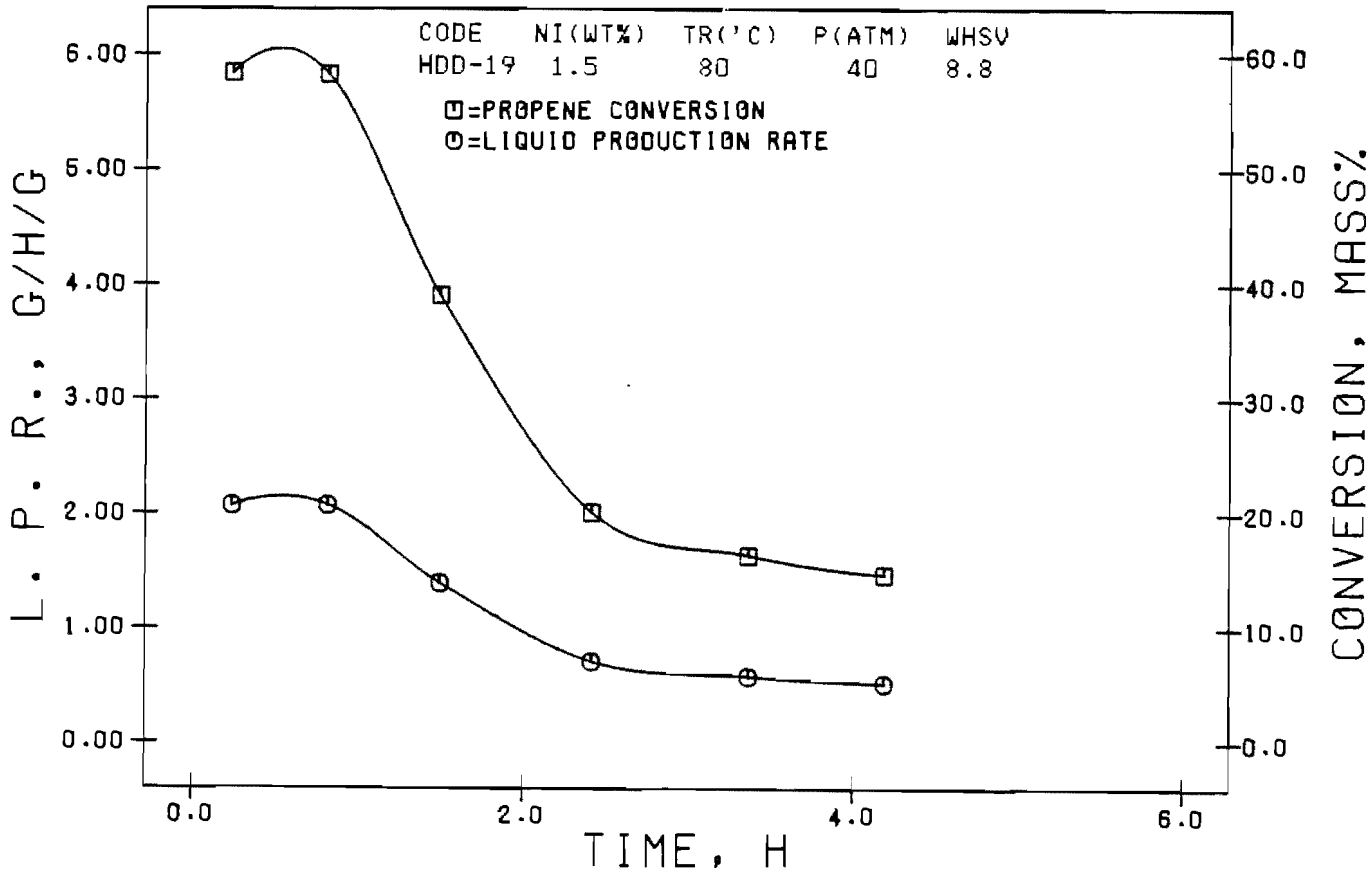

FIG 4.37 LIQUID PRODUCTION RATE (G/H/G) AND CONVERSION (MASS%) FOR PROPENE VS TIME (H); LIQUID (<69'C FRACTION) AND GAS FEED; HDD-19

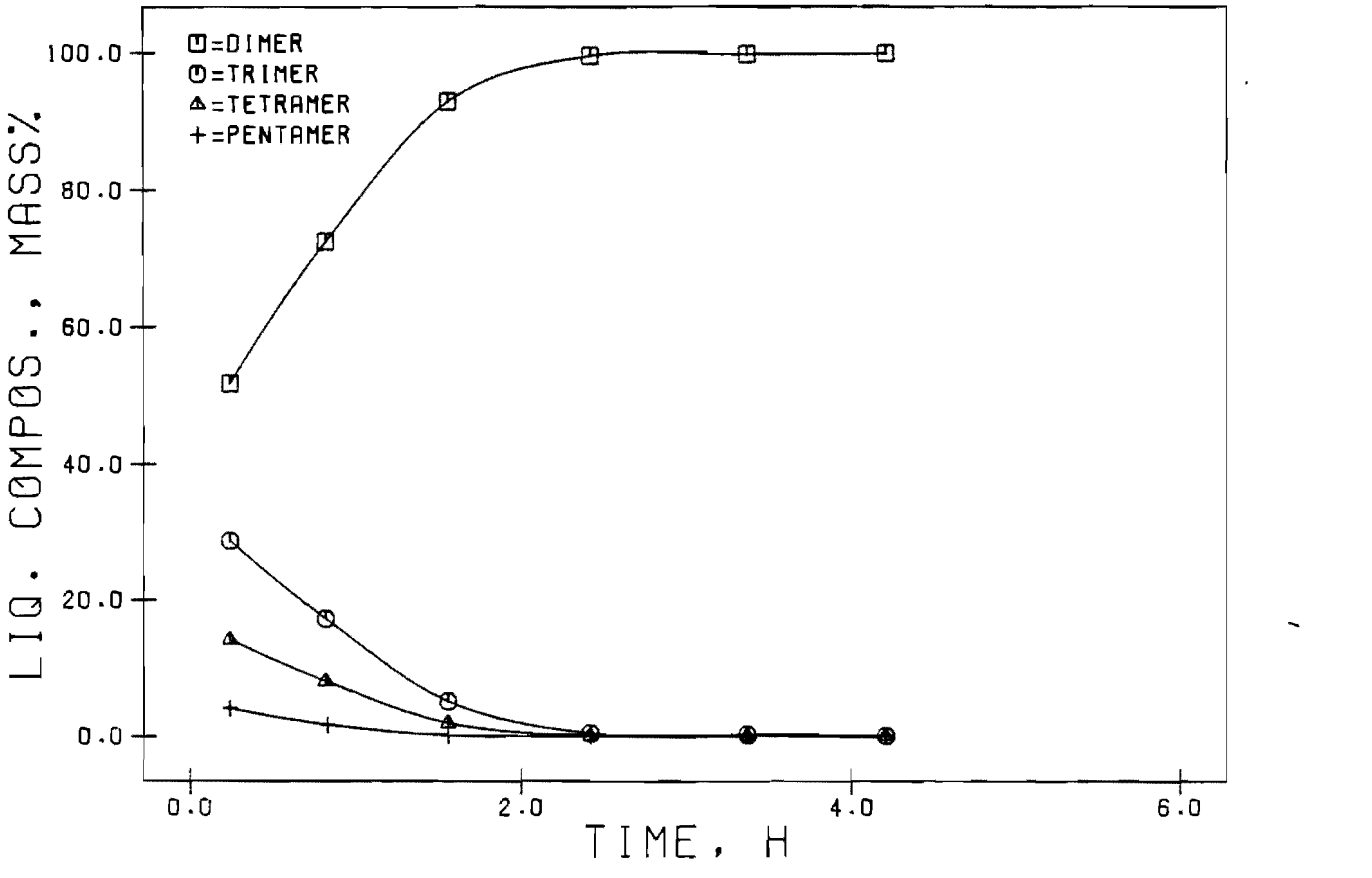

FIG 4.38 LIQUID COMPOSITION (MASS%) OF ENTIRE LIQUID EFFLUENT VS TIME (H); LIQUID (<69'C FRACTION) AND GAS FEED; HDD-19

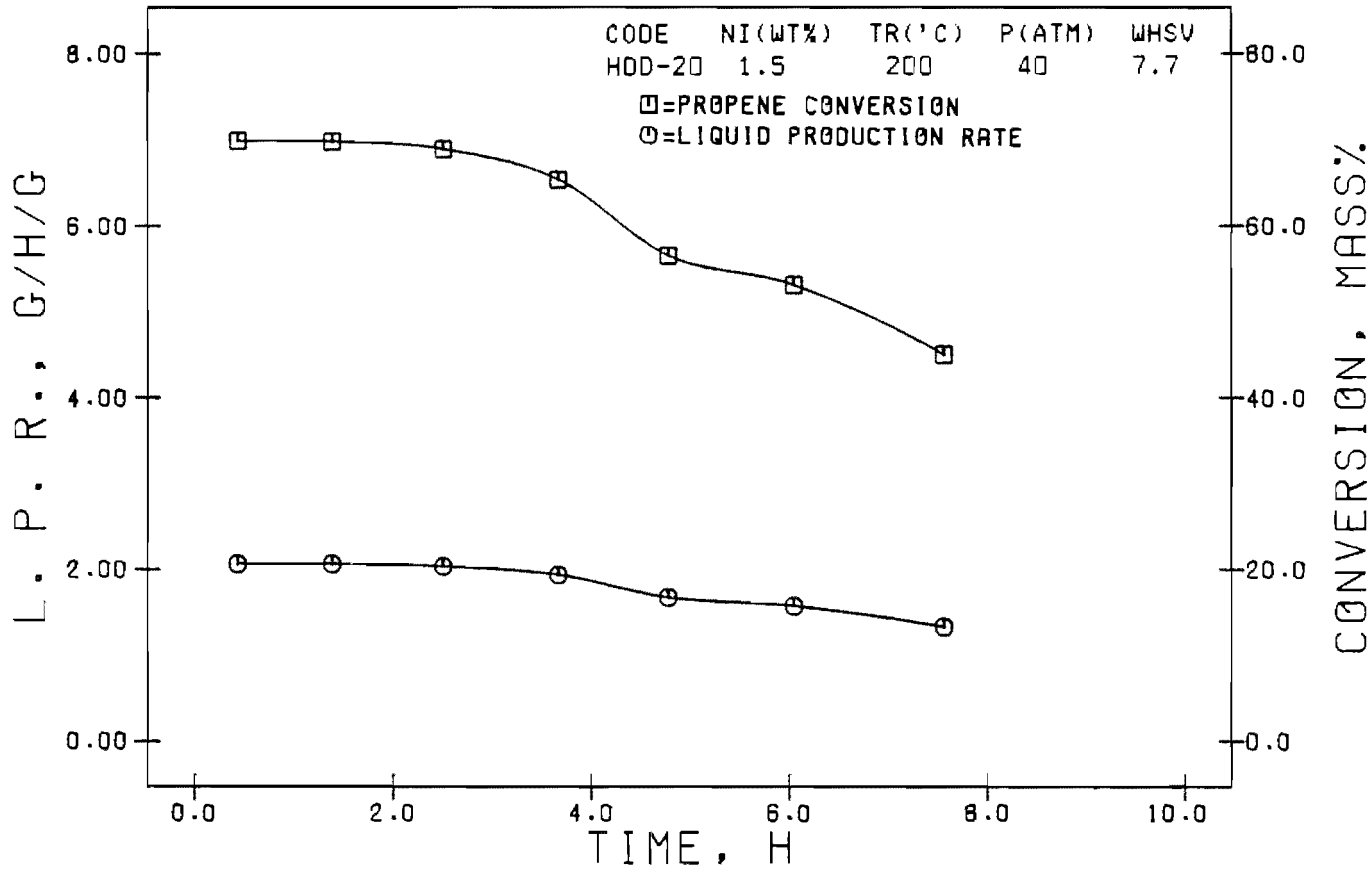

FIG 4.39 LIQUID PRODUCTION RATE (G/H/G) AND CONVERSION (MASS%) FOR PROPENE VS TIME (H); LIQUID (<69'C FRACTION) AND GAS FEED; HOD-20

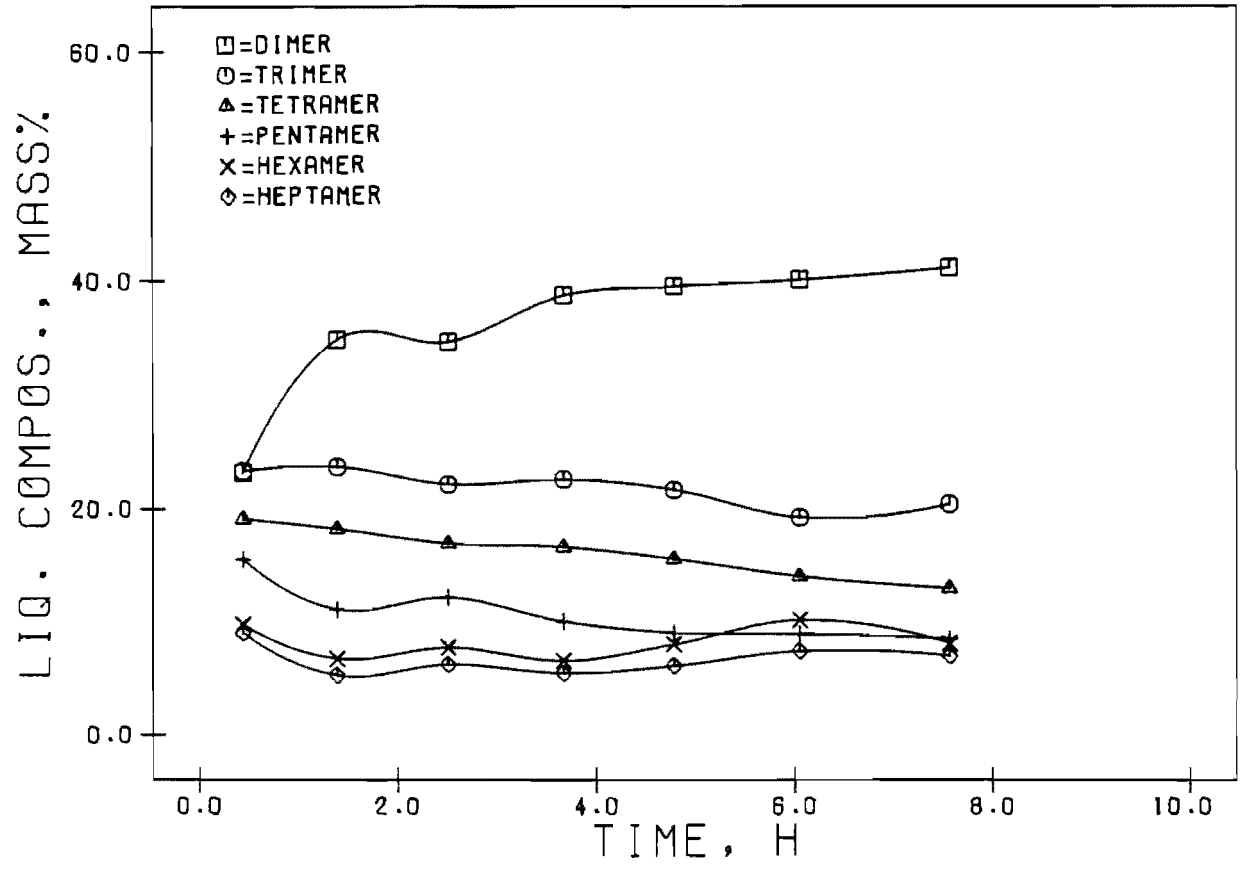

FIG 4.40 LIQUID COMPOSITION (MASS%) OF ENTIRE LIQUID EFFLUENT VS TIME (H); LIQUID (<69'C FRACTION) AND GAS FEED; HOD-20

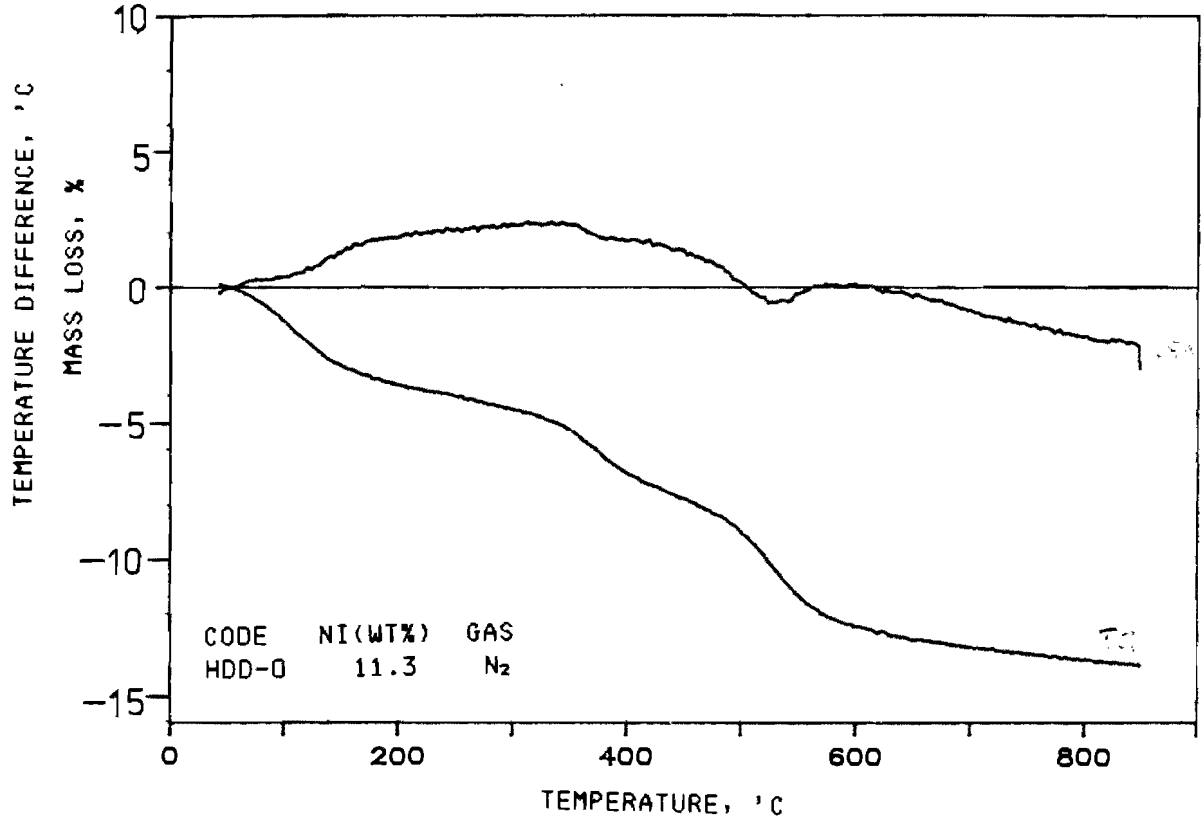

FIG 4.41 MASS LOSS (%) AND TEMPERATURE DIFFERENCE (°C) VS FURNACE TEMPERATURE (°C) FOR A FRESH CATALYST; 20 mg sample

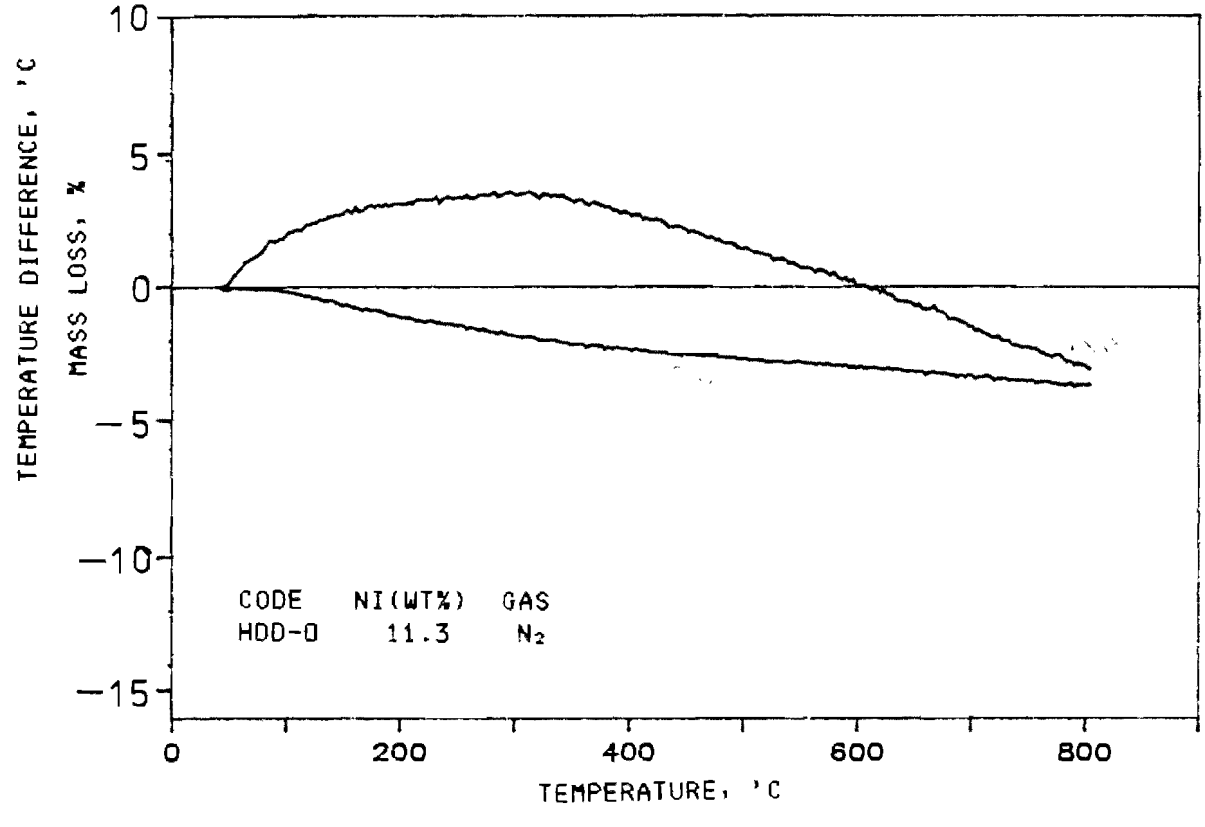

FIG 4.42 MASS LOSS (%) AND TEMPERATURE DIFFERENCE (°C) VS FURNACE TEMPERATURE (°C) FOR A CALCINED CATALYST WHICH HAS BEEN EXPOSED TO AIR; 19 mg sample

The DTA curve was exothermic below 400°C, probably as a result of combustion of the adsorbed hydrocarbons. No other thermal events occurred. The TG curve showed that the overall mass loss was 9.6 wt%.

To establish the effect of synthesis technique the TG and DTA curves of a SG, IMP and HDD type catalyst were recorded under flowing air. In each case the catalyst had been used for the oligomerisation of propene.

In Figure 4.44 the TG and DTA data for an IMP type catalyst with a nickel content of 0.83 wt% are shown. There were an exothermic peak at 340°C, and a shoulder at approximately 400°C probably due to the combustion of the adsorbed hydrocarbons. The TG curve also shown in Figure 4.44 shows that the overall mass loss was 17.3 wt%.
In Figure 4.45 the TG and DTA curves for an HDD type catalyst with a nickel content of 1.5 wt% are shown. The DTA curve showed a broad exothermic peak between 300 and 400°C. The overall mass loss was 12 wt%.

In Figure 4.46 the TG and DTA data for an SG type catalyst with a nickel content of 1.51 wt% are shown. The DTA curve showed that an exothermic peak in the vicinity of 300°C. The TG curve, showed a continual mass loss up to 600°C, the overall mass loss being 24.4 wt%.

4.12 NMR

The ^{1}H MNR spectra recorded were those of the bulk liquid collected throughout a run. For each type of catalyst the spectrum determined was that of the liquid collected at the reaction conditions deemed optimum, viz., 80°C and 40 atm over a catalyst with a nickel content of 1.5 wt%. The results obtained are shown in Table 4.2 and Table 4.3 while the spectra are shown in Figures 4.47, 4.48 and 4.49.

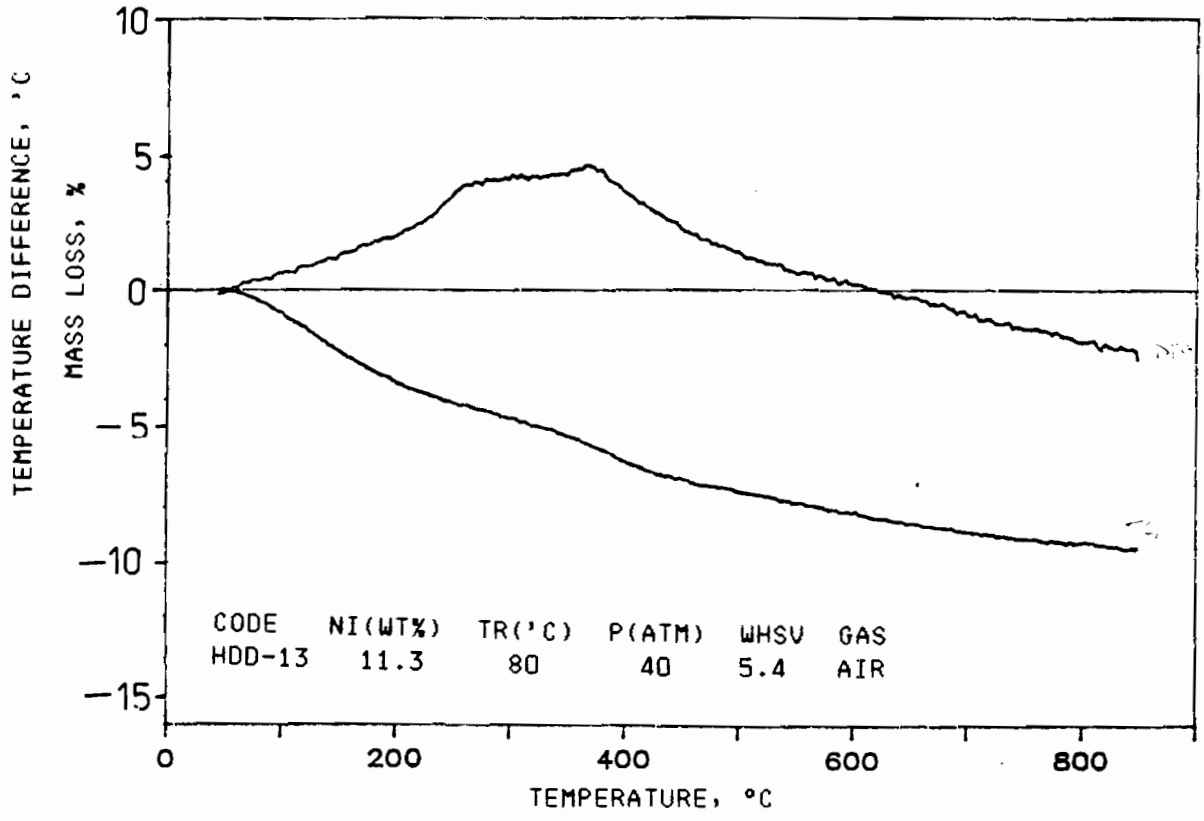

FIG 4.43 MASS LOSS (%) AND TEMPERATURE DIFFERENCE (°C) VS FURNACE TEMPERATURE (°C) FOR A USED CATALYST: HDD-13; 18.5 mg sample

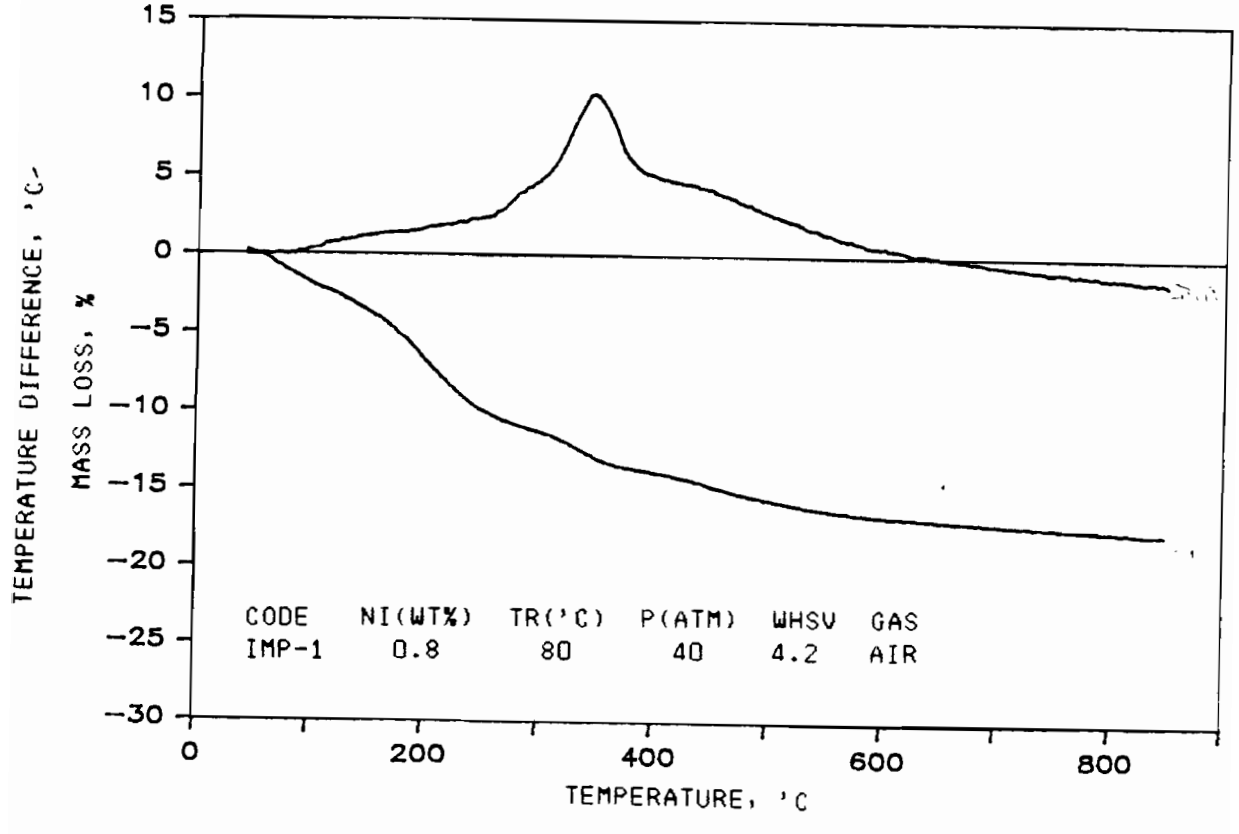

FIG 4.44 MASS LOSS (%) AND TEMPERATURE DIFFERENCE (°C) VS FURNACE TEMPERATURE (°C) FOR A USED CATALYST: IMP-1; 18 mg sample

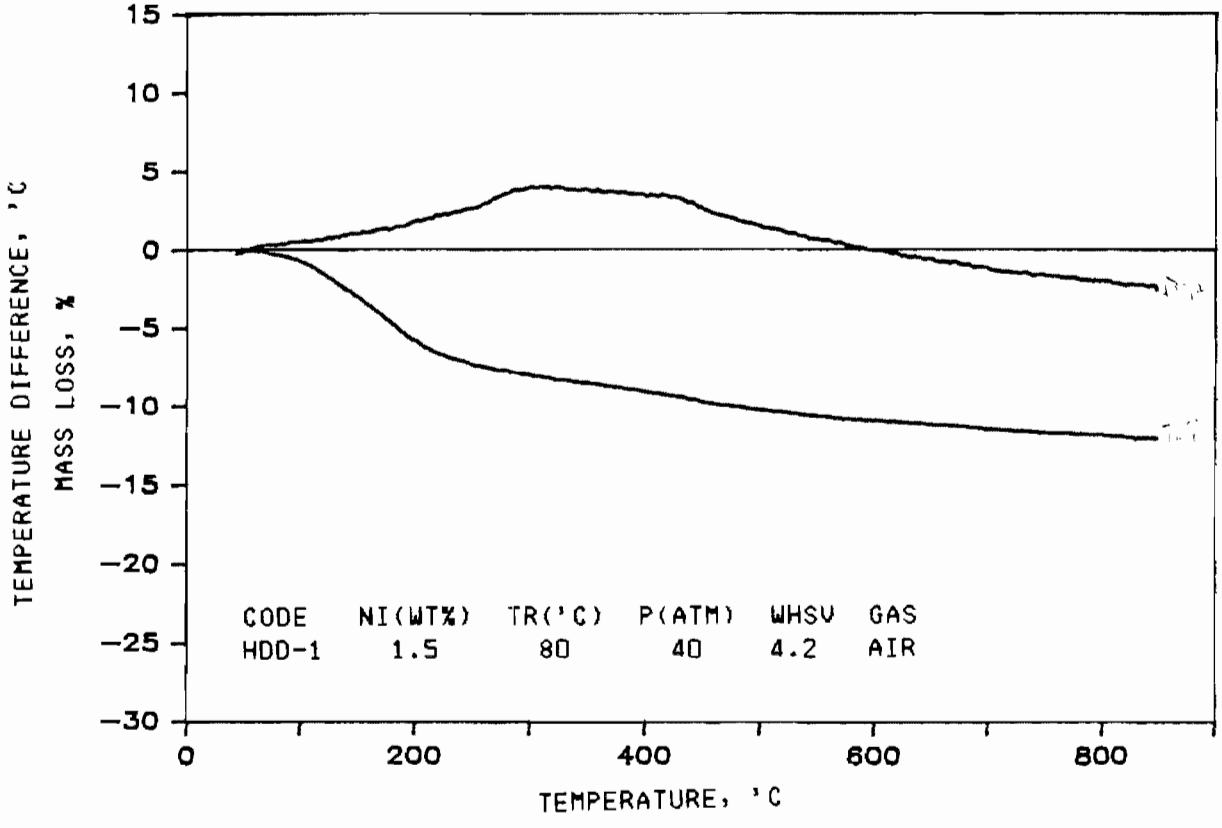

FIG 4.45 MASS LOSS (%) AND TEMPERATURE DIFFERENCE (°C) VS FURNACE TEMPERATURE (°C) FOR A USED CATALYST: HDD-1: 17 mg sample

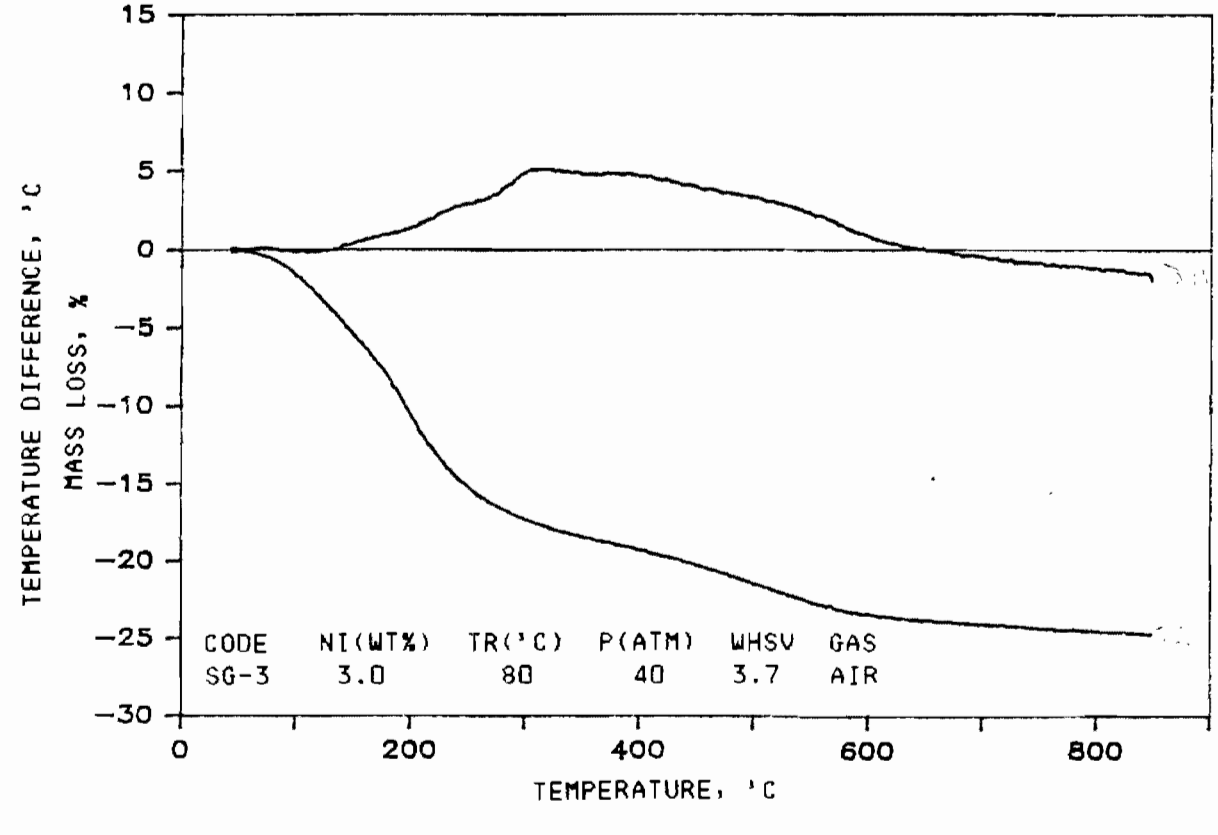

FIG 4.46 MASS LOSS (%) AND TEMPERATURE DIFFERENCE (°C) VS FURNACE TEMPERATURE (°C) FOR A USED CATALYST: SG-3: 17 mg sample

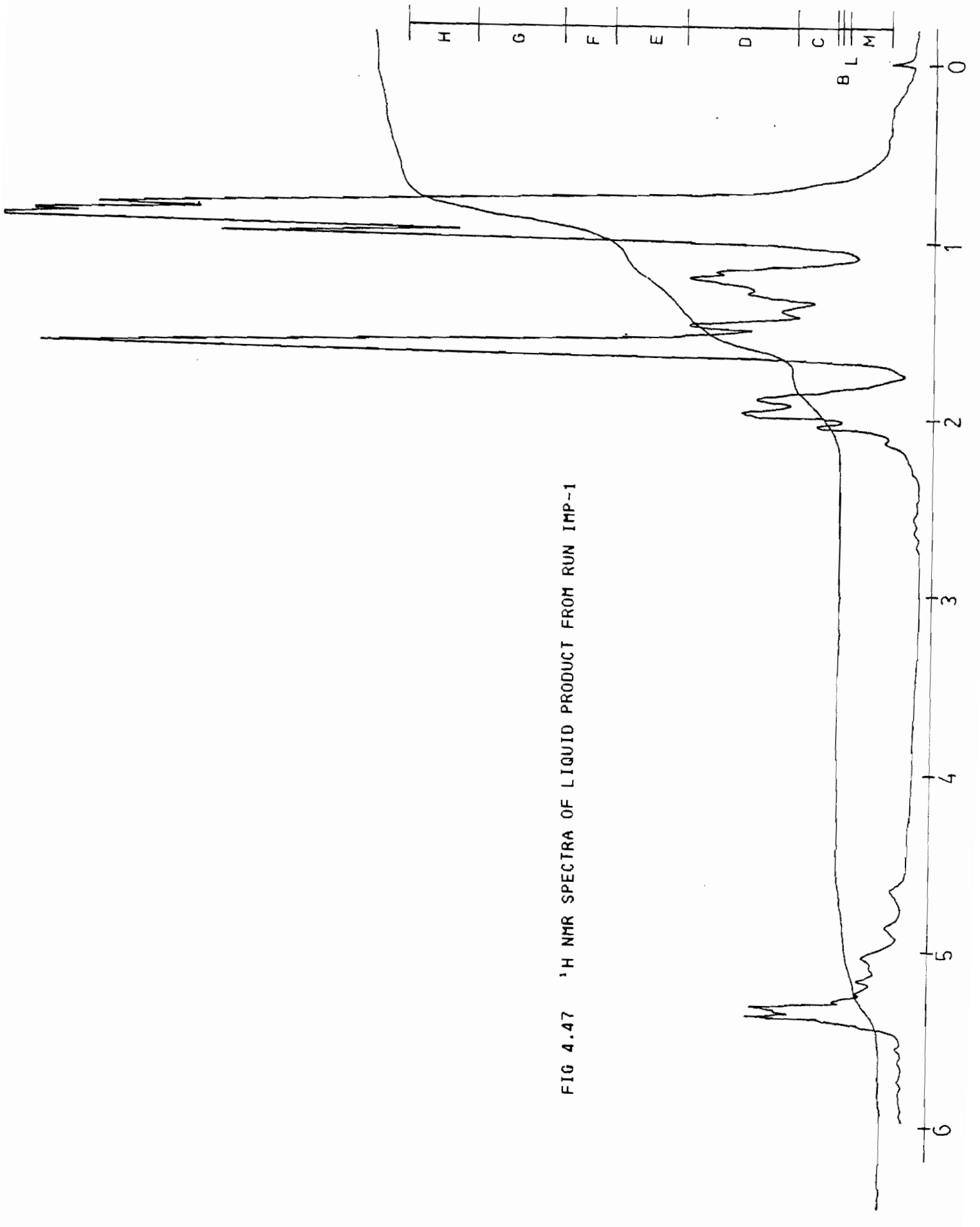

FIG 4.47 ^{1}H NMR SPECTRA OF LIQUID PRODUCT FROM RUN IMP-1

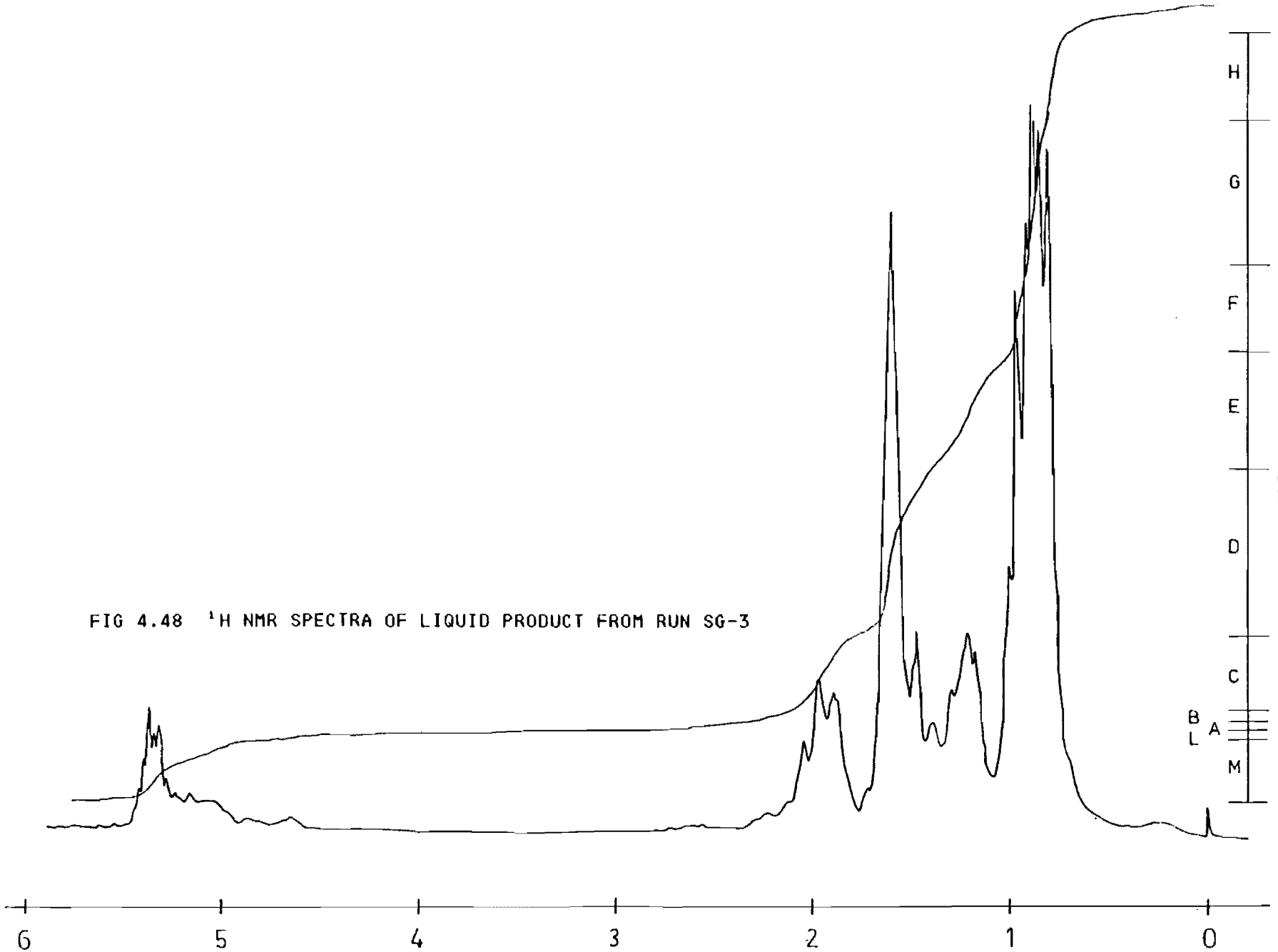

FIG 4.48 ^{1}H NMR SPECTRA OF LIQUID PRODUCT FROM RUN SG-3

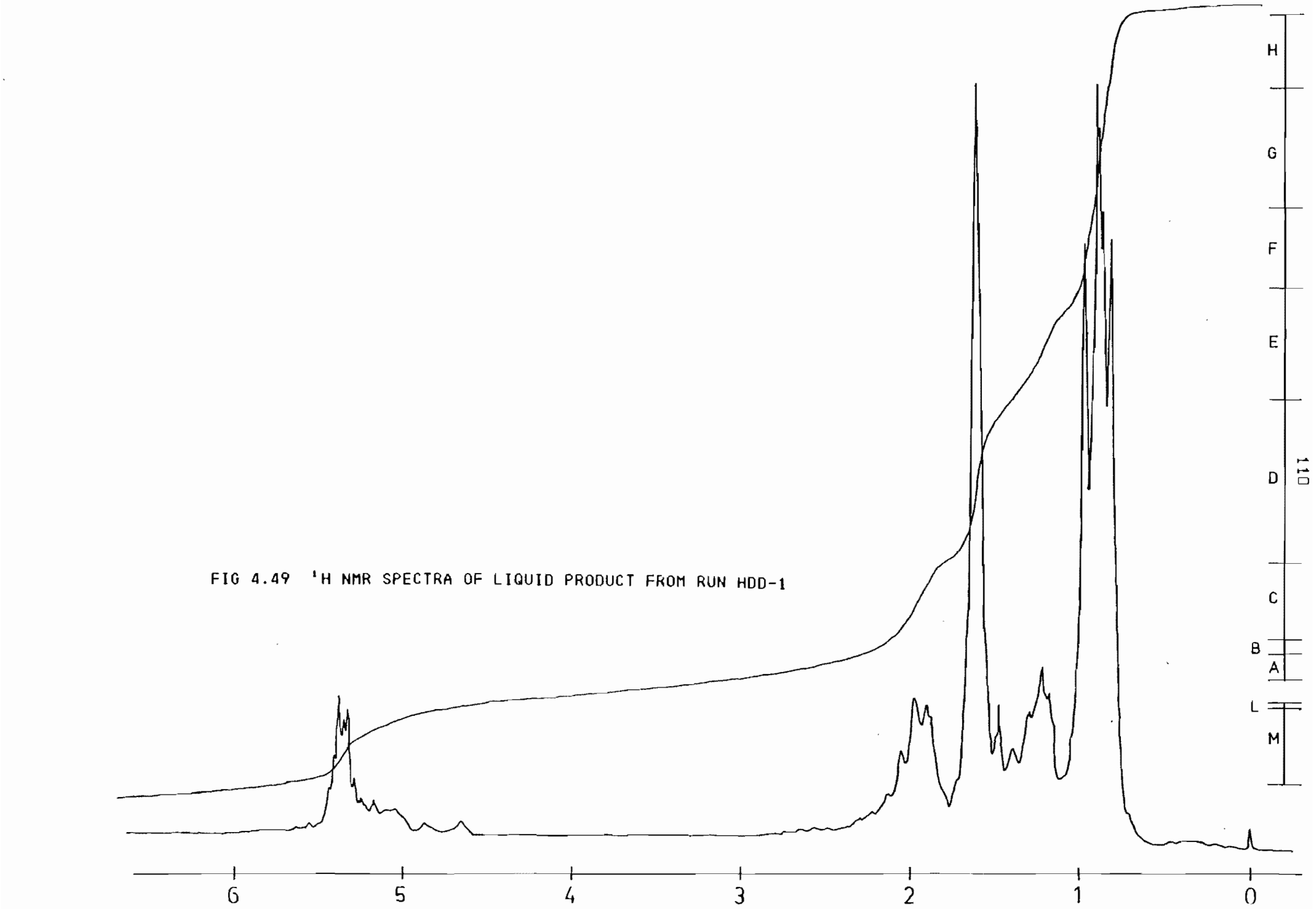

FIG 4.49 ^{1}H NMR SPECTRA OF LIQUID PRODUCT FROM RUN HDD-1

Table 4.2 : Integrated areas

Run code	Area code										
-	A	B	C	D	E	F	G	H	L	M	N
IMP-1	0.0	1.0	12.0	32.0	20.5	14.5	25.0	19.5	1.0	12.5	0.0
SG-3	2.0	3.0	19.0	43.0	30.5	22.0	36.5	22.5	1.5	15.8	0.0
HDD-1	7.5	5.0	23.0	49.0	33.2	23.5	35.5	22.2	2.0	22.0	0.0

Table 4.3 Carbon areas and branching

Code	CH_3	CH_2	CH	$\frac{CH_3}{CH_2}$	$\frac{CH_3}{CH}$	$\frac{CH}{CH_2}$
-	-	-	-			
IMP-1	25.8	27.5	21.0	0.94	1.23	0.76
SG-3	35.0	25.3	29.5	0.79	1.23	0.67
HDD-1	37.2	51.7	30.9	0.72	1.20	0.60

5. DISCUSSION

The effect of the synthesis procedure on metal distribution and dispersion in nickel silica catalysts was examined in detail by, amongst others, Hermans and Geus (1979), Blackmond and Ko (1984), Montes et al (1984) and in a more general sense by Maatman and Prater (1957).

The conclusions reached by these workers as to how the synthesis procedure effects the metal distribution and dispersion and hence, catalytic activity, has been discussed in Section 1.3, and are briefly summarised below. Using their conclusions an attempt was then made to explain the activity of an HDD type nickel oxide silica alumina catalyst.

Impregnation, as discussed in Section 1.3.2 and 3.6.2, involves the the homogeneous increase in concentration of the nickel precursor by the evaporation of the solvent. In terms of precipitation theory, as discussed in Section 1.3, the homogeneous increase in the concentration of the metal salt results in the formation of a limited number of large nuclei which are evenly distributed over the support. The reason for this is that, providing the concentration of the solution is kept homogeneous, the rate of increase in concentration is equal to the rate of crystal growth. Consequently the concentration of the solution will remain between that of the solubility and supersolubility curves where no new nuclei can develop. This has been discussed in Section 1.3.3.1. This was in fact found to be the case by Montes et al (1984) who in the case of an inpregnated Ni silica catalyst recorded an average nickel particle diameter of 5.2 nm. They further suggested that only a weak interaction exists between the metal precursor and the support. If this were so then upon calcination the crystal size should increase (Section 1.3.2.4) and the metal should be present in a form similar to that of the bulk oxide. They in fact found this to be so, i.e., the average nickel particle size increased to 45 nm after calcination for 16 h at 450°C in dry air. The fact that the metal was present in a form similar to that of the bulk oxide in calcined impregnated nickel silica catalysts had been established earlier by Houalla and Delmon (1981).

In the case of impregnated nickel silica alumina catalysts no data was available indicating the degree of interaction between the support and the metal. It is, however, assumed that, in the case of this catalyst, the interaction between the support and the metal precursor are also

weak and that a similar redistribution and corresponding increase in crystal size occurs during calcination. It is also suggested that the metal is present in a form similar to that of the bulk oxide.

It is well known that for optimum catalyst activity a large specific surface area and hence, a finely divided solid is required (Hermans and Geus 1979). Small crystallites ensure high specific metal areas but increasing nickel concentration results in agglomeration. In the case of impregnation the drying and calcination procedures result in the formation of a heterogeneity of crystal sizes when the nickel content is greater than about 5 wt%. Increasing the nickel content beyond 5 wt% results in broad and even binodal crystal size dispersion which not only affects the activity, due to loss of surface area but also the thermal stability, i.e., resistance to sintering (Richardson and Dubus 1978). It is proposed that this fact accounts for the observed loss in propene oligomerisation activity recorded by Hogan et al (1955) and Holm et al (1957) over impregnated nickel oxide silica alumina catalysts when the nickel content was raised beyond 5 wt%. This proposal was further supported by Dorling et al (1971) who predicted that when increasing the nickel content below 5 wt% the number of crystallites would increase but that the mean crystal size would remain approximately constant. Beyond 5 wt% nickel, on the other hand, they predicted that the number of crystallites would remain constant, as the nickel content was increased, but that the crystallites would increase in size. This has been discussed in detail in Section 1.3.2.3.

From the above discussion it can thus be concluded that the activity of impregnated catalysts is only a function of the the extent of metal distribution and dispersion which in turn is a function of the metal content.

It would thus be desirable to produce a catalyst in which the crystals generated during synthesis are held by the support and thus are prevented from migrating and agglomerating during subsequent heat treatments. One such method is co-precipitation. In the case of this synthesis procedure, as discussed in detail in Section 1.3.4 and 3.6.4, a reaction occurs between the support and the metal, i.e., the metal is held by the support and the crystals are uniformly distributed throughout the matrix. This type of catalyst was found to be much more active for the oligomerisation of propene than impregnated catalysts. According to Holm et al (1957), this is due to the high extent of distribution and dispersion of the nickel ions present in this catalyst. However, the same limitations of nickel content on the activity were

observed, i.e., the catalysts with a nickel content between 3 and 5 wt% were the most active (Holm et al 1957). In the case of SG type catalyst this cannot be explained in terms of loss of dispersion with increasing nickel content as it has been shown by Holm et al (1957) that the crystal size remained unchanged as the nickel content was raised from 3 to 20 wt%. The reason that the activity did not increase as the nickel content was raised beyond 5 wt% may either be due to the inaccessibility of the reactant molecules to the nickel, or due to the nickel being in an unsuitable form, i.e., Ni^0 as opposed to Ni^{+2} (NiO) after calcination. The latter was supported by the fact that the nickel was difficult to reduce, i.e., a reduction of only 50 % was achieved after 2 h on stream at 500°C by Holm et al (1957).

It is thus proposed that although crystal dispersion remained unchanged in co-precipitated nickel silica alumina catalysts, up to a nickel content of 20 wt%, the location and form of the crystals prevent total utilisation of the available metal.

Since most unsupported catalytically active materials sinter rapidly at the conditions of calcination and/or reaction (Hermans and Geus, 1979), the active compound has to be attached to a highly porous thermostable support such as silica or silica alumina. This support, which is often not catalytically active itself, increases the dispersion of the catalytically active material. Also the support is used most effectively when the active material is distributed densely and uniformly over it and is firmly held by the support. A rapid transportation of the reactants and products through the porous catalysts is also a prerequisite for an active solid catalyst. Silica alumina is such a support but the available method of loading nickel onto it viz., impregnation, does not lead to an adequate degree of interaction between the support and the metal. An alternative method of loading nickel onto silica alumina is thus required in which a uniform dispersion and distribution could be ensured together with a strong interaction between the support and the metal.

In the case of nickel silica catalysts such a method was developed by van Dillen (1976) and was termed homogeneous decomposition deposition (HDD). In this method, as discussed in detail in Section 1.3.3 and Section 3.6.3, the high degree of penetration of the solute into the support during impregnation was combined with a controlled ion exchange type precipitation.

In the case of nickel silica catalysts prepared by HDD, measurements of particle size distribution indicate a range of between 1 and 3 nm for loadings of up to 30 wt% nickel (Richardson and Dubus 1978). Furthermore a strong interaction exists between the support and the metal and consequently this type of catalyst was extremely resistant to sintering. Thus in the case of an HDD nickel silica catalyst with a nickel content of 8.3 wt%, Montes et al (1984) showed that after calcination in dry air at 450°C for 16 h the average diameter of the nickel particles decreased from 5.1 to 4.6 nm. In the case of an impregnated nickel silica catalysts with the same nickel content the average nickel particle size, after calcination at the same conditions, was 45 nm. From this it may be concluded that in the case of HDD nickel silica catalysts the metal is not present in the bulk oxide form. This was in fact confirmed by Montes et al (1984) using X-ray diffraction. The exact nature of the form of the metal on the surface is not known. Also the crystallites in HDD nickel silica were readily accessible. This was inferred from the results of Blackmond and Ko (1984) who recorded 100% reduction after 4 h on stream at 500°C.

From the discussion presented above it can be seen that the method of homogeneous decomposition deposition produces a nickel silica catalyst where the nickel is distributed densely and uniformly over the support and that a strong interaction between the support and the metal exists.

In the case of nickel oxide silica alumina catalysts, prepared by homogeneous decomposition deposition, no data was available in the literature either on the degree of dispersion or distribution or on the support-catalyst interaction. It is however thought that, in view of the results obtained from nickel silica catalysts, a high degree of interaction occurs and that the crystallites are uniformly and densely distributed throughout the support.

In this work the extent of metal distribution and dispersion on the support phase and the nature of the support metal interaction of nickel oxide silica alumina catalysts prepared by homogeneous decomposition deposition were not investigated. However, the catalytic activity and selectivity of this catalyst for the oligomerisation of propene were examined in detail and compared with the activity and selectivity of nickel oxide silica alumina catalysts prepared by impregnation and co-precipitation. A discussion of each aspect of the work is now given.

The reproducibility study (Section 4.1) indicated that the experimental results obtained in this study were reliable. Once steady state

operation was reached both the selectivity and LPR showed little variation between runs at similar reaction conditions.

The reaction conditions used were, unless otherwise stated (see Table 4.1), 80°C and 40 atm. It can be seen from the phase diagram shown in Appendix B that the reactants were in the liquid phase. Consequently a two phase system was studied. When the temperature was raised above the feed bubble point temperature of 86°C at 40 atm, i.e., when the reactants were in the vapour phase, a three phase system was studied.

The aim of this study was to compare the characteristics of a nickel oxide silica alumina catalyst synthesised via the HDD method adapted by the author from the work done by van Dillen (1979) on nickel oxide silica catalysts, with those of a catalyst prepared by the standard impregnation technique (referred to as IMP) and co-precipitation (referred to as SG) as discussed by Holm et al (1957).

The effect of synthesis procedure on the propene oligomerisation properties of nickel oxide silica alumina was investigated by Holm et al (1957) for an IMP type catalyst and a coprecipitated (SG) type catalyst. They found that the oligomerisation activity of SG type catalysts was approximately 1.5 times that of IMP type catalysts. HDD type catalysts on the other hand had an activity similar to that of IMP type catalysts but their performance was not as sensitive to the reaction conditions and nickel content as IMP and SG type catalysts were. With this in mind a comprehensive study of the effect of reaction conditions using nickel oxide silica alumina a catalysts prepared by homogeneous decomposition deposition, impregnation and to a limited extent coprecipitation were carried out.

Firstly the effect of the quantity of nickel loaded onto the catalysts was investigated. In the case of IMP type catalysts , Hogan et al (1955) had found that a nickel content between 3 and 5 wt% gave the most active catalyst. Holm et al (1957) examining the propene oligomerisation activity of IMP as well as SG type catalysts found that irrespective of synthesis technique catalysts with a nickel content between 3 and 5 wt% were the most active.

In the case of IMP type catalysts examined in the present study no such trend was observed. Increasing the nickel content from 2.2 wt% to 6.3 wt% at an average WHSV of 4.8 and 4.9 g/h/g respectively caused the LPR to decrease by 4.2%. Using, on the other hand, catalysts with a nickel content of 1.9 and 9.8 wt% at an average WHSV of 5.3 and 5.2 g/h/g,

respectively an increase of 5% in LPR was recorded. In view of the conflicting results obtained in this study and the differences in WHSV from run to run, no statement as to the effect of nickel content on the activity of impregnated nickel oxide silica alumina catalysts could be made.

In the case of an HDD type catalyst increasing the nickel content did not lead to a marked change in the LPR. Differences in the WHSV and the fact that the conversion was greater than 90 wt% in all the runs make a comparison of the results difficult. However, comparing runs with identical average WHSV, viz., 4.2 g/h/g, showed that changing the nickel content from 1.5 wt% to 7.2 wt% did not affect the LPR. Similarly at a WHSV of 4.9 and 5.0 g/h/g identical LPR were observed for catalysts with nickel contents of 11.7 and 2.2 wt%.

Thus although the study of the effect of the nickel content on the LPR in the case of both IMP and HDD type catalysts is not unambiguously conclusive, the available data seems to indicate that the activity of an HDD type catalyst was relatively independent of the nickel content, and that irrespective of nickel content HDD type catalysts were, on average, 20% more active than IMP type catalysts.

It was observed while examining the effect of WHSV on the activity and selectivity over HDD type catalysts that the selectivity was a function of the conversion, i.e., a shift to lighter products was recorded when the conversion decreased. Neither IMP type catalysts nor HDD type catalysts exhibited a strong dependence of product composition on nickel content. In the case of IMP type catalysts, the catalysts with 0.8 wt% nickel did show a greater selectivity towards trimers, but the overall trend observed was a gradual increase in dimer yield with increasing nickel content at the expense of the trimer (Section 4.2). The small increase in dimer yield with increasing nickel content observed in this work was in agreement with the data reported by Takahashi et al (1969) who recorded the maximum dimer yield for an impregnated nickel oxide silica alumina catalyst with a nickel content of 9.7 wt %.

The selectivity of HDD type catalyst was independent of the nickel content when the nickel content was held between 1 and 7 wt%. At a higher nickel content, viz., 11 wt% a decrease of 10% in dimer yield was observed. After careful examination of the data, however, it was found that after 4 h on stream the WHSV for the catalysts with 2.2 and 11.7 wt% nickel were 5.3 and 4.9, respectively. This 8% decrease in WHSV between the runs may explain the observed decrease in dimer yield.

It may thus be concluded that the activity and selectivity of HDD type catalysts were independent of the nickel content with in the range of nickel loadings of 1.5 to 11.7 wt%. In the case of IMP type catalysts, increasing the nickel content caused a shift to lighter products with no discernible effect on the activity.

The effect of varying the pressure at a fixed temperature on the activity and selectivity of an IMP type catalyst was investigated in detail by Takahashi et al (1969). In the present work the effect of varying the pressure at a fixed temperature of 80°C for an IMP as well as for HDD and SG type catalysts was investigated. For an IMP type catalyst the results obtained were similar to those of Takahashi et al (1969). Thus in the case of IMP type catalysts a drop in activity was recorded when the pressure was lowered from 40 atm to 20 atm at a constant temperature of 80°C, i.e., when the system moved into the vapour phase. In the case of an SG type catalyst it was found that the catalyst was inert at 20 atm.

In the case of a HDD type catalysts differences in WHSV and the fact that the conversion was greater than 88 wt% in all runs make an interpretation of the results difficult. From the available data it can, however, be seen that although the average WHSV increased from run to run, the LPR over HDD type catalysts remained constant as the pressure was dropped from 50 atm to 20 atm. From this it may be concluded that the activity of HDD type catalysts decreased as the pressure was decreased.

In respect of the effect of pressure on product selectivity, Takahashi et al (1969) found that when the system moved into the vapour phase at a constant temperature a shift to heavier products occurred. Using an IMP type catalyst this was also observed in this study, i.e., a drop of 52% in dimer yield, mainly in favour of the trimer, was observed when the pressure was dropped from 40 atm to 20 atm. In the case of HDD type catalysts an opposite trend was observed, viz., decreasing the pressure from 50 atm to 20 atm resulted in an almost linear increase in dimer yield.

From the above discussion it can be seen that IMP type catalysts contradict thermodynamics with regards to selectivity. It was expected from thermodynamics that as the pressure was decreased from 50 to 20 atm the dimer yield should increase. In the case of an HDD type catalyst this was found to be the case. In the case of IMP type catalysts, however, an opposite trend was was observed, i.e., a shift to heavier

products as the pressure was decreased from 50 to 20 atm. The observed shift to heavier products, with decreasing pressure, may be explained if it is assumed that at the lower pressures the heavier products are able to evaporate off. If this were so then in the case of HDD type catalysts the yield of heavier products should also increase as the pressure was decreased. This was infact found to be the case although the increase in trimer yield was very small. In the case of both IMP and HDD type catalysts the activity decreased as the pressure was decreased.

To complete the study of the effect of reaction pressure and temperature on the selectivity and activity, the effect of varying the temperature at a fixed pressure was investigated. Since the above results for IMP type catalysts were in agreement with those of Takahashi et al (1969) and much information is available in the literature on IMP type catalyst, no further experimental work using IMP type catalysts was done. Consequently the results obtained from the literature were used to compare IMP and HDD type catalysts.

In the case of IMP type catalysts Takahashi et al (1969) found that moving into the vapour phase, i.e., when the temperature was raised above approximately 90°C at a pressure of 50 atm, a slight drop in activity was observed. Increasing the temperature beyond the bubble point of the feed was accompanied by a shift to heavier products. The reason that the catalyst activity declined only slightly with increasing temperature at 50 atm was that the silica alumina support becomes active at the higher temperatures. At 35 atm on the other hand, crossing the phase boundary results in a rapid decline in propene conversion with increasing temperature. The reason for this is that silica alumina is only slightly active at 35 atm for the oligomerisation of propene. (Takahashi et al., 1971). The shift in product spectrum, i.e., a shift to heavier products can also be explained in terms of silica alumina activity. This is so because the preferential product of silica alumina, when the latter is used for the oligomerisation of propene, is a propene trimer (Feld'blyum and Baranova, 1971; Takahashi et al., 1971).

The nature of the products formed over silica alumina when used for the oligomerisation of propene and the effect of temperature on the activity and selectivity were examined. The results obtained were in agreement with those of Takahashi et al (1972), viz., silica alumina was active for the oligomerisation of propene as long as the system temperature remained above 150°C. Also the activity dropped with decreasing reaction temperature. At 80°C, i.e., in the liquid phase at 40 atm, the catalyst was inactive. This was not in agreement with the results of Feld'blyum

and Baranova (1971) who, in a batch reactor recorded 6% conversion at 64°C and 50 atm. The reason for the difference in the results was properly due to the different pressures used, i.e., 40 atm in this work as opposed to their 50 atm, and the different process, i.e., batch as opposed to fixed bed reactor. The product spectrum obtained agreed with that found by other workers, viz., decreasing trimer yield with increasing temperature and propene trimer being the main product.

In the case of an HDD type catalyst increasing the temperature at a fixed pressure resulted in the LPR dropping by approximately 50% when the system moved into the vapour phase. Increasing the temperature further did not result in any marked changes in the LPR. Thus, although the average WHSV increased from run to run, the LPR remained approximately constant as the temperature was increased. From this fact it may be concluded that the activity of the catalysts decreased as the temperature was increased.

The overall shift to heavier products when raising the temperature from 80°C to 150°C, i.e., an increase in propene trimer at the expense of the propene dimer, was expected in view of the catalytic role of the silica alumina support at the elevated temperatures. The increase in dimer yield as the temperature was raised further from 150°C to 210°C could be explained in terms of the increasing WHSV and hence decreasing activity of the catalyst. (See Section 4.4.1)

From the different trends in product spectrum recorded when operating in the vapour phase, i.e., an increase in trimer yield with increasing temperature when using nickel oxide silica alumina as opposed to a decrease in trimer yield when using silica alumina observed in this work it could be concluded that in supported nickel catalysts the nickel still played a role at the elevated temperatures. This conclusion was also supported by the results of Takahashi et al (1972) who found that a physical mixture of silica alumina and nickel oxide had the same activity as silica alumina alone thus indicating the importance of supporting the nickel. Also the conversion over nickel oxide silica alumina was less sensitive to the reaction temperature then was the case for silica alumina, when the system was operated in the vapour phase at 40 atm. Thus in the case of silica alumina a drop in LPR of 83% was recorded when the temperature was dropped by 50°C from 200°C while in the case of a HDD type catalysts an increase in LPR of 30% was recorded when the temperature was decreased over the same range.

The lifetimes of the catalysts were examined by the changes in the activity over the first 10 h on stream. In the case of an IMP type catalyst data was available in the literature on the lifetime when this type of catalyst was used for the oligomerisation of butene (Hogan et al., 1955, Allum, 1974). The results obtained by these researchers was that the activity of the catalyst did not change markedly after 100 h and 21 days on stream, respectively. No data was however available on the lifetime of this catalyst when used for the oligomerisation of propene.

As using the changes in activity over the first 10 h on stream as an indication of lifetimes was very sensitive to WHSV fluctuations, both the changes in LPR and WHSV have to be recorded. The average WHSV in this run was 5.3 g/h/g. In the case of an IMP type catalysts the LPR dropped by 17.5% after 5 h on stream during which time the WHSV dropped by 1%. In view of the fairly constant WHSV and the large drop in LPR it may be assumed that IMP type catalysts deactivate rapidly when used for the oligomerisation of propene. A slight shift to lighter products was also observed during this run which was expected in view of the decreasing activity.

In the case of SG type catalysts the LPR dropped by 9.6% while the WHSV dropped by 2.1% after approximately 6 h on stream. The average WHSV during this run was 5.2 g/h/g. The change in the WHSV was considered acceptable and so it may be concluded that this type of catalyst deactivates less rapidly than IMP type catalysts do when used for the oligomerisation of propene. This conclusion was also reached by Holm et al (1957). In the case of this catalyst a slight shift to lighter products was also observed with time on stream.

In the case of a silica alumina, when operated at 200°C, the LPR dropped by 31.5% while the WHSV over the same time period of 7.6 h dropped by 2.8%. The average WHSV during this run was 3.5 g/h/g. From these results it can be seen that this catalyst rapidly deactivates when used for the oligomerisation of propene at 200°C. A very slight shift to lighter products was observed during this run.

In the case of an HDD type catalyst no data as to the lifetime was available and hence a long run was performed. The LPR fluctuated during this run, due to WHSV fluctuations. The average WHSV during this run was 5.2 g/h/g. Using data points 105 h apart with nearly identical WHSV of 5.6 and 5.7 g/h/g respectively it was found that the conversion decreased by 12.6% over this period. The selectivity also changed during

this run, i.e., the quantity of dimer formed increased by 25% at the expense of the tetramer and pentamer after 120 h on stream.

The lifetime of the catalysts, as measured by the drop in activity over the first 10 h on stream, are in order of decreasing length, HDD > SG > IMP > SA. It may thus be concluded that HDD type catalysts are superior with respect to lifetime when used for the oligomerisation of propene than any of the other catalysts studied.

The effect of varying the WHSV on the activity and selectivity of IMP type catalysts was examined by Takahashi et al (1969) and by Hogan et al (1955) who also examined the effect of feed composition. They found, as discussed in detail in Section 1.5.2.4, that the rate of polymer production increased linearly with propene concentration, i.e., a first order relationship between propene concentration and rate of polymer formation was obtained. The optimum space velocity for maximum conversion was less than 2 g of propene per g of catalyst per hour (Takahashi et al., 1969). At higher WHSV Takahashi et al (1969) found that the conversion dropped rapidly.

In the case of HDD type catalysts the LPR increased with the WHSV. However, the catalysts deactivated rapidly at the higher WHSV, i.e., a WHSV greater than 11 g/h/g in this work resulted in a drop in the LPR of 28% after 7 h on stream. As expected the overall conversion decreased with increasing WHSV, dropping from 96% at the lowest WHSV of 4.9 g/h/g to 77% at a WHSV of 11.6 g/h/g.

The selectivity was also affected by the changing WHSV, viz., a shift to lighter products and an increase in dimer yield was observed with increasing WHSV. This trend is opposite to that observed by Takahashi et al (1969) who found using IMP type catalysts that dimer selectivity decreased for a WHSV greater than 3.2 g/h/g. Why this should be so is not known. The trends in conversion are however identical, viz., conversion decreased with increasing WHSV.

The effect of operating the catalyst initially at 200°C and then reusing it at 80°C was examined. The catalyst was calcined in the normal manner between the two runs. The effect on LPR and selectivity of operating the catalyst at 200°C has already been discussed.

From the results obtained in this study it was found that the activity of the catalyst at 80°C was affected by operating it first at 200°C, and the steady state conversion, after 4 h on stream, fell by 28% from that

of a catalyst used under normal conditions. The selectivity was also affected by this procedure, a shift to lighter products being recorded.

The reason for the decrease in activity was probably the same as that suggested by Hogan et al (1955) in the case of IMP type catalysts whereby the nickel oxide promoter underwent changes such as sintering or a change in oxidation state during the repeated calcination and high reaction temperature which caused the activity to decline. The catalyst when operated under normal conditions did not deactivate to any marked extent and hence, no data as to the effect of repeated calcination on the activity and selectivity was available.

The effect of feed contaminants was examined in detail by Hogan et al (1955) using an IMP type catalyst. This was discussed in detail in Section 1.5.2.5. In this work only the effect of water on the activity and selectivity was examined. In the case of an IMP type catalysts Hogan et al (1955) found that if the catalyst was allowed to absorb as little as 0.5 wt% moisture the catalyst deactivated. They found that this type of contamination was totally reversible.

In the case of an HDD type catalyst using an undried feed containing 112 ppm (v/v) water the catalysts deactivated after 4.5 h on stream as opposed to the more than 120 h recorded when using a dry feed. Using the average WHSV of 5.1 g/h/g to calculate the quantity of water fed to the reactor and assuming that all the water entering the bed was absorbed by the catalyst the mass of water absorbed by the catalysts was $5 \cdot 10^{-3}$ g·H_2O/g·cat, or 0.5 wt%. This result is consistent with to that obtained by Hogan et al (1955) for IMP type catalysts. Furthermore, the contamination was totally reversible as the catalysts regained its normal "dry feed" properties with respect to activity and selectivity after regeneration.

To examine the catalytic properties of the HDD type catalysts when used for the oligomerisation of propene dimer (C_6) the < 69°C fraction from previous runs was fed to the reactor. To quantify the activity of the catalyst the equations as discussed in Section 4.9 were used to calculate the LPR and conversion. At 80°C the catalyst was active for the oligomerisation of C_6 but deactivated rapidly. This was probably due to the high molar weight products formed, viz., a propene tetramer (C_{12}), staying on the catalysts and so blocking the active sites. Upon raising the temperature to 200°C the catalysts rapidly regained activity reaching a steady state conversion of 64%. The only product formed

during this run, to any significant extent, was a propene tetramer (C_{12}).

Feeding C_6 and C_3 simultaneously also caused the catalyst to deactivate after approximately 3 h on stream at 80°C. The main product formed during this run was a propene trimer (C_9). The reason for the rapid deactivation was probably the same as above, i.e., the accumulation of the propene trimer (C_9) in the system and consequent blocking of the active sites. After regeneration and reusing the catalyst at 200°C the catalyst was again active for the oligomerisation of the C_3/C_6 mixture. In this case the main product was also a C_9 oligomer with C_{12} through C_{21} formed in reasonable quantities. Co-feeding C_6 with C_3 thus has the effect of increasing the average molecular weight of the products over that when pure C_3 was fed although different temperatures are needed to ensure reasonable activity when C_6 or a C_6/C_3 mixture was used.

The oligomerisation activity of the silica alumina support when feeding C_6 or C_3/C_6 at 200°C was not examined. That the support does play a role can not be disputed as silica alumina is catalytically active for the oligomerisation of propene at temperatures > 150°C. The large quantity of C_9 formed when co-feeding C_3 and C_6 could be explained in two ways. Firstly it could be assumed that the co-oligomerisation of C_6 and C_3 was more rapid than the dimerisation of C_6, or secondly, that the trimerisation of propene was the main source of the trimer. The second option seems more likely as the preferential product of silica alumina when used for the oligomerisation of propene at 200°C is a propene trimer.

In the case of Ni-ZSM-5 Miller (1984) suggested the use of a two stage system whereby a high yield of propene tetramer was possible. The system suggested by Miller (1984) was that propene should first be dimerised in the normal way over Ni-ZSM-5 at 27 to 93°C and 27 to 109 atm followed by a distillation, to separate the dimer from the other products. The second stage would then be the oligomerisation of the C_6 stream at 121 to 232°C and 14 to 54 atm to propene tetramers, both reactions being conducted in the liquid phase. The final liquid product obtained contained as much as 60 wt% propene tetramer. From the results obtained in the present work it becomes apparent that HDD type nickel oxide silica alumina also achieves this product spectrum. The reaction conditions used in this work were 80°C and 40 atm for stage one, the product containing 65 wt% dimer, and 200°C at 40 atm for stage two. Here both reactions were also in the liquid phase, and the final product obtained contained approximately 45 wt% propene tetramer.If on the other

hand the feed to stage two is a mixture of C_3 and C_6, also at 200°C and 40 atm, the final liquid product contained 20 wt% C_9 with C_{12} to C_{21} also being formed in reasonable quantities. Thus depending on the feed used, the products obtained can range from predominantly dimer, obtained when pure C_3 is fed. to almost pure tetramer, when a C_6 feed is used, to a high molecular weight product, C_9 to C_{21} when C_3 and C_6 are fed. No information was however available as to the degree of branching of the products formed.

The effect of the activation procedure in the case of IMP type catalysts was studied in detail by Takahashi et al (1969) with respect to acidity, structure and propene dimerisation activity. They found that a temperature between 500°C and 600°C was needed to activate the catalyst and that the activity increased with increasing activation time up to 5 h above which the activity did not change. A more detailed discussion on the effect of activation procedure on the nature of the catalyst is given in Section 1.5.2.6.

In the case of an HDD type catalyst, using TG/DTA the only thermal event recorded was an endotherm between 500°C and 600°C. This was probably due to the decomposition of organic intermediate, incorporated in the catalysts during the synthesis, to nickel oxide. Below 600°C the mass loss was 12.2 wt% while 1.5 wt% was lost between 600 and 800°C. In view of the work done by Takahashi et al (1969), as discussed above, it was assumed that in the case of HDD type catalysts the optimum calcination temperature also lay in the region of 500 to 600°C.

To determine the quantity of water that the catalyst absorbed, the previously calcined catalysts was re-exposed to air and the mass loss recorded. In this run the rate of mass loss was fairly uniform, the overall mass loss being 3.7 wt%. From the results obtained it was concluded that below 600°C, i.e., below the endothermic event observed in the case of the unused catalyst, the only species removed from the catalyst was water.

To determine the quantity of hydrocarbon held by the catalyst after it had been used for the oligomerisation of propene as a function of nickel content, the TG/DTA curves for an HDD type catalysts with a nickel content of 11.3 and 1.5 wt% were recorded. In view of the above discussion the mass loss recorded below 600°C was probably due to the removal of water and, in this case, light hydrocarbons. As the catalysts upon completion of a run were not stored in air tight containers they probably absorbed water from the atmosphere. Consequently to make the

comparison meaningful only the mass loss above 600°C was considered. Below 600°C the mass loss recorded were 8.1 and 10.5 wt% for HDD type catalysts with a nickel content of 11.3 and 1.5 wt% respectively. From this result it can be seen that the higher the nickel content the lower the amount of adsorbed hydrocarbon and hence the lower the degree of active site contamination. In view of this result it may be concluded that a high nickel content is desirable to ensure a long catalyst lifetime. Above 600°C the mass loss was independent of the nickel content and in both cases was approximately 1.5 wt%.

To compare the effect of synthesis procedure and the quantity of hydrocarbon held by the catalyst after it had been used for the oligomerisation of propene, the TG/DTA curves for an IMP, HDD and SG type catalyst were recorded. In this case the total mass loss was considered and it was found that the SG type catalyst had the highest mass loss (24.4 wt%) followed by the IMP type catalyst which had a mass loss of 17.3 wt% and an HDD type catalyst which showed a mass loss of 12.0 wt%. From these results it can be seen that the HDD type catalysts held the least amount of hydrocarbon which gave a further indication that the extent of deactivation of this catalyst was not as great as that of the other catalysts examined.

The products obtained when propene was oligomerised over an IMP type catalyst were found by Hogan et al (1955) to contain as much as 70 vol% C_6 of which 35 vol% were linear hexenes. In the case of this work the degree of branching, i.e., the CH_3 to CH_2 and CH to CH_2 ratio was determined using ^1H NMR. From the results obtained the products formed over the IMP type catalyst were the most branched followed by the products formed over SG type catalysts. The products formed over HDD type catalysts were the least branched. From the above results, if it is assumed that the degree of branching found in this work for the products formed over IMP type catalysts correspond to the product spectrum quoted by Hogan et al (1955) then the products formed over HDD and SG type catalysts contain more linear C_6's than the products formed over IMP type catalysts do.

From the present work two questions arise. They are:

(I) Why is nickel oxide silica alumina active for the oligomerisation of propene at 30°C and silica alumina only at temperatures greater than 150°C ?

(II) Why is the preferential product of nickel oxide silica alumina when used for the oligomerisation of propene, a propene dimer while that of silica alumina, when used for the same reaction, a propene trimer ?

It is proposed that the differences observed are due to the nature of the active site and hence the oligomerisation mechanism.

In the case of silica alumina the nature of the active site is controversial because of the lack of conclusive evidence. The various schemes that have been proposed (8 in total) are discussed in Section 1.2.3.1. It can however be concluded from the structure of the products formed, as established in detail by Feld'blyum and Baranova (1971) and discussed in detail in Section 1.2.3.2, that silica alumina oligomerises propene via a carbonium ion mechanism. This in turn would explain why a high reaction temperature is needed for silica alumina to be active for the oligomerisation of propene.

In the case of nickel oxide silica alumina, 5 schemes have been formulated as to the nature of the active site and hence oligomerisation mechanism. The various schemes proposed have been discussed in Section 1.2.4.1.

An early indication of the nature of the active site was given by Clark (1953) who suggested that the nickel crystals in nickel oxide silica alumina contained an excess of metal ions. Hence the active center may either be an anion vacancy or a nickel atom not directly linked to an oxygen atom and situated at lattice or interstitial points. This suggestion was used by Feld'blyum et al (1974) who then continued to draw a comparison between the oligomerisation mechanism over homogeneous catalysts, based on nickel salt and organoaluminium compounds, and heterogeneous catalysts based on nickel oxide on acid carriers. This has been discussed in detail in Section 1.2.4.2. and summarised in Table 1.1. The conclusion reached by Feld'blyum et al (1984) was that the oligomerisation of propene over nickel oxide silica alumina proceeds via a complex hydride. This mechanism, proposed by them, accounts for the observed activity and selectivity of nickel oxide silica alumina.

Thus although no evidence exists to support or discount the mechanism proposed by Feld'blyum and Baranova (1971) to explain the activity and selectivity of silica alumina, and Feld'blyum et al (1974) to explain the activity and selectivity of nickel oxide silica alumina, they serve

as a good model. It is however clear that more work is required to explain these observations.

In conclusion

(I) The incorporation of nickel into silica alumina enhances the catalyst activity at low temperatures and affects the selectivity, i.e., causes a shift to lighter products.

(II) The method of incorporating the nickel affects the activity and selectivity of this catalyst.

(III) The activity and selectivity of nickel oxide silica alumina catalysts prepared by the HDD method are independent of the nickel content. In the case of IMP and SG type catalysts this is not the case.

(IV) The selectivity and activity of HDD, SG and IMP type catalysts are all sensitive to the reaction temperature and pressure.

(V) The lifetime of HDD type catalysts, when used for the oligomerisation of propene was superior to that of the other catalysts studied.

(VI) HDD type catalysts are more active than any of the other catalysts examined.

(VII) HDD, IMP and SG type catalysts are all sensitive to the feed moisture content. The introduction of a wet feed results in high initial activity followed by rapid deactivation. The rapid deactivation may be due to the conversion of Lewis acid sites to Bronsted acid sites in the presence of water.

(VIII) The product spectra of HDD and IMP type catalysts are similar. SG type catalysts, however, exhibit a greater selectivity towards heavier products.

(IX) HDD type catalysts can be used for the oligomerisation of high molar weight oligomers

REFERENCES

Allum, K.G., United States Patent Application, No. 3816555 (1974)

Bartlett, P.D., Condon, F.E., and Schneider, A., J. Am. Chem. Soc., 66, 1531 (1944)

Blackmond, D.G., and Ko, E.I., Appl. Catal., 13, 49 (1984)

Boreskov, G.K., in Preparation of Catalysts, (Delmon, B., ed.), Elsevier, Amsterdam, 223 (1976)

Brookes, C.S., and Christopher, G.L.M., J. Catal. 10, 211 (1968)

Cartwright, P.F.S., Newman, E.J., and Wilson, D.W., "The Analyst", 92, 663 (1967)

Cervello, J., Hermana, E., Jimlne'z, J., and Milo, F., in Preparation of Catalysts, (Delmon, B., eds.), Elsevier, Amsterdam, 251 (1976)

Clark, A., Ind. Eng. Chem., 45, 1476 (1953)

Coulson, J.M., and Richardson, J.F., Chemical Engineering, Vol. II, Pergamon Press, New York (1980)

Couper, A., and Eley, D. D., Discussions Faraday soc., 8, 172 (1950)

Dorling, T.A., Lynch, 13. W.J., and Moss, T.L., J.Catal, 20, 190 (1971)

Dow, W.M., and Jakob, M., Chem. Eng. Prog., 47, 637 (1951)

Dowden, D.A., J. Chem. Soc., 242 (1950)

Dutkuwicz, R.K., Energy 1980 An Energy Policy Discussion Document, The Energy Research Institute- U.C.T., 1980

Evans, A.G., and Polanyi, N., Nature, 152, 738 (1947)

Fel'dblyum, V.Sh., and Baranova, T.I., Zhurnal Organichesoi Kimii, 7, 2257 (1971)

Fel'dblyum, V. Sh., Petrushanskaya, N.V., Lesheheva, A.I., and Baranova, I.I., Zhurnal Organischeskoi Khimii, 10, 2265 (1974)

Finch, J.N., and Clark, A., J.Catal., 13, 147 (1969)

Fontana, C.M., and Kidder, G.A., J. Am. Chem. Soc., 70, 3745 (1948)

Forni, L., Catalysis Reviews, Vol. 8, (Heinemann, H., ed.), Marcell Dekker, New York, (1974)

Galya, L.G., Occelli, M.L., and Young, D.C., J. Mol. Cat., 32, 391 (1985)

Heertjies, P.M., and Mc Kibbins, S.W., Chem. Eng. Sci., 5, 161 (1956)

Hermans, L.A.M., and Geus, J.N., in Preparation of Catalysts II, (Delmont, B., Grange, P., and Jacobs, P., eds), Elsevier, The Netherlands (1979)

Higley, D.P., European Patent Application, No. 84305214.3 (1984)

Hill, F.N., and Selwood, P.W., J. Am. Chem. Soc. 71, 2522 (1949)

Hirschler, A.E., Am. Chem. Soc. Meet., Chicago. Sept. 1970, Reprints, Div. of Petrol. Chem., 15, A97 (1970)

Hogan, J.P., Banks, R.L., Lanning, W.C., and Clark, A., Ind. Eng. Chem., 47, 4 (1955)

Holm, V.C.F., Bailey, G.C., and Clark, A., Ind. Eng, Chem., 49, 250 (1957)

Holm, V.C.F., and Bailey, G.C., and Clark, A., J.Phys. Chem., 63, 129 (1959)

Houalla, M., and Delmon, B., Surface and Interface Anal., 3, 103 (1981)

Hunter, W.H., and Yohe, R.V., J. Am. Chem. Soc., 55, 1248 (1933)

Imai, H., and Uchida, H., Bull. Chem. Soc. Japan, 38, 925 (1965)

Imai, H., Hasegawa, T., and Uchida, H., Bull. Chem. Soc. Japan, 41, 45 (1968)

Johnson, O., J. Am. Chem. Soc., 59, 827 (1955)

Langlois, G.E., Ind. Eng. Chem. 45, 1470 (1953)

Leva, M., Fluidisation, McGraw and Hill (1959)

Levenspiel,O., Chemical Reaction Engineering, 2nd ed., John Wiely and Sons (1972)

Maatman, R.W., and Prater, C.D., Ind. Eng. Chem., 49, 2 (1957)

McNair, H.M., and Bonelli, E.J., Basic Gas Chromatography, 5th ed., Varian Instrument Division (1969)

Mickley, H.S., and Fairbanks, D.F., A.I. Ch. E.J., 1, 374 (1955)

Miller, S.J., U.S. Patent, 4,608,450 (1986)

Mizuno, K., Ikeda, M., Imokawa, T., Take, J., and Yoneda, Y., Bull. Chem. Soc., Japan, 49, 1788 (1976)

Montes, M., Penneman de Bosscheyde, C., Hodett, B.K., Delannay, F., Grange, P., and Delmon, B., Appl. Catal. 12, 309 (1984)

Norrish, R.G.W., and Russell, K.E., Trans. Faraday Soc., 48, 91 (1952)

Ozaki, A., and Kimura, K., J.Catal., 3, 395 (1964)

Ozaki, A., Ali, H., and Kimura, K., Fourth Int. Cong. Catal., Moscow, 40 (1968)

Peri, J.B., J.Catal., 41, 227 (1976)

Ramser, J.H., and Hill, P.B., Ind. Eng. Chem., 50, 1 (1958)

Richardson, J.T. and Dubus, R.J., J. Catal., 54, 207 (1978)

Sato, M., Aonuma, T., and Shiba, T., Proc. Third Int. Cong. Catal., Amsterdam, 1964, 1, 396 (1965)

Schmerling, L., and Ipatieff, V.N., Advances in catalysis, II, New York Academic Press Inc., 21 (1950)

Schultz, R. G., Schuck, J.M., and Wildi, B.C., J.Catal., 6, 385 (1966)

Shepard, F.E., Rooheg, J.J., and Kemball, C., J.Catal. 1, 379 (1962)

Smith, J.M., and Van Noss, H.C., Introduction to Chemical Engineering Thermodynamics, 3rd Edition, McGraw and Hill International Book Company, New York (1981)

Takahashi, K., Sasaki, O., Aomura, K., and Ohtsuka, H., Hokkaido Daigaku Kogakubu Kenkyu Hokoku, 53, 201 (1969)

Takahashi, K., Nishi,H., Yoneda, N., and Ohtsuka, Sekiyu Gakkai Shi, 15, 482 (1972)

Tamele, M.W., Ind. Eng. Chem, 8, 270 (1950)

Thomas, C.L., Ind. Eng. Chem., 37, 543 (1945)

Ublad, A.G., Mills, G.A., Heinemann, H., Polymerization of Olefins, Emmet, (ed.) Catalysis, 5, New York (1958)

Uchida, H., and Imai, H., Bull. Chem. Soc. Japan, 35, 995 (1962)

Van Dillen, J.A., Geus, J.W., Hermans, L.A.M., and Van Der Mejden, Proc. Sixth Int. Cong. Catal., B7 (1976)

Walton, A.G., in Dispersion of Powders in Liquids, (Parfitt, G.D., ed.), Elsevier, Amsterdam, 122 (1969)

Ward, J.W., and Hansford, R.C., J. Catal., 13, 154 (1969)

Weeks, T.J., Jr., Angell, C.L., Ladd, I.R., and Bolton, A.P., J.Catal., 33, 256 (1974)

Whitmore, F.C., Ind. Eng. Chem., 26, 94 (1934)

Yagi, S., and Kunii, D., Fifth Int. Symp. on Combustion, Reinhold, (ed.) New York, 231 (1955)

APPENDIX A

1 Gas chromatograph data

1.1 Gas samples

The settings used on the Gow-Mac 750p gas chromatograph for all feed and tail gas analyses are listed below

Chromatograph	Gow Mac 750p
Detector	Flame ionisation
Attenuation	1
Range	10^{-10} amps/mV
Data system	Varian 4270
Column length	5.5 m
Column diameter	4 mm
Column pressure	28 psig at 50°C
Packing	n-Octane/Poracil C
N_2 flowrate	41 ml/min
H_2 flowrate	31 ml/min
Air flowrate	300 ml/min
Injector temp.	150°C
Detector temp.	250°C
Temp. prog.	10 min at 50°C: 10°C/min to 120°C: 5 min at 120°C
Sample volume	10µl

1.1.1 Calibration

It is well established in the literature that the area percents of components are not directly proportional to the mass percent, i.e., different components have different detector responses. It is therefore necessary to determine correction factors. Once determined, these correction factors can be used to calculate the composition on a mass basis. Two gas standards were available, the composition of which are shown in Table A-1.

Table A-1 : Gas standards composition

Standard	Species	Mole %	Mass %
1	Methane	22.8	10.1
	Ethane	29.2	24.3
	Propane	29.8	36.3
	Butane	18.2	29.3
2	Propane	52.0	53.2
	Propene	48.0	46.8

Each standard was injected M times ($M \geq 3$) into the G.C. and the area counts and retention times recorded. The results were then normalized to eliminate any discrepancies while injecting, using the equations shown below. These equations were adopted from McNair and Bonelli (1969). To normalize area counts use

$$AP_i' = \left\{ \frac{\sum_{j=1}^{N} AC_{ij}}{\sum_{i=1}^{M} \sum_{j=1}^{N} AC_{ij}} \right\} \cdot 100 \qquad \text{For } i = 1 \text{ to } M,$$

where

M is the number of samples,
N is the number of components,
AC_{ij} is the area count of component i in sample j as recorded by the G.C., and
AP_i' is the mean area percent of component i.

and to normalize retention times use

$$RT_i' = \left\{ \frac{\sum_{j=1}^{N} (RT_{ij} \cdot AC_{ij})}{\sum_{i=1}^{M} \sum_{j=1}^{N} AC_{ij}} \right\} \qquad \text{For } i = 1 \text{ to } M,$$

where

RT_{ij} is the retention time of component i in sample j, and
RT_i' is the mean retention time of component i.

Once the mean area percent of each component had been established the ratio (AR_i) of the area percent (AP_i) to mass percent (MP_i) was calculated using:

$$AR_i = AP_i'/MP_i$$

The response factors (RF_i) are calculated using:

$$RF_i = AR_{Propane}/AR_i$$

These factors are relative to propane, i.e., the response factor for propane was arbitrarily set equal to unity. A detailed sample calculation using the above procedure is given in Table A-2.

Table A-2 : Area percent and retention time normalisation

Standard 1

Species: (N=4)	Methane (i=1)	Ethane (i=2)	Propane (i=3)	Butane (i=4)
$AC_{i,j=1}$	94792	241206	346861	371930
$RT_{i,j=1}$	3.5	4.3	6.2	11.1
$AC_{i,j=2}$	82857	213323	308409	332568
$RT_{i,j=2}$	3.5	4.3	6.2	11.1
$AC_{i,j=3}$	86832	215668	314257	322218
$RT_{i,j=3}$	3.5	4.3	6.1	11.1
AP_i'	9.0	22.9	33.1	35.0
RT_i'	3.5	4.3	6.1	11.1
MP_i	10.1	24.3	36.3	29.3
AR_i	0.89	0.94	0.91	1.2
RF_i	1.02	0.97	1.00	0.76

Table A-2 : Area percent and retention time normalisation (continued)

Standard 2

Species: (N=2)	Propane (i=1)	Propene (i=2)
$AC_{i,j=1}$	521001	593387
$RT_{i,j=1}$	6.1	7.4
$AC_{i,j=2}$	55278	64241
$RT_{i,j=2}$	6.2	7.4
$AC_{i,j=3}$	45750	56275
$RT_{i,j=3}$	6.1	7.4
AP_i'	46.6	53.4
RT_i'	6.1	7.4
MP_i	53.2	46.8
AR_i	0.88	1.14
RF_i	1.000	0.77

Under the same detector conditions these factors can be used time and time again to calculate the mass percent of the components in the standards relative to propane.

To calculate the composition on a mass basis of an unknown mixture the equation used is

$$MP_i = (RF_i . AC_i)/(_i \sum^{N}_{i} RF_i \cdot AC_i)$$

A sample calculation using the above equation and the G.C. output from an independent injection of Standard 1 is shown in Table A-3.

Table A-3 : Error determination

Species	$AC_{i,j=4}$	RF_i	MP_i	MP_{calc}	Error %
Methane	109318	1.02	10.1	10.3	1.6
Ethane	273475	0.97	24.3	24.3	0.3
Propane	394953	1.00	36.3	36.4	0.1
Butane	414146	0.76	29.3	29.0	0.9
				$\Sigma(\epsilon^2)$ =	3.4

A typical spectrum obtained (feed gas) is summarised in Table A-4 and shown in Figure A-1. Traces of species found in the feed but for which no standards were available were assigned response factors of unity. As the total contribution of these on an area basis was less than one percent, the error introduced should be negligibly small.

Table A-4 : Feed composition

Species	Retention time	Response factor	Mass %
Methane	3.5	1.02	0.0
Ethane	4.3	0.97	0.92
Propane	6.1	1.00	19.8
Propene	7.4	0.77	78.0
Iso-Butane	11.0	1.00	0.19
N-Butane	11.1	0.76	0.23
1-Butene	13.6	1.00	0.43
Iso-Butene	14.7	1.00	0.04
T2-Butene	15.3	1.00	0.09
C2-Butene	15.9	1.00	0.05
C_5^+	19.3	1.00	0.17

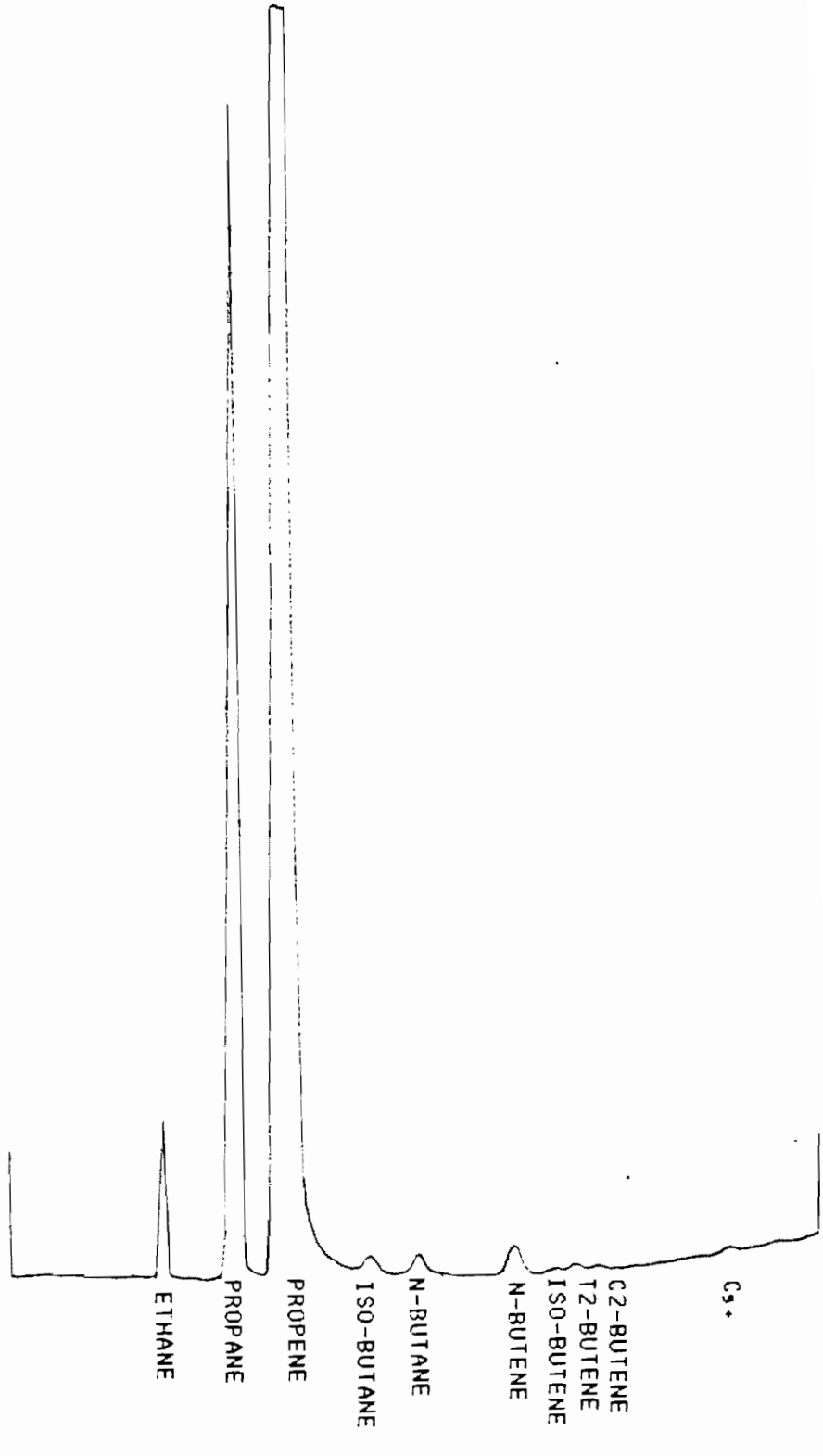

Fig A-1 G.C. SPECTRA OF FEED

1.2 Liquid samples

The settings listed below were used for all liquid samples.

Chromatograph	Varian 3400
Auto sampler	Varian 8000
Data system	Varian CDS 401
Detector	Flame ionisation
Attenuation	1
Range	10^{-9} amps/mV
Column length	3 m
Column diameter	4 mm
Column press.	18 psi at 40°C
Packing	3% Silicon/OV-101 on Chromosorb W-HP 100/120 mesh
N_2 flowrate	30 ml/min
H_2 flowrate	30 ml/min
Air flowrate	300 ml/min
Injector temp.	250°C
Detector temp.	300°C
Temp. Prog	5 min at 40°C: 10°C/min to 180°C: 30°C/min to 300°C: 5 min at 300°C
Sample volume	1 µl

1.2.1 Calibration using mass spectroscopy

Due to the complex nature of the liquid products the analysis of the liquid spectra was difficult. To facilitate product analysis it was decided that the liquid product analysis be based on carbon number groupings rather than on individual components. A direct comparison between the spectra obtained by the G.C. and M.S. was not possible due to hardware and software differences. The trends in the spectrum obtained were however the same and in this way carbon numbers could be allocated to the G.C. spectrum.

A typical spectrum of the G.C.-M.S. is shown in Figure A-2. The molecular weights of the components responsible for the peaks as determined by mass spectroscopy are shown in this figure. As a comparison a gas chromatogram using the Varian 3400 is shown in

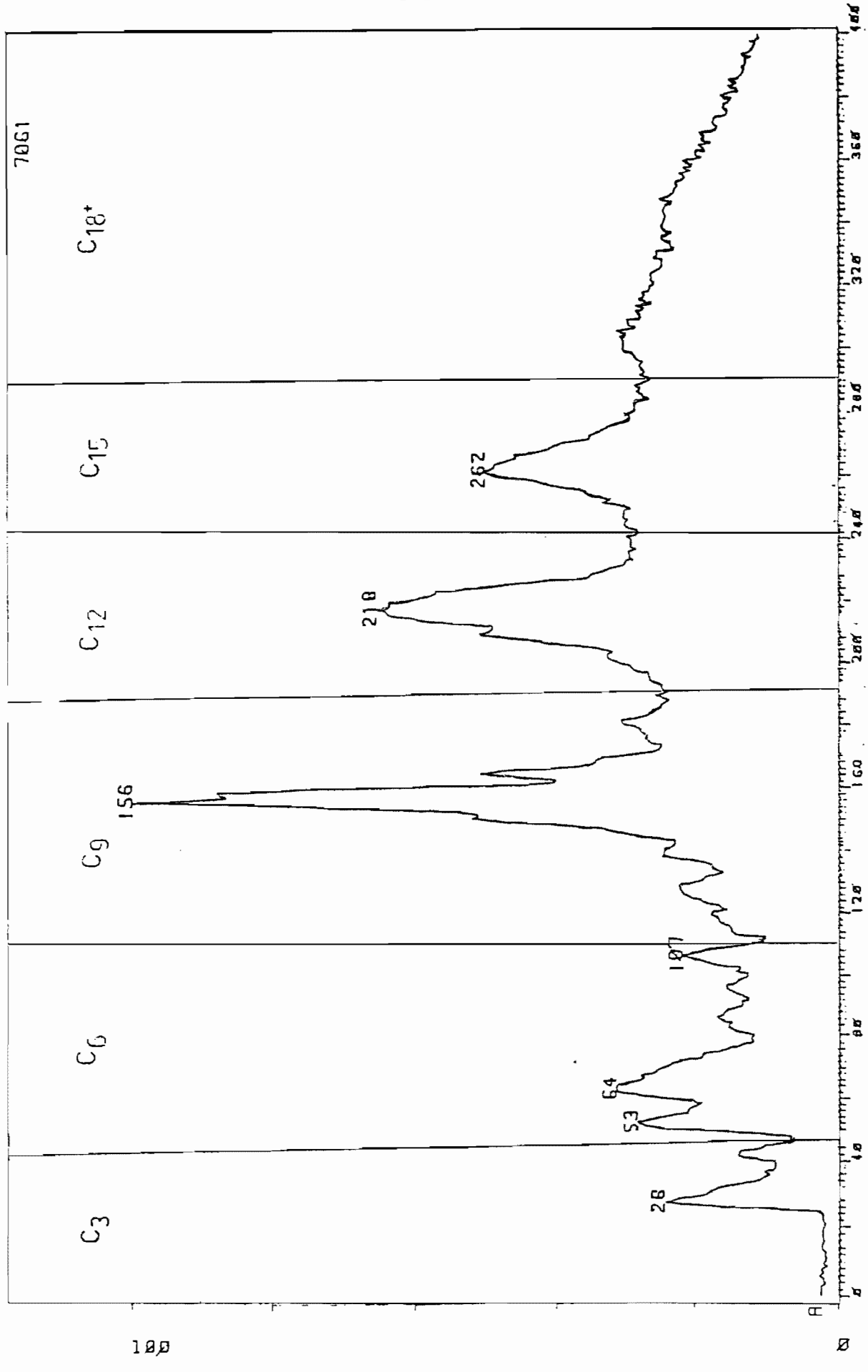

FIG A-2 TYPICAL G.C.- M.S. SPECTRA OF LIQUID PRODUCT

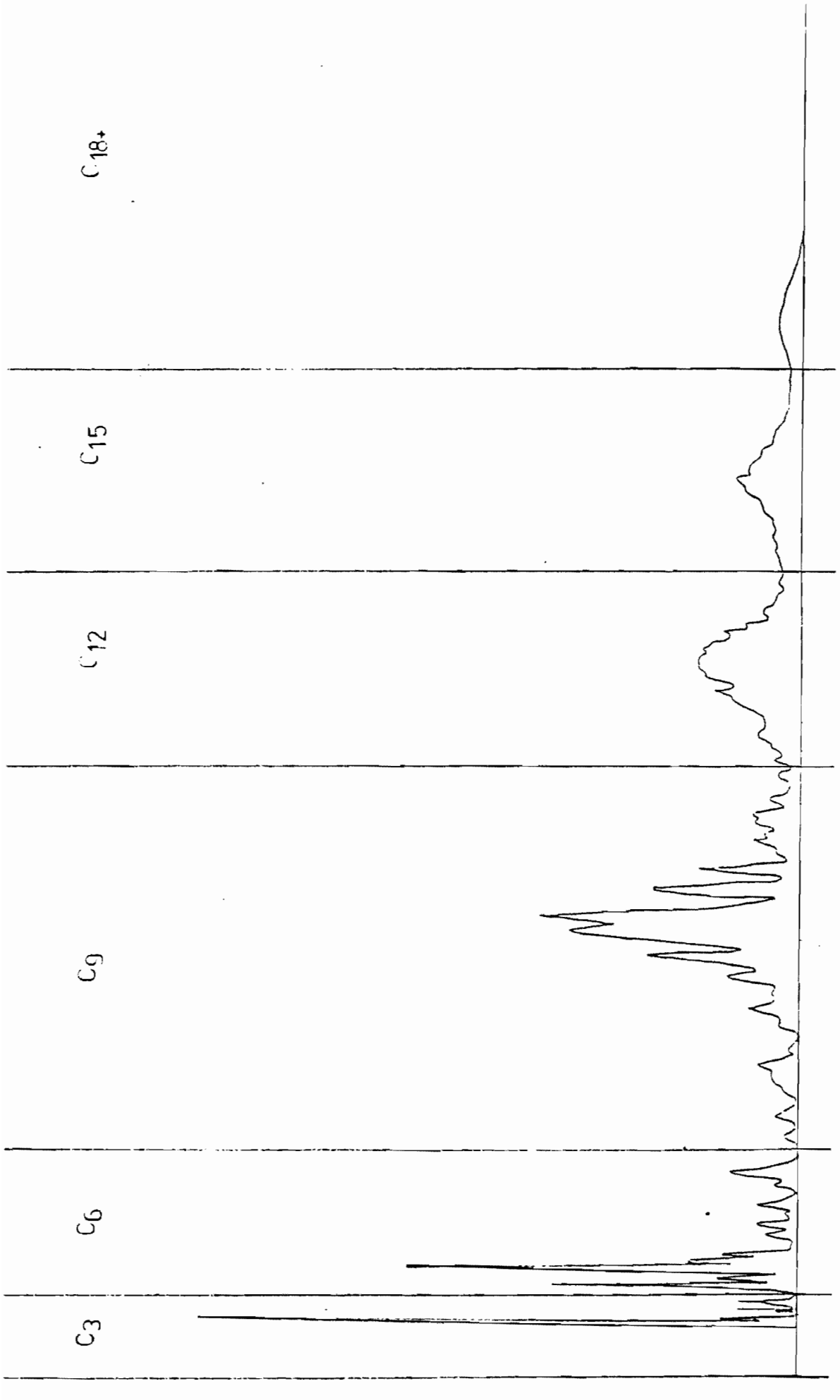

FIG A-3 TYPICAL G.C. SPECTRA OF LIQUID PRODUCT

Figure A-3. Using the data from the M. S., carbon numbers could be assigned to the peaks on the gas chromatogram, and so the start and end times of the various groups established. The groupings used are shown in Table A-5 as is a typical liquid composition

Table A-5 : Typical liquid composition and retention time windows

Group	Mass %	Retention times	
		start	stop
Monomer	4.95	0.00	1.02
Dimer	61.0	1.02	4.70
Trimer	24.3	4.70	11.2
Tetramer	8.13	11.2	15.7
Pentamer	1.62	15.7	18.5
Hexamer	0.00	18.5	20.5
Heptamer	0.00	20.5	28.0

The response factors of these groups were taken as unity, which was justified in view of work done by Dietz (1967) on the relative sensitivity of hydrocarbons. The results reported in mass percent are therefore a reasonable representation of the actual composition.

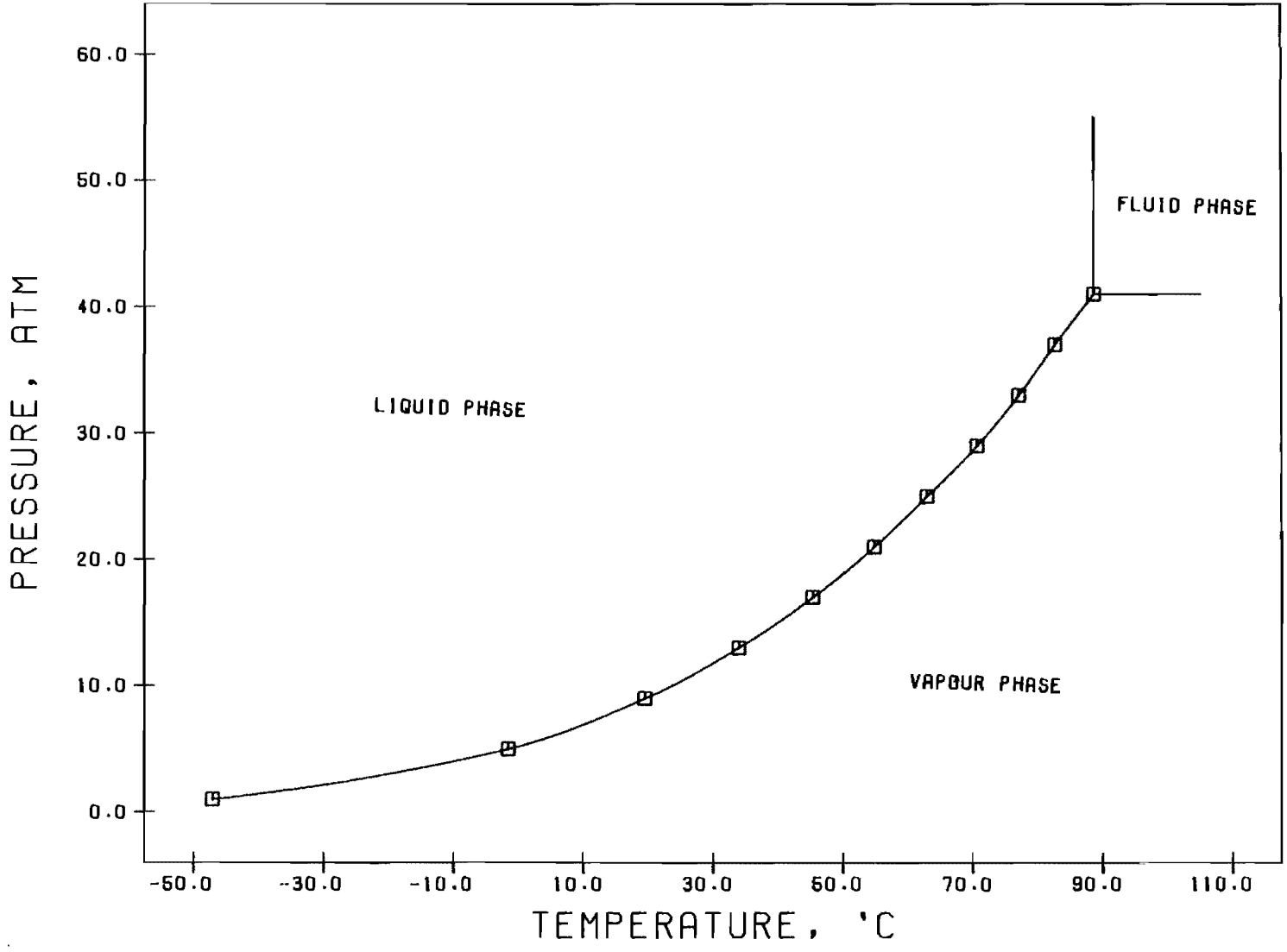

FIG B-1 DEW POINT TEMPERATURE ('C) AND BUBBLE POINT TEMPERATURE ('C) VS PRESSURE (ATM); 20 MOLE% PROPANE AND 80 MOLE% PROPENE